Development, Validation, Uptake Rate Modeling and Field Applications of a New Permeation Passive Sampler

by

Suresh Seethapathy

A thesis

presented to the University of Waterloo

in fulfillment of the

thesis requirement for the degree of

Doctor of Philosophy

in

Chemistry

Waterloo, Ontario, Canada, 2009

AUTHOR'S DECLARATION

I hereby declare that I am the sole author of this thesis. This is a true copy of the thesis, including any required final revisions, as accepted by my examiners.

I understand that my thesis may be made electronically available to the public.

Abstract

Passive air sampling techniques are an attractive alternative to active air sampling because of the lower costs, simple deployment and retrieval methods, minimum training requirements, no need for power sources, etc.. Because of their advantages, passive samplers are now widely used not only for water and indoor, outdoor and workplace air analysis, but also for soil-gas sampling required for various purposes, including vapor intrusion studies, contamination mapping and remediation.

A simple and cost effective permeation-type passive sampler, invented in our laboratory, was further developed and validated during this project. The sampler is based on a 1.8 mL crimp-cap gas chromatography autosampler vial equipped with a polydimethylsiloxane (PDMS) membrane and filled with a carbon based adsorbent. Apart from the low material costs of the sampler and ease of fabrication, the design allows for potential automation of the extraction and chromatographic analysis for high-throughput analysis. The use of highly non-polar PDMS reduces water uptake into the sampler and reduces early adsorbent saturation. The thermodynamic properties of PDMS result in moderately low sampling rate effects with temperature variations. Further, the use of PDMS allows for easy estimation of the uptake-rates based on the physicochemical properties of the analytes such as retention indices determined using capillary columns coated with PDMS stationary phase.

In the thesis, the theoretical and practical aspects of the new design with regards to uptake kinetics modeling and the dependence of the calibration constants on temperature, humidity, linear flow velocity of air across the sampler surface, sampler geometry, sampling duration, and analyte concentrations are discussed. The permeability of polydimethylsiloxane toward various analytes, as well as thermodynamic parameters such as the energy of activation of permeation through PDMS membranes was determined. Finally, many applications of the passive samplers developed in actual field locations, vital for the field validation and future regulatory acceptance are presented. The areas of application of the samplers include indoor and outdoor air monitoring, horizontal and vertical soil-gas contamination profiling and vapour intrusion studies.

Acknowledgments

Firstly, I would like to extend profuse thanks to my research supervisor Dr. Tadeusz Górecki for giving me the opportunity to work on this interesting project and making my past few years at the University of Waterloo wonderful, challenging and interesting. I am indebted to him for encouraging and guiding me not only to do true scientific work in the laboratory, but also to present my research work at prestigious conferences in Europe and in North America. This has resulted in my building acquaintances with leading scientists in the field, understanding the hottest research areas, and as a bonus, improving my skills in making presentations to the scientific community. On the research front, Dr. Górecki has been extremely receptive of any new ideas while being rightfully critical on their scientific merits and demerits. His methods of problem solving in the laboratory are something I will use for the rest of my career.

I wish to thank Dr. James J. Sloan, Dr. Jean Duhamel and Dr. Jacek Lipkowski, members of my advisory committee, for their helpful suggestions and critical review of my graduate work.

I greatly appreciate the support and encouragement of Dr. Jacek Namieśnik, Dr. Bożena Zabiegała and Dr. Monika Partyka at the Gdańsk University of Technology. The discussions with them on passive sampling technology during my four week visit to Gdańsk, Poland, have been very useful in further advancing my research at the University of Waterloo.

My sincere thanks to the staff of the department of chemistry, especially Cathy Van Esch, for guiding me smoothly through the administrative requisites during my graduate studies. Jacek Szubra, Harmen Vander Heide, Andy Colclough and others at the Science Technical Services have always been pleasant and helpful with anything I required to build my experimental setup. My sincere thanks to them.

My special thanks to Todd McAlary, Hester Groenevelt, David Bertrand, Robin Swift, Todd Creamer, Chapman Ross, Duane Graves, and many others at Geosyntec Consultants for agreeing to test our invention at various field sites including those at Raritan Arsenal

at New Jersey, contaminated sites at Knoxville in Tennessee, Harvard university, Maxxam school and Simmons residence at locations in Massachusettes, Thyez in France, and various sites in Philippines, Mexico and Italy. I would like to extend my sincere appreciation to Todd McAlary for giving me a glimpse of what large project management is all about and for his relentless pursuit of commercialization of the passive sampling technology developed within this project.

My thanks to Michael Dumas of Tauw scientifique and Birgitta Beuthe of SPAQuE SA, both operating in Belgium, for chosing my passive samplers for a huge pollutant mapping study at a contaminated site in Belgium. My special thanks to them for providing me with crucial field data, which is perhaps the best proof for validation of the newly designed passive samplers.

I would like to extend my heartfelt thanks to Dr. Alina Segal for being a constant motivator to begin my endeavour at the University of Waterloo. The acknowldegment will be incomplete without mentioning my special gratitudes to Ms. Maria Górecka, for always being there for me and my wife, personally as well as professionally, throughout our stay here at the University of Waterloo.

Timely help in numerous ways from past and present members of Dr. Górecki's research group is gratefully acknolwedged.

No amount of gratitude is enough to shower on my parents, brothers, sister, uncle (Duraikannan Srinivasan), aunt (Parimala Duraikannan), cousins (Aravin and Anita) and friends (Nandagopal Polamoda, Tom Blashill and Navin Madras) for all their support and pride they have for me. The endeavor was certainly made easy due to the constant motivation and support from Jyothi Thanigai, Athilesh Thanigai and Thanigai Ranganathan.

Finally, I would like to thank my wife, Manjula, for not just motivating me to begin this endeavor, but also for supporting me through all the ups and downs of the last few years. She is truly the woman behind my successful completion of the degree.

This thesis is dedicated to my brother,
Sundar Seethapathy

Table of Contents

List of Figures

List of Tables

List of Abbreviations

ASTM	American Society for Testing and Materials
BTEX	Benzene, Toluene, Ethylbenzene, and Xylene
CEN	Comitée Européen de Normalisation
CS_2	Carbondisulphide
E_a	Energy of activation of permeation
ECD	Electron capture detector
FID	Flame ionization detector
GC	Gas chromatography
HSE	Health and Safety Executive
ISO	International Standards Organization
ITRC	Interstate Technology and Regulatory Council
LC/ToF	Liquid chromatography/Time of Flight Mass Spectrometry
LTPRI	Linear temperature-programmed retention index
MESI	Membrane extraction with a sorbent interface
MIMS	Membrane inlet mass spectrometry
MLPE	Micro liquid-phase extraction
MS	Mass spectrometry
MW	Molecular weight
NIOSH	National Institute for Occupational Safety and Health
PAH	Polycyclic aromatic hydrocarbons
PCB	Polychlorinated biphenyls
PDB	Polyethylene diffusion bag

PDMS	Polydimethylsiloxane
POCIS	Polar Organic Chemical Integrative Sampler
PRC	Performance reference compound
PSD	Passive sampling device
PUF	Polyurethane foam
PVD	Passive vapour diffusion
SIM	Selected ion monitoring
SPMD	Semi-permeable membrane device
SPME	Solid phase microextraction
SVOCs	Semi-volatile organic compounds
TAGA	Trace atmospheric gas analyzer
TWA	Time-weighted average
US-EPA	United States – Environmental Protection Agency
VOCs	Volatile organic compounds

CHAPTER 1

Introduction and scope of the thesis[i]

A significant fraction of chemicals produced by the chemical industry is invariably released into the environment during their production, usage and disposal. Physicochemical properties of these man-made chemicals are wide-ranging, and so are their effects on the global environment and the quality of life of many living species. Monitoring of the presence and quantity of these chemicals in the environment is therefore not a question of choice, but rather a prudent decision on what to look for, when, where, how and why. This is often a challenging task, as the pollutants might be present as complex mixtures, in minute quantities and in varied matrices such as indoor air, workplace air, ambient air, surface and ground water, soil, sediments and aerosols, to name a few. The task is further complicated by spatial and temporal variations in the amount of these pollutants present in the environment due to their complicated flow paths between various environmental compartments. Owing to its simplicity and cost effectiveness, passive sampling is one of the few practical technologies able to meet the enormous sampling requirements posed by the presence and impact of anthropogenic chemicals in the environment.[1]

Górecki and Namieśnik defined passive sampling as "any sampling technique based on free flow of analyte molecules from the sampled medium to a collecting medium, as a result of a difference in chemical potential of the analyte between the two media".[2] Any device based on this principle can be called a passive sampler. This generalized definition takes into account analyte transport into the passive sampler resulting from various driving forces, including concentration, pressure, temperature and electromotive force gradients, which can be reduced to fundamental chemical potential gradients. By virtue of this definition, techniques such as aerosol sampling and analysis of fish adipose tissue for persistent organic pollutants (which partition into the tissue from water) in aquatic environment also fall into the category of passive sampling. Knowledge of the conventional methods of air sampling (active air sampling) is important in order to recognize the need for passive samplers as an attractive

[i] This chapter is partly based on the author's review article "Passive sampling in environmental analysis"[1]

alternative. Therefore, a brief discussion of active sampling methods will be presented here before the discussion of the passive sampling technology.

1.1 Active air sampling

Since the focus of this thesis is on the quantification of Volatile Organic Compounds (VOCs) in air, only the active sampling methods for their sampling and analysis will be discussed here. Many definitions of VOCs have been adopted by different regulatory authorities. In this thesis, the definition according to directive 2004/42/EC of the European Parliament will be adopted because of its broad nature. The definition according to the Directive is the following: "Volatile Organic Compound means any organic compound having an initial boiling point less than or equal to 250 °C measured at a standard pressure of 101.3 kPa".[3]

Active air sampling methods involve collection of contaminants onto a sampling medium by means of a pump. The sampling medium can be an empty container, solid sorbent packed in an inert tube, or liquid enclosed in an impinger. In the case of sampling with a solid sorbent or a liquid, the sampled air is drawn through the sampling medium; the air stripped of the contaminants is vented into the atmosphere. One such widely used method is the United States Environmental Protection Agency (US EPA) method TO-17 (similar to National Institute of Occupational Safety and Hygiene (NIOSH) method 1500 and Occupational Safety and Health Administration (OSHA) method 07) illustrated in Figure 1-1.[4] In this method, sampling is done by drawing a known amount of air through a solid sorbent contained in a deactivated glass or metal tube (often referred to as a sorption tube). The analytes are then desorbed either by extracting them with a solvent (solvent desorption) or by heating the sorbent (thermal desorption). Sorbents commonly used with solvent desorption include silica gel, activated carbon-based sorbents (such as Anasorb® 747), carbon molecular sieves (e.g. Carboxens®), and porous polymers. In the solvent desorption method, only a small aliquot of the solvent extract can be used for gas chromatographic (GC) analysis and quantification. The volume of the solvent aliquot that can be used depends on the sample introduction system in the GC. In the thermal desorption method, the instrumentation allows for a much larger fraction or even all of the analytes trapped by the sorbent to be introduced into the chromatographic system for quantitation. Thermal desorption is therefore preferred

at times to improve the sensitivity of the method. Sorbents used in this method include Tenax® TA, Chromosorb® 106, graphitised carbon, carbon molecular sieves, and multi-bed combinations.[5] The multi-bed combination is used when a single sorbent is not efficient in trapping the entire range of VOCs in the sample matrix. While the sample collection is done in the field, desorption and gas chromatographic analysis are usually done in the laboratory. The concentration of the analyte in the air is determined from the amount of analyte collected by the sorbent and the volume of air drawn into the sampler.

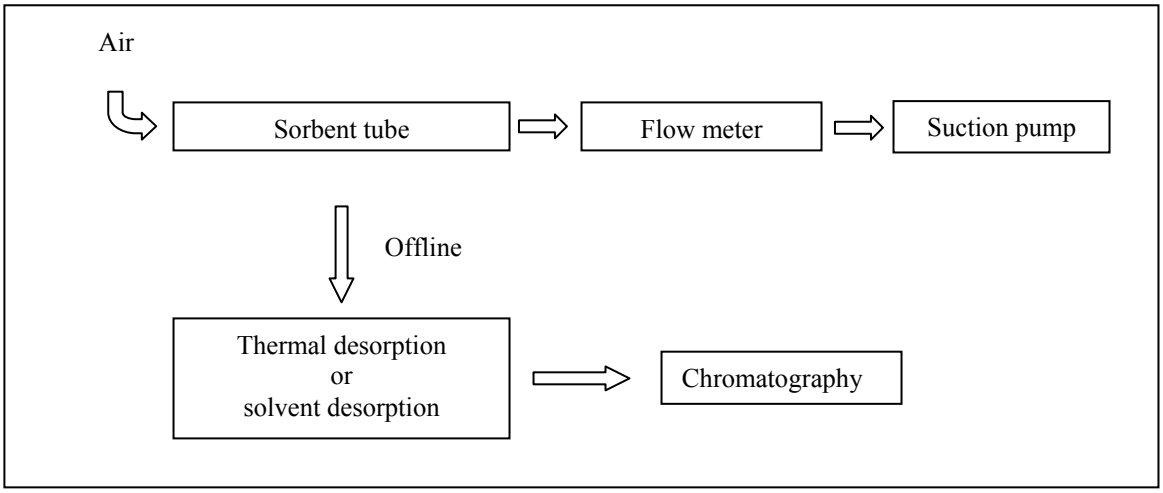

Figure 1-1: Schematic of EPA method TO-17

Active air sampling can also be performed by collecting the air sample in a container made of an inert material. Samples obtained in this way are often termed "grab samples". Depending on the analytes of interest, the containers may be deactivated glass or metal bottles, or bags made of Saran™, Mylar™, Teflon™ or Tedlar® polymers.[6] Tedlar® is the material used most often, and has been referenced in EPA methods 3, 18 and 40. The collected sample is then transported to the laboratory, and the sampled air is analyzed using suitable quantification methods. For the quantification of VOCs, gas chromatography with flame ionization detection (FID), electron capture detection (ECD) or mass spectrometry (MS) is most often used.

Although the final sample analysis is usually performed in the laboratory, there are often situations, like emergencies due to chemical spillage, when real-time measurements of analyte concentrations are needed. Some of these methods are discussed in the next section.

1.1.1 Real-time pollutant measurement

Various analytical methods are available for real-time analysis, which are capable of quantifying low concentrations of VOCs. They include differential optical absorption spectroscopy (limit of detection (LOD) ~2.6 $\mu g/m^3$ for benzene), low-pressure chemical ionization/tandem mass spectrometry (MS^2) (LOD ~2.0 $\mu g/m^3$ for benzene), atmospheric pressure chemical ionization/MS^2 (LOD ~38.3 $\mu g/m^3$ for benzene) and proton-transfer reaction MS (LOD ~0.3 $\mu g/m^3$ for benzene and toluene).[7] The instruments are generally installed in a vehicle for easy use at various locations based on the needs. US EPA's Trace Atmospheric Gas Analyzer (TAGA) is one such mobile laboratory which makes use of triple quadrupole (QqQ) MS^2 for real time analysis of various pollutants. In this method, the ambient air is sampled continuously at a specific flow rate (typically 90 ml/min) and part of it is directed into the ion source of a QqQ mass spectrometer for ionization, fragmentation, detection and quantification. The specificity of MS^2 (based on a series of ionization, fragmentation and detection events) allows for quantification of the target analytes in real-time.

The instruments mentioned in the above paragraph are expensive and require highly trained personnel for their operation. Cheaper, hand held devices which can provide an estimate of the total contaminant concentration in the vapor phase are also available. These include photoionization detectors (PID) and flame ionization detectors (FID).

The PID is based on the ionization of chemical species in the sample using an ultraviolet (UV) lamp, followed by detection of the ions formed. Commercially available PIDs have lamps with specific ionization energies (e.g. 9.8, 10.6 or 11.7 eV); any chemical species that can be ionized with the specific UV lamp used are detected by the PID.[8] The ions created by the action of the UV lamp generate a current in an external circuit. This current is used as a measure of the concentration of the ionizable chemicals in the sample. The PID is often calibrated based on the response of isobutylene, and the total concentration is expressed in terms of isobutylene concentration. While these are handy instruments, they have a number of disadvantages: PIDs cannot detect all the organic vapors in the sample, are not analyte

specific, and are affected by humidity and the presence of non-ionizable gases such as methane.

Portable FIDs are based on ionization of organic compounds in a hydrogen flame followed by quantification based on the signal generated by the resulting ions. This is similar to the FIDs available for detection in GC. Any chemical species with a C-H bond is ionized and detected by the FID. It is generally calibrated using a known concentration of methane, and the total VOC concentration is expressed in terms of this calibrant. Both the FIDs and the PIDs are capable of detecting concentrations in the range of 0.1 – 0.5 ppmV (as methane for FID and as isobutylene for PID). Like PID, FID also has the disadvantage of not being analyte-specific.[9]

The methods described in this section are just examples of the many variations of active air sampling methods, with each variation being devised according to the sample matrix, analyte type, sensitivity required, available resources, analysis time constraints, etc. Active sampling has been used and perfected over the last few decades and led to numerous scientific breakthroughs regarding volatile organic pollutants and their effects on animals and vegetation. In spite of that, these methods have many disadvantages, the most important of which cause researchers to look for alternative sampling techniques.

In the case of sampling systems using pumps, the pumps used to deliver the known amount of air sample into the sorbent have to be calibrated. Also, such pumps are often noisy and require electricity for their operation. The need for electricity, usually supplied from batteries, introduces the requirement for frequent checking to ensure that the pump is operating for its pre-determined period of time.

In the field of occupational exposure, the portable pumps are cumbersome for the employees to carry around for prolonged periods of time. Even though the present day technology has been able to miniaturize the sampling pumps, their presence has mostly been perceived as an obtrusion in the normal work of an employee.[10]

Many pumps and other pieces of sampling equipment are required in order to collect large numbers of samples simultaneously, e.g. when trying to map the contaminant source. Due to

the significant costs involved in procuring large amounts of equipment for sampling, the number of samples collected in any given study is often limited by the amount of equipment available. Also, costly equipment installed in the field is often prone to vandalism.

The biggest disadvantage of active sampling methods is their poor applicability to time weighted average concentration (TWA) determination. TWA is defined as the average concentration of a pollutant over a particular period of time. Active sampling can provide data only on pollutant concentrations present during the short period of sampling, typically not exceeding 24 hours. For longer time periods, active sampling requires many discrete measurements to provide TWA concentration. Because of all the disadvantages of active air sampling methods, passive sampling is used widely today for many applications.

1.2 Passive sampling

Since the first demonstration of truly quantitative passive sampling by Palmes and Gunnison in 1973,[11] numerous scientific peer-reviewed articles have been published on this topic. Passive samplers were initially designed for gaseous pollutants in air, followed by their application to aqueous matrices, and, more recently, solid matrices such as soils and sediments. According to the definition of Górecki and Namieśnik presented earlier, air sampling using evacuated containers such as SUMMA™ canisters can also be classified as passive sampling. The discussion of the passive sampling technique in this section does not apply to SUMMA™ canisters (they are covered in detail in section 1.5.1).

As an analytical chemistry tool, passive sampling is used to achieve some or most of the basic sample preparation goals. These include among others isolation of the analytes from the matrix and their pre-concentration to increase the selectivity and sensitivity of the measurements, chemically changing the analyte to a form suitable for the analytical measurement, and/or reduction of, or complete elimination of solvent use (green chemistry). With most passive samplers, reduction and/or elimination of matrix interferences can be easily achieved, although new matrix components might be introduced with certain passive samplers, prompting the need for further sample clean-up.

Passive sampling has many practical advantages, including cost effectiveness, little training required to handle the devices, and no need for power sources for their operation. Furthermore, it is often useful to be able to determine TWA concentrations. Many passive samplers can easily provide TWA concentrations, which is difficult (though not impossible) to obtain with active/grab sampling technologies, as explained above.

Many passive samplers are available commercially or from various research groups today. Factors affecting the design of these samplers include:

i. The sampled medium, or the matrix (air, water, soil, or various combinations of these, such as sediments or aerosols);
ii. Chemical and physico-chemical properties of the analyte(s) of interest;
iii. Analyte form (ionized, non-ionized, sorbed, etc.) and concentration range in the sample;
iv. Quantitative or semi-quantitative type of measurement required;
v. Sampling duration required (e.g. 8 hr workplace exposure vs. several weeks exposure in environmental monitoring);
vi. Variability of environmental parameters around the sampler or in the sample in which the samplers are to be deployed;
vii. Cost and availability.

Since a number of variables have to be considered, there are situations where combinations of passive samplers have to be deployed to obtain the data required. While the physical deployment of passive samplers is fairly simple, the sampling strategy involved in choosing the number and type of passive samplers for deployment, their exact locations, time and duration of exposure, as well as quantification in the laboratory, require careful consideration. The knowledge of the pollution source, quantity and potential fate in the environment, as well as of the analytical methods used for quantification, are required for proper data interpretation.

The sampler presented in this thesis was developed for the analysis of VOCs in the vapor phase, with main applications including indoor/outdoor air and soil-gas analysis. In the following sections, the principle of operation of passive sampling devices will be explained, followed by a review of a selection of currently available passive samplers and their designs.

The knowledge of the effect of various environmental parameters on different types of samplers is very important, hence this aspect will be discussed next. While proposing a design/model for a passive sampler to be applicable for routine use, it is important to understand and consider the regulatory requirements put forward by various agencies as applied to the validation of the passive sampling technology. Consequently, a summary of the relevant regulatory documents will be presented. The scope of the thesis will then be defined and listed.

1.3 General principles of operation

Even though many different designs of passive samplers are available on the market today, nearly all of them (with some exceptions, like the SUMMA™ canisters) consist of a barrier and a sorbent, the material and geometry of which are carefully chosen for the specific type of analyte and matrix. The barrier is generally one of two types: a static layer of air (diffusion-type samplers) or a polymer membrane (permeation-type samplers), as depicted in Figure 1-2. Within the barrier, convective transport of analytes is preferentially avoided, so that the net transport across it occurs mainly due to molecular diffusion following Fick's laws. For the sake of clarity, "barriers" in this thesis will not include the boundary layers (see later). The function of the sorbent is to adsorb or absorb analyte molecules reaching its interface with the barrier. Chemical reaction between the analyte and the sorbent can also be used to trap the analytes; the phenomenon is referred to as chemisorption. Adsorption is a surface phenomenon in which a chemical species (an adsorbate) associates with the surface of the material (adsorbent) due to intermolecular forces acting between the two. Absorption is a process in which a substance (an absorbent, usually a liquid) takes up (or dissolves) a chemical species (absorbate) uniformly within its matrix. Adsorbents, absorbents and chemically reacting materials are collectively referred to as "sorbents" in this thesis. Sorbents in various passive samplers are described later in the review.

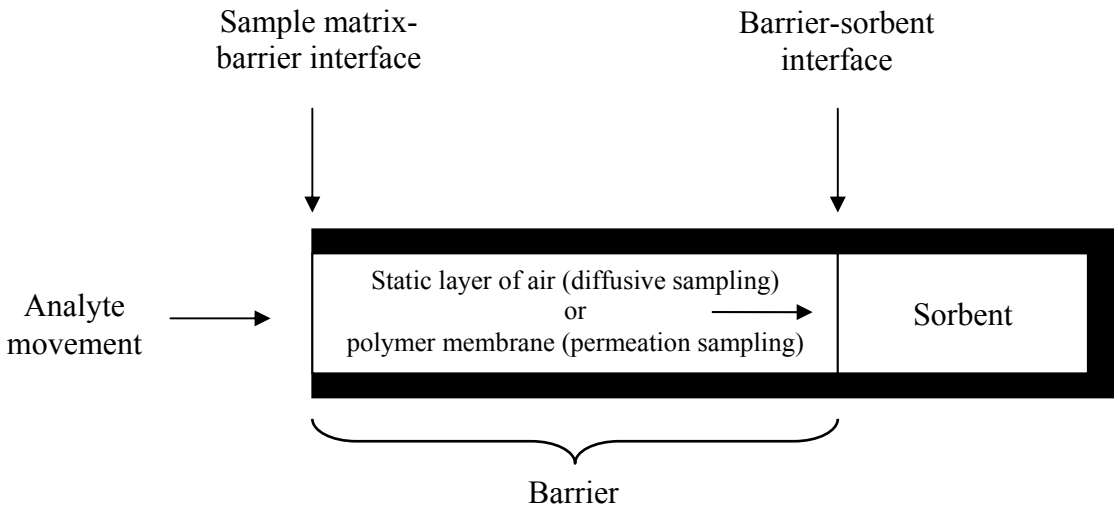

Figure 1-2: Conceptual design of a passive sampler

When a passive sampler of such a design is exposed to the sample matrix, analyte molecules are transferred into the sampler spontaneously under a concentration or partial pressure gradient existing between the barrier-sample matrix interface and the sorbent-barrier interface. The function of the sorbent is to completely absorb (or adsorb) all the analyte molecules reaching the interface between the sorbent and the barrier of the sampler so that the concentration at this interface is practically zero. Under such conditions, the kinetics of analyte transfer to the sorbent in a given period of time obey Fick's laws of molecular diffusion. Consequently, analyte concentration in the sample matrix can be calculated from the measured mass of the analyte present in the sorbent.

Analyte collection by the sorption material begins when the sampler is exposed to the sample matrix. The uptake of the analyte into the sampler can be generally represented by a one-compartment model shown in Figure 1-3.[12] According to the model, analyte uptake proceeds until the chemical potentials of the analyte in the sorbent and in the sample matrix become equal. Depending on the barrier type, the sorption material, the sampler geometry and the sampling duration, a passive sampler can function in the following three regions (Figure 1-3): the kinetic region, the equilibrium region, or the intermediate region. In the kinetic region, the sorbent is far from saturation (or equilibration) and therefore any molecule arriving at its

surface is effectively trapped. The analyte amount collected by the sampler is then directly proportional to the time period for which the sampler is exposed to the sample medium. Within the equilibrium region, either the active sites are all blocked (adsorbents) or equilibrium has been reached (absorbents). In this case, the analyte amount collected by the sampler is independent of the exposure time. Between the kinetic and the equilibrium region, the analyte uptake is non-linear, hence this region is seldom used for quantitative purposes.

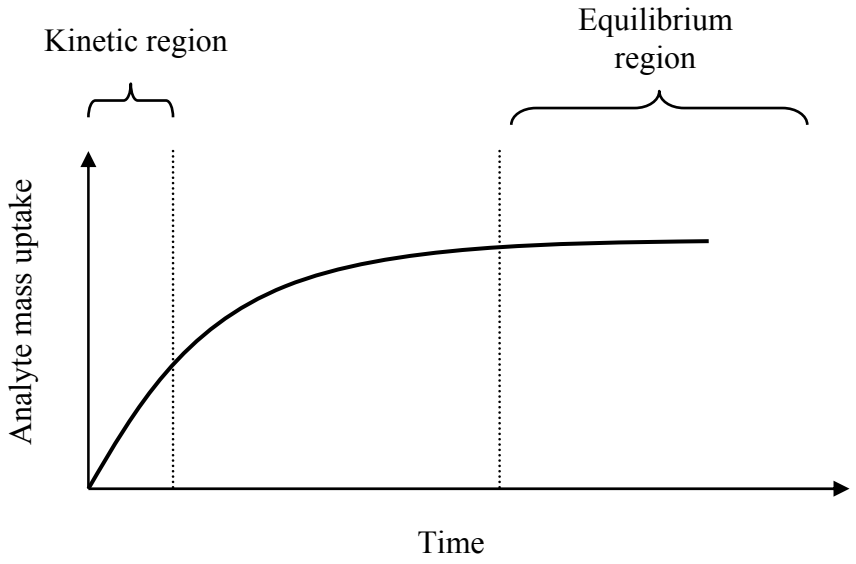

Figure 1-3: Analyte uptake as a function of time (based on ref. 12)

1.3.1 Passive air sampling

When sampling from air, a sorbent is often chosen that acts as a zero sink (i.e. analyte concentration at the sorbent-barrier interface is practically zero), which implies that the sampler functions in the kinetic region making TWA concentration determination straightforward. This is often accomplished by using adsorption or chemisorption-based sorbents. When adsorption-based sorbents are used, care must be taken to allow only for low mass loadings to minimize competitive adsorption processes, which become pronounced under high mass loading conditions.

Based on the conceptual design shown in Figure 1-2, various samplers of different geometry and materials are made depending on the type of application. Figure 1-4 illustrates a so-

called “tube-type” sampler, while Figure 1-5 illustrates a “badge-type” sampler. The latter uses either a semi-permeable membrane, or a porous material (such as ceramic) as the uptake rate-limiting barrier.

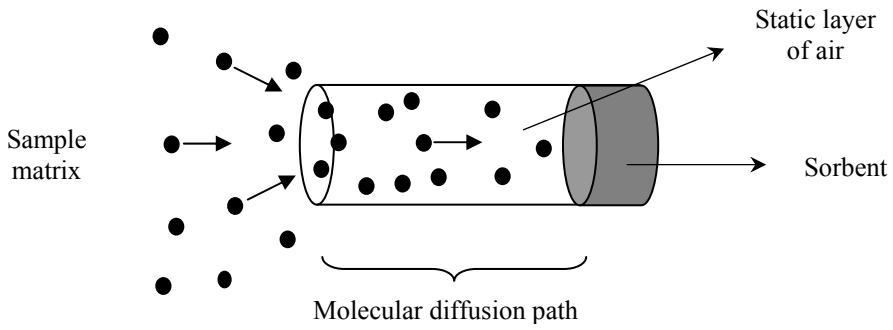

Figure 1-4: Tube-type passive sampler

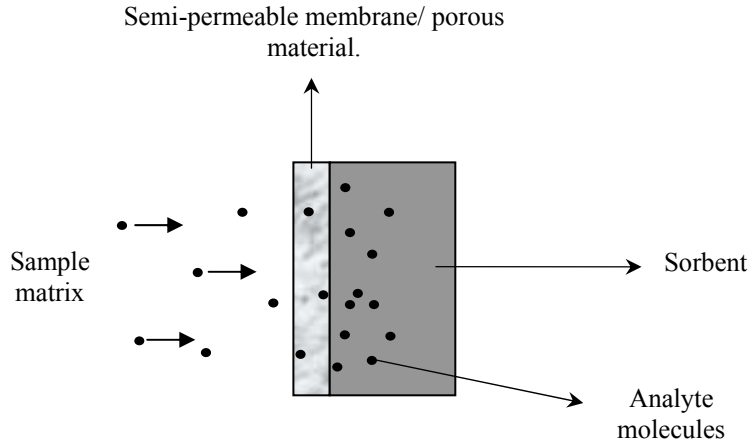

Figure 1-5: Badge-type passive sampler

The sampler used in this project is of permeation-type, resembling the badge-type sampler shown in Figure 1-5. When sampling under the kinetic region illustrated in Figure 1-3, ideal concentration profiles for analyte uptake from air by the diffusion- and permeation-type passive samplers are illustrated in Figures 1-6 and 1-7, respectively.[13] In the case of diffusion-type samplers, the analyte concentration within the barrier varies from a maximum

corresponding to the analyte concentration in the air to zero at the sorbent-barrier interface. In the case of permeation-type samplers, analyte transfer from the sample into the sorbent in the sampler (through the polymer membrane) involves three steps: dissolution of the vapor molecules in the polymer (determined by the partition coefficient of the analyte between air and the membrane material), diffusion of the molecules through the membrane material under a concentration gradient, and the release of the vapor from the polymer at the opposite side of the membrane.[14] The concentration of the analyte on the surface of the membrane exposed to the sample depends on its concentration in air and its partition coefficient between air and the membrane material. For polydimethylsiloxane (PDMS) membrane barriers, partition coefficients of VOCs are typically much greater than one (examples of partition coefficients of n-alkanes are provided in Chapter 2). The concentration of VOCs on the membrane surface on the sample side is therefore much higher than the concentration in the air. The relationships between analyte concentration in the air, sampler geometry, time of exposure and mass uptake into the sampler are summarized for the two types of samplers in Table 1-1.[15,16]

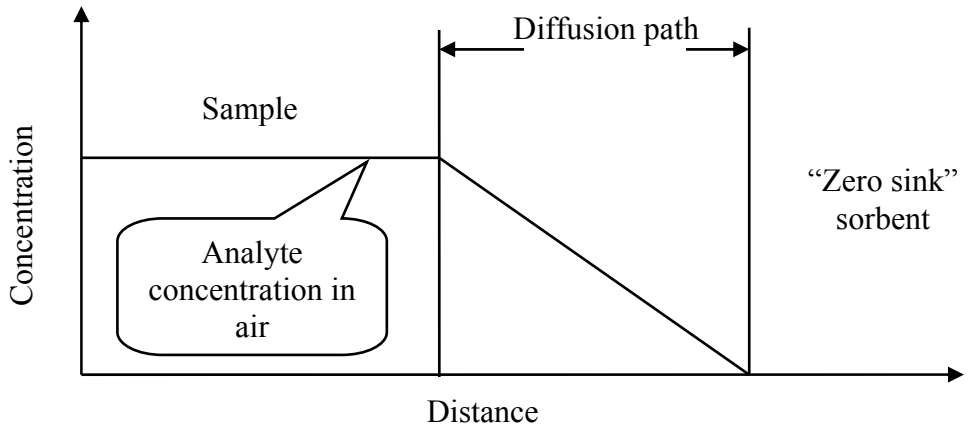

Figure 1-6: Ideal concentration profile for diffusion-type passive samplers (based on ref. 13)

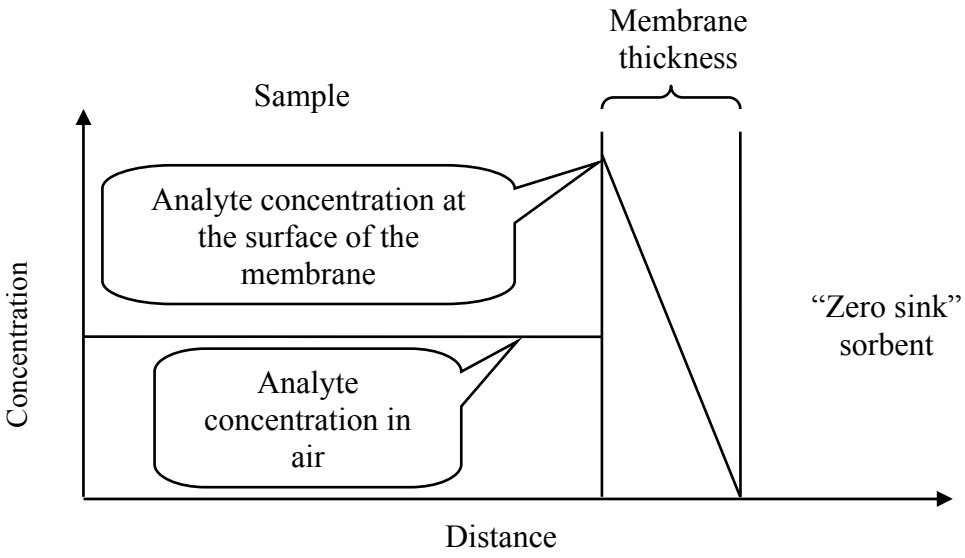

Figure 1-7: Ideal concentration profile for permeation-type passive samplers (based on ref. 13)

Table 1-1: Fick's law as applied to diffusive- and permeation-type passive samplers (based on refs. 15 and 16)

	Diffusion sampler	Permeation sampler
Application of Fick's law	$\left(\frac{M}{t}\right) = D\frac{A}{L_d}(C_0 - C)$ *D* - *D*iffusion coefficient of the analyte *A* - Area of the cross-section of the diffusion barrier L_d - Length of the diffusion path *C* - Concentration of the analyte near the diffusion path- sorbent interface C_0 - Concentration of the analyte in the vicinity of the diffusion barrier inlet	$\left(\frac{M}{t}\right) = D\frac{A}{L_m}(C_{ma} - C_{ms})$ *D* - Diffusion coefficient of the analyte in the membrane *A* - Surface area of the membrane L_m - Membrane thickness C_{ma} concentration of the analyte on the surface of the membrane exposed to air $C_{ma} = KC_o$ *K* - Partition coefficient of the analyte between the air and the membrane C_0 - Concentration of the analyte in air near the external membrane surface C_{ms} - concentration of the analyte on the membrane surface in contact with the sorbent.
Definition of the calibration constant *k*	$k = \frac{L_d}{AD}$	$k = \frac{L_m}{DKA}$
TWA concentration determination	$C_0 = \frac{kM}{t}$	$C_0 = \frac{kM}{t}$

1.3.2 Passive water sampling

When sampling from aquatic environments, the barriers are usually made of polymers such as polyethylene, PDMS, polysulfone, regenerated cellulose, silicone-polycarbonate, cellulose acetate, polytetrafluoroethylene (PTFE), nylon, polypropylene, polyvinyl chloride, etc. The polymeric membranes form a physical barrier to water molecules. Porous materials are also used as barriers, in which case analyte transfer is controlled by diffusion through water in the pores or through air trapped in the pores. In contrast to air sampling, where adsorption-based sorbents are most often used, water sampling usually involves samplers with sorbents that trap analytes via partitioning. In such cases, the sorption material is not a zero sink, and the analytes can reach equilibrium within a few minutes to several weeks depending on the amount and sorption capacity of the sorbent used.

The passive sampler developed in this project is for application in air and soil-gas analysis; consequently, a review focused only on passive sampling technologies currently available for these two matrices will be presented here.

1.4 Literature review

The reviews related to passive sampling technology published over the last three-and-a-half decades make it possible to follow its development with relative ease (Table 1-2). Immediately after its introduction, the technology was primarily adopted for workplace exposure measurements; the first notable review of such application was perhaps the one by Saunders, published as early as 1981.[17] By 1984, samplers such as PRO-TEK (DuPont), Palmes (MDA), VaporGard (MSA), GASBADGE (National Mine Safety), and 3M's mercury, organic and carbon dioxide monitors had appeared on the market. In 1986, an international symposium was held in Luxemburg on diffusive sampling with emphasis on workplace air monitoring, which resulted in the publication of one of the most comprehensive literature collections on diffusive sampling at that time in the following year.[18] Even though the first passive sampler for waterborne pollutants was patented as early as 1980 by Aylott and Byrne,[19] the technology growth was slow until Södergren developed and reported the in-situ mimetic passive sampling device in 1987.[20] By 2000, several such samplers were being used all over the world. Górecki and Namieśnik reviewed the status of

the technology in 2002. This review included the passive sampler's applications in air, water and soil matrices, and by virtue of the definition adopted (stated earlier) it also included bio-monitoring as a type of passive sampling based on accumulation of organic pollutants in the tissue of living organisms. The number of books dedicated specifically to passive sampling techniques is small, though many general air sampling-related publications include a section on this technology. Brown et al. compiled books containing the proceedings of international symposia held in Luxembourg in 1990.[21] A book authored by Huckins et al. provided a comprehensive treatment on semipermeable membrane devices (SPMDs).[22] A general treatise on passive sampling for environmental applications by Greenwood et al. is a recent addition to the list of available books.[23]

Table 1-2: Passive sampling reviews since 1980 (based on ref. 1).

Author/s	Publication year	Emphasis	Reference
Saunders	1981	Workplace exposure measurements.	17
Fowler	1982	Theory and fundamentals of passive vapor sampling applied to both permeation through membrane and diffusion through static air. Also discussed the effects of temperature, pressure, face velocity and sampler response time.	24
Rose and Perkins	1982	State-of-the-art of the technology, practical aspects and various commercially available passive samplers at the time.	25
Namieśnik et al.	1984	Quantitative and statistical aspects of commercially available passive samplers applied to inorganic and organic gases and vapors.	15
Harper and Purnell	1987	Theory and practical evaluation of the performance of diffusive samplers with the emphasis on the geometry and sorbent efficiency.	26
Berlin, Brown and Saunders	1987	Collection of articles presented at international symposium on diffusive sampling in workplace air monitoring.	18
Brown	1993	Technical report on the use of diffusive sampling for monitoring ambient air.	27
Levin and Lindahl	1994	Application of diffusive sampling for reactive compounds.	28
Kozdroń-Zabiegała et al.	1995	Application of passive samplers for indoor and outdoor air applied to volatile organic compounds.	29
Brown	2000	Environmental factors affecting the performance of passive samplers in ambient air, and European Union initiatives towards standardization.	30
Kot et al.	2000	Long-term monitoring of environmental pollutants in aquatic environments using passive samplers.	31
Lu et al.	2000	Background and applications of semipermeable membrane devices.	32
Górecki and Namieśnik	2002	Application of passive samplers in air, water and soil analysis, as well as bio-monitoring.	2
Cox	2003	Forest exposure to ozone, nitrogen dioxide and sulphur dioxide along with some case studies.	33
Mayer	2003	Equilibrium passive sampling devices.	12
Stuer-Lauridsen	2005	Passive sampling technology for organic micro-pollutants in aquatic environments and mathematical equations required for prediction of the concentration of the analytes in aqueous media.	34
Namieśnik et al.	2005	Passive sampling techniques for environmental analysis with special emphasis on solid-phase microextraction (SPME) devices.	35
ITRC publication	2005	Passive sampler technologies for groundwater sampling.	36
Vrana et al.	2005	Passive sampling techniques for monitoring pollutants in water.	37
Partyka et al.	2007	Monitoring organic constituents in air with emphasis on analytical methods required for the release and quantification of the analytes from the sorption media.	38
Mills et al.	2007	Application of passive samplers for the monitoring of pharmaceutical and personal care products In the environment.	39

1.5 Passive air samplers

A number of passive samplers are available for sampling VOCs from air. Selected passive samplers, representative of the different designs, materials of construction and analytes, are summarized here. Among the passive samplers discussed, the SUMMA™ canisters and 3M™ OVM samplers were used in this project and will be also dealt with in Chapters 6 and 7.

1.5.1 SUMMA™ canisters

Sampling of VOCs from air with SUMMA™ canisters has been widely employed and is generally considered and marketed as a passive sampling technique. Examples of validated air sampling methods using SUMMA™ canisters include EPA methodsTO-14A[40] and TO-15.[41] These canisters are specially designed and deactivated using a proprietary passivation technique called the "SUMMA" process, in which a series of chemical deactivation and electropolishing steps render the inner surface of the canisters chemically inert. The canisters are available in spherical or cylindrical shapes, and with volumes typically between 1 L and 6 L.

A schematic of the sample collection and analysis method using a SUMMA™ canister is illustrated in Figure 1-8.[42] The canister is first evacuated, typically to <0.05 mm Hg, and the canister inlet is opened to allow the sample air to flow into the canister by virtue of the differential pressure.[41] SUMMA™ canisters can be used to collect grab samples, with a typical duration of 10 to 30 seconds, or time weighted average samples of typically 1 to 24 hour duration by using a flow-controlled inlet attached to the canister. Generally, either a mass flow controller or a critical orifice flow controller are used for this purpose. With a critical orifice for controlling the flow, a reduction in the flow rate occurs as the pressure inside the canister approaches atmospheric pressure. On the other hand, the flow rate can be maintained constant throughout the sampling period using mass flow controllers. An interesting improvement was successfully tested and reported in 2005 by Rossner and Ferrant.[43] They used the same principle, but with a flow rate of 0.05 mL/min to collect samples for periods from one week to several weeks long using a 6 liter SUMMA canister, making it possible to obtain TWA concentrations for longer periods of time than achieved

earlier by canister methods. However this technique is not commercialized or used widely by field personnel.

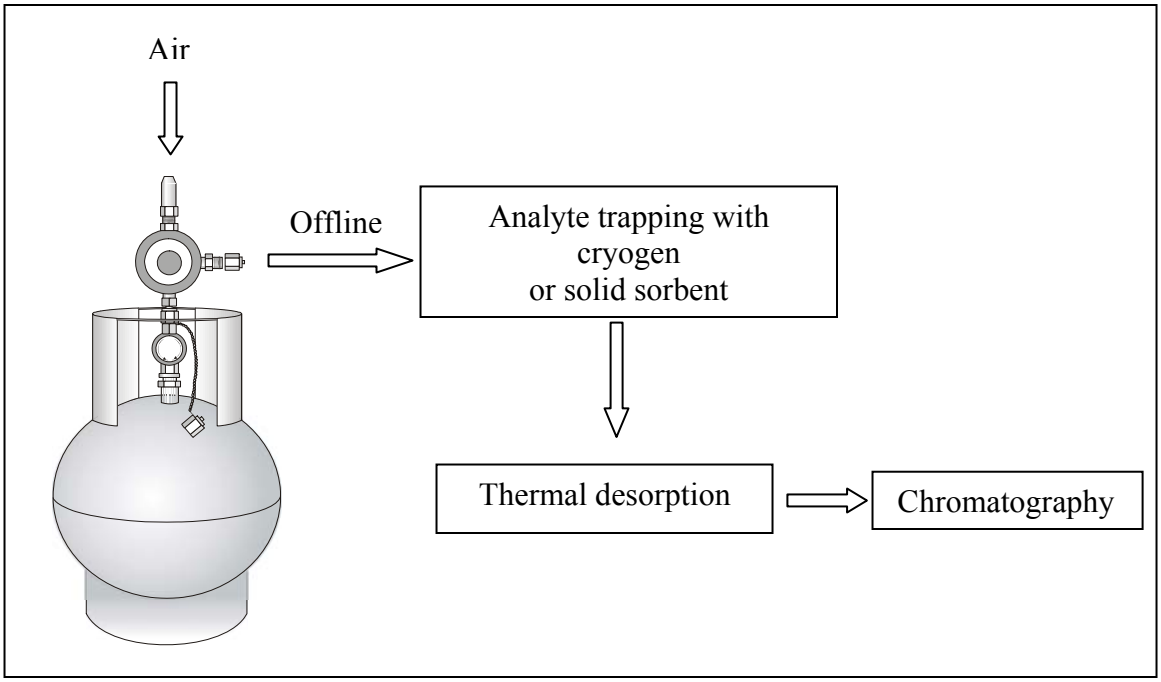

Figure 1-8: Schematic of EPA method TO-14 A and 15

Once the sample is collected in the canister, it is transported to the laboratory for analysis. Owing to inertness of the inner walls of the canisters, the samples can generally be stored in them for 14 to 30 days prior to the analysis without any significant decrease in analyte recovery. In the laboratory, the pressure in the canister is increased using zero-grade nitrogen as the diluent gas. After equilibration, this elevated pressure allows measured aliquots of the sample gas to be easily withdrawn for analysis. Analyte collection and pre-concentration from the diluted air sample in the canister is achieved through collection on thermally desorbable sorbent tubes or by using cryogenic techniques, followed by thermal desorption and gas chromatography. Method TO-14A utilizes chromatographic analysis with ECD or FID detectors, while method TO-15 utilizes chromatography combined with MS. Analyte concentrations in the range of parts per billion by volume can be easily determined using this method. The concentration of the analytes in the sampled air is then calculated based on the

initial pressure inside the canister before sampling, final pressure after sampling, and canister pressure after pressurization with zero grade nitrogen.

Analytical results obtained using SUMMA™ canisters are legally defensible and hence are routinely used for ambient air and indoor air applications where risk assessment is involved. Canisters have also found widespread use in soil gas sampling and analysis required for vapor intrusion monitoring. Such applications will be discussed in Chapters 6 and 7.

Even though SUMMA™ canisters have been found to be applicable to many areas, they have several significant disadvantages. Canister deployment, sample processing and analysis are more cumbersome with SUMMA™ canisters compared to most other passive samplers. The cost is relatively high (~$250 to $ 400$ per sample) as it includes canister rental, cleaning and certification, flow controller rental and cost of analysis. Further, the canisters are often considered obtrusive by occupants when used for indoor air sampling. Obtaining long term TWA concentration data (from 1 day to several weeks) from one canister is not currently possible with the commercially available SUMMA™ canisters.

1.5.2 3M™ Organic Vapor Monitor (OVM) 3500 sampler

OVM 3500 (Figure 1-9) is a diffusive-type passive sampler marketed by 3M Inc. (St. Paul, MN). Activated carbon-based material (160 mg), pressed to form a disc, is used as the sorbent in this sampler.[44] A thin microporous PTFE membrane (pore size 0.1 μm) serves as a wind screen.[45] The PTFE membrane and the sorbent disc are 1 cm apart, which defines the diffusion path for the analyte transport from the sample matrix to the sorbent. The cross-section area for diffusion is large at 7.07 cm^2. Once the sampling is completed, the sorbent is removed from the sampler and extracted with CS_2, followed by chromatographic analysis of the extract for quantification. Analyte uptake rate needs to be sufficiently high in order to sample enough analytes for quantification when the concentration is close to the regulatory limits. Because of the large cross section area and relatively short diffusion path length of the OVM samplers, the analyte uptake rates are high enough for use in routine 8 hour workplace exposure monitoring.

Figure 1-9: 3M™ OVM 3500 sampler (reproduced from ref. 46)

1.5.3 Solid-phase microextraction device

SPME device consists of a short fused silica fibre which is coated with an extracting phase (typically 1 cm long and 0.11 mm outer diameter).[47] The coated fibre is housed inside a stainless steel needle in such a way that it can be moved in and out of the needle for exposing the extraction phase to the sample matrix, as well as for introducing the fibre into a GC injector for thermal desorption and quantification of the extracted analytes. When the extraction phase is exposed to the sample matrix, the analytes are either adsorbed or absorbed, and the analyte uptake follows the profile as illustrated in Figure 1-3. The sampler is generally exposed for sufficient time for the analyte to equilibrate between the sampler and the extraction phase. The time to reach equilibrium is often on the order of a few minutes. Once the extraction is complete, the fibre is retracted into the stainless steel needle and then introduced into a GC injector using the needle as a guide. When the needle is in the injector, the fibre is exposed to the carrier gas flowing through the hot injector, which causes analyte desorption. The gas then carries the analytes into the GC column for separation and quantification. When the sample volume is large compared to the volume of the extraction phase, the amount of analyte (n) collected by the fibre at equilibrium is given by:

$$n = K_{fs} V_f C_0$$

where K_{fs} is the partition coefficient of the analyte between air and the extraction phase, V_f is the volume of the extraction phase and C_0 is the concentration of the analyte in air.

These devices are available commercially with many different extraction phases including PDMS, polyacrylate, PDMS/divinylbenzene, and Carboxen, and can be used in the extraction and analysis of different chemical species.

In conventional SPME sampling, analyte collection commences when the sorption material coated on the fibre is exposed to the sample matrix by pressing the plunger of the device and extending the fibre out of the metal needle housing of the device. As illustrated in Figure 1-10, the same fibre can be used for TWA concentration measurements by retracting the fibre into the metal housing so as to have a well defined diffusion distance for the analyte before it can be sorbed. Chen and Pawliszyn demonstrated the application of such a system for the analysis of VOCs in air.[48]

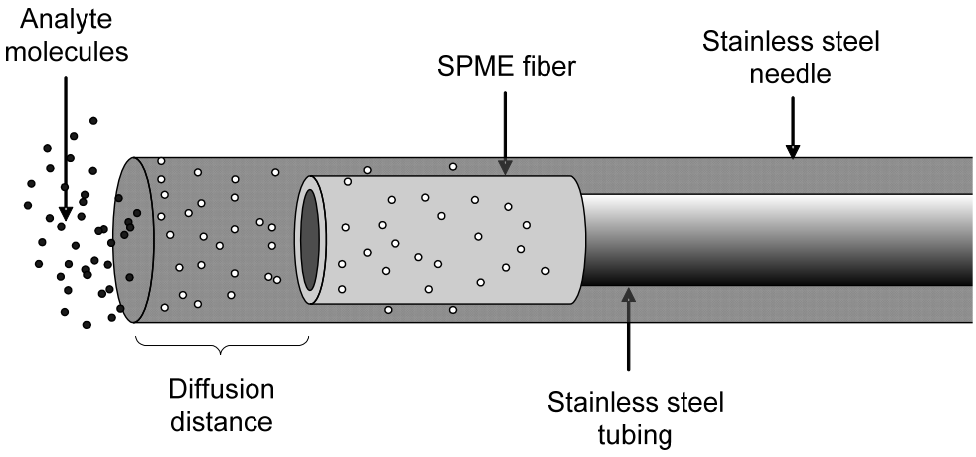

Figure 1-10: Solid-phase microextraction device used for TWA sampling (based on ref. 2).

1.5.4 Polyurethane foam passive sampler

Polyurethane foam (PUF) is routinely deployed as a sampling medium in classical active high-volume sampling devices.[49] Because of its advantageous properties, it has also been applied as a receiving phase in the form of PUF disks in diffusion type passive samplers.[50,51] Figure 1-11 shows the design of a typical PUF sampler. It consists of two stainless steel bowls connected with an external "S" metal clamp (not shown in the figure). The PUF

sorbent is placed in the bottom bowl with the help of a stainless steel support. The space between the two bowls and the openings in the bottom bowl provide air and analyte movement in and out of the arrangement. Shoeib et al. applied PUF disk passive samplers in the collection of perfluoroalkyl sulfonamides in indoor and outdoor air. The PUF disks (14 cm diameter, 1.35 cm thick) were suspended in a special chamber to prevent the deposition of coarse particles, as well as to eliminate ultraviolet radiation and minimize the effect of wind speed on the uptake in the case of outdoor applications. Because PUF has a high retention capacity for persistent organic pollutants (POPs) which are delivered by air movement, PUF disk passive samplers were applied by Shoeib et al. for the analysis of airborne POPs in Canada and Chile.[50,52,53] PUF disk passive samplers were also applied for the determination of PCBs across Europe.[54] Other examples include application of PUF passive samplers for polychlorinated naphthalenes (PCNs) and toxaphene,[55] polybrominated diphenyl ethers (PBDEs) and PCBs.[56]

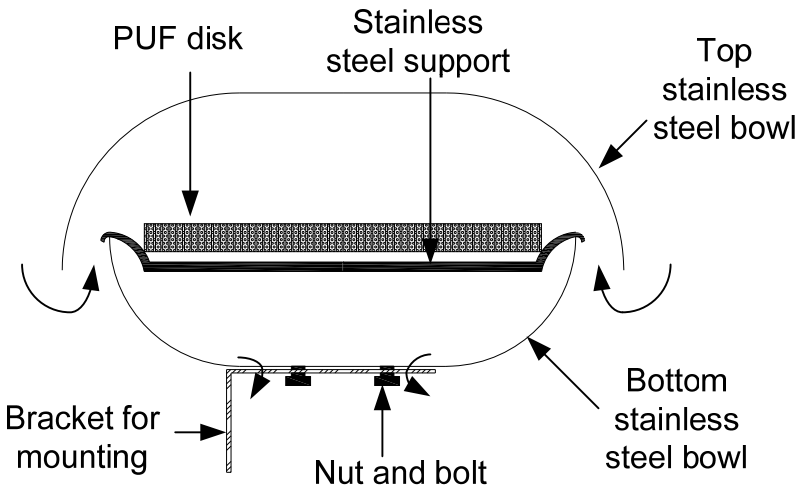

Figure 1-11: Design of a polyurethane foam diffusive sampler (based on ref. 57)

1.5.5 Other air samplers reported in literature

As depicted in Figures 1-2 and 1-3, passive samplers are composed of a barrier and a sorbent, and generally operate either in the kinetic or the equilibrium region. Table 1-3 provide details on various passive samplers used for sampling from air with these parameters in context, as well as information on the analytes for which specific passive samplers can be used.

Table 1-3: Diffusion/permeation barriers and receiving phases used in various passive samplers for the application in air (based on ref. 1).

Air sampling	Barrier type	Sorbent/receiving phase	Operation region	Analyte type	References
SUMMA canisters	None (flow regulated by various flow controlling devices)	None (electro-polished, evacuated canister)	Equilibrium	VOCs	41
Tristearin-coated fibreglass sheets	None	Tristearin on fibreglass cloth	Equilibrium	SVOCs	58
Polymer coated glass (POG)	None (sometimes partially enclosed in a stainless steel bowl)	Ethylene vinyl acetate (EVA) coated on a glass cylinder	Equilibrium	Persistent organic pollutants	59,60,61
Polyethylene-based passive sampling devices (PSD)	None	Low density polyethylene	Equilibrium	PAHs	62
XAD-2 resin-based sampler	None (stainless steel shelter)	XAD-2 resin (styrene-divinylbenzene)	Kinetic	Persistent organic pollutants	63
Palmes tube	Diffusion through static air in a tube	Stainless steel mesh impregnated with triethanolamine	Kinetic	NO, NO_2, SO_2	11,33,64
Reiszner-West badge	Permeation through silicone membrane	Sodium tetrachloromercurate	Kinetic	SO_2, CO	65,66,67,68
Willems badge	Diffusion through microporous PTFE and air	Citric acid, NaI/NaOH,	Kinetic	NH_3,NO_2	33,69,70
Developed by Yanigasawa-Nishimura	Diffusion through perforated polypropylene	Cellulose fibre filter paper containing triethanolamine	Kinetic	NO_2 and NO	71
OVM 3500,3520 (3M)	Diffusion through static air	Single or double adsorbent depending on the analyte(s)	Kinetic	VOCs	72,73,74
Perkin-Elmer tubes	Diffusion through static air in the tube	Various thermally desorbable sorbents depending on analytes	Kinetic	VOCs	75,76
Ogawa sampler	Diffusion through air channels in plastic material.	Various pre-coated collection pads	Kinetic	NH_3,NO_x,SO_2, O_3	77,78,79
Ferm Dosimeter	Badge-type, diffusion through air and with wind-shielded inlet	Impregnated filter, various chemicals depending on analyte	Kinetic	NH_3,NO_2,SO_2	80,81,82,83
TOPAS (Combined with thermal desorption system of Gerstel)	Diffusion through microporous PTFE	Tenax/Thermal desorption	Kinetic	VOCs (not suitable for highly polar compounds)	84
ORSA-5 (Dräeger)	Diffusion through static air in a tube on either side of the sorbent	Activated charcoal/solvent desorption	Kinetic	VOCs	85,86,87

Table 1-3 (continued): Diffusion/permeation barriers and receiving phases used in various passive samplers for the application in air (based on ref. 1).

Air sampling	Barrier type	Sorbent/receiving phase	Operation region	Analyte type	References
PRO-TEK, G-AA/G-BB (Dupont)	Diffusion through perforated plastic placed on either side of the sorbent strip	Activated carbon strip/solvent desorption	Kinetic	Most organic vapors	88,89
Analyst	Diffusion through stainless steel mesh and air cavity in the badge	Granular activated charcoal/solvent desorption	Kinetic	VOCs	90,91
Radiello	Diffusion through microporous polyethylene film and air	Carbograph 4 thermal desorption	Kinetic	VOCs	91,92
Gas Adsorbent Badges for Individual Exposure (GABIE) sampler	Diffusion through porous PUF windscreen and static air.	Activated carbon solvent desorption	Kinetic	VOCs	91,93
SKC 575 series of samplers	Diffusion through channels in plastic body (badge-type).	Activated charcoal, Anasorb 747®, Anasorb 727® solvent desorption	Kinetic	VOCs	94,95,96
SKC 590 series of samplers	Diffusion through channels in plastic body (badge-type).	Tenax, Carbopack-X thermal desorption	Kinetic	VOCs	97
Shibata gas-tube sampler	Porous PTFE tube	Granular activated carbon	Kinetic	VOCs	98
Namieśnik et al.	Permeation through PDMS membrane	Activated carbon	Kinetic	VOCs	99,100
Sep-pak Xposure DNPH cartridge	Diffusion through porous polyethylene filter and static air	2,4-dinitrophenylhydrazine-coated silica cartridge (Waters Sep-Pak XpoSure)	Kinetic	Selected aldehydes and ketones	101
GMD sampler (UMEx – 100)	Diffusion through channels drilled into polypropylene plate	Papers impregnated with various reagents for different analytes	Kinetic	Aldehydes, amines etc.	101,102,103
Seethapathy and Górecki	Permeation through PDMS	Activated carbon-based sorbents solvent desorption	Kinetic	VOCs	104
PUF sampler	Diffusion through air	Polyurethane foam (enclosed between stainless steel bowls)	Kinetic	VOCs and SVOCs	49,50,51,52,53,54,55,56, 105, 106, 107
Designed by Yamamoto et al.	Porous PTFE membrane (0.1 μm pore size)	Carbopack B (60-80 mesh)	Kinetic	VOCs	45
SPME	Diffusion through static air (SPME fibre retracted into the needle)	Various sorbents	Kinetic	VOCs	48
SPMD	Low density polyethylene. Historically, silicone, polypropylene and polyvinyl chloride have also been tried	Triolein	Kinetic, non linear, equilibrium	Non-polar hydrophobic compounds	22

1.6 Passive soil gas sampling

Compared to passive sampling techniques applied to air and aqueous matrices, the application to solid matrices (such as soil, sediment, and compost) has a relatively short history. Concentration of chemical species in soil gas is dependent on many variables, such as soil particle size and mineralogy, organic and moisture contents, temperature and overall heterogeneity of particle size and composition. As a result, most passive soil gas sampling applications are restricted to qualitative or screening purposes only, and few provide truly quantitative data. Sample spacing, sample collection depth, exposure period, etc., are key factors for both passive and active approaches. A detailed description of these factors has been provided by Morrison.[108] An adoption of these concepts can be found in a site assessment manual used in the USA.[109]

Passive soil gas samplers have been used for many purposes, including pollutant monitoring, soil gas/vapor survey in site assessment, evaluation of soil remediation performance, underground pipeline leak detection, soil/rock radiation detection, petroleum resource exploration, as well as soil fertility surveys.[110,111]. In these applications, sampling and measurement of chemicals of all kinds, such as VOCs, semi-volatile organic compounds (SVOCs), petrochemicals, non-aqueous-phase liquids (NAPL), pesticides, radon gas, explosives, carbon monoxide and nitrogen dioxide have been reported. Currently, GORE™ Module, PETREX sampler, SPMD, solid phase microextraction (SPME) and selected other samplers are used for soil gas sampling. A brief description and application of these soil gas sampling systems is provided in the following sections.

1.6.1 GORE™ modules

Since they were patented in 1992, GORE™ modules have been widely used for air, water and soil gas sampling applications.[23] These modules make use of expanded polytetrafluoroethylene (GORE-TEX®) membrane as the barrier material, and various proprietary polymeric and carbonaceous resin mixtures as adsorbents. The adsorbents are capable of trapping a wide variety of organic compounds including VOCs and SVOCs ranging from ethane (C_2) to phytane (C_{20}). The sorbent is enclosed by the GORE-TEX®

membrane and takes a flexible tubular form to which a support chord (also made of GORE-TEX®) is attached for installation and retrieval purposes. Because of the high surface tension of water and hydrophobic nature of the GORE-TEX membrane (with pore size of 0.2 μm), liquid water does not cross the membrane.[112] However, the membrane still allows water vapor to diffuse through it. The GORE-TEX™ membrane also protects the adsorbent from soil particles, enabling sensitive soil gas sampling. The GORE™ modules are generally installed inside 1-2 cm diameter holes drilled into the ground to a depth of typically 50-100 cm. After deployment, exposure and retrieval, the modules are transported to the laboratory for analysis. The modules are then analysed using thermal desorption-GC-MS.

The GORE™ module has been deployed in virtually all geological settings (from low permeability clays to high permeability sands) at all moisture levels (from dry to saturated soils) to detect VOCs and SVOCs. In a field test conducted by the United States Environmental Protection Agency (US-EPA) Environmental Technology Verification (ETV) program using GORE™ Module passive soil gas sampling system in 1997, its applicability was demonstrated at two sites: one composed primarily of clay soil, and the other composed primarily of medium to fine-grained sandy soil.[113] The results showed that the GORE™ method could detect VOCs (including vinyl chloride, cis 1,2-dichloroethylene (cis DCE), 1,1-dichloroethane, 1,1,1-trichloroethane (1,1,1 TCA), trichloroethylene (TCE) and tetrachloroethylene (PCE)) at lower concentrations in the subsurface than the reference active soil gas sampling method. However, at higher concentrations, the ratio between the mass of contaminant in soil gas detected using the GORE™ module and the concentration of contaminant in soil gas detected using the reference soil gas sampling method decreased. The authors suggested that sorbent saturation may have occurred at high concentrations. Monks et al. described the use of GORE™ modules consisting of chemical-specific organic compound-sensitive resins.[114] The samplers were inserted 3 feet into the ground inside predrilled holes for the determination of VOCs and SVOCs at a naval facility. The study demonstrated that the GORE™ module method could be used to determine the presence of both VOCs and SVOCs in the subsurface, whereas conventional active methods are limited mainly to VOC screening.

1.6.2 PETREX sampling system

The PETREX sampling system is a soil gas sampling technology developed by Northeast Research Institute (NERI). These samplers consist of two or three activated carbon adsorption elements fused to ferromagnetic wire collectors (to enable Curie point desorption) housed in a glass test tube. Soil gas samples are collected by unsealing the sampler and exposing the collector to the soil gas of the subsurface environment. Samplers are typically buried 30 to 45 cm (12 to 18 in.) deep with the open end down, and left in place from overnight to three weeks (two weeks is common). The method was originally developed for petroleum exploration and has been used for mapping trace levels of hydrocarbons diffusing from natural sources.[115] In recent years, the system has been adapted to the environmental field for the characterization of a wide range of VOCs and SVOCs such as chlorinated, aliphatic and aromatic compounds.

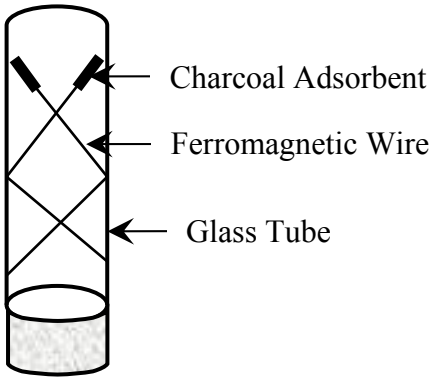

Figure 1-12: Design of a PETREX soil gas sampler (based on ref. 115)

The PETREX method is highly sensitive for the detection of very small concentrations of organics, allowing collection of semi-volatile hydrocarbons with detection limits as low as parts per trillion.[116] For this reason, the method is currently widely used for trace VOC and SVOC detection. Example applications of PETREX method for soil gas survey or site assessment are described by Anderson et al. and Gomes et al.[115,117] Final determination is often carried out by GC combined with mass spectrometry (GC-MS) for reliable identification of the analytes.

1.6.3 Semipermeable membrane devices

Huckins et al. introduced SPMDs in 1990 for the bioavailability studies of hydrophobic organic chemicals to aquatic organisms.[118] The sampler consists of a lay-flat LDPE tube (typical film thickness between 50 μm and 100 μm) filled with high purity triolein and sealed at both ends. Since both the membrane and the receiving phase are hydrophobic, SPMDs can be used only for hydrophobic contaminants, which are typically characterized by log *K*ow >3.[22] The samplers are available commercially with various sampling surface areas and different enclosure cages. A representative design of an SPMD rack is illustrated in Figure 1-13. Determination of low levels of contamination in a sample using SPMDs might require extensive cleanup procedures. SPMDs provide time-integrated concentrations for periods ranging from days to months, depending on the analyte concentration and deployment conditions. SPMDs have been used to determine the relationship between the partial pressure and mobility for monoaromatic and PAH contaminants in source area soils.[119] Caslavsky et al. performed soil sampling from a depth from 5 to 20 cm with SPMDs for the analysis of selected PAHs using liquid chromatography/time of flight mass spectrometry.[120] Lanno et al. used SPMDs to collect samples from soils for bioavailability screening of soils containing petroleum hydrocarbons (BPHs).[121] The results of the study showed the benefits of a screening methodology based on SPMD, including reduced reliance on the use of live test organisms and reduced cost of estimating the bioavailability of non-polar organic contaminants in soils.

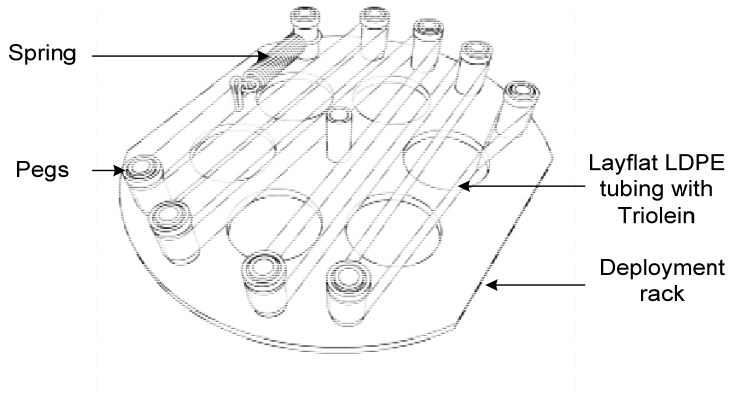

Figure 1-13: Design of a semipermeable membrane device in a deployment rack (based on ref. 122)

1.6.4 Solid-phase microextraction

SPME technique, as discussed in Section 1.5.3, is not only widely used for air and water sampling, but can also be applied to solid matrices.[123] There are three different extraction modes for SPME: direct, headspace and membrane,[124] among which headspace SPME is the most suitable for sampling from solid matrices. In this mode, the SPME fibre is placed in the air directly above the soil sample contained in a vial, and analytes partition from the sample matrix through the air to the fibre coating. The air in the vial serves as the barrier between the SPME fibre and the sample matrix, thus preventing the fibre from potentially being contaminated by the interferences in the sample medium. Headspace SPME was introduced by Zhang and Pawliszyn to extend the SPME technique to more complex samples which contain solid or high molecular weight materials, such as soil and sludge.[125]

1.6.5 Other samplers reported in literature

Polyethylene membrane vapor-diffusion (PVD) sampler is made from 20 or 40 mL glass crimp-top or volatile organic analysis (VOA) vials. The empty vials are uncapped and wrapped with two layers of low density polyethylene (LDPE) sheets.[126] When the samplers are exposed to soil gas, analyte equilibration occurs between the soil gas matrix and the air trapped inside the vial. Once the equilibration process is complete, the samplers are capped and returned to the laboratory for analysis. The PVD samplers were used as passive soil gas samplers in the unsaturated zone at a petroleum tank farm for the detection of toluene.[127] Based on this study, PVD samplers were found effective in the vadose zone.

EMFLUX® passive soil gas sampling system consists of a 7 mL, screw-top, glass vial with a plastic sampling cap. The cap has a hole in it covered with a fine-mesh screen to allow for analyte diffusion into the glass vial. A cartridge containing 100 mg of a hydrophobic, thermally desorbable adsorbent placed inside the vial serves as the sorbent for trapping SVOCs and VOCs in the vapor phase. A retrieval wire is connected to the sampler's mouth and the vial is inserted upside down into a 2 cm wide and 10 cm deep core hole drilled into the soil matrix. The soil is then collapsed onto the sampler and the sampler is allowed to collect analyte vapors for a predetermined amount of time. After sampling, the sampler is removed from the soil, and the adsorbent cartridge is analyzed by thermal desorption/GC-MS

method. The application of EMFLUX® samplers for soil gas analysis of VOCs and SVOCs was tested as part of the US EPA's Environment Technology Verification Program and was found to be applicable in clay and sandy soil matrices and provided positive identification and semi-quantitative concentrations of target VOCs at the contaminated site.[128] The EMFLUX® sampling system has been used at mixed waste landfill,[129] city schools in Memphis,[130] and sewer locations[131] among others.

1.7 Effect of environmental parameters

Even though passive sampling has been widely used and recognized as a valuable tool in environmental monitoring, the reliability of this technique under varying environmental conditions has always been a subject of controversy. This is because the theoretical treatment using Fick's laws of diffusion is based on the assumption that steady-state conditions apply to passive samplers. In reality, the concentration profile and the analyte flux across the membrane at a particular instant during sampling is a function of many variables, including temperature, atmospheric pressure, fluid velocity at the sampler face, sorbent effectiveness, analyte concentration in air, humidity, etc. The potential dependence of the results on such a large number of factors is the reason for the National Institute of Safety and Health (NIOSH) to accept results with an accuracy of ± 25 % and a bias of ± 10 % for passive sampler applications in air. In addition, passive samplers have to be validated by comparing their performance with active sampling conducted in parallel. The major factors affecting these parameters are discussed below, keeping both diffusive-type and permeation-type passive samplers in context.

1.7.1 Temperature

Temperature plays an important role in determining the uptake rate of a sampler and is an important factor in the validation of passive samplers. In the case of air sampling, molecular diffusion coefficients in air increase with temperature, which results in increased uptake rates of the analytes. The increase can be easily estimated, as the change in the rate of molecular diffusion with temperature is well explained by the kinetic theory of gases. According to this theory, diffusion coefficient varies as $T^{3/2}$ (K) and is inversely proportional to pressure. In practice, the uptake rate has been found to vary approximately by 0.2-0.4% per K.[30]

Nevertheless, knowledge of temperature variations is often required to apply the necessary corrections to the uptake rate of diffusive samplers.

Temperature dependence of permeability through polymers is determined by both the diffusion coefficient of the molecule in the polymer, and its partition coefficient between air and the polymer. For polymers such as PDMS, the diffusion coefficient of a molecule in the polymer increases with temperature, while the partition coefficient decreases. This trade-off results in permeability being generally a weak function of temperature. On the other hand, for polymers such as PTFE and polyethylene, permeability is found to increase with increasing temperature.[132,133]

1.7.2 Pressure

The diffusion coefficient of molecules in air is inversely proportional to pressure, hence pressure variations must be known accurately for accurate sampling rate corrections. While the effect of pressure for sampling from air has been discussed,[30] to the best of our knowledge no studies have been done so far for sampling from aqueous matrices. However, Booij et al.[134] reported the use of SPMDs, low-density polyethylene (LDPE) strip samplers and PDMS strip samplers in the sea at depths up to 5 km (hence under very high pressures) for 1 to 1.5 years without any specific problems.

1.7.3 Face velocity

When the sampler is collecting analytes from the sample matrix, there exists a region in the immediate vicinity of the sampler where the analyte concentration is lower than that in the sample matrix away from the sampler. The presence of such a region of depleted analyte concentration and its extent are both a function of the air flow pattern around the sampler. These effects are often studied by determining the uptake rates as a function of linear flow velocity of air across the surface of the sampler. Hori and Tanaka reported that for 3M™ OVM 3500 diffusive-type passive sampler, the uptake rate did not change from 0.5 m s^{-1} to 2.0 m s^{-1} but the uptake was substantially lower when the face velocity of air was zero.[80] Such effects can theoretically be discussed based on the concept of boundary layer effect, which is presented in detail in Chapter 2.

Positive bias often occurs when the air flow pattern around the sampler substantially alters the diffusion path distance in diffusive-type passive samplers, or causes advective uptake via turbulence. Hori and Tanaka found that for Pro-tek, G-AA Gasbadge passive sampler (See Table 1-4 for more information on the sampler), the concentration determined was twice the actual concentration when the face velocity of air was 2.0 m s^{-1}. This could be attributed to the effective reduction in the diffusion path distance. However, such effects can often be reduced using a wind shield, such as that for 3M™ OVM 3500 sampler discussed earlier. Permeation-type samplers are in principle immune to high air flow velocities or turbulent air flow around the sampler because permeation through the membrane (the rate limiting step) remains largely unaltered.

1.7.4 Sorbent strength, analyte concentration and humidity

For sampling VOCs from air, adsorbents are most often used. Adsorbents have finite sorption capacity for chemical species depending on their surface characteristics such as polarity, molecular weight, temperature, surface area, and porosity.[135] When the sampler is exposed to the sample matrix, the adsorbent at first functions in the linear isotherm region (similar to the kinetic region in the profile shown in Figure 1-3).[5] When a critical number of adsorption sites have been occupied by the sorbed molecules (the analyte and any matrix component undergoing sorption, usually including water), the sorbent can no longer maintain a zero analyte concentration at the sorbent-barrier interface of the sampler. This alters the uptake rate of the analytes depending on the competitive sorption properties (competition between different chemical species for the same adsorption site on the sorbent) of the sorbent and the analytes. Such non-ideal functioning of the adsorbents is generally observed when the concentration of the analyte and/or other co-adsorbed matrix components (including water vapor) is high, or when the exposure time of the sampler to the sample matrix is long. For example, it was found with a tube-type Perkin-Elmer diffusion sampler that an average uptake rate of benzene for a two week exposure was 20% lower than the average of two one week exposures.[136] Another study with a radial diffusive sampler and thermal desorption technique showed that the uptake of benzene decreased with increased exposure time.[137] The situation is particularly complicated when using thermally desorbable sorbents, since they have to be strong enough to maintain practically zero concentration of the analyte at the

sorbent-sample interface, while at the same time weak enough at higher temperatures to enable thermal desorption of the analytes.

The analytical recovery of pollutants from the samplers was also found to be dependent on the analyte concentration and the type of adsorbent used. In some cases, desorption efficiency has been found to vary by more than 20% depending on the analyte concentration.[138,139] Overall, proper choice of the sorbent is a key factor in both diffusive and permeation-type sampling.

Humidity has a negligible effect on the diffusion coefficients of the analytes in air, and consequently does not alter the transport kinetics of diffusive-type samplers as long as there is no moisture condensation in the diffusion path. Analyte concentration also has no effect on the diffusivity of the molecules in air. In the case of permeation passive samplers, non-ideal concentration gradients in the membrane theoretically might occur due to concentration-dependent diffusivity and solubility in the polymer. It should be pointed out, though, that this scenario is highly unlikely in practice when applied to passive samplers because such effects occur only at very high analyte concentrations, not typically encountered in indoor or ambient air.

The effects of various environmental parameters and sorbent characteristics are summarized in Table 1-4. Due to the dependence of the passive samplers operation on various parameters, their performance needs to be evaluated thoroughly with regard to analytical recovery, sampling capacity and uptake rate, reverse diffusion, storage stability, effects of temperature and fluid flow across the sampler, accuracy and precision, shelf life, and the effect of humidity on sampling from air. The uptake kinetics of passive samplers while sampling from water is also a function of the bioorganisms growth on the sampling surface of the passive sampler (biofouling). For samplers such as SPMD, a 1.4 to 3.3 fold reduction in the uptake rates has been reported.[140] Methods including dipping the SPMD in various chemical mixtures (either initially or intermittently during exposure) and constructing cages made of different metals to discourage organism growth have been researched.[141,142]

Table 1-4: Effect of environmental parameters and sorbent characteristics for diffusive- and permeation-type passive samplers

Effect of:	Air Sampling	
	Diffusive-type	Permeation-type
Temperature	Defined by diffusion coefficient as a function of temperature based on kinetic theory of gases.	Defined by permeability as a function of temperature based on Arrhenius-type relationships.
Atmospheric pressure	Defined by diffusion coefficient as a function of pressure based on kinetic theory of gases.	Unaffected as permeability does not depend on atmospheric pressure
Face velocity	Variable; depending on the sampler geometry. Worst for tube-type-samplers, moderate for porous material barriers	Insignificant at moderate and high face velocities, but potentially significant at low face velocity
Sorbent strength	Strong sorbents are typically used under kinetic uptake regime	Strong sorbents are typically used under kinetic uptake regime
Analyte concentration	Unaffected	Sorption and diffusion coefficients in the polymer might change at very high analyte concentrations resulting in variable uptake rates
Humidity	Can saturate the sorbent early, especially with adsorption based sorbents	Unaffected with hydrophobic membranes like PDMS

The uptake rate variations due to the effect of changing environmental parameters led to the development of performance reference compounds (PRCs) for correcting such errors. PRCs and their applicability are discussed in the next section.

1.8 Performance reference compounds

Uptake rates of samplers towards various analytes are often determined in the laboratory under known conditions of temperature, flow velocity around the sampler and without biofouling (in the case of aquatic sampling). However, such conditions are rarely

encountered when the samplers are deployed in the field, resulting in non-ideal uptake rates. Researchers have at times resorted to computational fluid dynamics modeling to understand the flow patterns around the sampler face, which can enable proper sampler design to eliminate or reduce such environmental effects. Thomas et al. performed one such computational study on two passive sampler designs based on PUF for sampling PCBs, PAHs, and pesticides ('flying-saucer' and the 'open-bowl' samplers).[143] To correct for the non-ideality, PRCs can also be used and are gaining importance. PRCs are compounds that are added to the extraction phase of the passive sampler prior to sampling and dissipate into the sample matrix at a rate depending on the same environmental factors that affect the uptake rates of the analytes. Therefore, the loss of PRCs helps quantify the uptake rate of target compounds from the matrix being sampled. An essential condition is that PRCs should have properties (such as diffusion coefficients in the boundary layer and polymer membrane and solubility in the polymer) as close as possible to the target analyte(s), and should not be present in the sample. An ideal PRC is an isotopic analog of the target analyte. Depending on the passive sampler design, the dissipation rate (also called depuration rate) is related to the uptake rate and provides a method to estimate the uptake rate "in-situ". An essential condition for using PRCs with a particular passive sampler is that the sorbent in the sampler should have sorption strength low enough for depuration of the PRC into the sample matrix when exposed, and that the PRCs exhibit isokinetic exchange. This rules out the use of PRCs for sorbents involving adsorption such as activated carbon, but allows for their use in devices such as SPME and SPMD, where analyte partitioning is involved. Examples of application of PRCs can be found in references 144 to153.

Chen et al. described the theory of PRCs as applied to SPME, demonstrating their applicability to sampling BTEX from water and predicting the potential application to other microextraction techniques, such as micro liquid-phase extraction (MLPE), membrane extraction and headspace extraction.[154] Bartkow et al. showed the potential applicability of the technique to the polyethylene-based passive sampling device (PSD) for the analysis of PAHs from air using wind tunnel experiments to generate a wide range of air flow velocities across the samplers.[155] Tuduri et al. touched on the applicability of depuration compounds for polyurethane foam (PUF) disk-based samplers.[156] Harner et al. showed the applicability of depuration compounds in their study using PUF samplers to determine the concentrations of

polychlorinated naphthalenes in Great Lakes air.[157] With growing scientific interest in the use of PRCs, perhaps future passive sampling designs should incorporate this concept whenever possible for accurate analyte concentration determination in the field.

1.9 Passive sampling and regulatory guidelines/protocols

Passive sampling technology has been widely accepted throughout the world for environmental sampling, as evidenced by many regulatory guidelines, manuals and protocols published by various environmental and standards authorities throughout the world. The contributing organizations include the US-EPA, NIOSH, American Society for Testing and Materials (ASTM), Health and Safety Executive (HSE), Occupational Health and Safety Administration (OSHA), International Organization for Standardization (ISO), Comitée Européen de Normalisation (CEN), Interstate Technology and Regulatory Council (ITRC), etc. Any new research and development of passive samplers should be aimed at satisfying the minimum performance criteria required by the various protocols developed so far. As noted by Harper, before the advent of the validation and evaluation protocols for diffusive samplers, their usage resulted in disappointing performance.[96] In 1983, HSE's method MDHS-27 was introduced to address these issues and assess the performance of the diffusive samplers prior to their use.[158,159] Brown et al. examined this protocol with emphasis on three important factors: determination of the accuracy of the standard test atmospheres used for the calibration of the diffusive samplers, field testing and acceptance criteria.[160] This was followed by a presentation on the successful applicability of the protocol during the Luxembourg Diffusive Sampling Symposium in 1986.[161] Also during the same symposium, Cassinelli et al. presented the details of the protocol developed at NIOSH for the evaluation of the passive monitors, in which the acceptance criteria were fixed at ±25% accuracy and ±10% difference at 95% confidence interval.[162] In his review in 1993, however, Brown noted that most of the protocols at that time were for workplace exposure measurement and that no formal validation protocol for environmental application of passive samplers was available (notwithstanding the application of certain general principles of HSE MDHS 27, NIOSH manual of analytical methods[163] and CEN's prEN 838 available at that time). Since then, and within two decades of the invention of the passive samplers, various guidelines and protocols

have been published with extensive collaboration between various organizations and with common and/or interrelated protocols and guidelines.

The HSE publication MDHS 27 contains the protocol for assessing the performance of diffusive samplers.[164] MDHS 80 describes a method for the quantification of VOCs in air using diffusive sampling with tube-type samplers and solid sorbents, followed by thermal desorption/GC for quantification.[165] MDHS 88 describes a method for VOC analysis with diffusive samplers using solvent desorption from the sorbent followed by gas chromatographic determination.[166] The ISO guidelines for passive diffusive sampling followed by solvent desorption for VOCs in workplace atmospheres are included in ISO 16200-2.[167] For diffusive sampling as applied to ambient, indoor and workplace atmospheres utilizing thermal desorption instead of solvent desorption, the method guidelines are described in ISO 16017-2.[168] ASTM suggests the diffusive samplers to be evaluated according to ASTM method D 6246-02, which includes an essential requirement to estimate the sampler accuracy under actual conditions of use and differentiates correctable bias (arising due to a difference in pressure) and non-correctable bias against NIOSH's requirement of less than 10% of the latter.[169] ASTM 4597-03 deals with diffusive sampling in workplace atmospheres using solid sorbents;[170] ASTM 4598 (now withdrawn) dealt with the same problem, but with liquid sorbents,[171] and D 4599-03 deals with standard practices with length-of-stain dosimeters for the time-weighted average concentration determination of toxic gases and vapors.[172] ASTM also came up with guidelines for properly placing the samplers in indoor air (while sampling for gases and vapors) in method D6306-98.[173] As applied to workplace atmospheres, EN 482:1994 developed by CEN provides general requirements for the performance of measuring methods and requires a measurement uncertainty of less than 30% (compared to NIOSH's ± 25%) in most cases.[174] Its subsidiary protocol EN 838 describes the requirements and test methods specific to diffusive sampling.[175] As applied to ambient air quality measurements, the general requirements for quantifying gases and vapors are elaborated in EN 13528-5;[176] specific requirements and test methods are described in EN 13528-2,[177] and the guide to passive samplers selection, use and maintenance is contained in EN 13528-3.[178] It is interesting to note that few such protocols are available for sampling of analytes from soil and water. In early 2004, ITRC published guidelines for using the widely used PDB samplers for analyzing VOCs in water.[179] A

comprehensive publication of ITRC in 2005 with an overview of twelve widely used passive samplers for the monitoring of various analytes in water (mostly ground water application) dealt with several aspects, including working principle, cost, applications, deployment, and regulatory guidance.[36] In early 2007, ITRC published a protocol for the use of 5 commonly used diffusive samplers for contaminant monitoring in groundwater, including the GORE™ module, hydrasleeve, snap sampler, regenerated-cellulose dialysis membrane sampler and rigid porous polyethylene sampler.[180] All these numerous regulatory guidelines and protocols available for the practitioners in the field of air sampling have resulted in a wider acceptance of the passive sampling technology.

1.10 Summary

Passive sampling technology is more advantageous compared to traditional active/grab sampling techniques due to its low cost, low maintenance requirements, unattended operation and independence from power sources. The accuracy of the passive sampling technology is generally considered to be on par with traditional techniques, but in practice depends on various factors such as environmental conditions affecting the uptake rates and the accuracy of the determination of the uptake rates in the laboratory. Nevertheless, for many applications including long-term monitoring to determine TWA concentrations, only passive sampling techniques can be practically used. Furthermore, it is impractical to use the expensive and often complicated traditional techniques when simultaneous large area monitoring at multiple locations is called for. Passive samplers are cheap, smaller and easy to hide when compared to SUMMA™ canisters. The chance of vandalism is therefore smaller and losses are minimal when it happens.

An important issue with the performance of passive samplers is the sampling rate variations when environmental conditions considerably deviate from the laboratory conditions under which the sampling rate was determined. To address these issues, performance reference compounds were proposed, and their applicability as demonstrated to date seems very encouraging.

Passive sampling technology has some disadvantages, such as unsuitability for the determination of short-term pollutant variations and difficulty with automation. The single

biggest disadvantage of the passive sampling technology is the long time required for calibration in the laboratory. The calibration procedure generally involves the generation of a standard gas mixture, exposure of the sampler to this controlled atmosphere, and quantification of the analytes trapped in the sampler. The uptake rate (expressed as the calibration constant) can be obtained from the knowledge of the concentration of the analyte generated, the exposure time, and the amount of analyte trapped in the sampler. At sites where a complicated mixture of pollutants is present (e.g. gasoline range of compounds), it becomes practically impossible to calibrate the samplers for each and every pollutant. This creates an enormous burden on the time required for the calibration of the passive samplers.

Passive sampling technology today is well developed and applicable to various areas, including workplace exposure, indoor and outdoor air quality determination, aquatic sampling for ground and surface water pollution, and sediment and soil pollution monitoring, to name a few. Groundwater remediation is another important area where passive samplers are regularly used for the monitoring of the remaining pollution levels. In the past decade, vapor intrusion into indoor dwellings started receiving considerable attention. The modeling of this process requires pollution data from surface and subsurface water/aquifer, soil, as well as outdoor and indoor air. Passive sampling is playing an increasingly important role in such vapor intrusion studies. These applications have been fueled by the availability of various regulatory guidelines and protocols for the selection, deployment and interpretation of data acquired using the different samplers available on the market today, complemented by growing acceptance of the technology by the regulatory agencies.

1.11 Scope of the thesis

1. Design a sampler which has the potential to function better than currently existing samplers with regards to the effects of humidity, temperature, and linear flow velocity of air across the sampler surface. The sampler design should be inexpensive, make it amenable to automation, and lead to reduced sample preparation steps in the analytical procedure. The design aspects of the sampler are dealt with in Chapter 3.
2. Determine the calibration constants of model compounds and develop models to estimate the calibration constants based on the physicochemical properties of the analytes. The

analytes used for the study included environmentally important compounds such as BTEX, chlorinated methanes, ethanes and ethenes, as well as n-alkanes, esters and alcohols. The developed model should make it possible to deploy the samplers in the field without prior knowledge of the analyte identity. This aspect is covered in Chapter 3 of the thesis.

3. Determine the fundamental transport properties of PDMS towards various analytes. The transport properties studied were the diffusion coefficient, energy of activation of permeation, and permeability of PDMS towards various analytes. Determination of such fundamental properties would be important scientific information for similar analytical sampler preparation/introduction techniques such as PDMS membrane extraction with a sorbent interface (MESI), PDMS thin film extraction and PDMS membrane inlet mass spectrometry (MIMS).[181,182] This is dealt with in Chapter 3 and partly in Chapter 4.

4. Determine the effects of temperature, humidity, linear flow velocity, sampler geometry, concentration and time period of exposure on the uptake rates of the samplers. These parameters form an important part of the validation process of passive samplers and are dealt with in Chapters 4 and 5 of the thesis.

5. Perform field sampling and analysis to confirm applicability of the samplers under real world conditions. Field sampling involved indoor air, outdoor air, and soil-gas (including sub-slab gas) matrices.

An important goal of the thesis has been to balance the research work between the following three ideas:

1. Detailed research on the calibration aspects, functioning and specific advantages and disadvantages of the sampler designed in the laboratory.

2. Obtaining research data for general use in techniques other than the specific type of passive sampler developed in the process. This in most part involved determining the fundamental transport properties of the PDMS membrane.

3. Performing field sampling and analysis and laying groundwork for the future of the passive sampling technology developed within the project for routine use in the field.

CHAPTER 2

Theory

In this Chapter, the theoretical aspects of the uptake kinetics of the sampler developed in this project will be discussed. A hypothesis will be presented to correlate the uptake kinetics of the sampler to the physicochemical properties of the analytes. The need for such a hypothesis will be discussed and the hypothesis testing will be presented in Chapter 3.

In the case of permeation-type samplers, the idealized concentration profile of the permeating vapor in and around the sampler during deployment is shown in Figure 2-1. As discussed in Chapter 1, the analyte transfer from the sample into the sorbent in the sampler (through the polymer membrane) involves three steps: dissolution of the vapor molecules, diffusion of the molecules through the membrane material under a concentration gradient, and the release of the vapor from the polymer at the opposite side of the membrane.

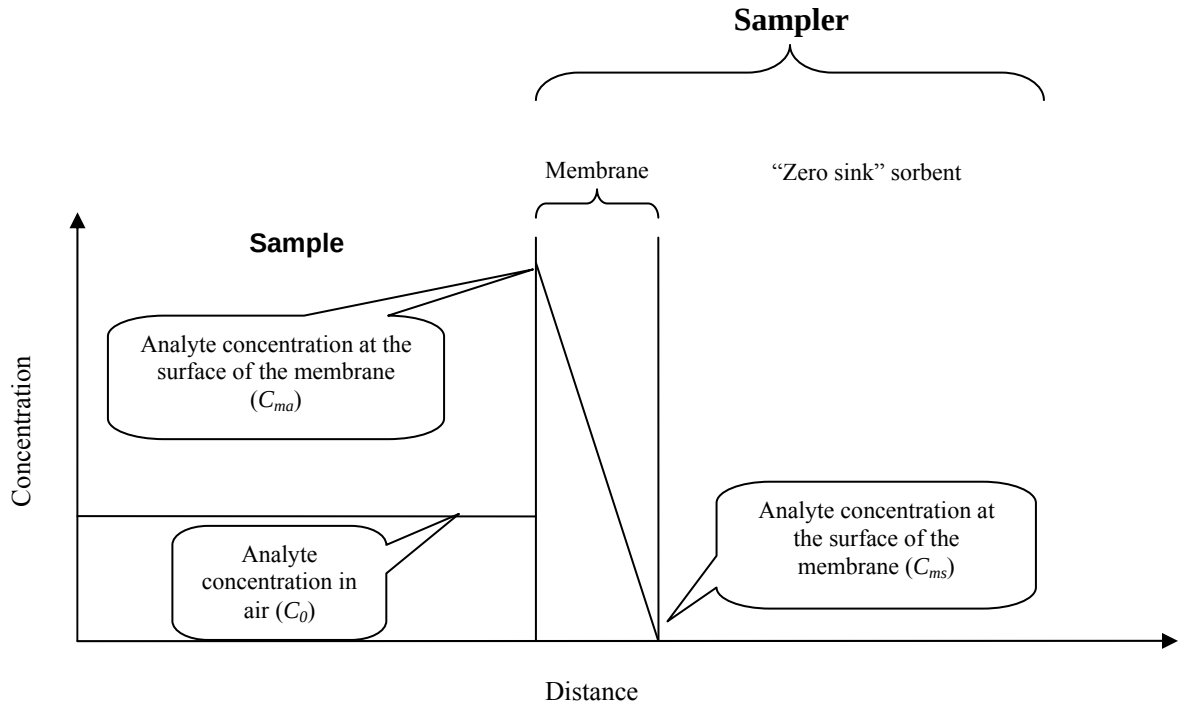

Figure 2-1: Ideal concentration profile for permeation passive samplers during deployment

Applying Fick's law to permeation-type passive samplers, the amount of analyte M (kg) collected in time t (min) by the sampler is given by

$$\left(\frac{M}{t}\right) = D\frac{A}{L_m}\left(C_{ma} - C_{ms}\right) \tag{2.1}$$

where D is the diffusion coefficient of the analyte in the membrane (cm^2/min), A is the surface area of the membrane (cm^2), L_m is the membrane thickness (cm), C_{ma} is the concentration of the analyte on the surface of the membrane exposed to air (kg/cm^3), and C_{ms} is the concentration of the analyte on the membrane surface in contact with the sorbent (kg/cm^3). The concentration of the analyte at the membrane-sorbent interface is practically zero due to removal of the analyte from the gas phase by the sorbent, hence C_{ms} is approximately zero. At a given temperature, the concentration of the analyte on the membrane surface exposed to the air is related to the concentration of the analyte in air by the following relationship:

$$C_{ma} = KC_0 \tag{2.2}$$

where K (dimensionless) is the partition coefficient of the analyte between the air and the membrane. Under the conditions of constant temperature, the diffusion coefficient, partition coefficient, as well as membrane area and thickness are all constant and can be replaced by a new constant, k.

$$k = \frac{L_m}{DKA} \tag{2.3}$$

where k is the calibration constant of the passive sampler. The product of the analyte's diffusion coefficient D in the membrane and its partition coefficient K is defined as the permeability of the polymer (P, $cm^2\ min^{-1}$) towards that particular analyte, and defines the relative calibration constants of the passive sampler towards various analytes. From equations (2.1), (2.2) and (2.3), one can calculate the concentration of the analyte (C_0) in the sample when the amount collected by the sampler is experimentally determined and the exposure duration (t) is known.

$$C_0 = \frac{kM}{t} \tag{2.4}$$

By definition, as per equation (2.3), the calibration constant k for permeation-type passive samplers depends on the geometry of the sampler and the permeability of the polymer (PDMS in the case of the sampler used in this project) towards the particular analyte. Membrane area and thickness can be adjusted if needed to increase or decrease the calibration constant.

In the field of passive sampling, the inverse of the calibration constant (k^{-1}) is often referred to as either the "uptake rate" or "sampling rate" of the sampler for a particular analyte. The advantage of using uptake or sampling rate is that the unit is mL/min (volume/time in general). This essentially is similar to active sampling techniques using sorption tubes, where the analytes are collected onto the sorbent from a fixed volume of air flowing through the tube, except that with passive samplers a given analyte mass is taken up via diffusion from an equivalent volume of gas. The term calibration constant will be mostly used in this thesis for mathematical convenience, and the term uptake rate will be used wherever it is thought to be more appropriate.

The fundamental prerequisite for a passive sampler to be used in the field is the need for calibration prior to its application. Determination of the calibration constant involves generating a standard test gas atmosphere with a precisely known and controlled analyte concentration (C_0), exposing the sampler for a predetermined time period (t) followed by determining the analyte mass (M) trapped by the sorbent using a chromatographic method. The calibration constant is then determined using equation (2.4). This is generally a time-consuming and laborious process.

2.1 Non-ideal conditions

The above method for the determination of the calibration constant and its relation to analyte concentration in air (C_0) and mass collected (M) in time t is based on the assumption that the rate of supply of the analytes to the outer surface of the membrane exceeds the uptake rate (i.e. no starvation of the analytes occurs near the external membrane surface). In addition, it

is assumed that the sorbent acts as a zero sink throughout the exposure period, and that temperature, pressure and concentration all remain constant. Such ideal conditions are not often encountered in practice. The experimentally determined variations in the calibration constants with changes in environmental parameters such as temperature, humidity and linear flow velocity of air across the surface of the sampler will be dealt with in Chapter 4. A brief theoretical treatment of the concepts of boundary layer and residence time, as well as their role in non-ideal functioning of the sampler, are provided in the next two sections.

2.1.1 Boundary layer width

Irrespective of whether the sampler application is for airborne, aqueous or soil pollutants, the function of the barrier in the passive sampler is to define the rate of analyte uptake into the sampler. However, if the air flow velocity is not sufficient to supply analytes to the sampling surface faster than they are taken up by the sampler, there will always exist a region around the sampler where the analyte concentration is lower than the concentration of the analyte in the sample matrix away from the sampler. This region of depleted analyte concentration is called the boundary layer and plays a significant role in affecting the uptake rate of the sampler towards various analytes, especially when the fluid flow across the sampler face is low.[22] The reduced uptake rate results in a negative bias in the concentration determined using the passive sampler. The process can be explained based on the boundary layer model as applied to extraction techniques in analytical chemistry as follows.[183]

According to the boundary layer model, for a defined convection in the sample, a width δ, called the boundary layer thickness, can be assigned to each analyte (Figure 2-2). The model then assumes that the analyte transport within this layer is controlled solely by the specific analyte's diffusion coefficient in air. The boundary layer "region", in a strict sense, is however considered as a region where the analyte transport is progressively more dependent on diffusion alone when moving from the bulk of the sample towards the surface of the membrane. The position δ is where the effect of convection becomes the same as the effect of diffusion of the analyte.

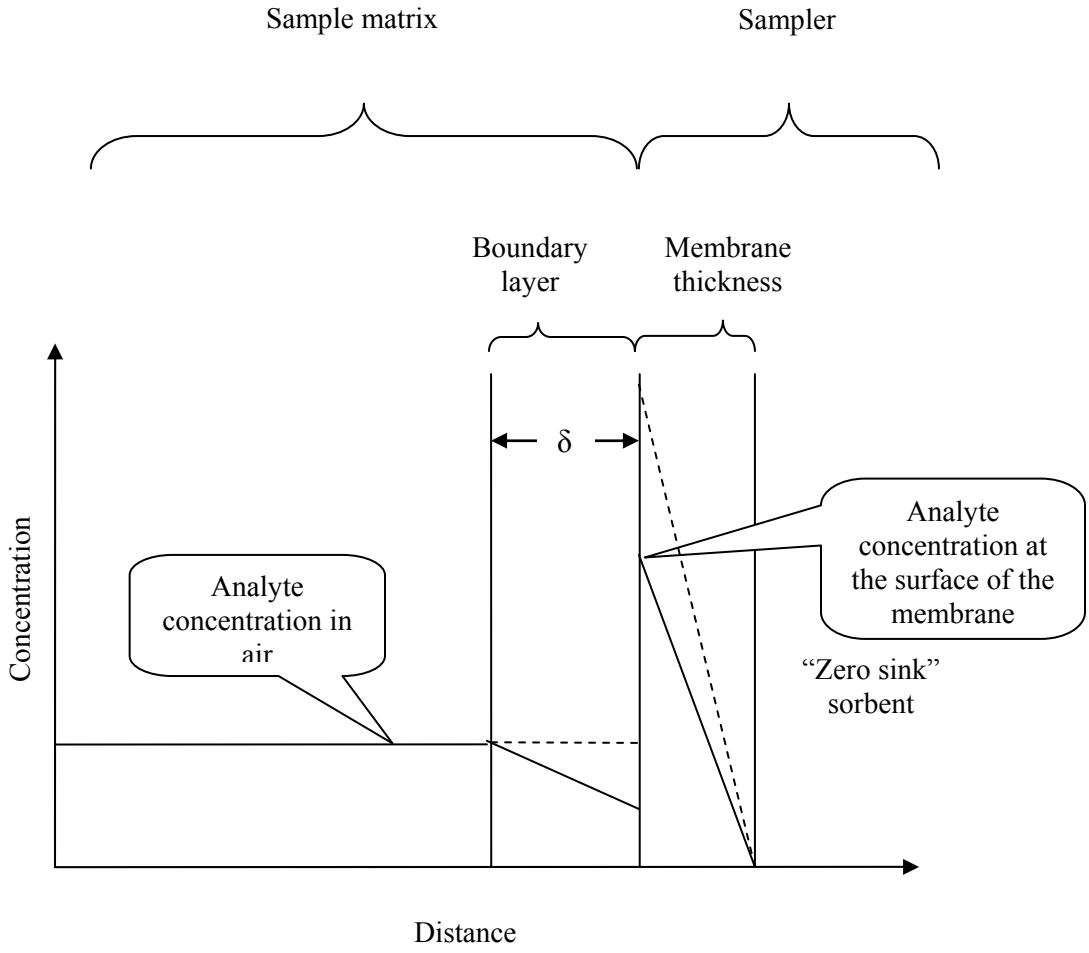

Figure 2-2: Concentration profile for permeation passive samplers with boundary layer effect and with an ideal sorbent. Dotted lines indicate the ideal concentration profile in the absence of boundary layer effect.

When applied to TWA sampling, the boundary layer thickness can be attributed to three parameters; the diffusion coefficient of the analyte in air, permeability of a specific analyte in PDMS, and the air flow patterns in the sample matrix. In the field of passive sampling, the effect of this boundary layer thickness on the actual concentration determined by the sampler is often referred to as the "starvation" effect.[184] Higher diffusion coefficients of the analyte in air and lower permeability result in lower starvation effect. If the linear flow velocity of air across the surface of the sampler is higher than a critical flow velocity, then the boundary layer thickness for all analytes becomes negligible, and the resultant concentration around the

face of the passive sampler is close to the true concentration in the bulk of the sample matrix. The effect of the linear flow velocity of air on the uptake rate of various kinds of passive samplers and the sampler developed in this project will be discussed in Chapter 4.

The effects of temperature and pressure on the diffusion coefficients of the analytes in the boundary layer are also important. Boundary layers can also exist in the sorption material within the sampler at the membrane/sorption material interface. Bartkow et al. considered such effects in their article on mathematical modeling of the uptake rates of semi-volatile organic compounds.[185]

2.1.2 Dynamics of the sampler response

The calibration constant (equation 2.4) has been mathematically derived based on the assumption that a steady state concentration profile exists within the membrane. In practice, concentrations of analytes can often change over the duration of the exposure. When such changes occur, there is an intermittent period when steady state concentration profile does not exist. A measure of the time the sampler takes to respond to this change in concentrations and reach the steady state again is quantitatively expressed using various terms such as residence time[184], relaxation time[186], lag time,[22] and response time[186]. The term residence time was introduced by Tompkins and Goldsmith and is now widely used. It is defined as the average residence time of an analyte in the diffusion region at steady-state conditions and is given below:

$$t_r = \frac{L_m^2}{2D_r} \tag{2.5}$$

where t_r is the residence time of the analyte with diffusion coefficient D_r in the membrane. The lower this value is, the shorter is the time required for the sampler to respond to a change in analyte concentration in the sample matrix. A similar relationship exists for diffusive-type samplers with the membrane thickness being replaced by the molecular diffusion distance in the diffusion barrier and D_r replaced by the diffusion coefficient of the analyte within the barrier (it is different depending on the dimension of the diffusion barrier and whether it is porous) as depicted in Equation 2.6.

$$t_r = \frac{L^2}{2D_a} \qquad (2.6)$$

The diffusion coefficient of any analyte in PDMS is often four to five orders of magnitude lower compared to that in air. However, the membrane thickness used in this project was on the order of micrometers, whereas the diffusion distances for diffusive-type samplers are on the order of millimeters or centimeters. Consequently, the effective residence times for both types of passive samplers are essentially of the same order of magnitude. For example, the residence time of toluene for diffusive-type passive samplers, GABIE and Perkin Elmer, are 4.05 s and 25.5 s, respectively.[187] Considering a diffusion coefficient of 1.15 x 10^{-6} cm^2s^{-1} for the diffusion of toluene through PDMS[188] and a 75 µm PDMS film thickness generally used in this project, the residence time can be calculated to be 24.5 s. PDMS membranes are available commercially with a thickness as low as 25 µm, which could lead to residence times of merely 2.7 s as shown in Figure 2-3 below.

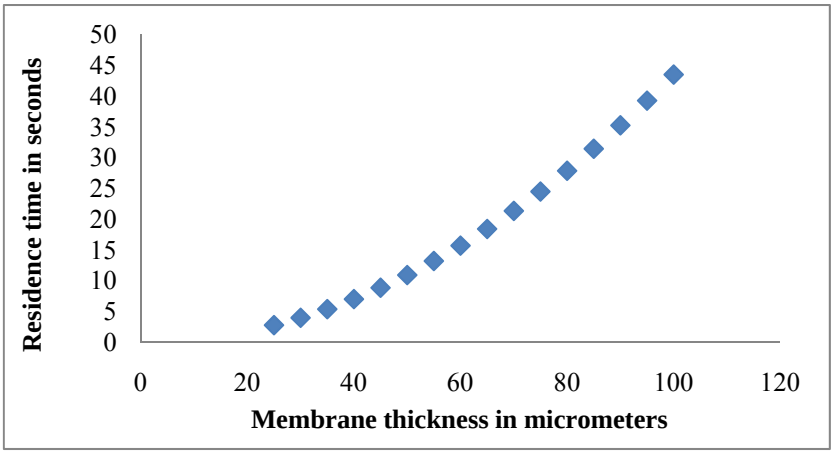

Figure 2-3: Effect of the membrane thickness on the residence time of the analytes in the membrane.

Nevertheless, various researchers working on this aspect have determined that when the total sampling time is substantially longer than the residence time, say 20 times, the contribution of the error due to delayed response by the sampler is negligible.[189] The TWA-PDMS sampler is typically deployed for days or weeks, so this is more than ample time to fulfill the above condition.

2.2 Estimation of the calibration constant

The requirement that the calibration constant be known prior to sampler deployment necessitates the analyte identity to be known prior to the sampler deployment, which is not always possible. In such cases, it becomes important to arrive at an estimate of the calibration constant for an analyte after analyzing the sorbent in the laboratory. For diffusive-type samplers, such estimation boils down to using either available or estimated diffusion coefficients of the analytes in air to calculate the calibration constants, while for permeation passive samplers it has thus far not been possible to arrive at an estimate without conducting tests under controlled conditions.

Various physicochemical properties of the analytes were researched to explore the possibility of using them to develop a model for the estimation of the calibration constants. One such property was linear temperature-programmed retention index of the analytes determined using PDMS as the stationary phase in a capillary GC column. Such correlations were reported in the author's M.Sc thesis[190] and by Zabiegała et al.[100] The hypothesis that calibration constants could be estimated based on the linear temperature-programmed retention indices (LTPRI) of the analytes was developed based on the theory of permeability of PDMS towards organic vapors and the concept of linear temperature-programmed retention index. To understand how and why LTPRI and the calibration constant should be related to each other, a simple mathematical approach can be developed based on the fact that relative permeabilities of PDMS towards various analytes (and hence the calibration constants) are a strong function of the partition coefficient, and so is LTPRI. The relationship between these parameters is discussed in the next three sections.

2.2.1 Contribution of analyte partition coefficient to permeability

Graham described the basics of the solution-diffusion model for permeation of organic compounds as early as in the 1800s.[191] According to this model, the transfer of gas or vapor across a polymer takes place in three steps: dissolution of the vapor molecule in the polymer, diffusion of the molecule under a concentration gradient, and the release of the vapor from the polymer at the opposite side of the membrane.[192] It can be shown that the permeability

coefficient *P* of a molecule is a product of its diffusion coefficient *D* in the polymer membrane and its partition coefficient *K*.

$$P = DK \tag{2.6}$$

It has long been known that vapor molecules permeate faster through rubbery polymers (such as PDMS) than through glassy polymers (such as Teflon®).[192] The structure of PDMS is shown in Figure 2-4. PDMS, of all the rubbery polymers, has one of the lowest diffusivity selectivity for permeation because of the flexible (-Si-O-Si-) backbone of the polymer chains, as well as the relatively weak binding forces between the individual segments.[193] In fact, PDMS has one of the lowest glass-transition temperatures for polymers of -127˚C which allows long-range segmental motions even at very low temperatures. As a result, the relative differences in permeability of vapor molecules are mostly governed by their solubility (or, in other words, the partition coefficient) in the polymer rather than the diffusivity in the polymer.[192] Results of various studies reported in the literature support the assumption that diffusivity of molecules in PDMS is of the same order of magnitude for most volatile organic compounds. This is illustrated in Table 2-1, using data on diffusion and partition coefficients reported by Kong et al. at 321 K.[194] Within the homologous series, the diffusion coefficients of the compounds decrease with increasing molecular size, but the relative decrease is marginal when compared to the exponential increase in the partition coefficients of the compounds.

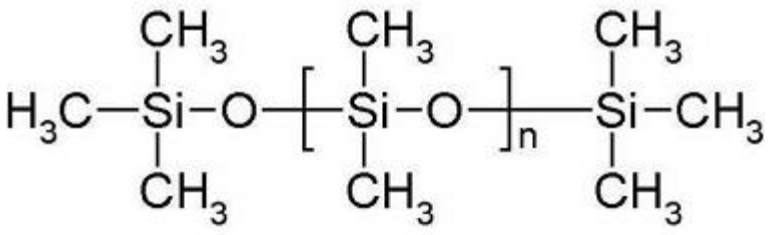

Figure 2-4: The structure of PDMS (reproduced from ref. 195)

Table 2-1: Partition coefficients and diffusion coefficients of n-alkanes (based on ref. 194).

Compound	Diffusion coefficient D x10^{10} (m^2 sec^{-1})	Partition coefficient K
n-pentane	6.5	40
n-hexane	6.0	95
n-heptane	5.3	218
n-octane	4.2	516
n-nonane	2.9	1267

A mathematical relationship between the calibration constant and the partition coefficient can then be derived under the assumption that D is constant for volatile organic compounds. Under these conditions, taking the natural logarithms of both sides of Equation (2.3), one gets,

$$\ln k = Z - \ln K \tag{2.7}$$

where Z is a constant defined by:

$$Z = \ln\left[\frac{L_m}{AD}\right] \tag{2.8}$$

In a homologous series of compounds, even though the diffusion coefficients are of the same order of magnitude, they typically decrease with increasing molecular weight of the compound. Under such conditions, constancy of the $D \times MW$ product can also be considered, and the correlations explored.

The assumption that the product of diffusion coefficient and molecular weight can be considered a constant was studied for the diffusion coefficients available from literature sources, and the results are tabulated in Tables 2-2[194] and 2-3.[196] For the n-alkane homologous series (Table 2-2), the relative standard deviations (RSD) of D, ln D, and ln (MW*D) show that the spread in ln (MW*D) was negligible when compared to the 29% RSD for D and 2.6% RSD for ln D. Similarly, for the n-alcohols homologous series (Table 2-3), the RSD of D, ln D, and ln (MW*D) show that the spread in ln (MW*D) was negligible when

compared to the 43% RSD for *D* and 2.5% RSD for ln *D*. These values are as expected for a homologous series of compounds.

Table 2-2: Variation in diffusivity with molecular weight for n-alkanes (based on ref.194)

Compound	Diffusion coefficient *D* x10^{10} (m^2 sec^{-1})	Molecular weight (MW)	MWx*D*x10^{10}	ln *D*	ln (*MW*x*D*)
n-pentane	6.5	72.15	470	-21	-17
n-hexane	6.0	86.177	520	-21	-17
n-heptane	5.3	100.203	530	-21	-17
n-octane	4.2	114.23	480	-22	-17
n-nonane	2.9	128.257	370	-22	-17
Average	5.0	100.2	474	-21	-17
Standard deviation	1.4	22.18	62	0.55	0
% RSD	29	22.13	13	2.6	0

Table 2-3: Variation in diffusivity with molecular weight for n-alcohols (based on ref. 196).

Compound	Diffusion coefficient *D* x10^{10} (m^2 sec^{-1})	Molecular weight (MW)	*MW*x*D*x10^{10}	ln *D*	ln (*MW*x*D*)
Methanol	10	32.042	320	-21	-17
Ethanol	7.1	46.069	330	-21	-17
Propanol	6.2	60.096	370	-21	-17
Butanol	5.5	74.122	410	-21	-17
Pentanol	5.1	88.149	450	-21	-17
Hexanol	4.2	102.176	430	-22	-17
Heptanol	4.1	116.203	480	-22	-17
Octanol	3.9	130.23	510	-22	-17
Nonanol	3	144.256	430	-22	-17
Decanol	2.5	158.283	400	-22	-17
Average	5.2	95.16	413	-21.5	-17
Standard deviation	2.21	42.47	61	0.53	0
% RSD	43	44.63	15	2.5	0

With the assumption that the product of diffusion coefficient and molecular weight can be considered a constant , the mathematical relationship takes the form

$$\ln\left[\frac{k}{MW}\right] = Q - \ln K \tag{2.9}$$

where Q is a constant defined as

$$Q = \ln\left[\frac{L_m}{AD \times MW}\right] \tag{2.10}$$

Equations 2.7 and 2.9 show the relationship between the calibration constant and partition coefficient. The calibration constant can then be related to LTPRI based on the relationship between LTPRI and the partition coefficient as described in the next section.

2.2.2 Relationship between the linear temperature-programmed retention index and partition coefficient of the analyte

Partition gas chromatography involves the partitioning of the solute between a liquid stationary phase and a gaseous mobile phase. Therefore, the retention properties of a compound in such a chromatographic separation are a function of the analyte partition coefficient between the carrier gas and the stationary phase (PDMS in this case). Under isothermal conditions, the partition coefficient of a solute at a given temperature is related to the retention time of the solute in the following manner,[197]

$$\frac{t'_r}{t_m} = \frac{t_r - t_m}{t_m} = K\ \frac{V_s}{V_m} \tag{2.11}$$

where $t`_r$ is the adjusted retention time, t_m is the retention time of an un-retained compound, t_r is the retention time of the solute, K is the partition coefficient of the solute, V_s is the volume of the stationary phase, and V_m is the volume of the mobile phase.

Van den Dool and Kratz[198] introduced the concept of LTPRI (dimensionless), which involves calculation of the retention index while achieving chromatographic separation under the conditions of linear temperature programming. LTPRI is defined as:

$$LTPRI = 100\left[\frac{t_r - t_n}{t_{n+1} - t_n}\right] + 100n \qquad (2.12)$$

where t_r is the retention time of the analyte, t_n is the retention time of the *n*-alkane eluting directly before the analyte, t_{n+1} is the retention time of the *n*-alkane eluting directly after the analyte, and n is the number of carbon atoms in the *n*-alkane eluting directly before the analyte. The exact correlation between LTPRI and the partition coefficient is complicated, and involves fluid dynamics inside the capillary column.[199] However, various researchers working on determining empirical relationships and/or mathematical approximations have found that LTPRI for a homologous series of compounds is related to the partition coefficient of the analytes at a particular temperature as[9]

$$LTPRI = N \ln K + B \qquad (2.13)$$

where N and B are constants. The relationship for a homologous series of n-alkanes can be quickly verified using data obtained by Kloskowski et al.[200] at 298 K using a capillary column with PDMS stationary phase (Figure 2-5). The correlation was found to be excellent with a correlation coefficient of 0.9999. Further validity of this concept can be drawn from data presented by Martos et al., who used solid phase micro-extraction techniques for compounds including benzene, toluene, ethyl benzene, n-propyl benzene, n-pentyl benzene and n-hexyl benzene among others (Figure 2-6).[201] The above relationship was successfully used to estimate the calibration constants of various analytes in solid-phase microextraction with PDMS-coated fibres.

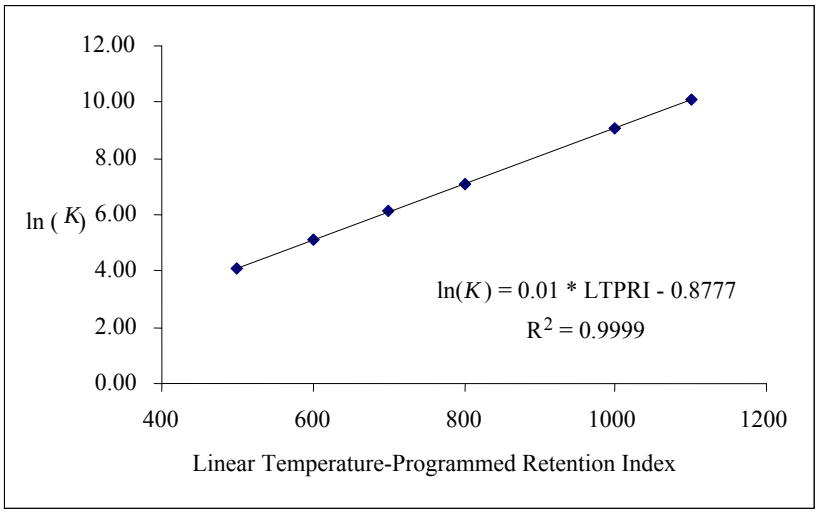

Figure 2-5: Partition coefficient – LTPRI correlation for n-alkanes (based on ref. 200).

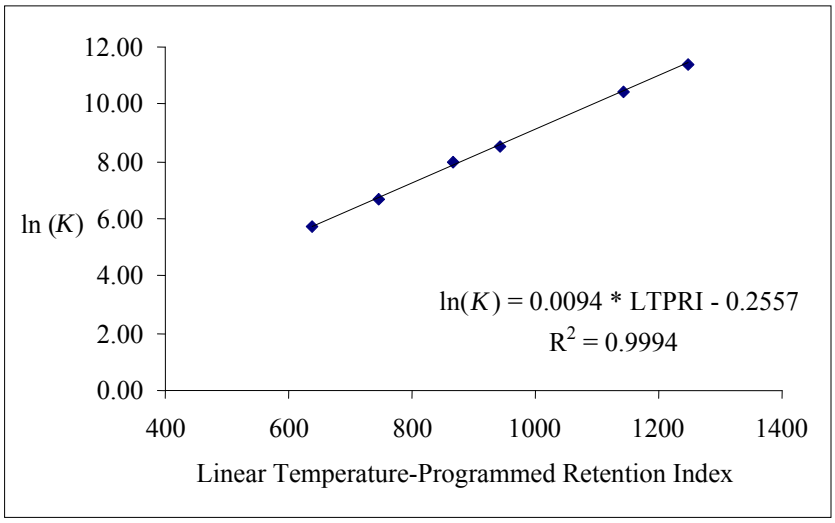

Figure 2-6: Partition coefficient – LTPRI correlation for aromatic compounds (based on ref. 201).

Since relative calibration constants are mainly a function of the partition coefficients of the analytes between air and PDMS as discussed in section 2.2.1, the relationship between LTPRI and the partition coefficient discussed in this section can be used to correlate calibration constants with LTPRI.

2.2.3 The calibration constant – LTPRI correlation

From equations (2.7), (2.8) and (2.9), the relationship between the calibration constant *k* and LTPRI can theoretically be obtained and can be studied under two scenarios:

Case 1: When *D* is assumed to be constant, equations (2.7) and (2.13) suggest that ln(*k*) is directly proportional to LTPRI. If this is true, then the major advantage would be the ability to estimate the calibration constants for analytes without knowing their identity (because it is not required to know the identity of a compound to determine its LTPRI)

Case 2: When ln (*D*×*MW*) is considered constant, equations (2.9) and (2.13) suggest that ln(*k/MW*) is directly proportional to LTPRI. In this case, the calibration constant could be estimated using LTPRI, but the identity of the compound would have to be known in order to determine its molecular weight. The identities of unknown analytes (thus their molecular weights) can often be established when using mass spectrometry for analyte detection.

It should be noted that the physical form of PDMS within the capillary column may differ from that which forms the membrane. The physical nature of PDMS depends on the degree of polymerization, cross-linking and the amount of fillers added in the manufacturing process. A low degree of polymerization (short chain lengths) and cross-linking result in a liquid-like physical form. A high degree of polymerization and cross-linking, along with addition of fillers such as SiO_2, result in the formation of a more rigid material. Cramers et al. noted that the LTPRI was nearly the same on PDMS stationary phases with and without cross-linking.[202] Therefore, the hypothesis that the calibration constant should be related to LTPRI should still be valid.

Calibration constants of 41 model compounds having different functional groups were determined and the above two cases were investigated. The details of the experiments will be discussed in the next Chapter.

CHAPTER 3

Experimental determination of the calibration constants and their correlation with physicochemical properties of the analytes

The knowledge of the calibration constants of the sampler towards the target analytes is required to determine the analytes' concentration in the vapor phase. When the calibration constant has not been experimentally determined, it is desirable to be able to estimate it based on the physicochemical properties of the analytes and the membrane material used for the fabrication of the sampler. The present chapter deals with the experimental determination of the calibration constants and using them to arrive at a model for the estimation of the calibration constants of analytes for which they are unknown.

The passive sampler design developed in this project and the idea of using physicochemical properties of the analytes for estimating the calibration constants is based on a similar design and concept first presented by Zabiegała, Górecki and Namieśnik.[100] The reason for redesigning the sampler and proposing a different theoretical model for the estimation of the calibration constant of the newly designed sampler was first presented in the author's M.Sc thesis.[190] Since the project presented in this thesis was a logical continuation of that presented in the author's M.Sc. thesis, a brief background of that research and its outcomes will first be provided.

3.1 Background to original sampler design, development of the new design and previous research observations

The original design of the sampler, as shown in Figure 3-1, was first developed at the Gdańsk University of Technology (Poland) using a PDMS membrane as the permeation barrier and activated carbon as the sorbent.[100] The sampler was equipped with a metal screen (2) for mechanical protection of the membrane, and the membrane (4) was mounted between this screen and the PTFE washer (7). Active carbon was used as the sorbent (5). It was held in contact with the membrane by a glass wool plug (6) and plastic plug (11) screwed into the body of the sampler (8). The above ensemble was mounted in a screw cap (1), which was

prevented from loosening by tightening a setscrew (12). The body of the sampler (8) and the internal chamber of the sampler were sealed using an O-ring (9) made of Buna-S rubber.

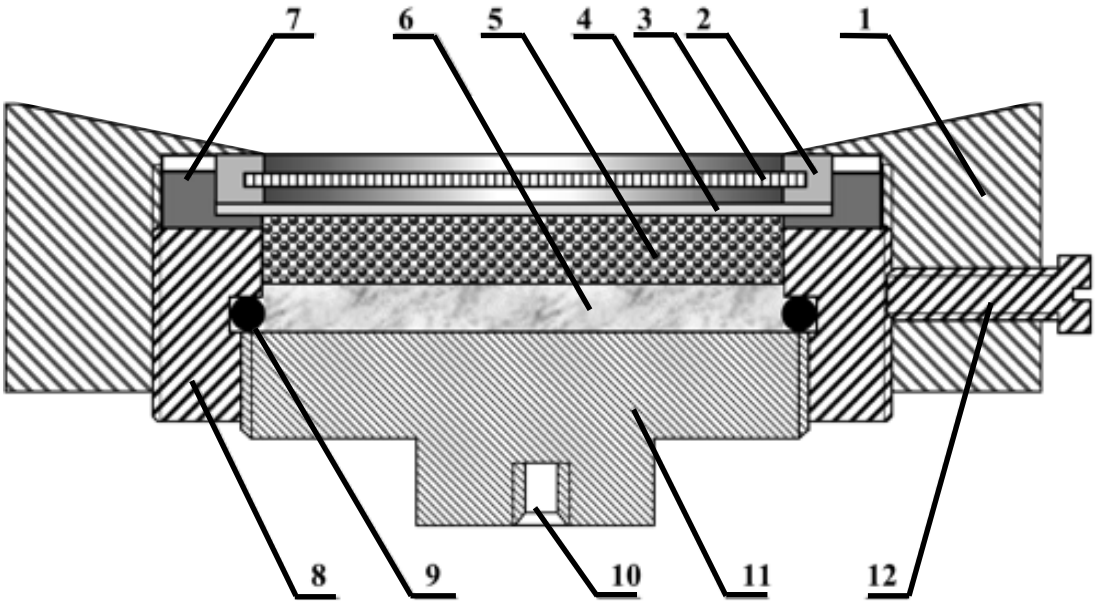

Figure 3-1: Passive sampler designed at the Gdańsk University of Technology. 1**.** screw cap**;** 2**.** protective screen mount; 3**.** protective screen; 4**.** PDMS membrane; 5. active carbon; 6. glass wool; 7. washer; 8. main body; 9. O-ring; 10. opening for a screw-in holder; 11. plug; 12. set screw (reproduced from ref. (100).

This permeation-type passive sampler was equipped with a 50 µm thick PDMS membrane and Zabiegała et al. determined the calibration constants of this sampler towards various groups of analytes. During the author's M.Sc. thesis work, the same sampler design but without the set screw shown in Figure 3-1 was used in the experiments. As a 50 µm thick membrane was not available at that time, a 75 µm thick membrane was employed instead. Also, the same experimental setup (as used by Zabiegała et al.) was used with some improvements in the flow controlling system in the experimental setup. The calibration constants obtained by the author for n-alkanes did not match the data published by Zabiegała et al., according to which there was a linear relationship between LTPRI and k (as against a linear relationship between ln(k) vs. LTPRI discussed in the Chapter 2), as shown in Figure

3-2. This resulted in a detailed investigation to explain the discrepancy and was one of the main focuses of the author's M.Sc. thesis.

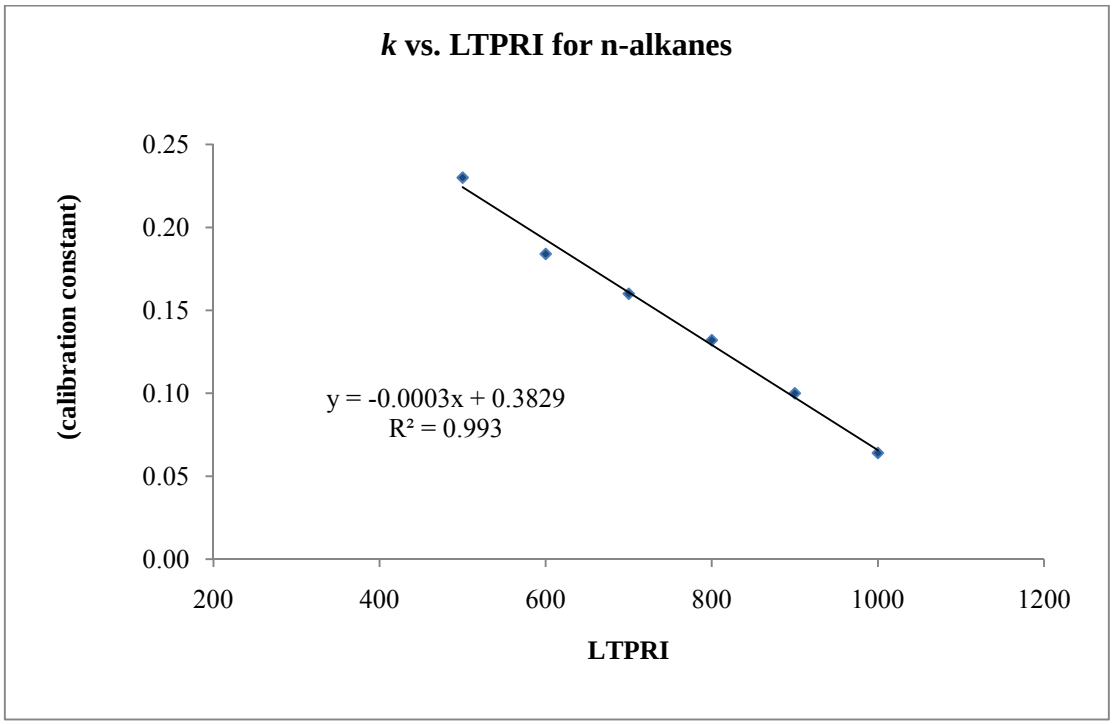

Figure 3-2: Calibration constant vs. LTPRI correlation for n-alkanes obtained by Zabiegała et al. (reproduced from ref (100)).

The investigations revealed the important reasons for the observations. The thickness of the membrane used earlier (50 µm) was different from that used by the author (75 µm). This would affect the uptake rates of the sampler towards various analytes to a different extent, as the starvation effect is different for different analytes (discussed in more detail in Chapters 1, 4, 6 and 7). This was further exaggerated as there was no proper air circulation inside the exposure chamber in which the samplers were exposed to standard test gas atmosphere to determine the calibration constants. A new exposure chamber was then built (described in detail later in this chapter), in which a fan was incorporated to allow proper air circulation around the sampling surface of the samplers. The calibration constants obtained using the new chamber and for the same analytes by the author along with the calibration constants obtained by Zabiegała et al. are shown in Table 3-1.

Table 3-1: Calibration constants and retention indices for n-alkanes observed by Zabiegała et al. and Seethapathy (reproduced from ref. (100) and (190))

Compounds	LTPRI	Calibration constant reported by Zabiegała et al., k (min cm^{-3})	Calibration constant reported by the author of this thesis with modified experimental set up, k (min cm^{-3})
n-pentane	500	0.230	n/a
n-hexane	600	0.184	0.156
n-heptane	700	0.160	0.087
n-octane	800	0.132	0.054
n-nonane	900	0.100	0.037
n-decane	1000	0.064	0.023

The calibration constants obtained by the author were lower than those reported by Zabiegała et al., which confirmed that starvation effect was indeed reduced to a great extent by the fan in the exposure chamber. Further, a plot of ln(k) vs. LTPRI (Figure 3-3) using the data obtained by the author supported the hypothesis presented in this thesis (and earlier in the Master's thesis). This could further be confirmed based on the data by Kong et al., which indicate that the permeability of PDMS (which is inversely proportional to the calibration constant) towards n-alkanes from pentane to nonane increases exponentially as shown in Figure 3-4.[194] It was difficult to recognize this correlation from the data reported by Zabiegała et al., as the calibration constants were all within one order of magnitude. Should the differences be greater than that, the true character of the relationship could have been possibly observed.

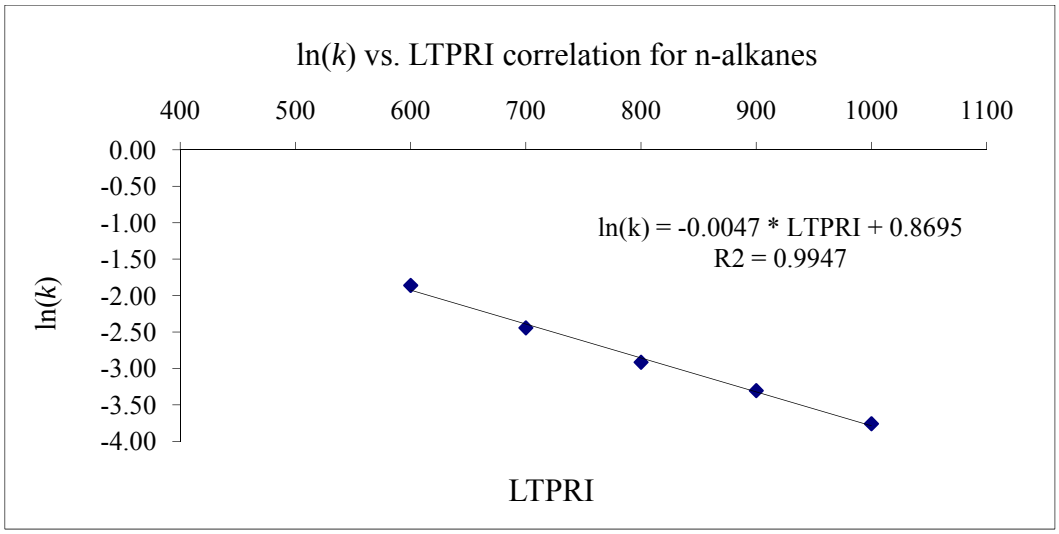

Figure 3-3: ln (*k*) vs. LTPRI correlation for n-alkanes observed with a fan incorporated in the calibration chamber (from ref. (190)).

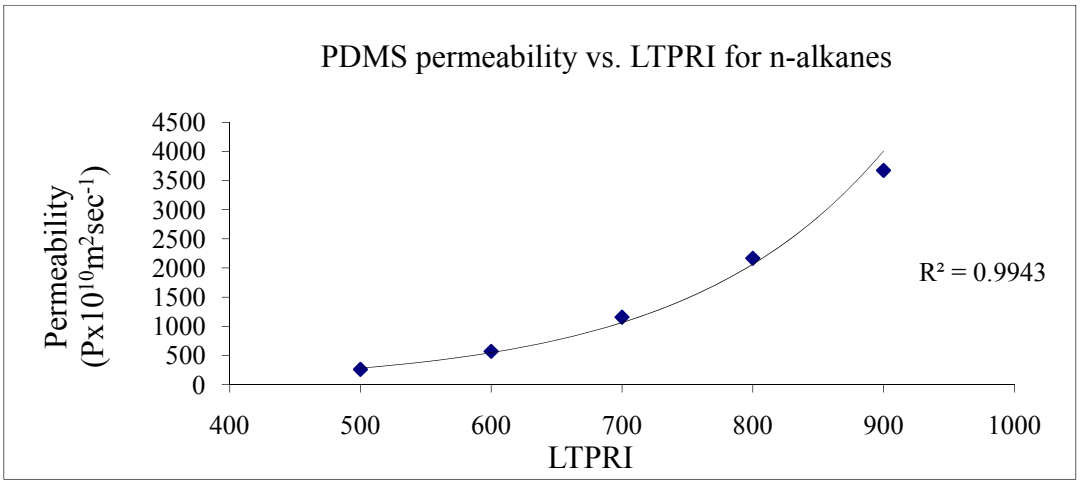

Figure 3-4: Data showing exponential increase in the permeability of PDMS towards n-alkanes with an increase in LTPRI (based on ref. (194)).

Though the sampler design shown earlier worked well, a new design was proposed during the author's M.Sc. thesis work for three main reasons:

(i) To reduce the cost of sampler fabrication to enable large scale studies which require large numbers of samplers,

(ii) To reduce the area of the cross section of the membrane exposed to the sample matrix, and consequently reduce the starvation effect, and

(iii) To allow for sampling and sample extraction in the same sampler housing if required.

The new design functioned in exactly the same manner as the earlier design, but was based on a 1.8 mL crimp-cap auto sampler vial used as a housing for the PDMS membrane and the sorbent (described later in detail). Various experiments were conducted to determine the calibration constants of this sampler towards n-alkanes (hexane to decane), aromatic hydrocarbons (benzene, toluene, ethyl benzene, propyl benzene, and butyl benzene) and chlorinated compounds (1,1-dichloroethylene, dichloromethane, cis-dichloroethene, chloroform, 1,1,1-trichloroethane, 1,2-dichloroethane, trichloroethylene and tetrachloroethylene). The results had confirmed a linear correlation between ln(k) and LTPRI for n-alkanes and aromatic hydrocarbons, but not the chlorinated compounds for which there was a linear correlation between ln (k/MW) and LTPRI. Based on these observations and to further investigate the LTPRI and calibration constant relation, more model compounds from moderately polar esters to polar alcohols were chosen for further experimentation, which forms a part of this thesis.

The experimental setup described in this chapter, as well as the methods of determining the calibration constants were the same as those used during the author's M.Sc. thesis work. The calibration constants of the sampler towards n-alkanes and aromatic hydrocarbons were determined again to confirm the correlation and are presented in this thesis. The calibration constants of the newly designed sampler towards chlorinated compounds determined during the author's previous work were essential in order to arrive at the overall relationship between LTPRI and the calibration constants and were extensively used for field sampling applications discussed in Chapters 6 and 7. Therefore, the data related to the chlorinated compounds as well as the model developed for estimating the calibration constants, are included in this thesis as well. However, only those data and methods necessary and sufficient to enable the readers to understand the overall functioning of the sampler have been included in this thesis.

3.2 Chemicals used in the experiments

High purity CS_2 required for the preparation of standard solutions of the analytes for gas chromatographic quantification and for analyte desorption from sorption tubes and passive samplers was purchased from VWR CANLAB (Mississauga, ON). Chromatography grade compressed air, helium, nitrogen, and hydrogen were purchased from Praxair (Kitchener, ON). All high purity, analytical grade chemicals were purchased from Sigma-Aldrich (Bellefonte, PA). The minimum purity, molecular weights, boiling points and CAS numbers of these chemicals are listed in Table 3-2.

Table 3-2: Purity and physical properties of model compounds used in the experiments.

Group	Name of the compound	CAS-No	% Purity	Molecular weight	Boiling point (˚C at STP)
Esters	Ethyl acetate	141-78-6	99.7	88.106	77.1
	Propyl acetate	109-60-4	99.5	102.133	102
	Methyl butyrate	623-42-7	99	102.133	102-103
	Sec-butyl acetate	105-46-4	99	116.160	112
	Ethyl butyrate	105-54-4	99	116.160	121
	Butyl acetate	123-86-4	99.7	116.160	126.1
	Propyl butyrate	105-66-8	99	130.187	142-143
	Butyl butyrate	109-21-7	98	144.213	166
Chlorinated compounds	1,1- Dichloroethylene	75-35-4	98	96.944	31.7
	Dichloromethane	75-09-2	99	84.933	39.8
	Cis-1, 2-Dichloroethylene	156-59-2	99	96.944	60
	Chloroform	67-66-3	99	119.378	61.7
	1,1,1-Trichloroethane	71-55-6	98	133.405	74.1
	1,2-Dichloroethane	107-06-2	98	98.960	83.5
	Carbon tetrachloride	56-23-5	99	153.823	76.7
	Trichloroethylene	79-01-6	99	131.389	86.7

Table 3-2 (continued): Purity and physical properties of model compounds used in the experiments.

Group	Name of the compound	CAS-No	% Purity	Molecular weight	Boiling point (˚C at STP)
n-Alkanes	n-hexane	110-54-3	99.5	86.177	69
	n-heptane	142-82-5	99	100.203	98.4
	n-octane	111-65-9	99	114.230	126
	n-nonane	111-84-2	99	128.257	150.8
	n-decane	124-18-5	99	142.284	174.1
Aromatic hydrocarbons	Benzene	71-43-2	99	78.113	80.1
	Toluene	108-88-3	99	92.140	110.6
	Ethyl benzene	100-41-4	99	106.167	136.2
	Propyl benzene	103-65-1	98	120.194	159
	Butyl benzene	68411-44-9	99	134.221	183
Alcohols	2-methyl-1-propanol	78-83-1	99	74.122	107.9
	n-butanol	71-36-3	99	74.122	117.6
	2,3-dimethyl-2-butanol	594-60-5	99	102.176	119
	n-pentanol	71-41-0	99	88.149	137.9 - 139
	2-hexanol	626-93-7	99	102.176	136
	2,4-dimethyl-3-pentanol	600-36-2	99	116.203	139
	n-hexanol	111-27-3	99	102.176	156 - 157
	n-heptanol	111-70-6	98	116.203	176
	2-octanol	123-96-6	99	130.230	180
	2-ethyl-1-hexanol	104-76-7	99	130.230	183
	n-octanol	111-87-5	99	130.230	195
	2-methyl-1-butanol	137-32-6	99	88.149	129
	3-Octanol	589-98-0	98	130.230	174-176
	6-methyl-2-heptanol	4730-22-7	99	130.230	172

3.3 Experimental

In this section, the design of the permeation passive samplers will first be presented. The general aspects of the experimental setup will then be described, followed by detailed experimental methods employed for the determination of LTPRI and the calibration constants of the sampler towards various analytes.

3.3.1 Passive sampler design

A simple passive sampler was designed and fabricated using a 1.8 mL standard mouth, crimp cap, chromatography auto-sampler vial, a PDMS membrane and a sorbent, as illustrated in Figure 3-5. The PDMS membrane (Product code: SSP-M823) used in the samplers was procured from Specialty Silicone Products Inc., (Ballston Spa, NY). The membrane had a nominal thickness of 75 μm. Even though the information was provided that silicon dioxide was added as a filler to increase the physical strength of the membrane, the manufacturer did not reveal its exact percentage in the finished product. The translucent PDMS membrane was supplied with a brown, nylon support sheet. The membrane along with the nylon support sheet was first cut to the shape of the top surface of the 1.8 mL glass vial using a cutting tool shown in Figure 3-6. The membrane was then separated from the support and weighed. Since the specific gravity of the commercially available PDMS membrane (1.17 ± 0.2)[203] and the area cut by the cutting tool were constant, the weight of the membrane served as a control for the membrane thickness. The thicknesses of the membranes procured were measured at the Department of Mechanical Engineering, University of Waterloo, using an Olympus U-PMTVC optical microscope (Tokyo, Japan) coupled to a digital image capture system. A typical cross section of the membrane as observed using the optical microscope is depicted in Figure 3-7.

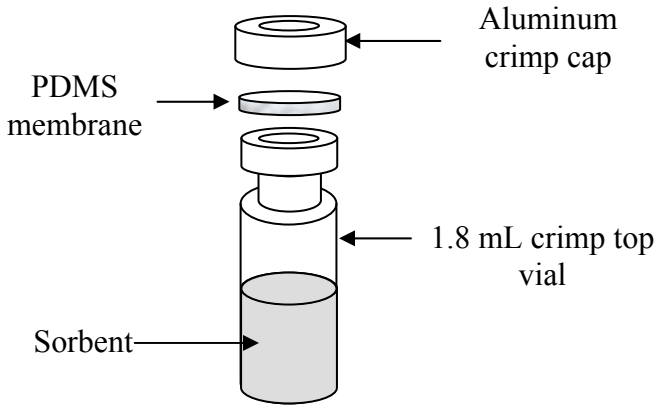

Figure 3-5: 1.8 mL crimp cap vial-based permeation passive sampler.

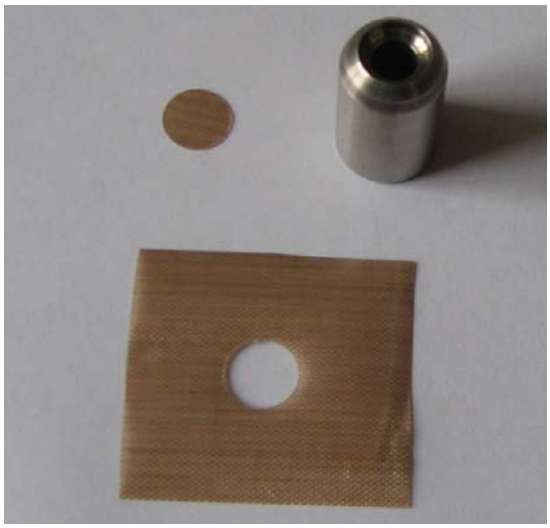

Figure 3-6: Photograph of a membrane with nylon backing and the membrane cutting tool

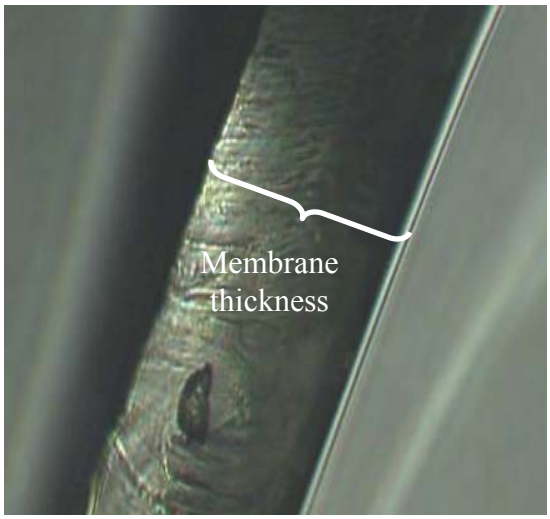

Figure 3-7: Photograph of a membrane cross-section

The samplers were then fabricated using the procedure illustrated in Figure 3-8. Anasorb 747®, an activated carbon-based sorbent available commercially in bulk quantities of 100 g from SKC Inc., (Philadelphia, PA), was used as the sorbent for the samplers. Approximately 250 mg of Anasorb 747® were weighed into the glass vial and the PDMS membrane was placed on top of the vial. An aluminum cap was then placed on top of the membrane and crimped using a crimper. A support made of heavy gauge PTFE tape procured from G.F.Thompson Co. Ltd. (Newmarket, ON), also shown in Figure 3-9, was attached to the

vial, and labeled prior to sampling. The rubbery nature of the PDMS membrane provided an air-tight seal between the aluminum cap and the glass vial, which could be verified by warming the vial (either by holding it in the palm of a hand or by blowing hot air on the vial) and watching the membrane bulge. The PDMS membrane is thinner than the PTFE-backed septum accompanying the crimp cap. This requires that a section of about 1 mm of the rim of the cap be trimmed before use, in order to crimp with a competent seal. The fabricated samplers were stored in 20 mL scintillation vials prior to exposure to the standard test atmospheres in the laboratory or deployment in the field. During sampling, the vial was turned upside down so that the sorbent was in contact with the PDMS membrane (Figure 3-9). This ensured that the organic vapors permeating through the membrane were quickly sorbed at its inner face. A concentration of effectively zero at the inner surface of the membrane at all times was one of the assumptions inherent in correlating the analyte concentration in air to its mass sorbed in the sampler. When the exposure with such a sampler was complete, the sampler was returned to the 20 mL overpack vial prior to extraction and analysis. In the case of samplers deployed in the field, the same packing procedure was followed for return transportation to the laboratory for analysis. The threads of the overpack vial were also wrapped inside and out with Teflon tape to minimize blank contamination during transit. The sorbent in the sealed samplers in the 20 mL overpack vials continued to draw and trap the analytes until the concentration in the membrane eventually diminished to near-zero. The sampler design will be referred to as the "TWA-PDMS sampler" throughout the rest of the thesis.

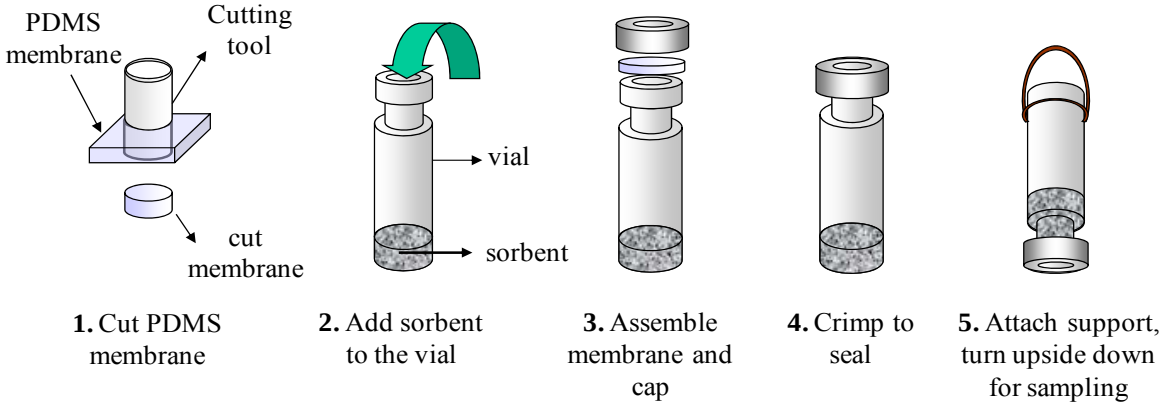

Figure 3-8: Fabrication sequence of TWA-PDMS sampler

Figure 3-9: Deployment of the TWA-PDMS sampler in the field

A summary of the reasons for the use of the specific design and material of fabrication has been provided below for the benefit of the readers at this point of the thesis. Detailed explanations of the advantages of this design will be dealt with in the remainder of the thesis.

- The 1.8 mL crimp top vial used in the fabrication of the sampler is the same as the vial used for autoinjectors in most gas chromatography instruments. The same vial can also be used for solvent desorption. This drastically reduces the sample preparation steps, reduces cost and errors, and allows for potential complete automation of the sample preparation and quantification process.
- Polydimethylsiloxane used for the membrane has properties that are well suited for passive sampling of VOCs from air. It has high permeability towards many organic compounds, low permeability for water, and low energy of activation of permeation; it is easily available in membrane form, inexpensive and has been studied and used widely since the 1960's. It is the same material as that used as the stationary phase in capillary GC columns, which (as discussed in Chapter 2) provides a valuable opportunity for estimating uptake rates using a correlation to published GC retention indices.
- Anasorb 747® is a granular, activated carbon-based sorbent which has been widely used for sorption of volatile organic compounds in various other active and passive sampling systems. This commercially available sorbent is often touted as a universal sorbent for the sorption of volatile organic compounds and analyte recoveries from the sorbent after solvent desorption are generally high and reproducible.

3.3.2 Experimental setup

The function of the experimental setup was to generate a test gas atmosphere with measurable concentrations of the analytes, where the passive sampler could be exposed for a predetermined amount of time for determining its calibration constant towards the analytes. The overall design of the experimental setup is illustrated in Figure 3-10. Nitrogen was passed through an air purifier (containing activated carbon) to remove traces of VOC impurities at a flow rate controlled by a mass flow controller (model MDF-52000L0N-0L) purchased from Pneucleus Technologies Inc., (Hollis, NH). The mass flow controller had an operating range of 0 to 1000 mL/min and was connected in series with an MKS Instruments (Andover, MA) Type 247 4-channel readout system for setting and monitoring the flow. The purified gas was then passed through a standard gas mixture generator whose design is described next.

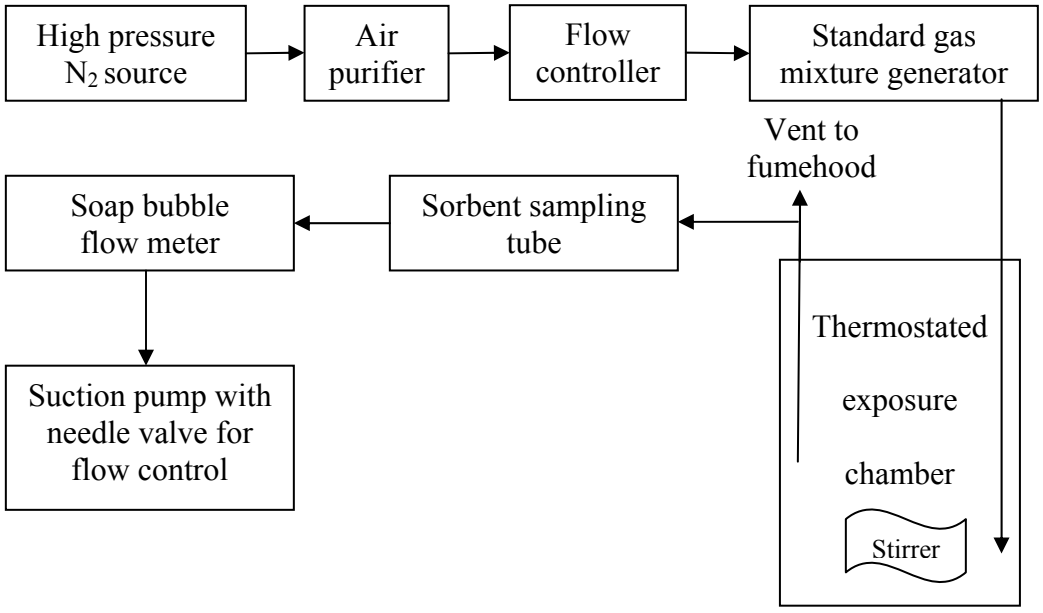

Figure 3-10: Schematic of the experimental setup used for the determination of the calibration constants.

The standard gas mixture generator used permeation tubes as the source for analyte vapors. Neat liquid enclosed in these permeation tubes (shown in Figure 3-11) permeated through the walls of the tube at a constant rate, and the vapors were swept by purified gas which entered the calibration chamber. The permeation tubes were made from virgin PTFE tubing cut into

segments of the desired lengths. The tubes prepared in this way were filled with neat liquids of the test compounds and sealed by means of PTFE plugs and Swagelok® ferrules compressed using a custom-made, removable fitting.[204] The PTFE tubes used for the fabrication of the permeation tubes had an outer diameter of ¼" and a wall thickness of 250 μm. The PTFE plugs were standard, ¼" diameter rods, which were machined on a lathe to reduce the thickness by approximately 250 μm to tightly fit the tubing. The brass Swagelok® ferrules were those used for standard ¼" outer diameter metal tubing. The permeation tube lengths ranged from 5 cm to 10 cm, depending on the volatility of a compound (longer tubes for less volatile compounds so as to have larger surface area of permeation, and hence increased flux). Depending on the composition of the standard gas mixture required, the respective permeation tubes (each tube containing one neat liquid) were enclosed in a flow-through vessel maintained at a constant temperature by placing them inside a GC oven as shown in Figure 3-12. Different sets of compounds were thermostated at different temperatures based on the permeation rates of the compounds through PTFE. The outlet of the standard gas mixture generator was connected to the inlet of the calibration chamber. The calibration chamber design and construction are detailed in the next paragraph.

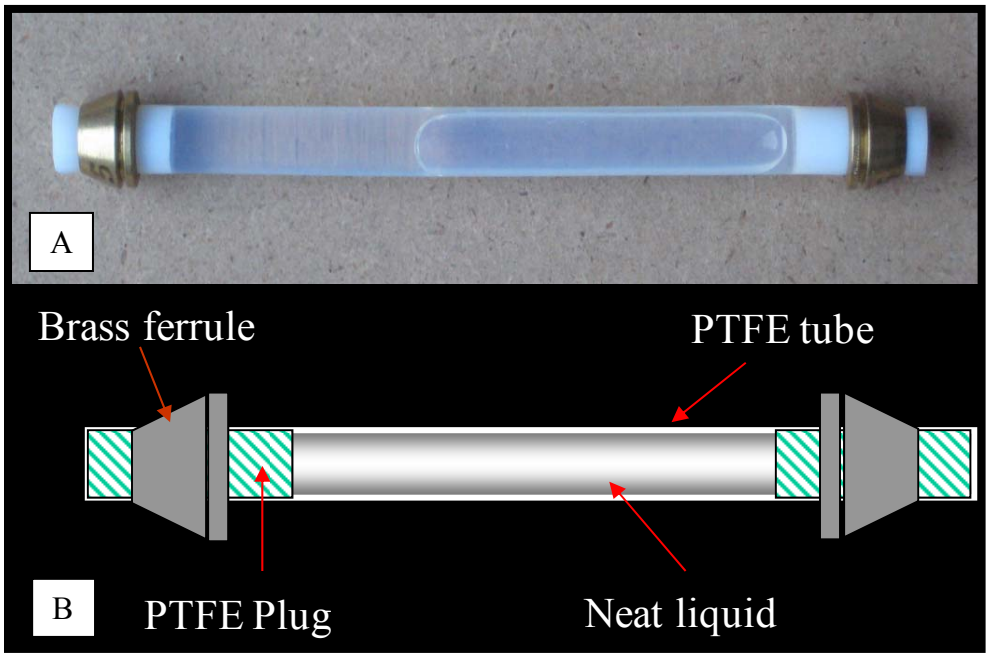

Figure 3-11: (A) Photograph and (B) schematic of a permeation tube used for the generation of standard test gas atmospheres.

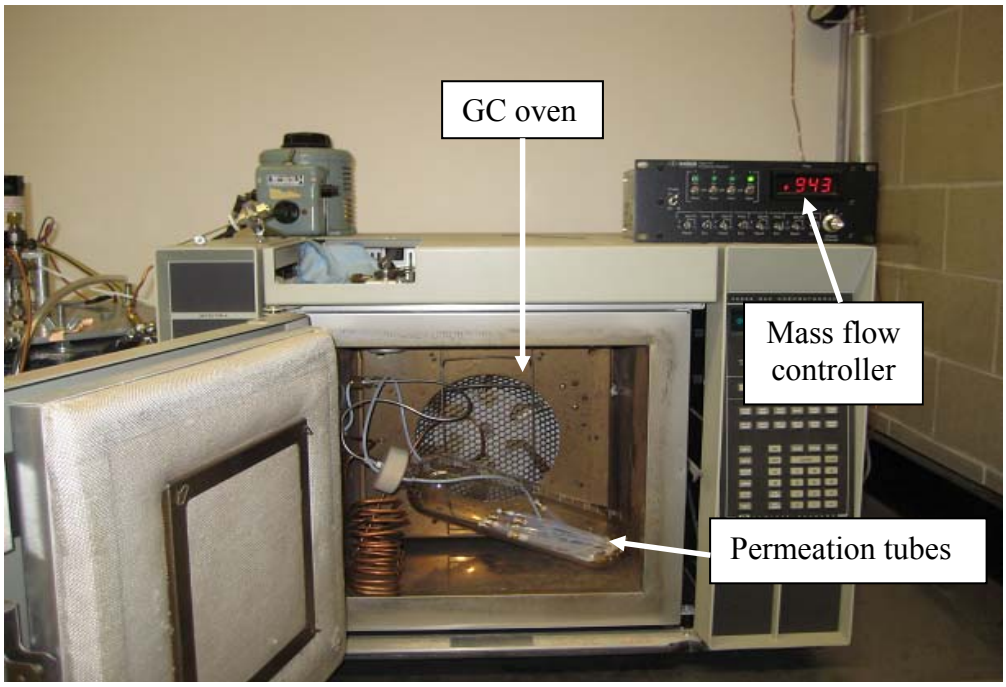

Figure 3-12: Photograph of the standard gas mixture generating system.

A schematic and a photograph of the calibration chamber used for the experiments are shown in Figures 3-13 and 3-14, respectively. The calibration chamber was constructed using a 10-liter cylindrical glass jar. A PTFE plate of ¼" thickness was used as the top lid for the glass jar, with an O-ring (made of PTFE-encapsulated Viton) between the plate and the jar for better sealing. The PTFE plate was held in place with the help of two aluminum plates, one placed on top of the Teflon® plate and another below the glass jar and the cooling jacket. These plates were held together by means of stainless steel rods, threaded on both ends, which were fixed to the bottom and top aluminum plates with the help of nuts. A motor (model Number JB2PO21N, Universal Electric Company, MI) was fixed on top of the aluminum plate, and a hole was drilled in the centre of the PTFE and aluminum plates to allow the shaft from the motor to run through this hole. A fan blade made of high-density polyethylene was attached to the bottom of the shaft. The motor itself was connected to a Powerstat® variable autotransformer (model 3PN116B, Superior Electric Company, CT) to enable control of the speed of the circulation fan. Also connected to the chamber was a ¼" diameter copper tubing inlet, through which the standard gas mixture entered the chamber. Holes were drilled in the segment of the inlet tubing positioned parallel to the bottom of the chamber to allow uniform introduction of the analyte gas mixture. Eight holes were drilled through the top plates (aluminum and PTFE) with diameters small enough to hold the vial-based passive samplers snugly, and the vials were inserted membrane down during exposure. The whole chamber was placed in a thermostated jacket and the outside of the jacket was insulated by wrapping it with glass wool insulation material. The calibration chamber was maintained at the required temperature throughout the period of sampling by circulating radiator fluid through the jacket with the aid of a circulation thermostat (model number 000-5744, HAAKE, Germany). The ½" inner diameter rubber tubing connecting the thermostat and the chamber were also wrapped with the glass wool insulation material.

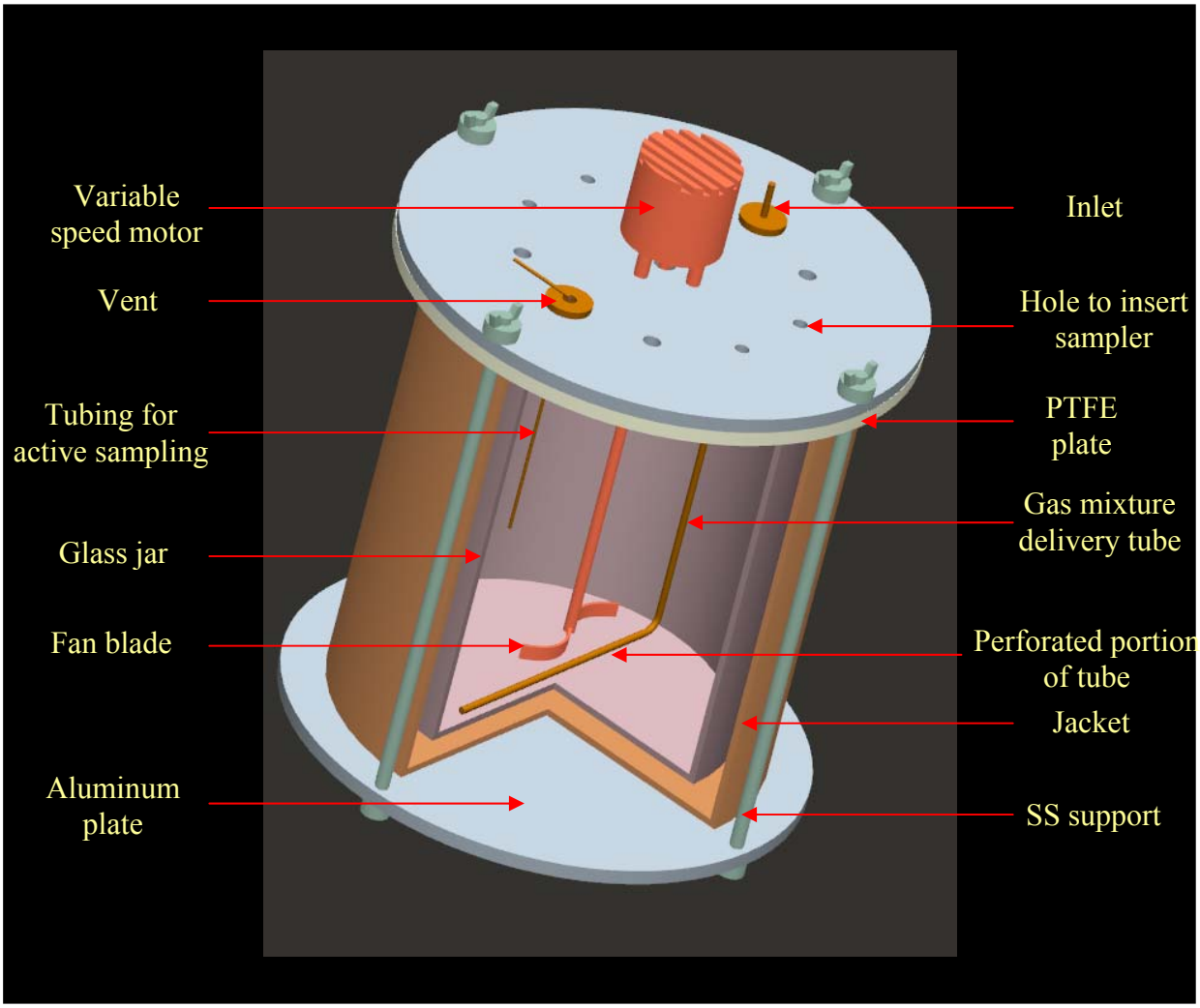

Figure 3-13: Schematic of the calibration chamber used for the exposure of the TWA-PDMS samplers to standard test gas mixtures.

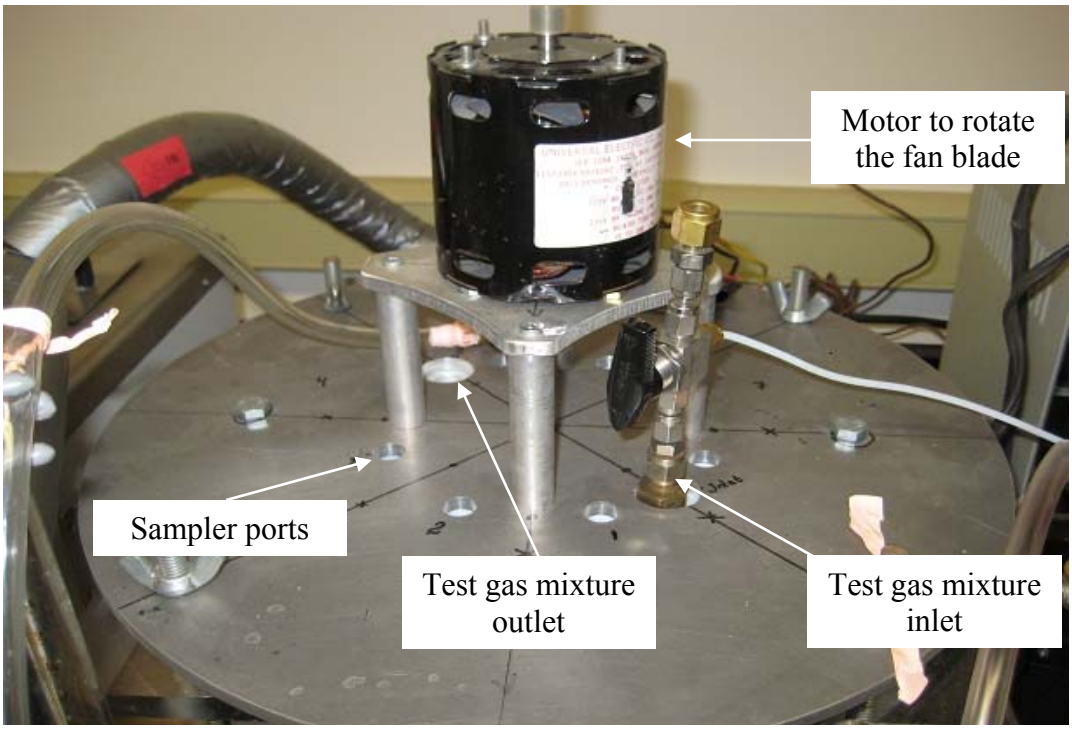

Figure 3-14: Photograph of the top part of the calibration chamber showing the sampler ports, test gas mixture inlet, motor and the test gas mixture outlet ports.

The passive samplers, inserted into the sampler ports of the calibration chamber, were thus exposed to a dynamic standard gas mixture. A piece of 1/8" stainless steel tubing inserted into the chamber through the vent was used to draw a sample of the chamber atmosphere through a sorption tube. The custom-made sorption tubes (fabricated by the glass blowing shop, University of Waterloo) were loaded with 300 mg of Anasorb 747® in the sample section and 100 mg in the back-up section, as shown in Figure 3-15.

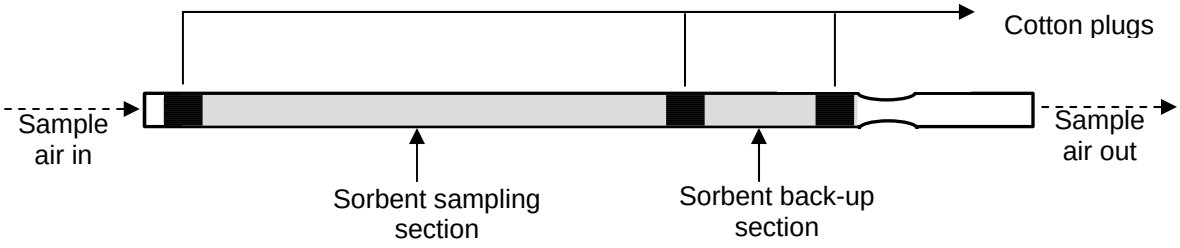

Figure 3-15: Schematic of a sorption tube used for the active sampling to determine analyte concentrations in the calibration chamber.

The sample was drawn at a constant rate of approximately 100 mL/min using a suction pump (Model MB-21) procured from Metal Bellows Corp. (Shanon, MA). The sample flow rate was measured using a bubble flow meter. Analyte concentrations in the calibration chamber were then determined based on the analyte mass trapped by the sorbent tube (determined by gas chromatography) in a given time, and the sample flow rate. These concentrations were then used to calculate the calibration constants of the samplers towards the analytes.

3.4 Experimental methods

In this section, the method used for the determination of LTPRI will first be described, followed by the determination of the calibration constants to enable the investigation of the correlation between the two parameters.

3.4.1 Determination of LTPRI

By definition, the retention indices of n-alkanes are 100 times the number of carbon atoms they contain (for example, it is 500 for n-pentane). Determination of LTPRI of all other analytes required the determination of their respective retention times, as well as the retention times of two n-alkanes (differing in number of carbon atoms by one) such that one of the alkanes had retention time shorter than the analyte, and the other longer than that of the analyte (Section 2.2.2). An Agilent 6890 GC (Santa Clara, CA) equipped with a split-splitless injector, an FID and an ECD was used for the analysis with the method described in Table 3-3. To correlate the calibration constants to LTPRI, it was necessary to use a capillary column with 100% PDMS stationary phase. The column was procured from Restek (Bellefonte, PA). For the determination of the LTPRI of aromatic hydrocarbons, a mixture of n-alkanes in CS_2 (from pentane to undecane) was prepared at concentrations of approximately 100 μg/mL each in CS_2. This solution was used for the determination of the retention times of the n-alkanes. Individual solutions of all the aromatic hydrocarbons listed in Tables 3-1a were also prepared at approximately 100 μg/mL in CS_2 and were used for the determination of the respective analyte's retention times for peak identification. Finally, another solution containing approximately 100 μg/mL of all the n-alkanes and aromatic hydrocarbons in CS_2 was prepared. This solution was injected 6 times, and the averages of

the retention times of each compound from the 6 injections were used for the calculation of LTPRI.

The LTPRI of different groups of compounds were determined at different points during the course of the project. The same method as described above for aromatic hydrocarbons was used for the determination of LTPRI of chlorinated compounds listed in Table 3-2. For the determination of the LTPRI of alcohols and esters, the same methods was used but with a Thermo Electron Corporation Focus GC (Waltham, MA) equipped with a split-splitless injector and an FID. The LTPRIs determined were then used for the investigation of their correlation with calibration constants whose determination is discussed next.

Table 3-3: Gas chromatographic method used for the determination of LTPRI.

GC Instrument	Agilent Technologies model 6890 GC
Detector	Flame Ionization Detector at 300˚C
Injection mode	Split, 275˚C, auto-injector
Split ratio	1:10
Injection volume	1 μL
Carrier gas	Helium at 1.2 mL/min
Oven temperature program	35˚C, 7˚C/min to 220˚C, held for 2 min
Data acquisition and processing	Chemstation software (Agilent)
Capillary column	RTX-1 (100% polydimethylsiloxane), 30 m x 0.25 mm, 0.25 μm film thickness

3.4.2 Determination of the calibration constants

The calibration constants were determined using equation 3.1:

$$k = \frac{C_0 t}{M} \tag{3.1}$$

The knowledge of the extraction efficiency of the analytes from Anasorb 747® was required to determine both the analyte mass trapped in the sampler (M) and its concentration (C_0) in the calibration chamber (by active sampling method using sorption tubes), and hence the method used for the determination of the extraction efficiency will be described next. The determination of the analyte mass trapped in the sampler (M) and the concentration of the analyte (C_0) in the calibration chamber will then be detailed.

3.4.2.1 Determination of analyte recovery rates from Anasorb 747®

Recoveries of all 41 compounds of interest from the Anasorb 747® sorbent were determined prior to the exposure experiments. This involved preparation of a stock solution of the respective analytes in CS_2, followed by the addition of 10 μL aliquots of this stock solution to six 4 mL vials containing 250 mg of Anasorb 747® each. The vials were capped and allowed to remain at room temperature for 24 hours for equilibration. Even though the extraction efficiency from Anasorb 747® was reported to be high for many VOCs using CS_2 as the desorption solvent (used at later stages of the project for field sampling and analysis), the extraction efficiency could be marginally increased according to the manufacturers specifications by using a polar solvent along with CS_2 for the extraction. Consequently, isopropyl alcohol (IPA) was used as a cosolvent in proportions depending on the polarity of the analytes studied. For alkanes and aromatic hydrocarbons, desorption of the analytes from the sorbent was performed by adding 1 mL of CS_2 to each of the six 4 mL vials, followed by shaking intermittently for 30 minutes. For alcohols, a 50:50 mixture of IPA and CS_2 was used for the extraction. For esters and chlorinated compounds, a 1% solution of IPA in CS_2 was employed. Some of the alcohols had similar retention times under the temperature programming conditions employed. To avoid difficulties imposed by co-elution, the recoveries were determined by analyzing 3-octanol, 2-methyl-1-butanol and 6-methyl-2-heptanol separately from the remaining alcohols listed in Table 3-2. The resulting extracts were transferred to 100 μL inserts placed inside 1.8 mL crimp-top vials, and the analyte amounts were quantified by GC. For the determination of the extraction efficiency of n-alkanes and aromatic hydrocarbons, the Agilent 6890 GC with the method described in Table 3-3 was used. A Thermo Focus GC with Chromquest data acquisition software was used

instead of the Agilent GC for quantifiying alcohols and esters by gas chromatography using the method described in Table 3-3.

In the case of chlorinated compounds, desorption was performed using a 1% solution of IPA in CS_2. Since the retention times of 1,1-dichloroethylene (1,1-DCE) and dichloromethane (DCM) were close with 100% PDMS-based stationary phase capillary columns, a slightly more polar HP-5 stationary phase (95% methyl and 5% phenyl) was used for their separation and quantification. The chromatographic separation and quantification was performed using the method detailed in Table 3-4.

Table 3-4: Gas chromatographic method used for the quantification of chlorinated compounds.

GC Instrument	Agilent Technologies, 6890 GC
Detector	Electron Capture Detector at 350˚C
Injection mode	Split, 275˚C
Split ratio	1:10
Injection volume	1 µL
Carrier gas	Helium at 1.2 mL/min
Oven temperature program	35˚C, 7˚C/min to 220˚C, held for 2 min
Data acquisition and processing	Chemstation software
Capillary column	RTX-5 (95% methyl and 5% phenyl), 30 m x 0.25 mm, 0.25 µm film thickness
Calibration method	External standard multipoint calibration

3.4.2.2 Determination of analyte mass in the samplers

The mass of analytes trapped in the adsorbent medium was determined using one of the two desorption methods illustrated in Figures 3-16 and 3-17 prior to chromatographic analysis. In the method illustrated in Figure 2-5, the aluminum cap was removed from the sampler with the help of a de-crimper (Chromatographic Specialties Inc., Brockville, ON), and the sorbent along with the PDMS membrane were transferred to a 4 mL vial for desorption. Since the

sorbent tended to stick to the surface of the membrane and it was cumbersome to try to separate them, it was decided to extract the membrane along with the sorbent. A 1 mL aliquot of the desorption solvent was introduced into the vial, which was then shaken intermittently over 30 minutes for desorption. After desorption, the vials were centrifuged if necessary, and aliquots of the extract were transferred to 1.8 mL crimp cap vials with 100 µL inserts for chromatographic analysis. Whenever the approximate analyte masses trapped in the samplers were unknown, the extracts were transferred to two 1.8 mL vials with 100 µL inserts in them. One of the two vials was used for GC analysis, while the other was reserved for dilution in cases when the concentrations of the analytes were higher than the calibration range of the GC (or GC-MS) method used.

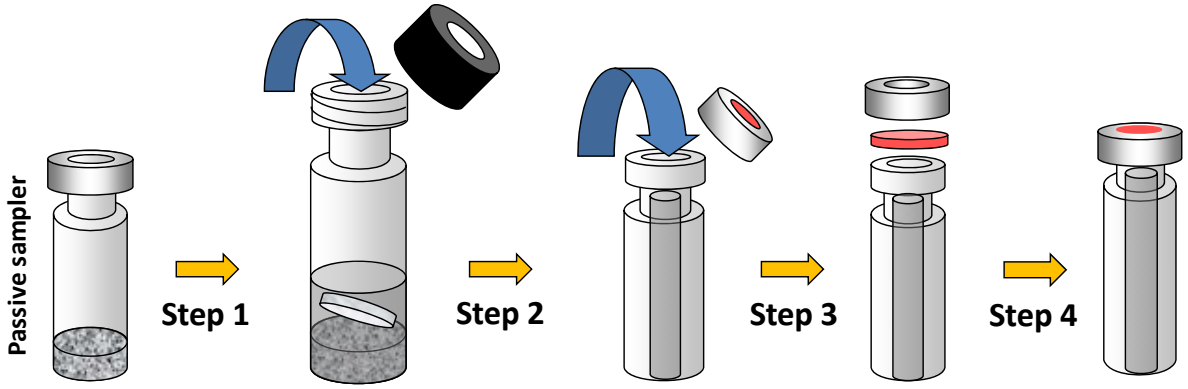

Figure 3-16: Solvent desorption using separate vials. Step 1: de-crimp the aluminum crimp cap, transfer the sorbent and the membrane into a 4 mL vial, add 1 mL of CS_2, cap the vial and extract for 30 minutes with intermittent shaking; Step 2: place a 200 µL glass insert inside a 1.8 mL crimp cap vial and transfer part of the extract from step 1 into it; Step 3: crimp with aluminum cap/Teflon lined septum to seal; Step 4: introduce the vial into the GC autosampler.

The second method involved using the sampler vial itself for solvent extraction as well as for introduction into the GC autosampler for chromatographic analysis. In this method, the aluminum crimp cap was first de-crimped and the membrane was transferred into the same 1.8 mL vial. 1 mL of CS_2 was then added to the vial and a new aluminum cap with Teflon® lined septum was crimped onto it. The advantage of this method is that the vial can be placed directly in the autosampler tray for injection without the need to transfer the CS_2 desorption solvent to another vial. Because of the granular nature of the sorbent, no syringe clogging

was observed during injection by the chromatographic autosampling/injection systems. In this method, the number of sample preparation steps as well as vials required for extraction was reduced, thereby increasing the throughput. The disadvantage of this method is that no separate extract aliquot is available for dilution if necessary, and the integrity of the extract in the original vial is compromised once the septum is pierced due to losses of the very volatile solvent.

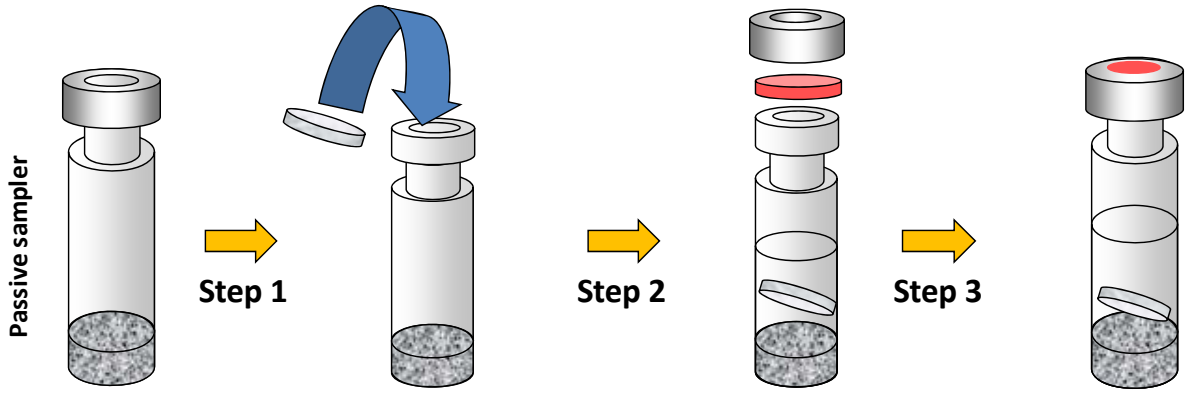

Figure 3-17: Direct solvent desorption in the sampler. Step 1: de-crimp the aluminum cap and transfer the membrane into the same vial; Step 2: Add 1 mL CS_2 and crimp with aluminum cap/Teflon lined septum and shake intermittently over a period of 30 minutes; Step 3: introduce the vial into the GC autosampler.

The sample preparation method involved extracting the sorbent as well as the PDMS membrane from the sampler using CS_2. It was therefore necessary to study the weight loss of the membranes on extraction with CS_2, what compounds were extracted from the membrane material and whether these compounds could interfere with the chromatographic analysis of the samples. To study this, 9 PDMS membranes cut with the tool shown in Figure 3-6 were weighed using a model UMT2 microbalance (Metler Toledo, Mississuaga, ON) and extracted separately by shaking them with 5 aliquots of 5 mL CS_2 in 20 mL vials. The membrane was made of cross-linked PDMS, and did not dissolve in CS_2.The membranes were then placed on Petri dishes and dried at 40˚C in a GC oven, cooled to room temperature and then weighed again.

To determine if the compounds extracted from the PDMS membrane affected the chromatographic separation and quantification of analytes, 10 PDMS membranes were extracted with 1 mL aliquots of CS_2 for 30 minutes and the extracts were analyzed by GC-MS, GC-FID and GC-ECD to identify any compounds that could interfere with the analysis of the samples.

3.4.2.3 Determination of analyte concentrations in the calibration chamber

Analyte concentrations in the chamber were measured using active sampling. They were then used for determining the calibration constants of the samplers towards the analytes. The permeation tubes were placed in a flow-through vessel inside the oven of an HP 5890 GC (with nitrogen flow) one week prior to the exposure experiments to stabilize the permeation rates of the analytes. The permeation tubes with n-alkanes, aromatic compounds and alcohols were maintained at 40˚C (± 1˚C); the tubes with chlorinated compounds were maintained at 30˚C (± 1˚C), and the permeation tubes for esters were maintained at 60˚C (± 1˚C) to account for differences in the permeability of PTFE towards each of these classes of compounds. Nitrogen flow rate was set at 800 mL per minute (controlled by the mass flow controller). The calibration chamber was maintained at 25˚C ± 1˚C throughout the period of sampling. The samplers equipped with 75 μm thick membranes were assembled as in Figure 3-8. The samplers were then inserted through the sample ports in the calibration chamber, and the start time of the exposure was recorded.

The concentrations of the analytes in the chamber were determined using sorption tubes that were changed every 24 to 48 hours. Flow through the tubes was determined using a soap bubble flow meter, and generally ranged from 80 to 120 mL/min. The flow rate measurement was performed at the beginning and the end of each sample collection cycle. The concentration in the chamber was first monitored without the samplers, and the exposure experiments were started when consecutive measurements showed concentrations within ±10% for each analyte. Typical exposure durations ranged from 3 to 16 days. After the exposure was completed, the passive samplers were removed and their contents were immediately transferred to separate 4 mL glass vials (along with the PDMS membranes) for extraction and analysis.

The chromatographic parameters used in the quantification of the compounds trapped by the sorbent in the passive samplers were the same as described in the method for the determination of analyte recoveries. The same extraction and chromatographic procedure was followed for the quantification of the analytes trapped by the sorption tubes. The breakthrough layers in the sorption tubes were extracted and analyzed separately to examine whether all the analytes were trapped by the front sampling portion of the tube, or whether there was breakthrough past the first segment of the adsorbent. Prior experiments were performed in order to make sure that the sorption capacity of the sorbent was sufficient (so as to not have breakthrough) for the analyte concentrations and standard gas mixture flow rates used in the chamber, yet it was considered prudent to test the breakthrough layer for confirmation following the protocol described in Figure 3.16.

3.5 Results and discussion

In this section, the LTPRIs determined for the model compounds will first be presented. Analyte recoveries from Anasorb 747® for the different analytes will then be discussed, followed by the observations made on membrane weight losses on extraction with CS_2. The calibration constants of the samplers towards the various analytes and their correlation with LTPRIs will then be discussed in detail. The calibration constants along with the knowledge of the dimensions of the PDMS membrane used in the fabrication of the sampler allowed the determination of the permeability of PDMS towards the various analytes.

3.5.1 LTPRI of the different groups of model compounds

Table 3-10 lists the LTPRIs of all compounds used in the study. The retention indices obtained in the laboratory were in close agreement with those reported in the literature. The injection-to-injection retention time precision was less than 0.1% RSD (n=6) for all the compounds. LTPRIs can often be determined within ±5 units for most chemical species.[205,206] For the purpose of the development of the model in this thesis, the LTPRI variability of ±5 units was considered insignificant.

Table 3-5: LTPRIs for the 5 groups of analytes determined using PDMS stationary phases in the GC column.

Analyte group	Analyte	LTPRI
Alkanes	Hexane	600
	Heptane	700
	Octane	800
	Nonane	900
	Decane	1000
Aromatic compounds	Benzene	649
	Toluene	757
	Ethyl benzene	853
	Propyl benzene	947
	Butyl benzene	1050
Alcohols	2-methyl-1-propanol	609
	n-butanol	643
	2,3-dimethyl-2-butanol	719
	n-pentanol	748
	2-hexanol	782
	2,4-dimethyl-3-pentanol	827
	n-hexanol	850
	n-heptanol	952
	2-octanol	985
	2-ethyl-1-hexanol	1016
	n-octanol	1055
	2-methyl-1-butanol	720
	3-octanol	983
	6-methyl-2-heptanol	951
Esters	Ethyl acetate	594
	Propyl acetate	693
	Methyl butyrate	703
	Sec butyl acetate	740
	Ethyl butyrate	780
	Butyl acetate	792
	Propyl butyrate	878
	Butyl butyrate	976
Chlorinated compounds	1,1- Dichloroethylene (1,1-DCE)	508
	Dichloromethane (DCM)	510
	Cis-1,2-Dichloroethylene (cis-DCE)	592
	Chloroform	603
	1,1,1-Trichloroethane (1,1,1-TCA)	625
	1,2-Dichloroethane (1,2-DCA)	633
	Carbon tetrachloride	655
	Trichloroethylene (TCE)	696

3.5.2 Analyte recoveries from Anasorb 747®

Analyte recoveries from the sorbent were used in the determination of the analyte masses trapped in the sampler, as well as analyte concentrations in the calibration chamber as determined by the active sampling method. Tables 3-6, 3-7, 3-8, 3-9 and 3-10 show the recoveries for the various groups of compounds used in this study. For n-alkanes and aromatic hydrocarbons, the maximum RSD was 2.2% for butyl benzene. The recoveries exceeded 95% in every case for the n-alkanes; the lowest recovery among the aromatic hydrocarbons was 93 % for propyl benzene and butyl benzene.

Table 3-6: Recovery rates of spiked n-alkanes from Anasorb 747®

Analyte	Amount added to sorbent (μg)	Average amount extracted from the sorbent (μg)	Average % recovery (n=6)	% RSD
Hexane	926	904	98	1.0
Heptane	742	719	97	1.0
Octane	658	636	97	1.0
Nonane	432	414	96	1.0
Decane	321	307	96	1.0

Table 3-7: Recovery rates of spiked aromatic hydrocarbons from Anasorb 747®

Analyte	Amount added to sorbent (μg)	Amount extracted from the sorbent (μg)	Average % recovery (n=6)	% RSD
Benzene	103	99	96	1.3
Toluene	96	93	97	1.3
Ethyl benzene	112	106	94	1.7
Propyl benzene	89	83	93	1.9
Butyl benzene	78	73	93	2.2

Table 3-8: Recovery rates of spiked alcohols from Anasorb 747®

Analyte	Amount added to sorbent (μg)	Amount extracted from the sorbent (μg)	Average % recovery (n=6)	% RSD
2-methyl-1-propanol	30.7	30.1	98	7.4
n-butanol	32.3	31.4	97	8.7
2,3-dimethyl-2-butanol	32.2	32.9	102	5.4
n-pentanol	38.1	40.5	106	7.0
2-hexanol	34.2	34.1	100	8.2
2,4-dimethyl-3-pentanol	32.1	32.1	100	4.2
n-hexanol	26.9	29.1	108	5.0
n-heptanol	27.8	29.3	105	5.3
2-octanol	29.6	32.1	108	3.6
2-ethyl-1-hexanol	39.2	39.4	100	7.6
n-octanol	37.4	37.8	101	6.8
3-octanol	31.6	35.7	113	6.6
2-methyl,1-butanol	32	32.5	102	3.7
6-methyl,2-heptanol	31.5	32.8	104	7.8

Table 3-9: Recover rates of spiked esters from Anasorb 747®

Analyte	Amount added to sorbent (μg)	Amount extracted from the sorbent (μg)	Average % recovery (n=6)	% RSD
Ethyl acetate	43.8	44.5	102	2.3
Propyl acetate	43.4	44.6	103	2.7
Methyl butyrate	44.1	45.3	103	2.9
Sec-butyl acetate	42.6	44.9	105	3.0
Ethyl butyrate	42.4	44.8	106	3.0
Butyl acetate	43.5	45.2	104	3.3
Propyl butyrate	42.5	44.5	105	3.0
Butyl butyrate	42.4	45.1	106	2.8

Table 3-10: Recovery rates of spiked chlorinated compounds from Anasorb 747®

Analyte	Amount added to sorbent (µg)	Amount extracted from the sorbent (µg)	Average % recovery (n=6)	% RSD
1,1- Dichloroethylene (1,1-DCE)	121.3	118.5	98	2.3
Dichloromethane (DCM)	119.9	117.5	98	2.0
Cis-1,2-Dichloroethylene (cis-DCE)	131.4	127.4	97	3.0
Chloroform	101.2	98.6	97	2.6
1,1,1-Trichloroethane (1,1,1-TCA)	8.54	8.3	97	3.1
1,2-Dichloroethane (1,2-DCA)	75.5	74.1	98	1.9
Carbon tetrachloride	3.07	3.0	98	2.2
Trichloroethylene (TCE)	38.34	37.2	97	3.1

Quantitative recovery of polar compounds from Anasorb 747® has always been a problem in the field of air sampling. The recoveries obtained for alcohols were all very high, but the reproducibility was not as good as for other groups of analytes, with a maximum RSD of 8.7 % for n-butanol and a minimum RSD of 3.6 % for 2-octanol (Table 3-8). The uncertainty in the recoveries of esters was comparatively low, with a maximum of only 3.3% RSD for butyl acetate (Table 3-9). Recoveries of polar alcohols and moderately polar esters were mostly higher than 100%. This was likely due to complete analyte desorption aided by isopropyl alcohol as a co-solvent and possible slight concentration of the extract, e.g. through sorption of the co-solvent by the sorbent. The recoveries of the chlorinated compounds and their uncertainties are shown in Table 3-10; they were all considered to be very good.

The efficiency of Anasorb 747® was studied by Gjølstad et al. with respect to extraction efficiency and storage stability for up to 28 days.[207] They found the sorbent to be highly suitable for a wide group of compounds including alkanes, alcohols, esters, chlorinated compounds, aromatic hydrocarbons, glycol ethers and ketones. Anasorb 747® has a very high

surface area of 1000 m^2 g^{-1}. Even though it is not as high as that of coconut charcoal, Anasorb 747® is more homogeneous and has more regular surface characteristics.[208] The shelf life of the sorbent is a minimum of 3 months and a maximum of 2 years, which is suitable for practical purposes such as sorbent storage, long deployment periods and storage before analysis in the laboratory.[209]

3.5.3 Determination of membrane weight loss and interferences on extraction with carbon disulphide

On washing the membranes with CS_2, the membranes lost an average of 3.1% of their weight, as shown in Table 3-11. Since the membranes retained their original appearance after drying, some of the membrane material was likely dissolving in CS_2. Analysis of the CS_2 extracts using GC-MS and GC-FID showed chromatograms similar to the one shown in Figure 3-18. GC-MS analysis indicated that the compounds extracted from PDMS with CS_2 were linear and cyclic siloxanes, with the first prominent peak indicated in Figure 3-18 eluting after hexadecane (boiling point 287˚C). The siloxanes were likely left behind in the membrane material because of incomplete polymerization of the monomers used in the manufacturing of the PDMS. Chromatograms obtained using GC-ECD indicated the absence of any compounds detectable by ECD. These experiments collectively indicated that the extraction method did not interfere in the quantification of the analytes from the samples.

Table 3-11: Mass loss of PDMS membranes on washing with CS_2

sample	Initial weight (mg)	final weight (after CS_2 wash) (mg)	difference (mg)	% weight loss
1	8.047	7.822	0.225	2.80
2	7.883	7.688	0.195	2.47
3	8.152	7.829	0.323	3.96
4	8.02	7.764	0.256	3.19
5	7.814	7.596	0.218	2.79
6	7.981	7.722	0.259	3.25
7	7.905	7.629	0.276	3.49
8	7.545	7.325	0.22	2.92
9	7.731	7.489	0.242	3.13
			Average % weight loss	**3.11**

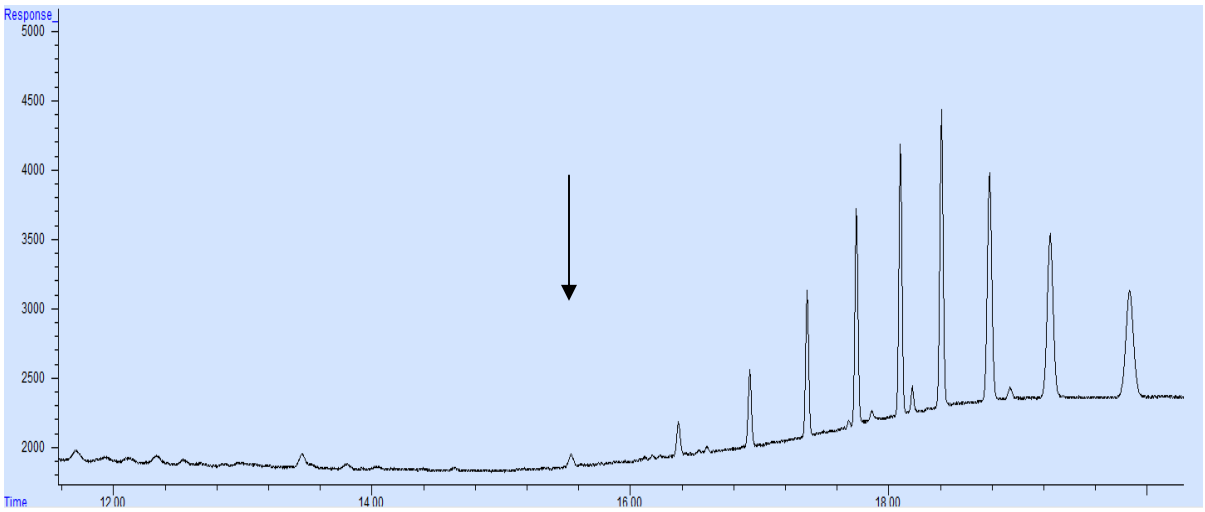

Figure 3-18: GC-FID chromatogram showing the compounds extracted from a PDMS membrane using CS_2. The arrow indicates the elution time of hexadecane.

3.5.4 Calibration constants and their correlation with LTPRIs

The calibration constants determined for all the compounds and their correlations with LTPRIs for each analyte group separately, as well as for all analytes put together, are discussed in this section. The exposure duration for each of the experiments, the average mass of each analyte trapped in the samplers during exposure in the calibration chamber, as well as the concentrations of the analytes in the calibration chamber are given in Table 3-12. The calibration constants determined using the TWA-PDMS samplers equipped with 75 µm thick PDMS membranes were determined using this data, and their %RSD values are also reported in Table 3-12.

The analyte concentrations in the exposure chamber ranged from 0.031 mg/m^3 to 34.3 mg/m^3. The concentrations in the chamber (determined using sorption tubes) were within ±14% of the average value reported in Table 3-12 for all exposure experiments. Variations in analyte concentrations were generally higher for analytes with higher boiling point in each of the groups. This was likely due to the increased sorption capacity of the inside walls and materials of the calibration chamber to higher molecular weight analytes.

Table 3-12: Calibration constants at 25˚C (± 1˚C); *k* is the average calibration constant observed when n passive samplers were employed during the exposure to the indicated set of compounds.

Analyte	LTPRI	Exposure duration (minutes)	Average mass in n samplers (µg)	Concentration in the chamber (mg/m^3)	*k* (min/mL)	n	% RSD
Hexane	600	5354	10.2	1.46	0.765	5	7.3
Heptane	700	5354	12.0	0.919	0.411	5	9.4
Octane	800	5354	11.5	0.473	0.220	5	9.4
Nonane	900	5354	9.9	0.219	0.119	5	7.8
Decane	1000	5354	8.5	0.117	0.074	5	8.7
Benzene	649	5354	17.4	1.35	0.414	5	7.3
Toluene	757	5354	33.7	1.33	0.213	5	7.9
Ethyl benzene	853	5354	21.4	0.538	0.135	5	7.8
o-xylene	885	5354	11.3	0.238	0.113	5	6.8
Propyl benzene	947	5354	17.8	0.300	0.090	5	7.0
Butyl benzene	1050	5354	12.2	0.139	0.061	5	8.5
2-methyl-1-propanol	609	16160	3.01	0.147	0.788	7	6.4
n-butanol	643	16160	11.1	0.351	0.512	7	6.6
2,3-dimethyl-2-butanol	719	16160	2.27	0.077	0.549	7	6.0
n-pentanol	748	16160	14.6	0.232	0.258	7	5.3
2-hexanol	782	16160	13.4	0.189	0.228	7	5.0
2,4-dimethyl-3-pentanol	827	16160	5.51	0.086	0.253	7	6.1
n-hexanol	850	16160	15.3	0.131	0.138	7	5.5
n-heptanol	952	16160	16.5	0.077	0.075	7	4.8
2-octanol	985	16160	19.3	0.082	0.069	7	5.0
2-ethyl-1-hexanol	1016	16160	7.83	0.031	0.064	7	6.1
n-octanol	1055	16160	13.3	0.043	0.052	7	6.7
2-methyl-1-butanol	720	22950	5.77	0.101	0.404	5	7.6
3-octanol	983	22950	9.46	0.049	0.120	5	9.7
6-methyl-2-heptanol	952	22950	23.4	0.096	0.095	5	12.2
Ethyl acetate	594	11628	218.4	14.2	0.754	7	2.5
Propyl acetate	693	11628	168.1	5.75	0.398	7	2.5
Methyl butyrate	703	11628	218.1	6.84	0.365	7	2.5
sec.butyl acetate	740	11628	34.1	1.15	0.392	7	2.4
Ethyl butyrate	780	11628	176.6	3.36	0.221	7	2.4
Butyl acetate	792	11628	169.6	2.95	0.202	7	2.0
Propyl butyrate	878	11628	151.1	1.66	0.128	7	2.0
Butyl butyrate	976	11628	134	0.927	0.081	7	2.4
1,1- Dichloroethylene	508	2925	82.3	34.3	1.22	5	5.1
Dichloromethane	510	2925	64.5	18.1	0.824	5	5.8
Cis-1,2-Dichloroethylene	592	2925	32.6	5.82	0.524	5	5.6
Chloroform	603	2925	26.1	4.58	0.514	5	5.1
1,1,1-Trichloroethane	625	2925	2.98	0.800	0.787	5	6.0
1,2-Dichloroethane	633	2925	24.3	3.22	0.388	5	5.4
Carbontetrachloride	655	2925	6.76	1.54	0.667	5	6.1
Trichloroethylene	696	2925	120.5	12.5	0.305	5	7.1

The calibration constants of the samplers towards the 41 model compounds reported here varied between 0.052 min/mL for n-octanol and 1.22 min/mL for 1,1-dichloroethylene. Sampler-to-sampler reproducibility was very good and better than 10% RSD for all the compounds studied with the exception of 6-methyl-2-heptanol, for which the reproducibility was 12.2% RSD. The reproducibility was exceptionally good for esters, with %RSD values equal to or less than 2.5% for all the analytes. For field applications, these variations can be considered minimal and errors arising from them negligible when compared to other factors involved in field studies, as will be discussed in the remaining chapters of this thesis.

The calibration constants of the TWA-PDMS samplers toward n-alkanes decreased exponentially from 0.765 min/mL for n-hexane to 0.074 min/mL for n-decane. Since the calibration constants were inversely proportional to the permeability of PDMS towards the analytes, this trend indicated an exponential increase in the permeability of PDMS from n-hexane to n-decane. This is in agreement with data on permeability of PDMS towards n-alkanes published in the literature, as discussed in Section 3.1. A plot of ln(*k*) vs. LTPRI for n-alkanes, depicted in Figure 3-19, showed a straight line correlation with a correlation coefficient of 0.9976. This supported the hypothesis that the relative calibration constants of the samplers were mainly determined by the analyte partition coefficients between the PDMS membrane and air (hence they were correlated to LTPRI), as discussed in Section 2.2.

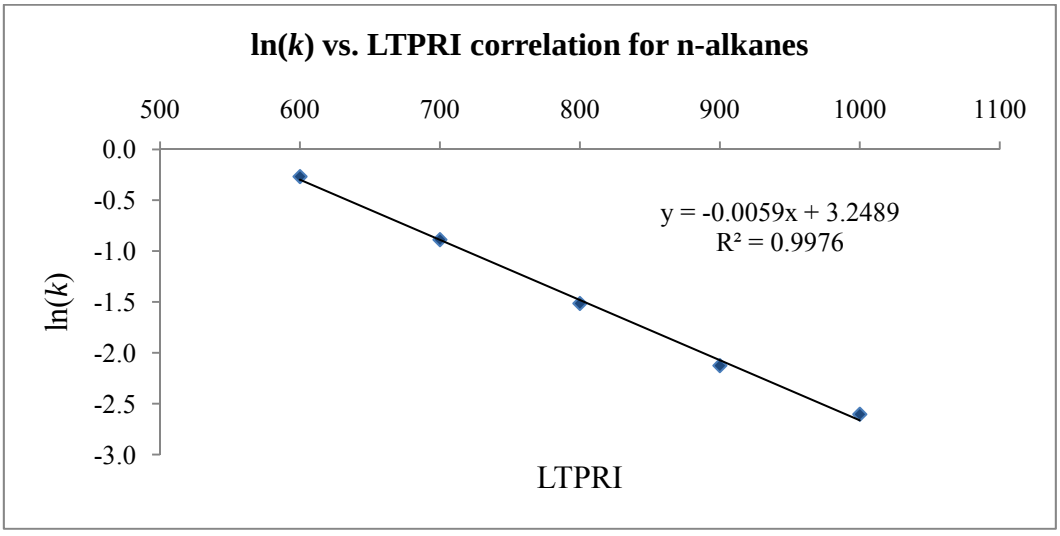

Figure 3-19: ln(*k*) vs. LTPRI correlation for n-alkanes

The calibration constants of the samplers towards aromatic hydrocarbons indicated a similar trend of exponential decrease from 0.414 min/mL for benzene to 0.061 min/mL for butyl benzene. Boscani and co-workers determined the permeability of benzene, toluene, ethyl benzene and propyl benzene using membrane inlet mass spectrometry, and found the same exponential increase in the permeability of PDMS from benzene through propyl benzene as was observed in this research.[188] Similarly to n-alkanes, the linear correlation between ln(*k*) and LTPRI for aromatic hydrocarbons (as shown in Figure 3-20) supported the hypothesis that the relative calibration constants were mainly a function of partition coefficients of the analytes.

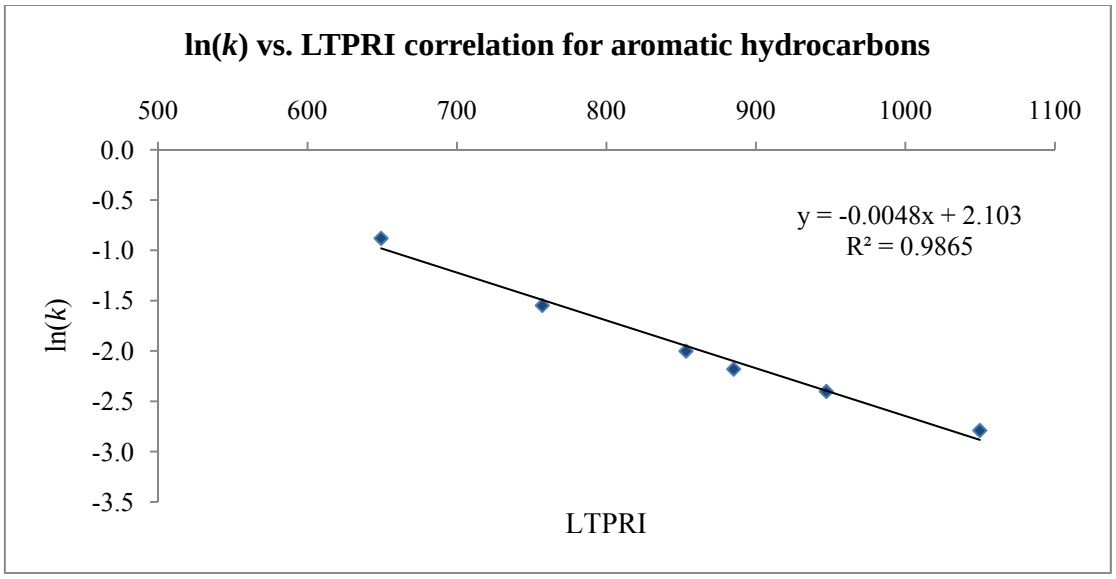

Figure 3-20: ln(*k*) vs. LTPRI correlation for aromatic hydrocarbons

The analytes in the alcohol group were either primary or secondary alcohols, and had either linear or branched alkyl chains in them. The calibration constants of the samplers towards n-alcohols from n-butanol to n-octanol showed a trend similar to those observed for n-alkanes and aromatic hydrocarbons, i.e. an exponential decrease in the calibration constants and consequently a linear correlation between ln(*k*) and LTPRI, with a correlation coefficient of 0.9903 (as shown in Figure 3-21). This correlation was again due to the dominant nature of partitioning in permeation through PDMS, as discussed in Section 2.2 (the diffusion coefficient data for n-alcohols are presented in Table 2-3). Even though there was also a

linear correlation for the ln(*k*) vs. LTPRI relationship for the alcohols with branched alkyl groups and secondary alcohols, the spread in the data points was much higher than for n-alcohols. This indicated that branching of the side chains and/or the nature of the alcohol (primary or secondary) played important roles in determining the permeability of PDMS towards these analytes, and consequently in determining the calibration constants.

Between a primary alcohol and the corresponding secondary alcohol with the –OH group in the 2 position a decrease in the permeability was observed. For example, the calibration constant of n-hexanol was 0.138 min/mL, while that for 2-hexanol was 0.228 min/mL. Similarly, the calibration constant of n-octanol was 0.052 min/mL, while that for 2-octanol was 0.069 min/mL. The decrease in permeability can be explained based on the mechanism of the partitioning process. When a molecule dissolves in the liquid polymer matrix, energy is required to disrupt the intermolecular attractions holding the individual PDMS chains together. Some of this energy is regained as a result of interactions between the analyte molecule and the PDMS matrix. Consequently, lower the energy required for dissolution, the higher is the tendency for the analyte molecule to partition into PDMS.

One of the important factors affecting the energy of dissolution of a molecule is its hydrophobic surface area. The larger it is, the stronger is the interaction between the analyte molecule and the hydrophobic PDMS chains. With linear alcohols such as n-hexanol, the long hydrophobic chains can align with the PDMS chains for maximum interaction. In the case of secondary alcohols, the hydrophobic surface area is reduced because of the geometric positioning of the –OH groups, thereby reducing the intermolecular attractions when compared to that for n-alcohols. Consequently, the partition coefficients for n-alcohols are greater than those for the corresponding 2-alkanols. Furthermore, the diffusion coefficients of n-alcohols are higher compared to those of the corresponding 2-alkanols due to the smaller "minimum cross section" of the former compared to the latter.[210] A similar observation was made by Favre et al., who found that the diffusion coefficient of n-butanol in PDMS (3.11 X 10^{-10} m^2 s^{-1}) was higher than that for s-butanol (2.25 X 10^{-10} m^2 s^{-1}) and t-butanol (2.66 X 10^{-10} m^2 s^{-1}).[211]

Branching in the alkyl chain of an alcohol molecule resulted in a decrease in the permeability through PDMS. For example, permeability of PDMS towards 2-methyl-1-butanol (k=0.404 min/mL) was lower than that for n-pentanol (k=0.258 min/mL). Similarly, the permeability of 2-methyl-1-propanol in PDMS (k=0.788) was lower than that for n-butanol (k=0.512). This can be explained based on the similar arguments presented for the primary and secondary alcohols above. Since branching reduces the hydrophobic surface area of a molecule, the partition coefficients of compounds with branched alkyl chains are smaller than those with linear alkyl chains. Furthermore, branching increases the minimum cross section of the molecules, thereby decreasing their diffusion coefficients.

When considering all the alcohols together, there was still a linear trend with a correlation coefficient of 0.9437. In general, it could be concluded that the trends for homologous groups of the highly polar alcohols were similar to those observed for the highly non-polar alkanes and aromatic hydrocarbons.

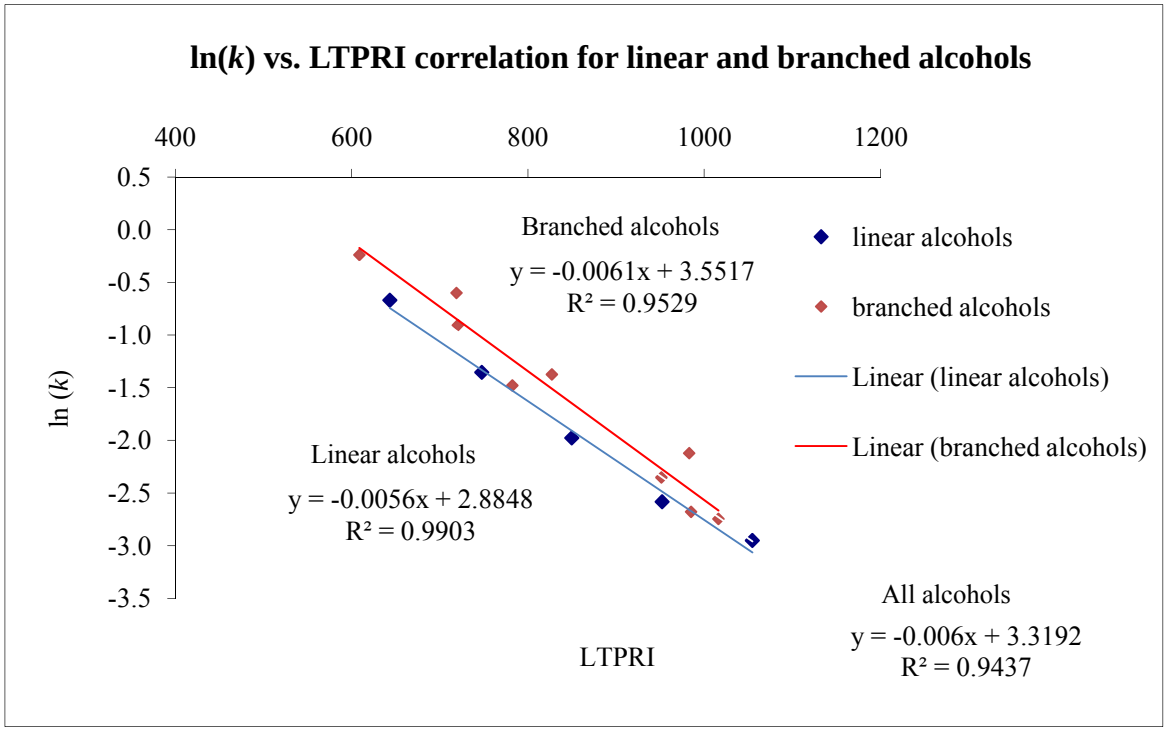

Figure 3-21: ln(k) vs. LTPRI correlation for alcohols

Esters have polarities ranging between those of n-alkanes and alcohols. As anticipated, there was a very good linear correlation between ln(*k*) and LTPRI (Figure 3-22) for the two homologous ester series, the acetates and the butyrates. Similarly to the trends observed for alcohols, PDMS had lower permeability for sec. butyl acetate (*k*=0.392 min/mL) when compared to that for butyl acetate (0.202 min/mL), which could be explained by the differences in the partition coefficients of the two compounds and the lower diffusion coefficient of sec. butyl acetate in PDMS due to steric hindrance caused by branching.

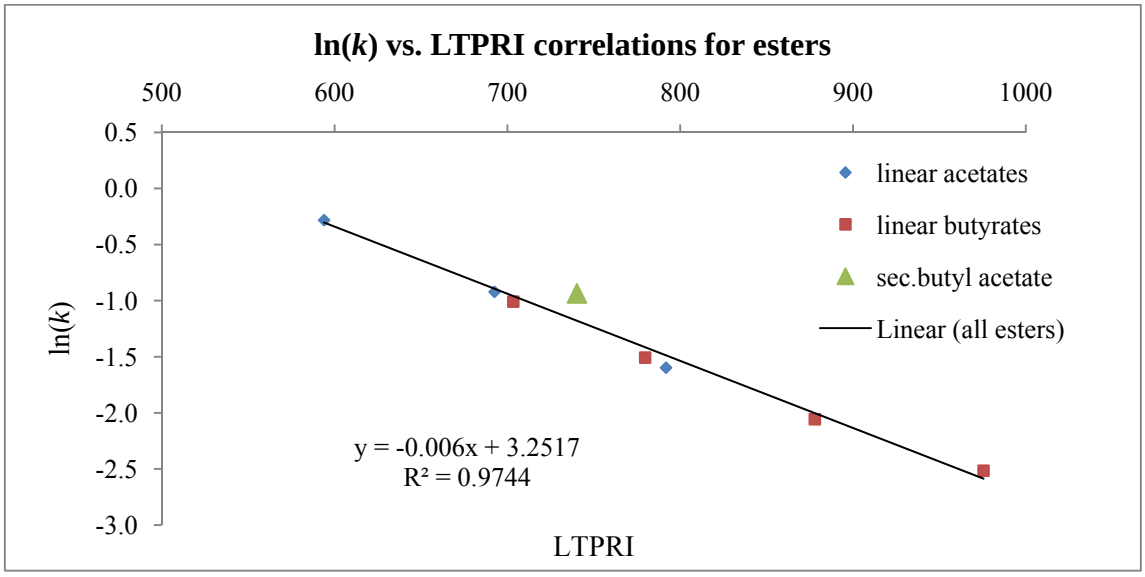

Figure 3-22: ln(*k*) vs. LTPRI correlation for esters

The trend in the calibration constants of DCM, chloroform, and carbon tetrachloride seemed at first counter-intuitive. Since the retention indices of these three compounds increase with the increase in the number of chlorine atoms in the molecule (Table 3-11), the calibration constants were expected to decrease accordingly from DCM to carbon tetrachloride. However, the average calibration constant for carbon tetrachloride (0.667 min/mL) was substantially greater than that for chloroform (0.514 min/mL). A subsequent literature search indicated that the diffusion coefficients of these three compounds in PDMS play an important role in determining the net permeability of the molecules through this polymer.[212] Even though the partition coefficients increase with the increase in the number of chlorine atoms, it is evident from the results that the decrease in the diffusion coefficients with the increase in

the number of chlorine atoms (and hence the molecular weight) plays a much more important role for these compounds compared with the remaining analytes. The significant role of the diffusion coefficients can be explained based on the molecular weights of these analytes (84.93 for dichloromethane, 119.38 for chloroform, and 153.82 for carbon tetrachloride), which change much more from one compound to another in the homologous series than for the n-alkanes and aromatic hydrocarbons. Dotremont et al. also reported that the diffusion coefficients decreased in the order CH_2Cl_2>$CHCl_3$>CCl_4, while partition coefficients decreased in the order CCl_4>$CHCl_3$>CH_2Cl_2, but because of their relative magnitudes, the permeability decreased in the order $CHCl_3$>CCl_4>CH_2Cl_2.[213] A similar observation can also be made for the calibration constant of 1,1,1-TCA, which has a higher LTPRI than cis-DCE and chloroform, but has a larger calibration constant than the other two.

As a consequence of the deviation from the general trend observed for other group of compounds, the ln(*k*) vs. LTPRI relationship for chlorinated compounds showed a significantly worse correlation coefficient of 0.6080 (Figure 3-23). Furthermore, the low value of the correlation coefficient indicated that alternative correlations should be considered (case ii, section 2.2.3). The diffusivity of a molecule in PDMS is inversely proportional to its molecular weight, which spans a wide range for the chlorinated compounds. A better correlation of 0.8938 could be obtained by plotting ln(*k*/MW) against LTPRI, as shown in Figure 3-24.

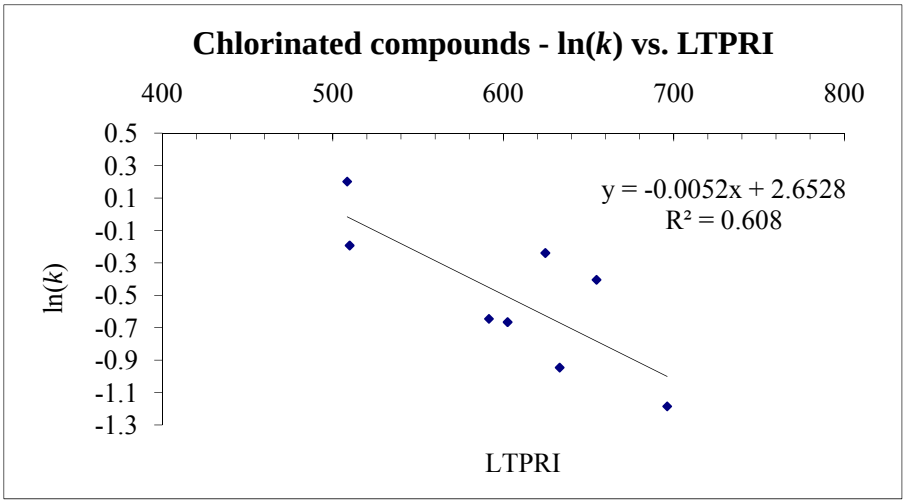

Figure 3-23: ln(*k*) vs. LTPRI correlation for chlorinated compounds

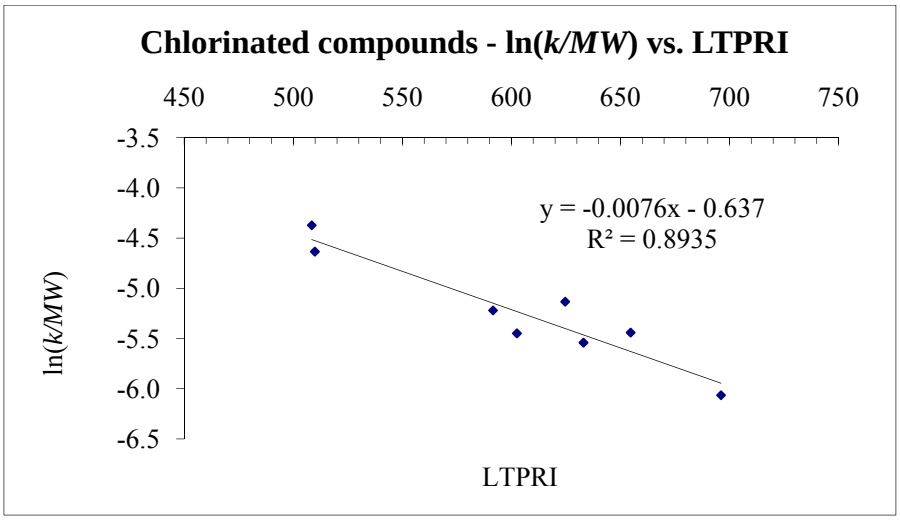

Figure 3-24: ln(*k*/MW) vs. LTPRI correlation for chlorinated compounds

The correlation coefficient for the relationship between ln(*k*) and LTPRI for all 41 compounds studied was 0.9475 (Figure 3-25). The ln(*k*/MW) vs. LTPRI correlations were also examined for the individual classes of compounds, as well as all compounds put together (Figure 3-26). The correlation equations and the respective correlation coefficients are tabulated in Table 3-13.

The correlation equations and correlation coefficients alone cannot determine if one method of estimation is better than the other, hence statistical analysis of the residuals was performed to determine if there were any significant differences between the experimentally determined calibration constants and the various estimated calibration constants.

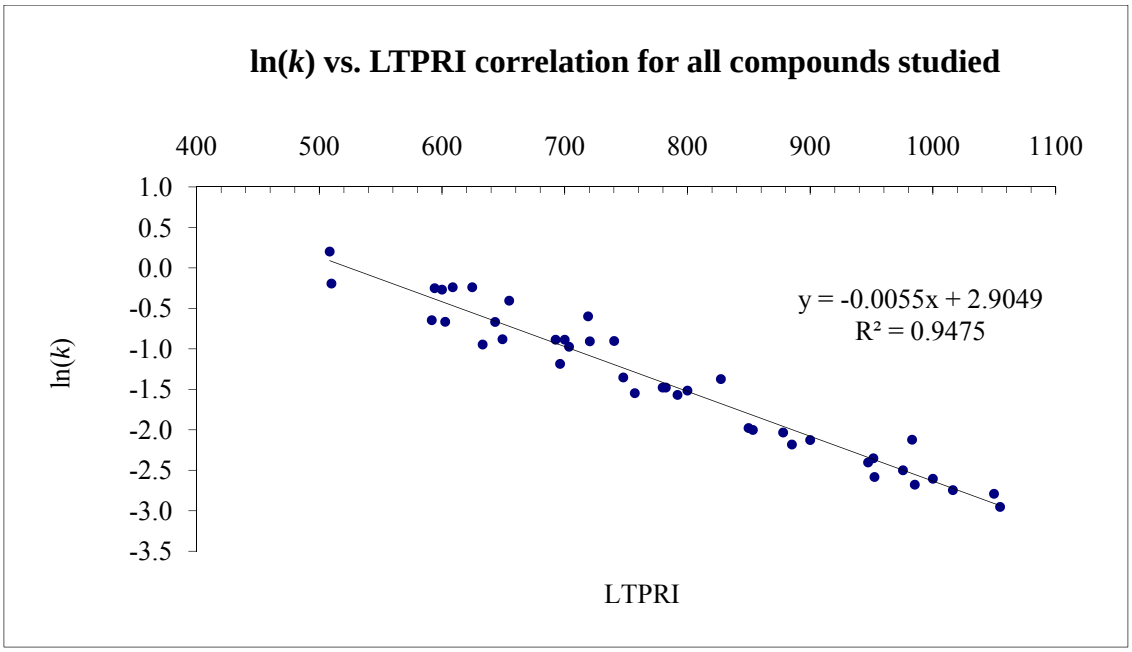

Figure 3-25: ln(*k*) vs. LTPRI correlation for all 41 compounds studied

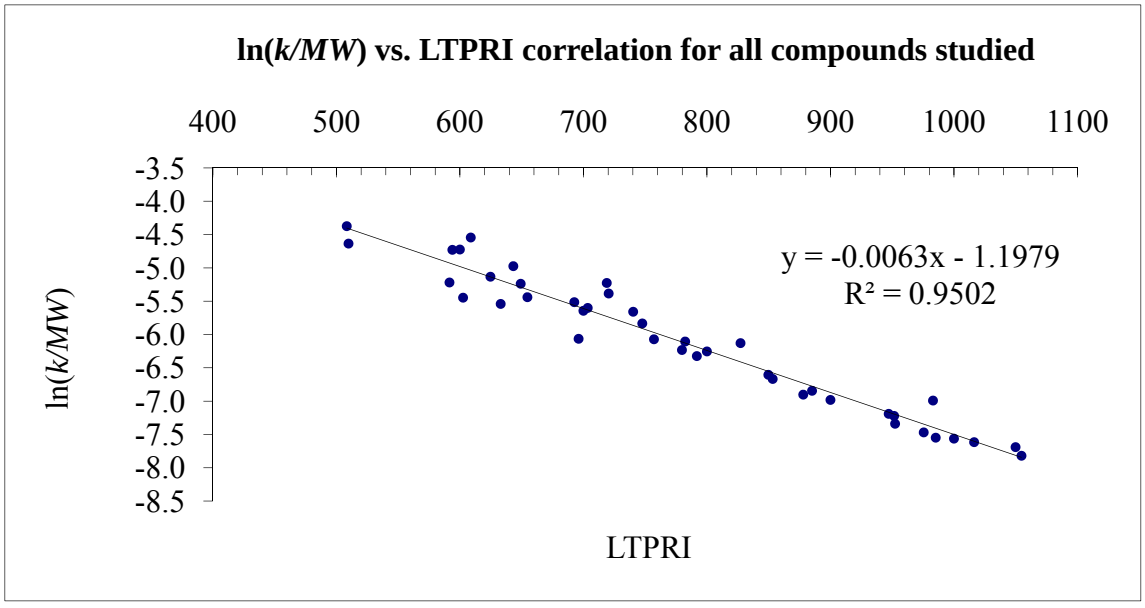

Figure 3-26: ln(*k*/MW) vs. LTPRI correlation for all 41 compounds studied

Table 3-13: Correlation coefficients and regression line equations for the calibration constants at 25˚C (± 1˚C) for different classes of compounds

Compound class	Parameter	ln(*k*)vs. LTPRI	ln(*k*/MW) vs. LTPRI
n-Alkanes	Correlation coefficient: Equation:	0.9976 ln(*k*) = -0.0059 * LTPRI + 3.2489	0.9936 ln(*k*/MW) = -0.007 * LTPRI - 0.6218
Aromatic hydrocarbons	Correlation coefficient: Equation:	0.9865 ln(*k*) = -0.0048 * LTPRI + 2.103	0.9903 ln(*k*/MW) = -0.0061 * LTPRI - 1.3874
Alcohols	Correlation coefficient: Equation:	0.9437 ln(*k*) = -0.006*LTPRI + 3.3192	0.9729 ln(*k*/MW) = -0.0073 *LTPRI - 0.2132
Esters	Correlation coefficient: Equation:	0.9744 ln(*k*) = -0.006*LTPRI + 3.2517	0.9865 ln(*k*/MW) = -0.0073*LTPRI - 0.4933
Chlorinated compounds	Correlation coefficient: Equation:	0.6080 ln(*k*) = -0.0052 * LTPRI + 2.6528	0.8934 ln(*k*/MW) = -0.0076 * LTPRI - 0.6371
Overall correlation for ln(*k*/MW) vs. LTPRI	Correlation coefficient / Equation	0.9502 /	ln(*k*/MW) = -0.0063 * LTPRI - 1.1979
Overall correlation for ln(*k*) vs. LTPRI	Correlation coefficient / Equation	0.9475 /	ln(*k*) = -0.0055 * LTPRI + 2.9049

3.5.5 Statistical analysis of the ln (*k*) vs. LTPRI and ln(*k*/MW) vs. LTPRI correlations

Statistical analysis was performed to determine if there were any significant differences between the various methods used for estimating the calibration constants. The two tailed, paired Student's *t* test was employed for this purpose. The significance of the differences was determined at the 95% confidence level by comparing the calculated *t* value with that of the critical (two tail) value for the respective number of paired observations (n).[214] The experimentally determined calibration constants and the estimated calibration constants using different methods are listed in Table 3-14. The results from the statistical tests are summarized in Table 3-15.

(1) When the experimentally determined calibration constants (k_{exp}) were compared separately with each of the four sets of estimated calibration constants (k_{est}) as in Table 3-14 for all 41 compounds studied (n=41), no significant differences between the values obtained using the different estimation methods and the experimental values were observed in any of the cases. The statistical tests also found no significant differences between the k_{est} values obtained from the class-specific ln(*k*) vs. LTPRI correlations and class-specific ln(*k*/MW) vs. LTPRI correlation, as well as between overall ln(*k*) vs. LTPRI and overall ln(*k*/MW) vs. LTPRI correlations.

The maximum difference between the k_{exp} and the k_{est} obtained using the overall ln(*k)* vs. LTPRI correlation was only 43.2% (1,2-dichloroethane). Analysis of the residuals in this case showed that out of the 41 compounds studied, the calibration constants for 14 of them could be estimated within ±10%, 26 within ± 20%, 37 within ± 30% and all the 41 compounds within ±50%. Considering that the identity of a compound does not have to be known at the time of sampling and analysis when using the ln(*k*) vs. LTPRI correlation, the error related to the estimation of the calibration constants could be considered fairly low.

Table 3-14: Analysis of the residuals (difference between actual and estimated calibration constants) for class-specific and non-class-specific correlations; k_{exp} is the experimentally obtained calibration constant, and k_{est} is the calibration constant estimated using the correlations specified in the Table.

	k_{exp}	LTPRI	Class-specific k_{est} using ln(k) vs. LTPRI correlation	% Diff	Class-specific k_{est} using ln(k/MW) vs. LTPRI correlation	% Diff	k_{est} using ln(k) vs. LTPRI correlation for all compounds studied	% Diff	k_{est} using ln(k/MW) vs. LTPRI correlation for all compounds studied	% Diff
n-hexane	0.765	600	0.747	2.2	0.615	19.5	0.667	12.8	0.587	23.2
n-heptane	0.411	700	0.414	-0.7	0.348	15.3	0.385	6.5	0.364	11.6
n-octane	0.220	800	0.230	-4.6	0.193	12.0	0.222	-1.0	0.221	-0.5
n-nonane	0.119	900	0.127	-6.8	0.106	11.4	0.128	-7.4	0.132	-10.8
n-decane	0.074	1000	0.071	4.5	0.057	22.8	0.074	0.0	0.078	-5.6
Benzene	0.414	649	0.363	12.4	0.372	10.3	0.508	-22.7	0.390	5.8
Toluene	0.213	757	0.216	-1.7	0.227	-6.8	0.281	-32.1	0.233	-9.8
Ethyl benzene	0.135	853	0.136	-0.9	0.146	-7.7	0.166	-22.5	0.147	-8.6
o-xylene	0.113	885	0.117	-3.6	0.120	-6.1	0.139	-23.0	0.120	-6.3
Propyl benzene	0.090	947	0.087	4.0	0.093	-2.7	0.099	-9.1	0.092	-1.6
Butyl benzene	0.061	1050	0.053	13.5	0.055	9.6	0.056	8.5	0.054	12.4
2-methyl-1-propanol	0.788	609	0.717	9.0	0.712	9.7	0.635	19.4	0.478	39.3
n-butanol	0.512	643	0.582	-13.7	0.551	-7.6	0.525	-2.6	0.385	24.9
2,3-dimethyl-2-butanol	0.549	719	0.370	32.6	0.434	20.9	0.347	36.9	0.329	40.0
n-pentanol	0.258	748	0.311	-20.6	0.303	-17.3	0.296	-14.6	0.237	8.2
2-hexanol	0.228	782	0.253	-10.9	0.271	-19.1	0.244	-7.3	0.221	3.1
2,4-dimethyl-3-pentanol	0.253	827	0.193	23.6	0.222	12.4	0.191	24.5	0.189	25.2
n-hexanol	0.138	850	0.169	-21.9	0.165	-19.1	0.169	-21.9	0.144	-4.3
n-heptanol	0.075	952	0.091	-20.8	0.088	-16.3	0.096	-27.2	0.086	-14.0
2-octanol	0.069	985	0.075	-9.0	0.077	-12.3	0.080	-16.6	0.078	-14.1
2-ethyl-1-hexanol	0.064	1016	0.062	3.2	0.061	4.5	0.068	-5.2	0.064	-0.4
n-octanol	0.052	1055	0.049	5.6	0.046	11.8	0.055	-4.6	0.051	3.2
2-methyl-1-butanol	0.404	720	0.367	9.2	0.370	8.3	0.344	14.9	0.281	30.3
3-octanol	0.120	983	0.076	36.7	0.078	34.6	0.081	32.4	0.079	33.7
6-methyl-2-heptanol	0.095	951	0.092	3.7	0.099	-4.0	0.096	-1.3	0.097	-1.9
Ethyl acetate	0.754	594	0.732	2.9	0.704	6.6	0.689	8.6	0.624	17.3
propyl acetate	0.398	693	0.405	-1.8	0.398	0.1	0.401	-0.7	0.389	2.3
methyl butyrate	0.365	703	0.380	-4.1	0.367	-0.7	0.377	-3.5	0.363	0.5
sec.butyl acetate	0.392	740	0.304	22.4	0.319	18.6	0.308	21.4	0.327	16.5
ethyl butyrate	0.221	780	0.240	-8.5	0.239	-8.1	0.248	-12.0	0.255	-15.3
Butyl acetate	0.202	792	0.223	-10.4	0.219	-8.2	0.232	-14.7	0.236	-16.9
propyl butyrate	0.128	878	0.133	-4.2	0.131	-2.4	0.145	-13.1	0.154	-20.5
butyl butyrate	0.081	976	0.074	8.2	0.071	11.9	0.084	-4.6	0.092	-14.3
1,1- Dichloroethylene	1.223	508	1.009	17.5	1.076	12.0	1.103	9.8	1.176	3.8
Dichloromethane	0.824	510	1.001	-21.5	0.932	-13.1	1.094	-32.8	1.021	-23.9
Cis-1,2-Dichloroethylene	0.524	592	0.655	-25.0	0.572	-9.1	0.698	-33.2	0.697	-33.0
Chloroform	0.514	603	0.619	-20.4	0.648	-26.1	0.657	-27.9	0.801	-55.9
1,1,1-Trichloroethane	0.787	625	0.551	29.9	0.612	22.2	0.582	26.0	0.778	1.1
1,2-Dichloroethane	0.388	633	0.528	-36.0	0.426	-9.7	0.556	-43.2	0.548	-41.1
Carbontetrachloride	0.667	655	0.472	29.3	0.562	15.8	0.493	26.0	0.743	-11.4
Trichloroethylene	0.305	696	0.380	-24.5	0.350	-14.6	0.393	-28.6	0.489	-60.0

Table 3-15: Results of the two tailed, paired, student's *t* test employed to determine the significance of the difference between various methods used to estimate the calibration constant at the 95% confidence level. "S" indicates a significant difference and "NS" indicates no significant difference between the two sets of data (variable 1 and variable 2) for the respective group of analytes and corresponding n values. "t Stat" indicates the calculated t value for the data and "t critical two-tail" indicates the tabulated t value at 95% confidence interval.

	Variable 1 →	k_{exp}	k_{exp}	k_{exp}	k_{exp}	k_{est} using class specific ln(k) vs. LTPRI correlation	k_{est} using overall ln(k) vs. LTPRI correlation
Analytes	**Variable 2 →**	k_{est} using class specific ln(k) vs. LTPRI correlation	k_{est} using class specific ln(k/MW) vs. LTPRI correlation	k_{est} using overall - ln(k) vs. LTPRI correlation	k_{est} using overall ln(k/MW) vs. LTPRI correlation	k_{est} using class specific ln(k) vs. LTPRI correlation	k_{est} using overall ln(k/MW) vs. LTPRI correlation
All compounds (n=41)	Significance	NS	NS	NS	NS	NS	NS
	t Stat	0.59	1.39	0.67	-0.42	0.89	-1.39
	t Critical two-tail	2.02	2.02	2.02	2.02	2.02	2.02
n-alkanes (n=5)	Significance	NS	NS	NS	NS	NS	NS
	t Stat	-0.03	2.12	1.38	0.98	2.51	0.06
	t Critical two-tail	2.78	2.78	2.78	2.78	2.78	2.78
Aromatic hydrocarbons (n=6)	Significance	NS	NS	NS	NS	**S**	NS
	t Stat	1.04	0.28	-2.31	-1.21	-4.68	1.66
	t Critical two-tail	2.57	2.57	2.57	2.57	2.57	2.57
Alcohols (n=14)	Significance	NS	NS	NS	**S**	NS	NS
	t Stat	0.85	0.74	1.71	2.25	-0.87	1.97
	t Critical two-tail	2.16	2.16	2.16	2.16	2.16	2.16
Esters (n=8)	Significance	NS	NS	NS	NS	NS	NS
	t Stat	0.48	1.00	1.00	0.14	1.28	-2.19
	t Critical two-tail	2.36	2.36	2.36	2.36	2.36	2.36
Chlorinated compounds (n=8)	Significance	NS	NS	**S**	NS	NS	**S**
	t Stat	0.03	0.16	-3.52	-0.35	0.18	-3.97
	t Critical two-tail	2.36	2.36	2.36	2.36	2.36	2.36

Using the overall ln(k/MW) vs. LTPRI correlations resulted in maximum differences of 23.2% for alkanes, -12.4% for aromatic hydrocarbons, 40.0% for alcohols, -20.5 % for esters, and -60.0% for the chlorinated hydrocarbons. Even though the correlation coefficients for the ln(k/MW) vs. LTPRI relationship were higher, the statistical analysis indicated that the estimated calibration constants were not necessarily more accurate than those obtained with the overall ln(k) vs. LTPRI correlation.

The maximum differences between the k_{exp} and the k_{est} obtained using class specific ln(k) vs. LTPRI correlation were -6.8% for alkanes, 13.5% for aromatic hydrocarbons, 36.7 % for alcohols, 22.4 % for esters, and –36.0% for chlorinated hydrocarbons. The maximum differences between k_{exp} and k_{est} obtained using class-specific ln(k/MW) vs. LTPRI correlations were 22.8% for n-alkanes, 10.3% for aromatic hydrocarbons, 36.9% for alcohols, 18.6% for esters, and –26.1% for chlorinated hydrocarbons.

(2) Statistical comparisons of k_{exp} values with the four sets of k_{est} values (Table 3-14) were also performed separately by considering the individual groups of analytes (n=5, 6, 14, 8, and 8 for n-alkanes, aromatic hydrocarbons, alcohols, esters and chlorinated compounds respectively). The tests indicated no significant differences between the respective pairs of methods for n-alkanes, and esters. In the case of chlorinated compounds, the tests indicated that there were no significant differences between the experimental values and the estimates obtained using the different methods with the exception of the k_{est} values obtained using the ln(k) vs. LTPRI correlation. As discussed earlier, this can be attributed to the disproportionate increase in the molecular weight of the chlorinated compounds with increasing number of chlorine atoms. For example, chloromethane is almost the same size as carbon tetrachloride, but its molecular weight is almost 3 times lower. Consequently, the relative diffusion coefficients of these analytes play an important role in determining the calibration constants of the samplers. Such drastic variations in molecular weights were not observed for the other homologous groups of compounds considered, hence no corrections for the diffusion coefficients were necessary. On the other hand, for alcohols a significant difference was observed between the k_{exp} values and the k_{est} values obtained from the overall ln(k/MW) vs. LTPRI correlation. In this case, the structure of the individual linear and branched alcohols played an important role in deciding both the partition coefficients and the

diffusion coefficients in PDMS, as discussed earlier. Consequently, corrections for the molecular weight did not account for the observed variations in permeability of alcohols through PDMS.

In the case of aromatic hydrocarbons, the calibration constants for all the individual analytes obtained using class specific ln(k/MW) vs. LTPRI correlation were consistently higher than those obtained using the class specific ln(k) vs. LTPRI correlation. Consequently, the test showed significant difference between the two methods used for estimating the calibration constants.

For n-alkanes and esters, there were no significant differences between k_{est} values obtained from the class-specific ln(k) vs. LTPRI correlations and the class-specific ln(k/MW) vs. LTPRI correlations, as well as between k_{est} values obtained from the overall ln(k) vs. LTPRI correlation and the overall ln(k/MW) vs. LTPRI correlation. In general, even though the correlation coefficients were consistently higher for the correlations obtained for all classes of compounds using the ln(k/MW) vs. LTPRI relationship, analysis of the residuals showed no significant improvement in the accuracy of the estimation of the calibration constants except for the chlorinated compounds. Applications of the various estimation methods in practical situations are described in the next section.

3.5.6 Application of the calibration constant – LTPRI relations for field analysis

The concept of estimating the calibration constants based on the LTPRI of the analytes can be used if necessary following the schematic shown in Figure 3-27. Determining analyte concentration over a specific time period by passive sampling requires the knowledge of two parameters in general: the calibration constant and the chromatographic response factor for the analyte. If the calibration constant is not known, it can be estimated based on the class-specific correlation or the overall correlation (depending on whether the identity of the analyte can be determined, e.g. using mass spectrometry). If the identity of the analyte is established after the analysis of the samplers, the chromatographic detector can be calibrated for that specific analyte; on the other hand, if the analyte identity cannot be established, a flame ionization detector can be used based on the assumption that the response factor for the unknown analyte is similar to that of a standard such as benzene or toluene.

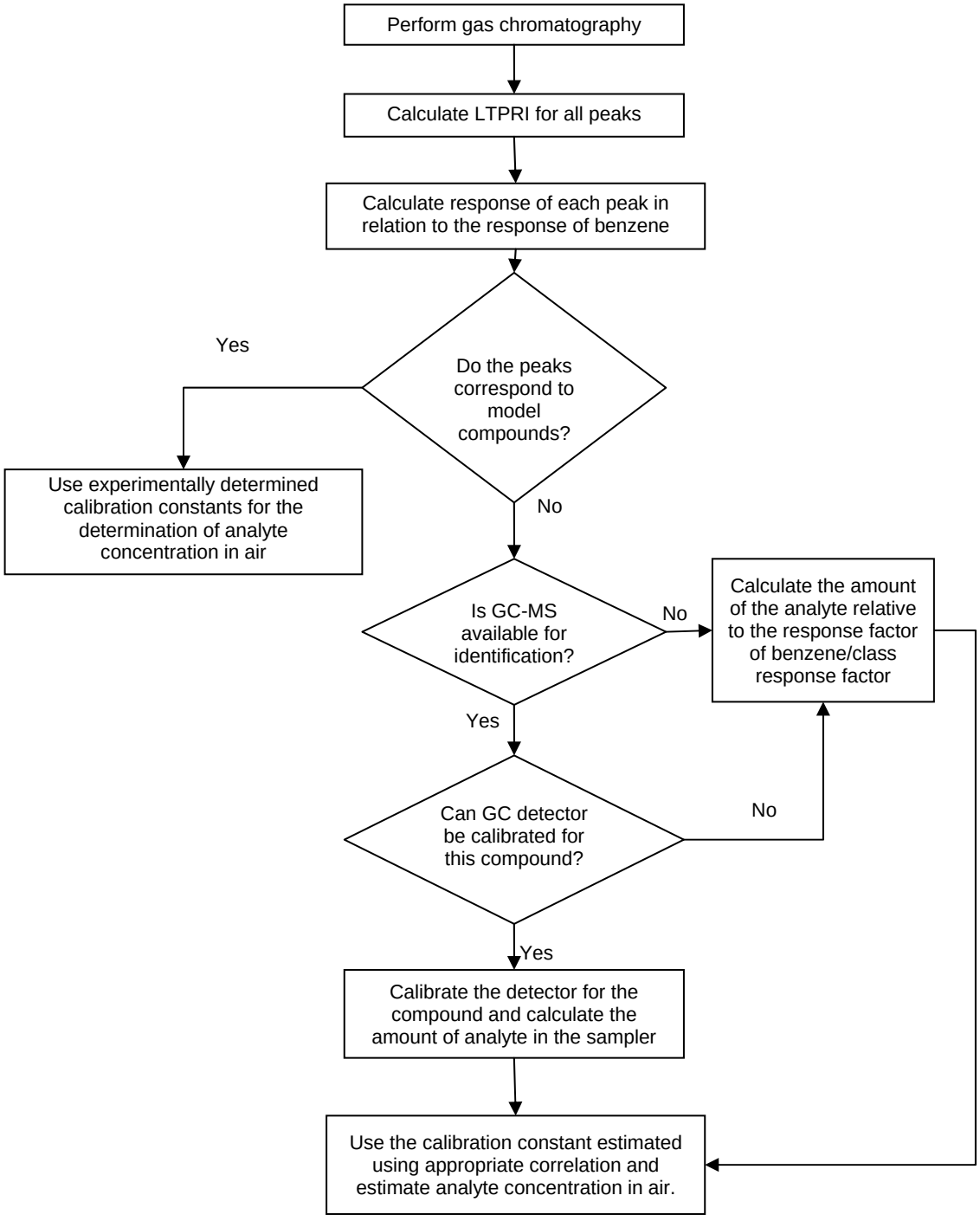

Figure 3-27: Schematic of the method for the determination/estimation of analyte concentrations in the vapor phase

Using the estimated calibration constant based on the overall correlation between ln(k) and LTPRI, combined with the use of FID as a detector for GC, can then be a powerful technique to estimate total parameters such as Total Petroleum Hydrocarbons (TPH) in vapor phase. Such approach to the determination of TPH is not possible with diffusive-type passive samplers.

The calibration constants determined in this study have not only enabled the development of models to estimate calibration constants for unknown compounds, but also allowed the determination of the permeability of PDMS towards the respective analytes for general use in analytical techniques based on the use of PDMS. This will be discussed in the next section of this thesis.

3.5.7 Determination of permeability of PDMS towards VOCs

Experiments reported in this section were conducted under ideal conditions of good air circulation in the calibration chamber; hence the calibration constants were dependent only on the permeability of the polymer towards the analytes and the geometry of the membrane. By definition, the relationship between the calibration constant and permeability (Chapter 2) is,

$$k = \frac{L_m}{PA}$$

Permeabilities of the PDMS membrane towards the 41 model compounds were determined based on this equation and are provided in Table 3-16. The permeabilities were valid assuming that the exposed membrane area was equal to the area of the opening of the sampler's aluminum crimp cap. The knowledge of PDMS permeability towards various analytes listed in the table might be valuable for the development of related analytical techniques (which use analyte permeation through PDMS membranes), such as membrane inlet mass spectrometry (MIMS) and membrane extraction with a sorbent interface (MESI).

Table 3-16: Permeability of PDMS towards various n-alkanes, aromatic hydrocarbons, alcohols, esters and chlorinated compounds determined based on the relationship between the calibration constant and permeability.

Compounds	P (cm^2 min^{-1})
n-hexane	0.041
n-heptane	0.077
n-octane	0.144
n-nonane	0.265
n-decane	0.428
Benzene	0.076
Toluene	0.149
Ethyl benzene	0.234
o-xylene	0.280
Propyl benzene	0.350
Butyl benzene	0.516
2-methyl-1-propanol	0.040
n-butanol	0.062
2,3-dimethyl-2-butanol	0.058
n-pentanol	0.123
2-hexanol	0.139
2,4-dimethyl-3-pentanol	0.125
n-hexanol	0.229
n-heptanol	0.419
2-octanol	0.461
2-ethyl-1-hexanol	0.493
n-octanol	0.605
2-methyl-1-butanol	0.078
3-octanol	0.264
6-methyl-2-heptanol	0.333
Ethyl acetate	0.042
Propyl acetate	0.080
Methyl butyrate	0.087
sec.butyl acetate	0.081
Ethyl butyrate	0.143
Butyl acetate	0.156
Propyl butyrate	0.248
Butyl butyrate	0.392
1,1- Dichloroethylene	0.026
Dichloromethane	0.038
Cis-1,2-Dichloroethylene	0.060
Chloroform	0.062
1,1,1-Trichloroethane	0.040
1,2-Dichloroethane	0.082
Carbontetrachloride	0.047
Trichloroethylene	0.104

3.6 Conclusions

Calibration constants of TWA-PDMS samplers were determined for 41 model compounds belonging to various chemical classes, including n-alkanes, aromatic hydrocarbons, alcohols, esters and chlorinated compounds. Reproducibilities of the extraction efficiencies and the calibration constants were very good. The extraction and the chromatographic method were free of interferences from compounds extracted with CS_2 from the PDMS membrane.

The correlations between ln(k) and LTPRI, as well as ln(k/MW) and LTPRI, were generally good for all classes except the chlorinated compounds. For the chlorinated compounds, ln(k/MW) vs. LTPRI was a better model than ln(k) vs. LTPRI. The approach proposed in this thesis allows easy and fast estimation of the calibration constants of permeation passive samplers equipped with PDMS membranes. Using LTPRI for the estimation of the calibration constants comes with the advantage that compound identity need not necessarily be known at the time of sampling. This is very important, as the decision to sample air or soil gas does not necessarily come with the knowledge of the identity of the analytes. Once the identity of the compound is known after the exposure in the field, class-specific correlations can be used to estimate the calibration constants with better accuracy. Also, the chromatographic detector can be calibrated for the target compounds once their identity is established. If not, detectors such as FID, with uniform response towards most organic compounds, can be utilized for analyte quantification. The results presented in the thesis should help in broader adoption of permeation passive sampling in different application areas
.

CHAPTER 4

Effect of temperature, humidity and linear flow velocity of air on the calibration constants

The three environmental variables which may directly or indirectly affect the uptake rates of passive samplers are temperature, humidity and air flow patterns around the sampler. In this chapter, the theoretical aspects and experimental results obtained in calibration experiments at different temperatures, humidity levels and linear flow velocities of air across the surface of the sampler will be discussed.

4.1 Theoretical considerations

4.1.1 Effect of temperature

Temperature can play an important role in determining the uptake rate of a sampler depending on the type of the polymer membrane used as the barrier. Temperature dependence of polymer permeability towards a given analyte is determined by the temperature dependences of the diffusion coefficient of the molecule in the polymer, as well as its partition coefficient between air and the polymer. The partition coefficient and diffusion coefficient of the molecule, and consequently the permeability of the polymer towards a particular analyte, can be expressed as a function of temperature using Van't Hoff's and Arrhenius equations:[2]

$$P = P_o \exp\left[- E_p \left(\frac{1}{RT} - \frac{1}{RT_o} \right) \right] \tag{4.1}$$

$$K = K_o \exp\left[- \Delta H_s \left(\frac{1}{RT} - \frac{1}{RT_o} \right) \right] \tag{4.2}$$

$$D = D_o \exp\left[- E_d \left(\frac{1}{RT} - \frac{1}{RT_o} \right) \right] \tag{4.3}$$

$$DK = D_o K_o \exp\left[- \left(E_d + \Delta H_s \right) \left(\frac{1}{RT} - \frac{1}{RT_o} \right) \right] \tag{4.4}$$

where P_o, K_o and D_o are the permeability constant, partition coefficient and diffusion coefficient at a temperature T_o, E_p is the activation energy for permeation, ΔH_s is the heat of sorption of the analyte in the membrane, and E_d is the activation energy for diffusion.[215] Combining equations (4.1), (4.2) and (4.3), we can express the activation energy of permeation as:

$$E_p = E_d + \Delta H_s \tag{4.5}$$

Equation (4.5) shows that the temperature dependence of permeability is a function of the analyte's heat of solution and its activation energy for diffusion. For PDMS, the diffusion coefficient of a molecule in the polymer increases with increase in temperature, and the partition coefficient of the molecule decreases with increase in temperature. In other words, E_d is greater than zero (positive), and ΔH_s is less than zero (negative) for most volatile organic compounds. This observation is in agreement with the permeability characteristics of PDMS membranes reported by Boscaini et al.[188] and Mark et al.[216] (among others). Since E_d and ΔH_s oppose each other, there is a trade-off in the net permeability with change in temperature. This eventually results in the permeability generally being a weak function of temperature when compared to many other polymers. Further, the net change in the permeability of the polymer membrane with temperature is decided based on which of these two parameters defining the activation energy of permeation is dominating.

To understand how the temperature affects the calibration constant, theoretical relationships between the two parameters were derived as follows.

Equation (4.1) suggests that

$$\ln P = \ln P_o - \frac{E_p}{RT} + \frac{E_p}{RT_o} \tag{4.6}$$

From the definition of the calibration constant introduced in Chapter 2 (Equation 2.4), we can arrive at the relationship as in Eq. (4.7).

$$\ln(k) = \ln\left(\frac{L_m}{A}\right) - \ln(P) \tag{4.7}$$

Equations (4.6) and (4.7) can then be used to derive the relationship between temperature and the calibration constant as in equation (4.8).

$$\ln k = \ln\left(\frac{L_m}{A}\right) - \ln P_o - \frac{E_p}{RT_o} + \frac{E_p}{R}\left(\frac{1}{T}\right) \tag{4.8}$$

According to equation (4.8), a linear relationship should exist between ln(k) and 1/T. Furthermore, it should be possible to calculate the activation energy of permeation from the slope of this linear relationship. Experiments can therefore be performed to determine the calibration constants of the samplers towards various analytes at different temperatures, and the E_p can be determined from the slope of the ln (k) vs. 1/T line.

4.1.2 Effect of humidity

One of the motivations to use a PDMS membrane as the barrier in the passive sampler is its low permeability towards water molecules. In the case of diffusive samplers, the uptake rates of various molecules are determined exclusively by their diffusion coefficients in air. The diffusion coefficients of water vapour and toluene in air at atmospheric pressure and 25°C are 0.251 cm^2s^{-1} and 0.0827 cm^2s^{-1}, respectively.[217,218] Consequently, the uptake rate of water for diffusive-type passive samplers is roughly 3 times higher than that for toluene. On the other hand, the permeability of toluene in PDMS is approximately 63 times higher than that of water vapour.[212] Accordingly, the uptake rate of water should be only about 0.0157 times that of toluene when using the TWA-PDMS sampler. Consequently, the chance of the sorbent getting saturated with water (eventually leading to non-linear sorption of the analyte molecules) should theoretically be very low when compared to that of diffusive-type passive samplers. In other words, by using the TWA-PDMS samplers, it should be possible to prolong the exposure period in humid atmospheres without risking sorbent saturation. This is particularly valuable when using the samplers for soil gas testing, where the relative humidity is typically very close to 100%.

4.1.3 Effect of linear flow velocity of air

During the discussion of the theory of the permeation-type passive samplers, it was assumed that the boundary layer effect is minimal as shown in Figure 2-1. In practice, the boundary

layer effect is minimal only when the air velocity around the sampler is sufficiently high. When the linear flow velocity is below a certain value, a boundary layer will always exist (Figure 4-1), as the analyte is supplied to the outside surface of the membrane at a rate slower than the rate at which it is transported into the sampler. The magnitude of this starvation effect depends on two parameters: the analyte transport rate through the membrane defined by the permeability of PDMS, and the analyte transport rate within the boundary layer defined by the diffusion coefficient of the analyte in air. The starvation effect is more pronounced for compounds for which PDMS permeability is higher because they are removed from the air near the sampler more rapidly. Since the mass transport across the boundary layer is generally slower for larger molecules (generally characterized by larger permeability), the magnitude of the starvation effect usually increases when the size of the molecule increases.

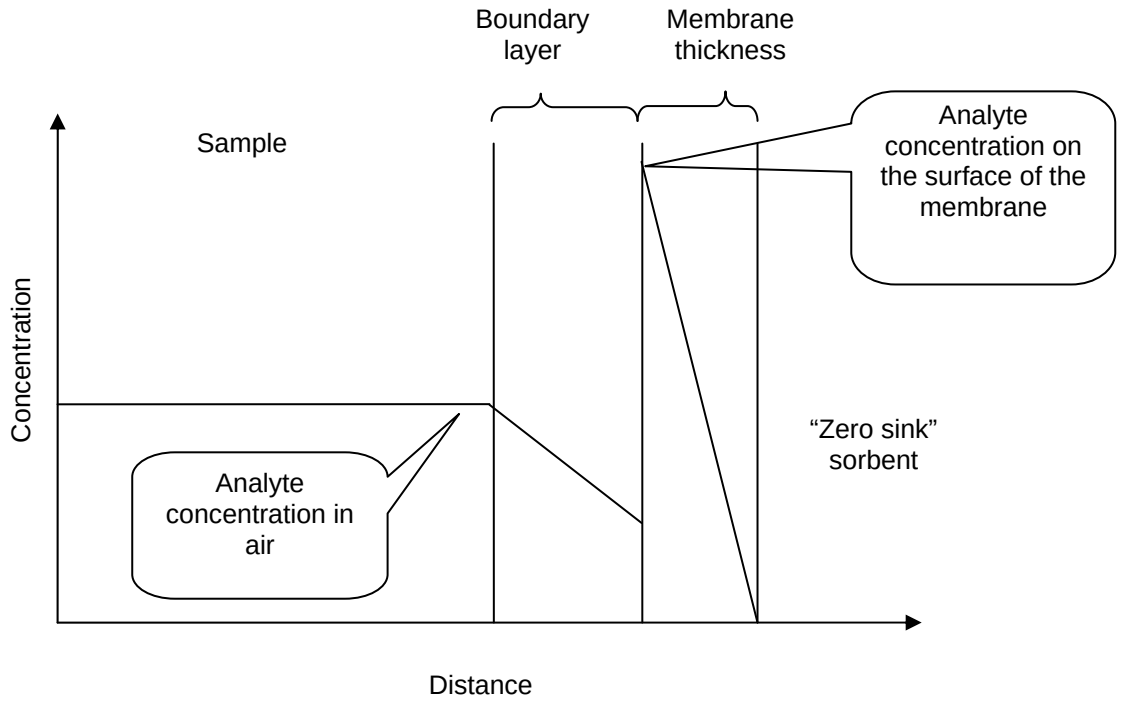

Figure 4-1: Concentration profile for permeation samplers with starvation effect and with an ideal sorbent.

In the case of diffusive-type passive samplers, the rate of mass transport of various analytes through the diffusion barrier decreases with a decrease in their diffusion coefficients.

Consequently, for such samplers, analytes with lower diffusion coefficients in air will be less depleted in the boundary layer and hence the starvation effect will be lower.

4.2 Experimental methods

The experiments to determine the effect of temperature, humidity and linear flow velocity of air on the calibration constants employed the same quantification methods and chemicals as described in Chapter 3. The necessary modifications in the sampler design and exposure chamber are described in the respective sections.

4.2.1 Effect of temperature

For determining the effect of temperature and humidity on the uptake rates of passive samplers, it is critical to keep all other variables affecting the uptake rate constant, including the membrane thickness. Since the sampler shown in Figure 3-5 cannot be re-used after one exposure, a re-usable vial was designed and fabricated in the glass shop at the University of Waterloo as shown in Figure 4-2.

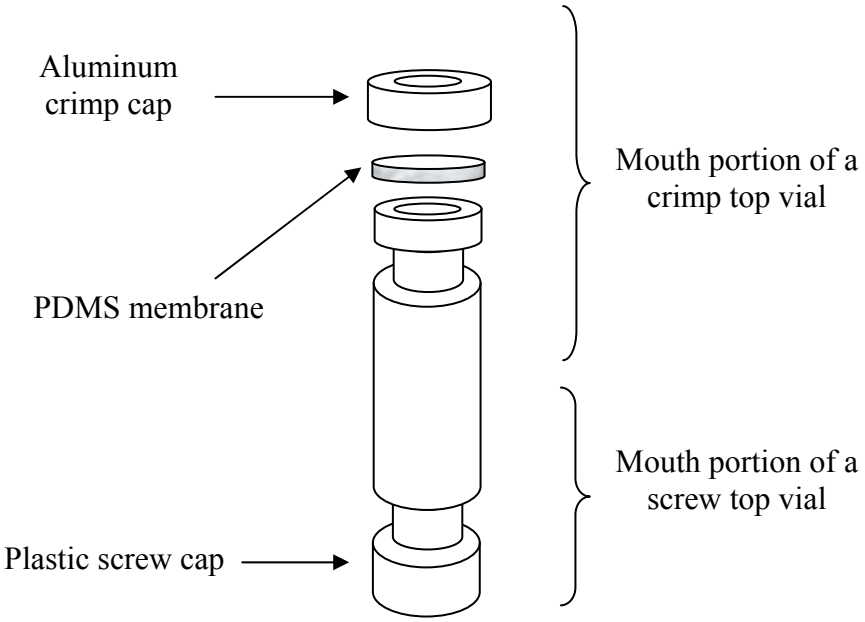

Figure 4-2: Design of a re-useable TWA-PDMS sampler

The sampler fabrication involved cutting the bottoms of a crimp cap vial and a screw cap vial (both of same internal and external diameters) and fusing the open vial ends together. This enabled removing the sorbent from the vials through the screw cap end without disturbing the membrane, followed by solvent desorption and chromatographic analysis as per the scheme illustrated in Figure 3-16. Consequently, the sampler design allowed the use of the same set of 7 samplers for the experiments at different temperatures.

Experiments were performed with three sets of compounds; alkanes and aromatic hydrocarbons together, linear and branched alcohols together and esters. The list of analytes is provided in Table 4-1. The experiments were performed at 4 different temperatures ranging from approximately 10 °C to 40 °C for each set of compounds. These experiments were conducted at 0% relative humidity, as the effect of humidity on the calibration constants had not been studied at that time. It was also desired to determine the energy of activation of permeation without introducing any error related to non-zero humidity (if any). Further, the fan in the calibration chamber was operated at the maximum speed in order to eliminate any starvation effects. The average weight of the 7 membranes used for the fabrication of the samplers was 8.6 mg ± 0.20 mg.

Table 4-1: List of analytes used in the experiments for determining the effect of temperature on the calibration constant.

Analyte group	Analytes
n-alkanes	n-hexane, n-heptane, n-octane, n-nonane and n-decane
Aromatic hydrocarbons	Benzene, toluene, ethyl benzene, propyl benzene, and butyl benzene.
Esters	Propyl acetate, methyl butyrate, sec-butyl acetate, ethyl butyrate, butyl acetate, propyl butyrate and butyl butyrate.
Linear and branched alcohols	n-butanol, n-pentanol, n-hexanol, n-heptanol, n-octanol, 2-methyl-1-propanol, 2,3-dimethyl-2-butanol, 2-hexanol, 2,4-dimethyl-3-pentanol, 2-octanol, and 2-ethyl-1-hexanol.

4.2.2 Effect of humidity

The experimental setup for the generation of the standard gas mixtures was modified to produce the desired humidity levels. The modified experimental setup, as shown in Figure 4-3, involved splitting the dry nitrogen gas prior to its delivery to the exposure chamber into two streams. One part was saturated with water by bubbling the gas through water in a 2.5 liter glass jar, while the other was passed through the vessel containing the permeation tubes. The flow rates of the two streams, and hence the humidity at the outlet, could be controlled using needle valves A and B. The humidity of the resulting standard gas mixture was measured using a hygrometer (Model 11-661-7D) procured from Fisher Scientific Inc., (Ottawa, ON). The experiments performed using the n-alkanes and aromatic hydrocarbons as the model compounds (see Table 4-1) were carried out at four relative humidity levels: approximately 0%, 29%, 60% and 91%. The exposure time durations in these experiments were 4705, 3230, 2997 and 8997 minutes, respectively. The 8997 minutes (6.24 days) exposure at 91% humidity was carried out to test the performance of the sampler under "worst case scenario" conditions of high humidity and long exposure duration. The temperature of the calibration chamber was maintained at 25°C ± 2°C for all the experiments.

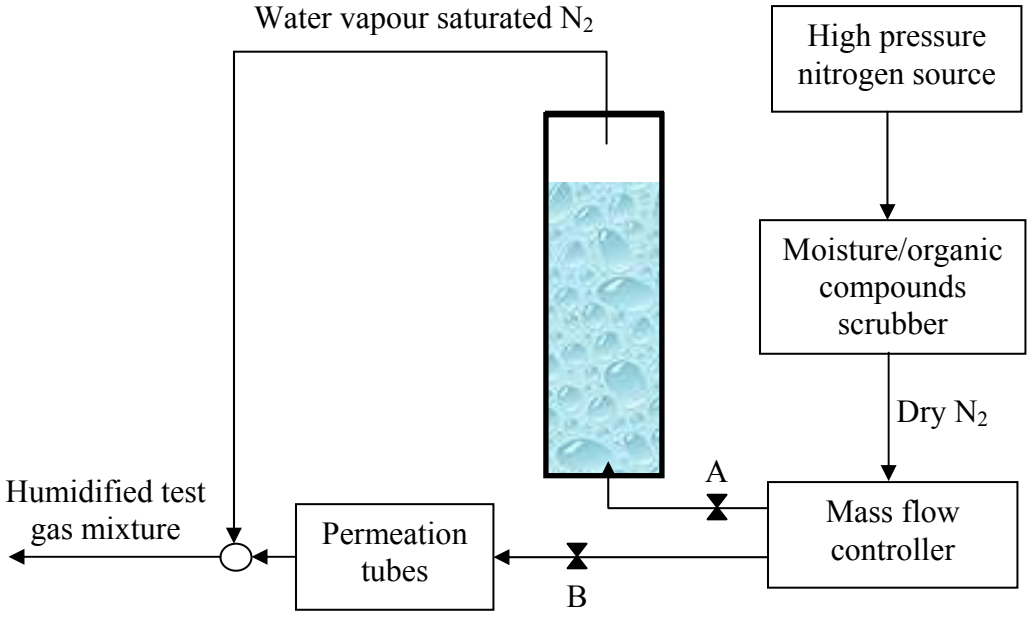

Figure 4-3: Schematic representation of the experimental setup used for generating the test gas atmosphere with the required humidity.

4.2.3 Effect of linear flow velocity of air

The calibration chamber was modified to expose the samplers to different linear flow velocities of air across their surfaces. Figure 3-13 in Chapter 3 illustrates the calibration chamber used for the experiments described so far. The shaft from the motor was originally attached to a fan blade. For the experiments aimed at determining the effect of face velocity, the blade was replaced by a custom made part made from PTFE as shown in Figure 4-4. Nine holes were drilled into the PTFE block so as to snugly hold the passive samplers. The holes were drilled in such a way that 8 samplers could be placed at distances from 2 cm to 9 cm, in steps of 1 cm, from the center of the PTFE block. A hole was also drilled at the center of the PTFE block to simulate zero flow velocity across the surface of the sampler. When the motor rotated, the shaft and the PTFE block also rotated. The sampler at the center of the PTFE block was then expected to experience practically no flow of air across its surface, while the other samplers experienced non-zero linear air flows, their magnitude being dependent on the samplers' distances from the centre of the shaft.

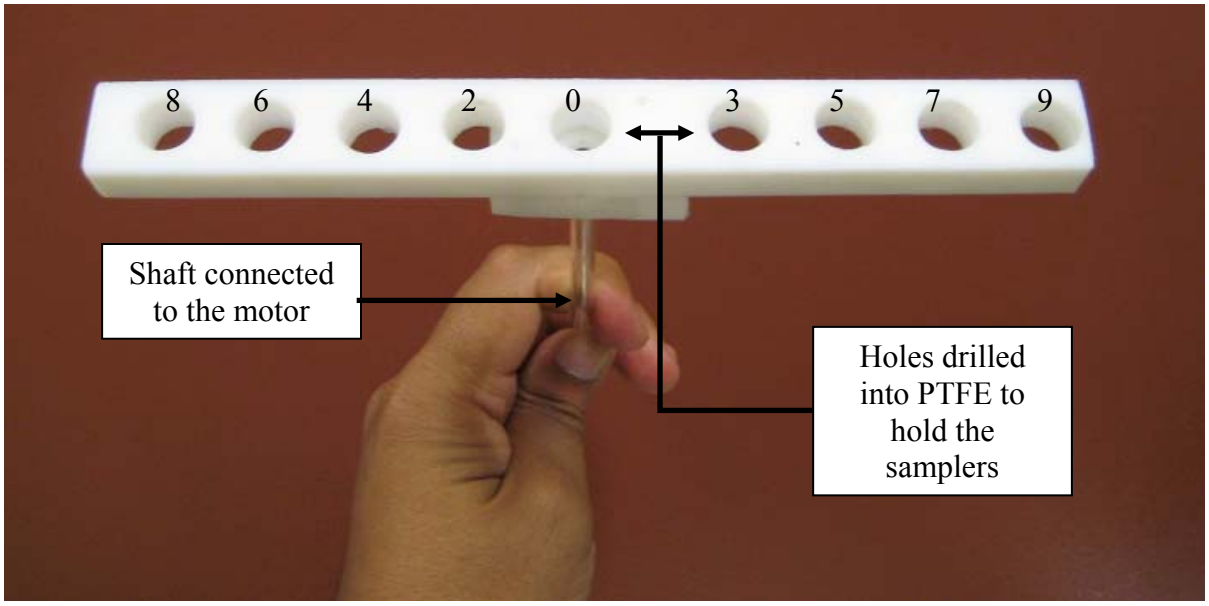

Figure 4-4: Photograph of the PTFE holder. The number next to each hole indicates the distance in centimeters from the centre of the PTFE block.

A single experiment was performed at a rotational speed of 64.5 revolutions per minute. The linear flow velocities of air across the surface of the samplers were calculated using the

circumference covered by each sampler. The experiments were performed at 25°C ± 2°C, and 0% relative humidity. The analytes used for this study were n-alkanes and aromatic hydrocarbons listed in Table 4-1.

4.3 Results and discussion

The results obtained from the experiments allowed the determination of the fundamental transport properties of PDMS (energy of activation of permeation) towards the model compounds used in the study and provided critical information on the variability of the calibration constants with temperature, humidity and linear flow velocity of air that should be carefully considered during field deployment of the samplers. The results are discussed in the next three sub-sections.

4.3.1 Effect of temperature

The calibration constants of n-alkanes and aromatic hydrocarbons determined at 10°C, 19.7°C, 29.9°C and 39.5°C are listed in Table 4-2. The calibration constants increased with increase in temperature in all cases. By definition, the calibration constant is inversely proportional to the permeability of PDMS towards an analyte. Consequently, the experimental results indicated that the permeability decreased with increase in temperature. This is in agreement with many observations on the permeability of PDMS as a function of temperature, as discussed in the theory section. A plot of 1/T vs ln(k) for each of the n-alkanes and aromatic hydrocarbons, as shown in Figures 4-5 and 4-6, reiterated the earlier observations noted in the literature that the permeability is related to temperature through Arrhenius-type relationships for PDMS. The correlation was good for all the analytes studied, with the correlation coefficients ranging from 0.9082 for n-hexane to 0.9990 for propyl benzene.

The slopes of the correlations were used to determine the energy of activation of permeation (using equation 4.8) and are listed in Table 4-3 along with the standard error of the slope. The energy of activation of permeation was negative, which shows that the heat of solution (ΔH_s) of the analytes in PDMS was the dominating factor when compared with the energy of activation of diffusion (E_d) within the polymer (refer to equation 4.5). Within the n-alkanes

homologous series, the E_p values decreased from -8 kJ mole^{-1} for n-hexane to -13 kJ.mole^{-1} for n-nonane, and then increased again to -7 kJ.mole^{-1} for n-decane. A similar trend within the aromatic hydrocarbons was noticed where the E_p decreased from -8 kJ mole^{-1} for benzene to -11 kJ mole^{-1} for ethyl benzene, and increased again to -5 kJ mole^{-1} for butyl benzene**.** Nevertheless, the E_p values were all within the same order of magnitude, as has been observed by other researchers.[188]

For n-hexane, the increase in temperature from 10°C to 39.5°C resulted in the uptake rate decreasing from 1.24 mL/min to 0.9 mL/min, a decrease of 27.3% in the uptake rate. This corresponds to an average decrease in the uptake rate of about 0.9% per °C change within the temperature range studied. Within the n-alkanes group, n-octane had the highest average percentage decrease of 1.4% in the uptake rate per °C increase in temperature. Mathematically, the closer the energy of activation of permeation is to zero, the smaller is the effect of a change in temperature on the calibration constant.

Table 4-2: Calibration constants of selected n-alkanes and aromatic hydrocarbons determined at 4 different temperatures. The average values are for n=7.

Temperature		n-hexane	Benzene	n-heptane	Toluene	n-octane	Ethyl benzene	o-xylene	n-nonane	Propyl benzene	n-decane	Butyl benzene
10°C	Average	0.804	0.428	0.356	0.194	0.167	0.115	0.097	0.093	0.075	0.065	0.055
	STD	0.051	0.023	0.026	0.012	0.012	0.008	0.006	0.007	0.006	0.005	0.004
	% RSD	6.4	5.4	7.2	5.9	7.4	7.1	6.6	7.6	7.4	8.1	7.9
19.7°C	Average	0.96	0.51	0.44	0.23	0.21	0.14	0.11	0.111	0.09	0.073	0.06
	STD	0.05	0.03	0.02	0.01	0.01	0.01	0.00	0.004	0.00	0.004	0.00
	% RSD	5.4	5.0	4.7	4.0	4.0	3.8	3.9	4.0	4.2	5.1	5.4
29.9°C	Average	1.099	0.569	0.517	0.273	0.245	0.161	0.130	0.123	0.098	0.080	0.064
	STD	0.068	0.035	0.033	0.016	0.016	0.009	0.008	0.007	0.005	0.004	0.003
	% RSD	6.2	6.1	6.4	6.0	6.4	5.8	5.8	5.8	5.5	5.2	4.9
39.5°C	Average	1.106	0.588	0.556	0.297	0.283	0.183	0.150	0.147	0.111	0.087	0.068
	STD	0.114	0.058	0.056	0.030	0.028	0.018	0.015	0.014	0.010	0.008	0.006
	% RSD	10.3	9.8	10.1	10.1	9.7	9.7	9.8	9.4	9.2	8.7	8.5

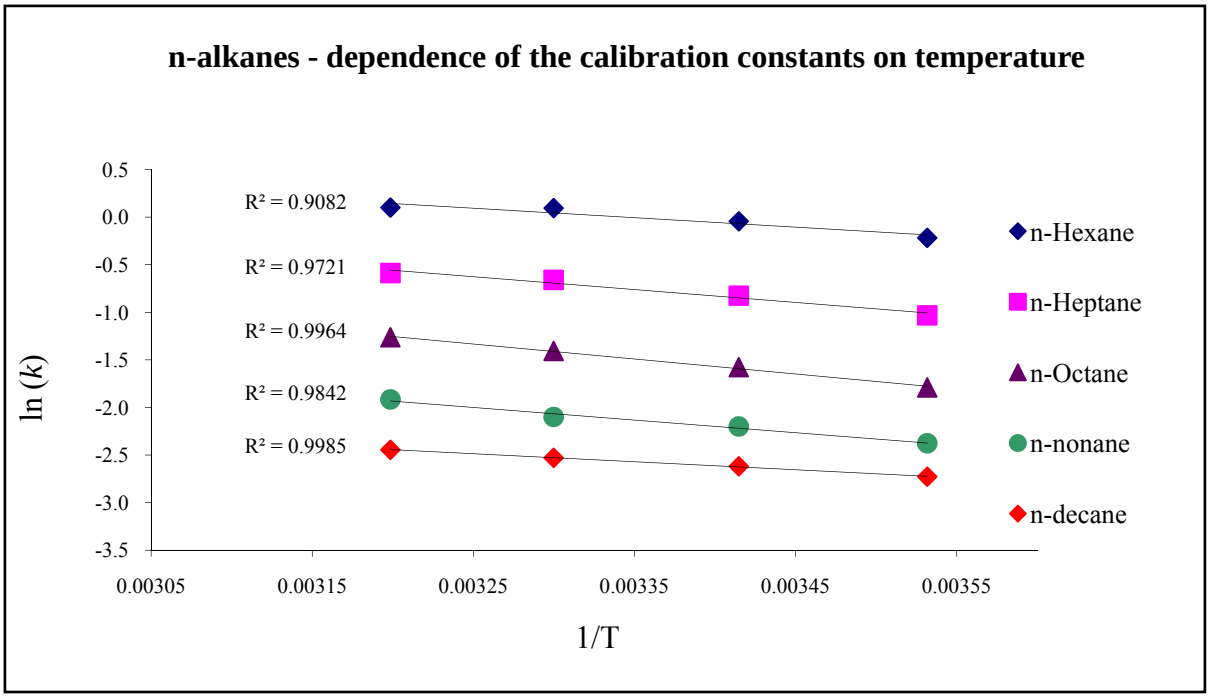

Figure 4-5: Arrhenius-type relationship between ln(*k*) and 1/T for n-alkanes.

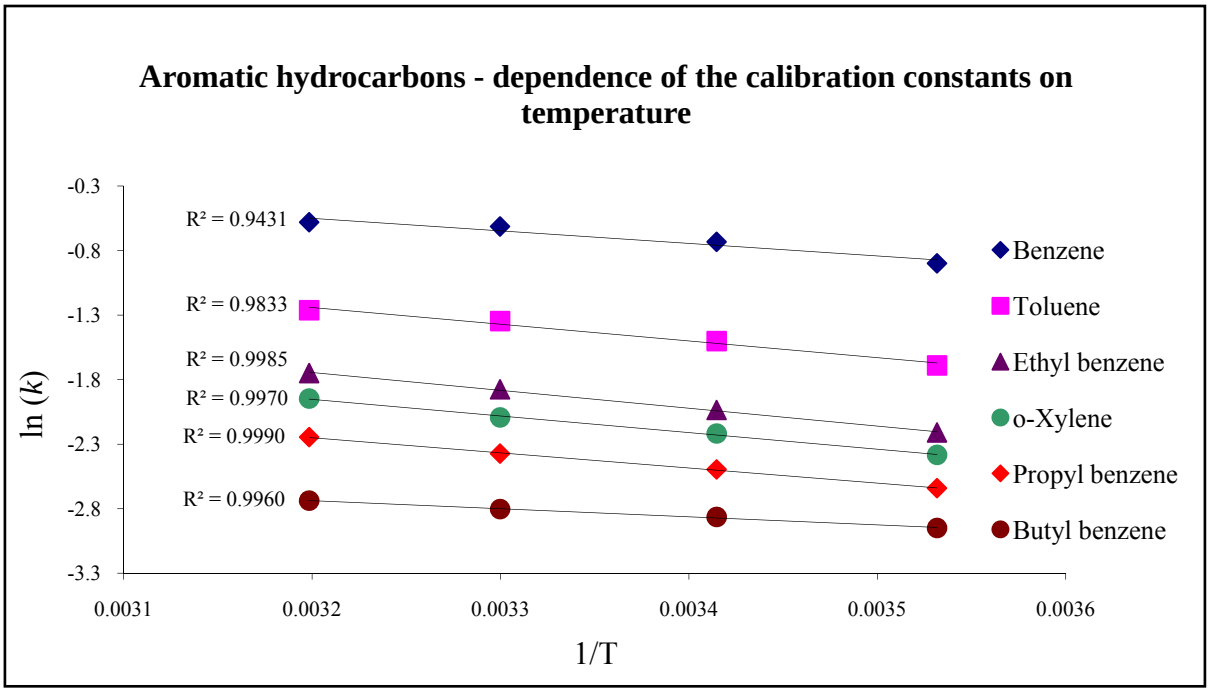

Figure 4-6: Arrhenius-type relationship between ln(*k*) and 1/T for aromatic hydrocarbons.

Table 4-3: Energy of activation of permeation for selected n-alkanes and aromatic hydrocarbons determined using the slope of the Arrhenius-type plots shown in Figures 4-5 and 4-6.

Compound	Slope $\times 10^{-3}$	Standard error of the slope $\times 10^{-2}$	E_p (kJ mole^{-1})	R^2 for the ln(k) vs. 1/T correlation
n-hexane	-1	2.2	-8	0.9082
n-heptane	-1.3	1.6	-11	0.9721
n-octane	-1.6	1	-13	0.9964
n-nonane	-1.3	1.2	-11	0.9842
n-decane	-1	0	-7	0.9985
Benzene	-1	1.7	-8	0.9431
Toluene	-1.3	1.2	-11	0.9833
Ethyl benzene	-1.3	0	-11	0.9985
Propyl benzene	-1.2	0	-9.7	0.9990
Butyl benzene	-1	0	-5	0.9960
o-xylene	-1.3	0	-11	0.9970

A similar trend of increasing calibration constants with increase in temperature (Table 4-4) was also observed for all esters. The linearity of the ln(k) vs. LTPRI curve was good for 5 out of the 7 compounds studied with the correlation coefficient greater than 0.98, as shown in Figure 4-7. The correlation for propyl butyrate and butyl butyrate deviated from the straight line, which could partially be attributed to their high uptake rates and consequently higher starvation effect despite the best efforts to have proper air circulation inside the calibration chamber. A slight deviation from linearity was observed for sec-butyl acetate, but the

correlation coefficient (0.9869) was not as bad as that for propyl butyrate and butyl butyrate. The energy of activation of permeation for all the esters was calculated (Table 4-5). The values were generally lower than those observed for the n-alkanes and aromatic hydrocarbons.

Table 4-4: Calibration constants of selected esters determined at 4 different temperatures. The average values are for n=7.

Temperature		Propyl acetate	Methyl butyrate	Sec-butyl acetate	Ethyl butyrate	Butyl acetate	Propyl butyrate	Butyl butyrate
12°C	Average	0.199	0.186	0.205	0.135	0.129	0.108	0.096
	STD	0.022	0.020	0.023	0.013	0.012	0.010	0.010
	% RSD	10.8	10.7	11.2	9.8	9.7	8.8	10.0
20°C	Average	0.232	0.217	0.236	0.153	0.144	0.115	0.099
	STD	0.026	0.024	0.027	0.016	0.015	0.011	0.009
	% RSD	11.1	10.9	11.4	10.3	10.3	9.5	9.0
30.5°C	Average	0.28	0.26	0.29	0.18	0.17	0.13	0.10
	STD	0.03	0.02	0.03	0.02	0.01	0.01	0.01
	% RSD	9.2	9.1	9.6	8.5	8.4	7.7	7.2
39.5°C	Average	0.326	0.302	0.367	0.209	0.198	0.155	0.120
	STD	0.034	0.031	0.041	0.021	0.019	0.014	0.011
	% RSD	10.5	10.4	11.2	9.9	9.8	9.1	8.8

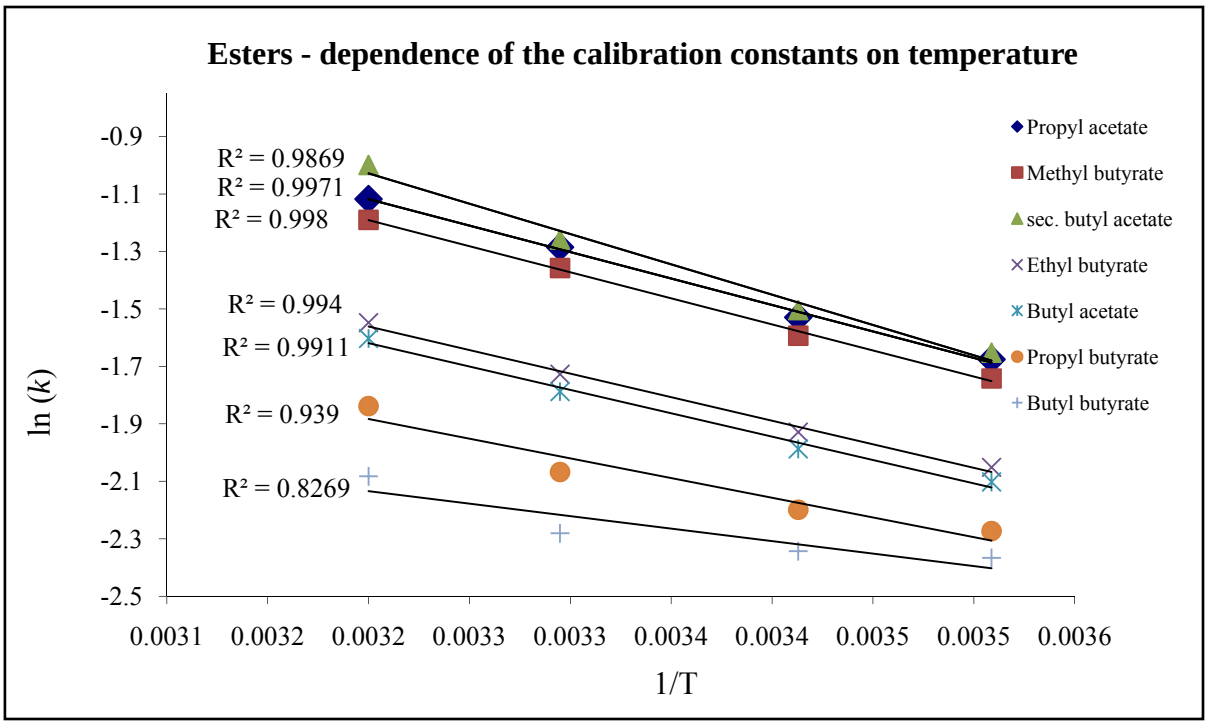

Figure 4-7: Arrhenius-type relationship between ln(k) and 1/T for esters.

Table 4-5: Energy of activation of permeation for selected esters determined using the slope of the Arrhenius-type plots shown in Figure 4-7.

Compound	Slope $\times 10^{-3}$	Standard error of the slope $\times 10^{-2}$	E_p (kJ mole^{-1})	R^2 for the ln(k) vs. 1/T correlation
Propyl acetate	-1.8	1	-15	0.9971
Methyl butyrate	-1.8	1	-15	0.998
Sec-butyl acetate	-2.1	1.7	-17	0.9869
Ethyl butyrate	-1.6	1	-14	0.994
Butyl acetate	-1.6	1.1	-13	0.9911
Propyl butyrate	-1.4	2.5	-11	0.9390
Butyl butyrate	-1	2.8	-7	0.8269

The alcohols also revealed an increasing trend in the calibration constants with temperature (Table 4-6). As shown in Figures 4-8 and 4-9, the 1/T vs. ln(k) plots showed generally good

correlations for all compounds except for 2,3-dimethyl-2-butanol ($r^2 = 0.6967$) and n-octanol ($r^2 = 0.8294$). Within the n-alcohols group, there was also a similar trend of increasing energy of activation of permeation from -13 kJ $mole^{-1}$ for n-butanol to -8 kJ $mole^{-1}$ for n-heptanol, followed by a reversal in the trend with -9.3 kJ $mole^{-1}$ for n-octanol.

From the results observed for all the different groups of compounds and from the literature data it can be concluded that for most VOCs, the energy of activation of permeation through PDMS is indeed mainly governed by the heat of solution of the analyte in the membrane, and to a much smaller extent by the energy of activation of diffusion. Furthermore, the results also indicate that the energy of activation of permeation is mostly of the same order of magnitude for all the compounds irrespective of their polarities.

The temperature variations of the uptake rates observed for the model compounds studied in this project were somewhat higher than the theoretically calculated ~0.4% per degree Celsius change for diffusive-type passive samplers reported in the literature.[219] It should be noted that when the temperature increases, the uptake rates should increase for diffusive-type passive samplers, while they decrease for the sampler designed in this project. In practice, the diffusive-type passive samplers have been reported to be dependent on temperature to various degrees by different researchers. For example, Penniquin-Cardinal et al. found that the uptake rate decreased by 0.6%/°C for benzene, while it increased by 0.35%/°C for toluene and 0.5%/°C for ethyl benzene and xylenes for the diffusive-type Radiello® samplers.[220] Piechocki-Minguy et al. observed an average 2%/°C change in the uptake rate of nitrogen dioxide between 5°C and 30°C using their custom-made diffusive-type passive sampler.[221] The variations in the uptake rates with temperature for the TWA-PDMS samplers are still relatively small compared to other sources of variability under field conditions, such as linear flow velocity of air across the sampler (discussed in the next section), temporal concentration variations, etc. Furthermore, for typical applications in indoor air and soil gas analysis, the temperature of the air is usually nearly constant. Consequently, temperature variations are expected to play only a minimal role in field applications. When more accurate results are desired, appropriate corrections to the calibration constants can be made based on the knowledge of temperature variations in the field.

Table 4-6: Calibration constants of selected n-alcohols and branched alcohols determined at 4 different temperatures.

Temperature		2-methyl-1-propanol	n-butanol	2,3-dimethyl-2-butanol	n-pentanol	2-hexanol	2,4-dimethyl-3-pentanol	n-hexanol	n-heptanol	2-octanol	2-ethyl-1-hexanol	n-octanol
10°C	Average	0.391	0.282	0.182	0.14	0.119	0.111	0.074	0.052	0.043	0.050	0.046
	STD	0.018	0.018	0.006	0.01	0.007	0.004	0.004	0.002	0.003	0.002	0.002
	% RSD	4.6	6.5	3.1	5.8	5.9	3.9	4.8	3.2	6.5	4.0	3.8
20.1°C	Average	0.455	0.338	0.209	0.165	0.14	0.128	0.087	0.059	0.049	0.057	0.046
	STD	0.012	0.008	0.003	0.004	0.00	0.004	0.004	0.003	0.005	0.004	0.003
	% RSD	2.7	2.3	1.6	2.5	2.9	3.0	4.0	4.5	10.0	7.5	6.7
29.9°C	Average	0.465	0.358	0.195	0.175	0.188	0.130	0.094	0.062	0.053	0.060	0.047
	STD	0.009	0.013	0.004	0.005	0.005	0.003	0.002	0.001	0.004	0.002	0.001
	% RSD	1.9	3.6	2.0	3.1	2.5	2.1	2.3	2.2	8.4	2.8	2.5
40.1°C	Average	0.611	0.491	0.233	0.226	0.194	0.148	0.112	0.074	0.066	0.076	0.052
	STD	0.019	0.020	0.007	0.007	0.01	0.004	0.002	0.002	0.01	0.003	0.002
	% RSD	3.2	4.1	2.9	2.9	3.1	2.8	2.2	2.2	7.6	3.6	3.1

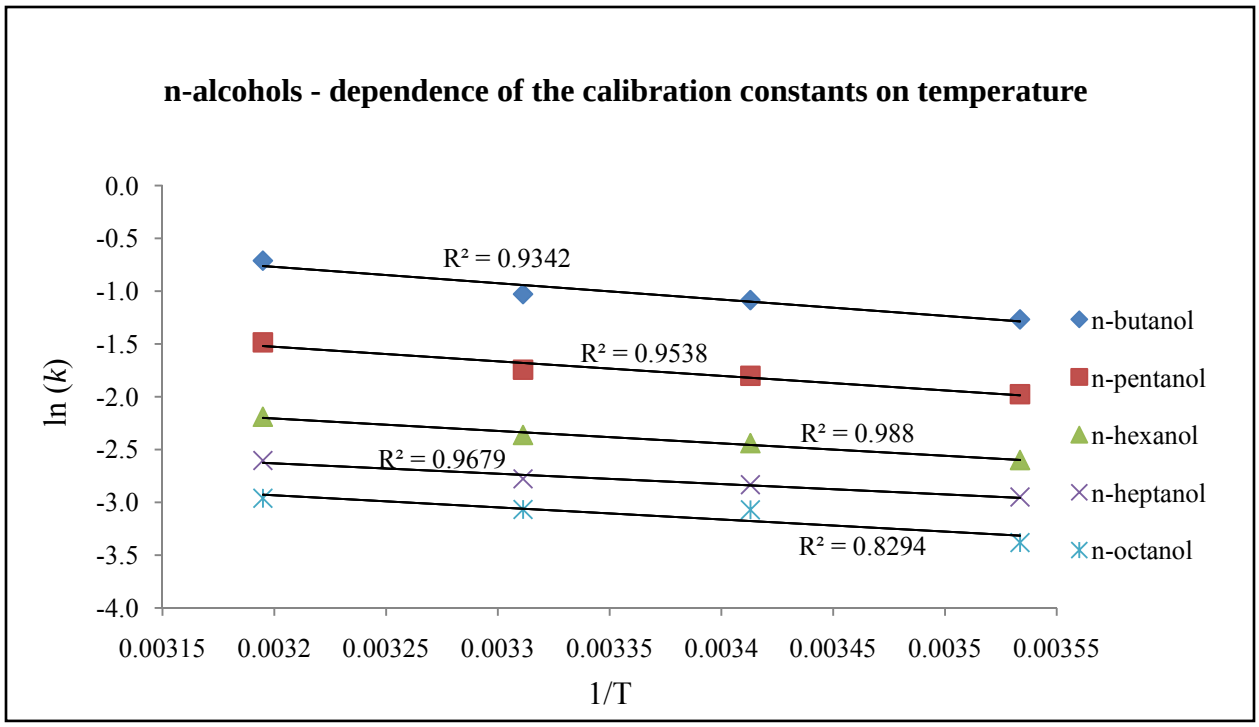

Figure 4-8: Arrhenius-type relationship between ln(*k*) and 1/T for n-alcohols.

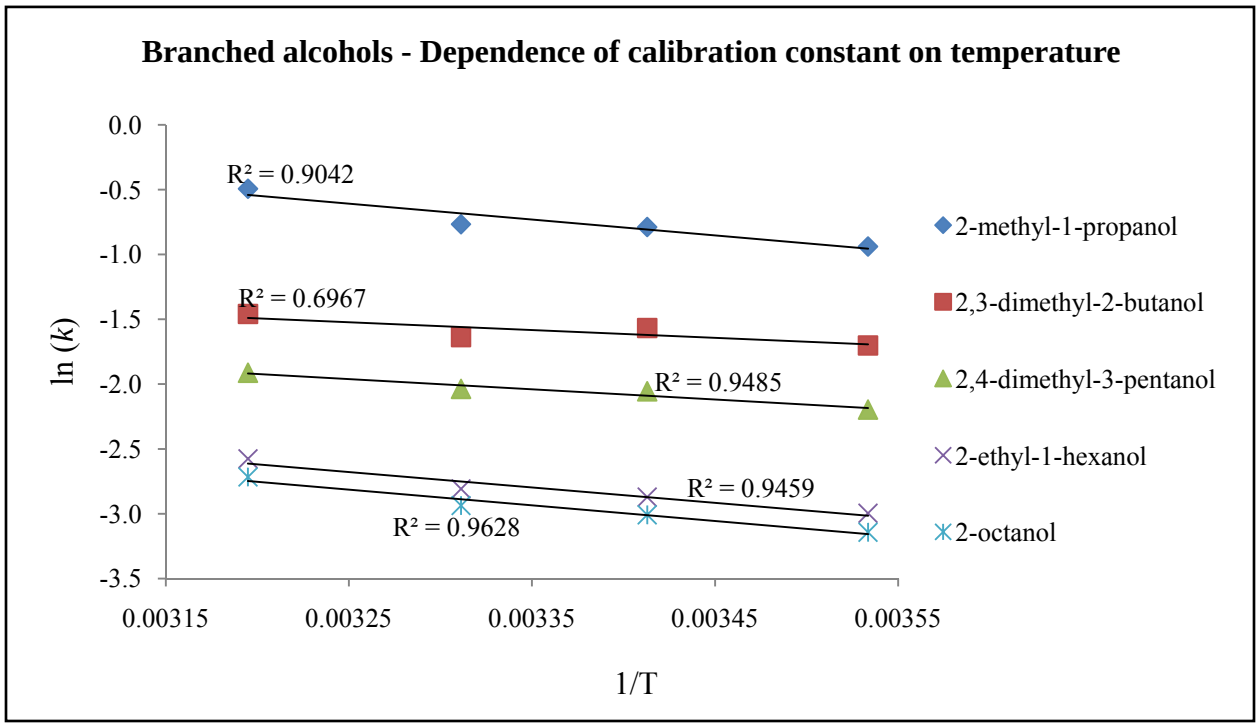

Figure 4-9: Arrhenius-type relationship between ln(*k*) and 1/T for branched alcohols.

Table 4-7: Energy of activation of permeation for selected alcohols determined using the slope of the Arrhenius-type plots shown in Figures 4-8 and 4-9.

Compound	Slope $\times 10^{-3}$	Standard error of the slope $\times 10^{-2}$	E_p (kJ mole^{-1})	R^2 for the ln(k) vs. 1/T correlation
n-butanol	-1.5	2.9	-13	0.9373
n-pentanol	-1.3	2.1	-11	0.9554
n-hexanol	-1.1	1	-9.6	0.9869
n-heptanol	-1	1.3	-8	0.9700
n-octanol	-1.1	3.7	-9.3	0.8139
2-methyl-1-propanol	-1.2	2.8	-10	0.9074
2,3-dimethyl-2-butanol	-5.9	2.8	-4.9	0.6931
2,4-dimethyl-3-pentanol	-1	1.3	-6	0.9432
2-octanol	-1.2	1.7	-9.7	0.9659
2-ethyl-1-hexanol	-1.2	2.0	-9.9	0.9502

4.3.2 Effect of humidity

The calibration constants obtained for the n-alkanes and aromatic hydrocarbons at 4 different humidity levels are listed in Table 4-8. The average calibration constants for all the analytes except n-decane studied at 91% relative humidity were somewhat higher than the calibration constants determined at lower humidity levels, but the differences proved to be statistically insignificant. In addition, the sampler to sampler variability was substantially higher at 91% relative humidity than at the other humidity levels for most of the analytes (Figure 4-10

illustrates this for n-hexane). This can be attributed to higher variability in the extraction efficiencies of the various analytes in the presence of different quantities of water in the sorbent. Such a phenomenon was noticed by Sunesson and co-workers when trying to desorb analytes from Anasorb 747® with thermal desorption methods.[222] A potential solution for reducing the variability would be to use a co-solvent for desorption, such as isopropyl alcohol, to enable partial miscibility of the traces of water which permeated through the PDMS membrane with the extraction solvent. Overall, the uptake rates were within 12.5% RSD for all the analytes when determined at the four different temperatures, which can be considered insignificant when compared to other uncertainties in measurement under field conditions.

The fact that the calibration constants change very little at different humidity levels is very advantageous when using the TWA-PDMS sampler for soil gas sampling applications, as the humidity in such matrices is often close to 100%. Further, the samplers can be deployed for a longer time than diffusive samplers (to reduce the limits of detection and quantification), as the saturation of the sorbent by moisture does not occur as early as it does for the latter.

Table 4-8: Calibration constants of selected n-alkanes and aromatic hydrocarbons determined at 4 different humidity levels.

Humidity		n-hexane	Benzene	n-heptane	Toluene	n-octane	Ethyl benzene	n-nonane	o-xylene	Propyl benzene	n-decane	Butyl benzene
0%	Ave.	0.624	0.343	0.299	0.171	0.154	0.109	0.097	0.096	0.079	0.074	0.063
	STD	0.046	0.025	0.022	0.013	0.011	0.009	0.008	0.007	0.006	0.006	0.005
	%RSD	7.5	7.3	7.4	7.4	6.9	7.9	8.2	7.8	8.1	8.1	7.8
29%	Ave.	0.591	0.316	0.27	0.153	0.136	0.096	0.083	0.081	0.067	0.062	0.053
	STD	0.04	0.018	0.017	0.009	0.008	0.006	0.007	0.006	0.006	0.007	0.006
	%RSD	6.7	5.8	6.1	5.9	6.1	6.8	8	7.4	8.7	10.7	11.3
60%	Ave.	0.611	0.329	0.275	0.158	0.133	0.096	0.080	0.081	0.065	0.059	0.050
	STD	0.024	0.012	0.011	0.006	0.006	0.005	0.005	0.004	0.004	0.005	0.004
	%RSD	3.9	3.6	3.9	3.8	4.4	5.1	6.6	5.1	6.7	8.1	8.1
91%	Ave.	0.643	0.354	0.306	0.168	0.145	0.104	0.081	0.083	0.065	0.057	0.048
	STD	0.084	0.055	0.047	0.022	0.022	0.013	0.01	0.011	0.007	0.005	0.004
	%RSD	13.1	15.5	15.2	13.2	14.9	12.8	11.8	13.5	11.3	8.1	7.9
Average *k*		0.617	0.336	0.288	0.163	0.142	0.101	0.085	0.085	0.069	0.063	0.054
% RSD		3.5	4.9	6.1	5.2	6.7	6.3	9.3	8.5	9.8	12.1	12.4

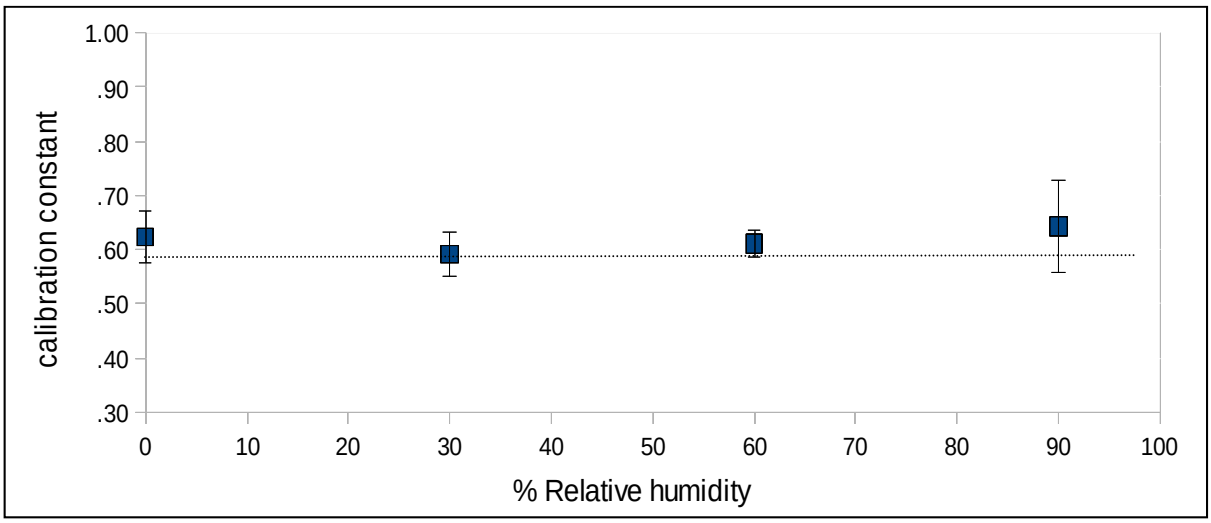

Figure 4-10: Variation of the calibration constants for n-hexane with changes in humidity. The error bars correspond to one standard deviation of the mean, and the dotted line indicates the average calibration constant.

4.3.3 Effect of linear flow velocity of air

Of all the environmental parameters that have been discussed in this chapter, the effect of linear flow velocity of air on the uptake rates is perhaps the most important. It should be noted here that while calculating the linear flow velocity of air experienced by each sampler, it was assumed that the air was stationary in the calibration chamber, and the rotation of the sampler alone contributed to the relative flow of air across the face of the sampler. This was not necessarily true, since the rotating component could drag the air and the samplers could therefore experience a linear flow velocity lower than the calculated rotational speed (except for the sampler positioned in the axis of rotation, which may have experienced some flow across the face via turbulence). Further, since there was a flow of 1000 ml/min of the standard test gas mixture through the chamber, there was bound to be some movement of air, which could contribute to errors in the calculation of the linear flow velocity of air across the surface of the sampler.

The uptake rate of the sampler is proportional to the ratio of the peak area (obtained from injecting the CS_2 extract of the sorbent in the sampler) to exposure duration (M/t). These

ratios for all the n-alkanes and aromatic hydrocarbons studied are tabulated for estimated linear air flow velocities from 0 m/s to 0.53 m/s in Table 4-9. In all cases, as expected, the uptake rate decreased somewhat when the air flow velocity approached 0 m/s. This can be attributed to the starvation effect discussed in Chapter 2. As the linear flow velocity increased, the starvation effect decreased, and the uptake rates stabilized at around 0.35 m/s for all the analytes. A plot of the peak area/exposure duration ratio against linear flow velocity for n-hexane and butyl benzene is shown in Figures 4-11 and 4-12, respectively. The uptake tended to reach a plateau at around 0.35 m/s. This is close to the 0.4 m/s reported by Cinnau for diffusive-type passive samplers.[223]

The magnitude of the percentage decrease in the uptake rate between the maximum flow velocity of 0.53 m/s and 0 m/s increased from n-hexane (39.7%) to butyl benzene (47.2%). As discussed earlier, the starvation effect is a function of the permeability (increased permeability leads to decreased availability of the analytes around the sampler), as well as the diffusion coefficient of the analyte in the boundary layer (smaller diffusion coefficient results in slower mass transfer through the boundary layer). Since the permeability of PDMS increases from n-hexane to butyl benzene, the starvation effect component due to permeability also increases in the same direction. In addition, the diffusion coefficient decreases from n-hexane to butyl benzene, which further worsens the net starvation effect by reducing the mass transport rate through the boundary layer. The results obtained, showing increasingly stronger starvation effect from n-hexane to butyl benzene (Table 4-9), were therefore in accordance with the theoretical predictions.

Table 4-9: Variation in the ratio of the peak area to exposure duration (proportional to uptake rates) of TWA-PDMS samplers towards various analytes at linear flow velocities from 0 to 0.53 m/s.

Analyte	Linear flow velocity of air (m/s)									% Decrease in uptake rate with change from 0.53 to 0 m/s
	0.00	**0.12**	**0.18**	**0.23**	**0.29**	**0.35**	**0.41**	**0.47**	**0.53**	
n-hexane	214	223	230	283	311	332	345	339	355	39.7
Benzene	489	520	530	646	708	748	792	776	807	39.4
n-heptane	229	252	255	309	337	358	381	374	382	40.0
Toluene	591	661	677	811	884	936	1008	983	991	40.4
n-octane	211	243	255	300	323	345	376	363	365	42.1
Ethyl benzene	352	408	435	507	543	584	635	609	610	42.3
o-xylene	245	288	310	358	387	414	453	432	432	43.1
n-nonane	155	187	207	235	248	271	297	281	281	44.8
Propyl benzene	194	233	262	295	312	340	374	350	352	44.9
n-decane	124	154	180	196	204	225	251	231	233	46.9
Butyl benzene	119	148	175	190	198	218	244	222	226	47.2

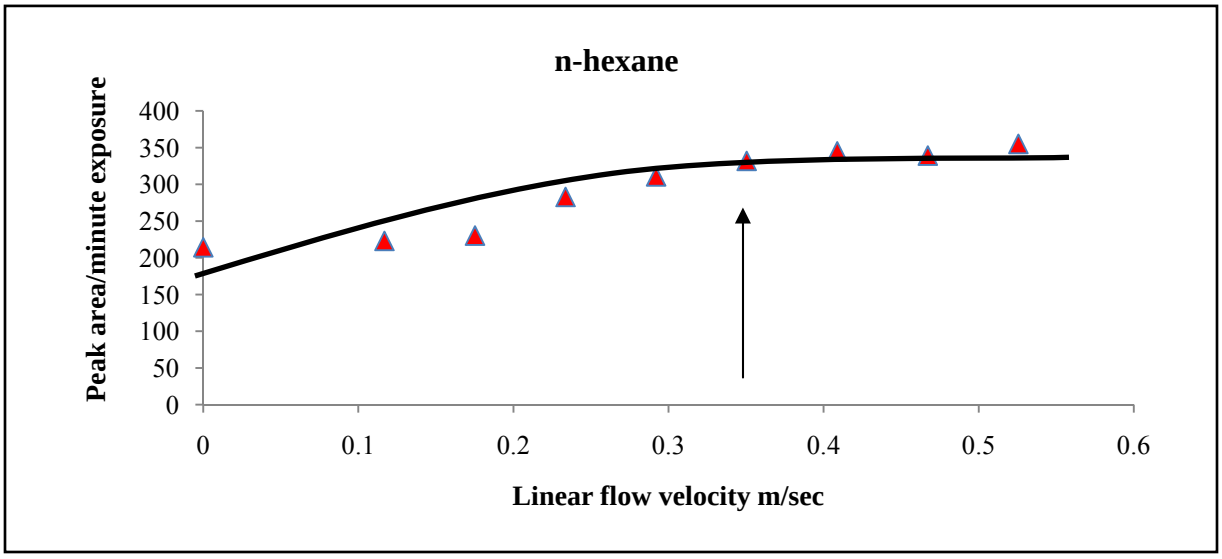

Figure 4-11: The effect of linear flow velocity of air on the uptake rate of n-hexane.

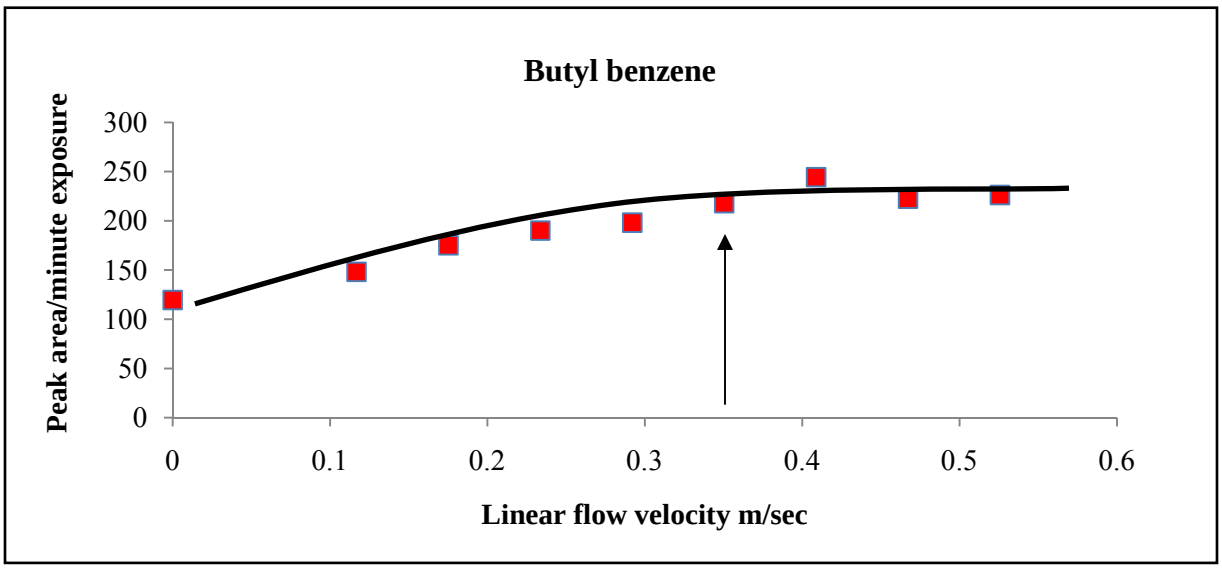

Figure 4-12: The effect of linear flow velocity of air on the uptake rate of butyl benzene.

In practice, the effect of linear flow velocity of air should always be considered in the context of the particular application of the TWA-PDMS samplers. In outdoor air sampling, the linear flow velocity of air is about 4 m/s on average, while for indoor air in well-ventilated buildings it is likely to be above 0.35 m/s in most cases. Consequently, the effect of face

velocity can be ignored in these cases. However, when using the TWA-PDMS samplers for soil gas sampling, with the samplers deployed inside sealed boreholes, the linear flow velocity of air across the surface of the sampler is essentially zero. Consequently, the starvation effect has to be taken into account when interpreting the data generated.

4.4 Conclusions

It is important to consider the effect of environmental factors on the uptake rates of any passive sampler for accurate determination of the analyte concentrations in the gas phase. The TWA-PDMS sampler has very significant advantages when considering the effects of humidity on the calibration constant or when considering the deployment duration of the sampler in the field. This is true because of the low permeability of PDMS towards water vapor. The negligible effect of humidity on the analyte uptake has been experimentally demonstrated by performing experiments at different humidity levels.

Increase in temperature results in decreased uptake rates for TWA-PDMS samplers, while it results in an increase in the uptake rates for diffusive-type passive samplers. The magnitude of the difference is slightly higher for the TWA-PDMS samplers, but can be considered negligible when averaging the temperature over a 24 hour period or multiples of 24 hours. The experiments performed to determine the variation in the calibration constants with temperature allowed the determination of the energy of activation of permeation of various analytes through PDMS.

Linear flow velocity of air can have a significant effect on the uptake rates of TWA-PDMS samplers when it is below 0.35 m/s. A similar effect has been observed for diffusive-type passive samplers. The difference in the uptake rates between that obtained at 0 m/s and the 0.53 m/s linear flow velocity was found to increase with the increase in the mass transport rate of the analyte within the membrane. The effect of face velocity can therefore be disadvantageous for soil gas applications, while it can mostly be ignored for indoor (with forced ventilation) and outdoor air analysis because of constant air movement.

CHAPTER 5

Effect of membrane geometry and exposure duration on the calibration constants for various analytes

The objective of this chapter is to show how the membrane geometry (thickness and surface area exposed to the sample matrix) and the sampler exposure duration affect the uptake rates of the TWA-PDMS sampler.

As discussed in the theory section of this thesis, the calibration constants of the sampler towards various analytes are functions of the thickness and the area of the membrane exposed to the sample matrix. According to Fick's laws, the uptake rate is directly proportional to the area of the membrane exposed to the sample matrix and inversely proportional to the thickness of the membrane. Apart from changes in the uptake rates, it should also be noted that the starvation effect should in principle be lower if the mass transport across the membrane is reduced either by increasing the membrane thickness, or by reducing the area of the membrane exposed to the sample. Increasing the membrane exposure area or reducing the membrane thickness, on the other hand, should aid in lowering the limits of detection and limits of quantification of the analytical procedure.

Three different thicknesses of PDMS membranes were used to study the effect of the membrane thickness on the calibration constants of the sampler towards various analytes. The sampler design discussed in Chapter 3 and all the experiments up to this point used the 1.8 mL crimp cap, autosampler vials. Vials and crimpers of other sizes are available commercially and can also be used to increase or decrease the membrane area exposed to the sample matrix. Samplers fabricated using vials of 0.8 and 1.8 mL volume were used to perform head-to-head comparisons of two different areas of the membrane exposed to the sample matrix.

Exposure duration and analyte concentrations have been reported to have substantial effects on the uptake kinetics of diffusive-type passive samplers (also discussed in Section 1.7.4). Both these parameters influence the uptake rate mainly because of non-ideal functioning of the sorbent used in the fabrication of the respective diffusive-type passive samplers. The non-

ideality arises because of premature saturation of the sorbent and/or competition for the adsorptive sites by water molecules over time. Since PDMS has low permeability towards water vapor compared to the compounds of interest, competition by water molecules should in principle be vastly reduced or eliminated altogether. Consequently, the sampler presented in this thesis should be able to function properly for a long time without changes of the uptake rates.

Separate experiments were not performed to determine the effects of exposure duration on the uptake rates, as sufficient information was available from earlier experiments. The uptake rates determined for n-hexane over the last 4 years using different exposure durations will be presented here.

5.1 Experimental methods

In this section, the experimental methods used for the determination of the effect of the membrane thickness, exposure area and sampling duration on the calibration constant of the sampler towards various analytes are described. These experimental methods were in general the same as described in Chapter 3, except as noted below in the respective sub-sections. The calibration constants were determined in the same manner as described earlier. The speed of rotation of the fan blades in the exposure chamber was kept high to minimize the starvation effect. The experiments were conducted at 0% relative humidity and at 25 ± 2˚C.

5.1.1 Effect of membrane thickness

The experimental study on the effect of membrane thickness on the calibration constant of the sampler towards various analytes was carried out prior to most of the experimental studies reported in this thesis. The analytes used for the experiments were n-alkanes from hexane to decane, benzene, toluene, ethyl benzene, propyl benzene and butyl benzene. In total, nine vials were deployed in the calibration chamber, among which three had 25 μm thick membranes, three had 75 μm thick membranes and three had 150 μm thick membranes procured from Specialty Silicone Products Inc., (Ballston Spa, NY). The membrane thickness was specified by the manufacturer with a tolerance of ±20%. The analyte concentrations

ranged between 279 μg/m^3 and 3438 μg/m^3 in the exposure chamber, and the total exposure duration was 8929 minutes.

5.1.2 Effect of membrane area

To determine the effect of membrane area, four 0.8 mL crimp cap vials (with an exposure area of 11.5 mm^2) and three 1.8 mL crimp cap vial (with an exposure area of 21.4 mm^2) were exposed in the chamber to n-alkanes (from hexane to decane) and aromatic hydrocarbons (benzene, toluene, ethyl benzene, propyl benzene and butyl benzene) at concentrations ranging from 41 μg/m^3 to 1025 μg/m^3 for a duration of 8715 minutes. The nominal membrane thickness used was 75 μm ±20% and the membranes required for all the samplers were cut from an area of 2" x 2" from the PDMS sheet procured from the manufacturer.

5.1.3 Effect of exposure duration

Over a period of time, a number of exposure experiments were performed for the determination of the calibration constants of the 40 compounds listed in Chapter 3. The permeation tube design and the specifications of the PTFE tubing used for the fabrication of the permeation tubes were the same in all these experiments. Since the permeation rates of the different analytes through PTFE were different (resulting in different concentrations of the analytes in the chamber), many trial and error experiments were conducted by changing the sampler exposure duration (in addition to changing the permeation tube temperature and length) in order to trap enough analytes in the sampler for quantification by the chromatographic method. The experiments were challenging as the sensitivity of different chromatographic detectors (FID, ECD) and the injection systems available on the instruments used for the analysis (cool on-column and split-splitless) were different. In-order to control the calibration chamber performance, n-hexane was sometimes used along with the respective sets of model compounds while determining the calibration constants. Some of the selected exposures of different duration at the same (or very close) n-hexane concentrations are discussed here. The concentrations of n-hexane ranged from 605 μg/m^3 to 923 μg/m^3 and the exposure duration ranged from 1 day to 9 days.

5.2 Results and discussion

The results obtained from the experiments described above provided important information on the parameters that have to be carefully assessed for future optimization of the uptake rate and sampler deployment duration in the field. For a specific concentration of the analytes in the sample matrix, the membrane geometry and exposure duration define the detection and quantification limits of the sampler towards the respective analytes. The observations and interpretations from these experiments are provided in the next three subsections.

5.2.1 Effect of membrane thickness

The calibration constants obtained for the test of different membrane thicknesses are given in Table 5-1. Samplers coded PS-1, PS-2 and PS-3 had 25 μm membranes; those coded PS-4, PS-5 and PS-6 had 75 μm membranes, and the ones coded PS-7, PS-8 and PS-9 had 150 μm membranes. The calibration constants should theoretically be linearly proportional to the inverse of the membrane thickness. The calibration constants for the samplers equipped with the 25 μm thick membranes were 25 to 50 % lower than those for the 75 μm thickness membrane samplers, which was consistent with the theory. However, even though the difference between the calibration constants for the 75 μm and 150 μm membranes should theoretically be 100%, it was found to be only around 30% to 40%. This could be explained by the thickness tolerance of ±20%, as quoted by the manufacturer of the PDMS membrane.

Table 5-1: Calibration constants obtained with vial-based passive samplers equipped with PDMS membranes of different thicknesses.

Membrane thickness	Sampler code	Hexane	Heptane	Octane	Nonane	Decane	Benzene	Toluene	Ethyl- benzene	Propyl- benzene	Butyl- benzene
25 µm	PS-1	0.216	0.114	0.070	0.050	0.041	0.131	0.072	0.054	0.043	0.036
	PS-2	0.228	0.120	0.075	0.056	0.046	0.139	0.076	0.056	0.047	0.040
	PS-3	0.231	0.123	0.077	0.056	0.046	0.139	0.078	0.059	0.048	0.043
	Average	0.225	0.119	0.074	0.054	0.044	0.136	0.076	0.056	0.046	0.040
	STD	0.008	0.004	0.003	0.003	0.003	0.005	0.003	0.003	0.002	0.003
	% RSD	3.36	3.61	4.67	6.04	6.67	3.43	4.10	4.51	5.28	8.76
75 µm	PS-4	0.964	0.463	0.250	0.141	0.090	0.501	0.250	0.157	0.108	0.079
	PS-5	0.939	0.375	0.224	0.133	0.083	0.382	0.209	0.140	0.100	0.072
	PS-6	0.993	0.475	0.258	0.147	0.094	0.514	0.251	0.155	0.108	0.080
	Average	0.965	0.438	0.244	0.140	0.089	0.466	0.236	0.151	0.105	0.077
	STD	0.027	0.055	0.018	0.007	0.005	0.073	0.024	0.009	0.005	0.004
	% RSD	2.80	12.53	7.25	5.16	5.80	15.69	10.02	5.95	4.43	5.29
150 µm	PS-7	1.409	0.683	0.382	0.215	0.141	0.727	0.352	0.218	0.154	0.112
	PS-8	1.334	0.626	0.332	0.176	0.118	0.680	0.325	0.198	0.133	0.097
	PS-9	1.350	0.630	0.342	0.180	0.118	0.696	0.330	0.201	0.138	0.109
	Average	1.364	0.646	0.352	0.191	0.126	0.701	0.336	0.206	0.141	0.106
	STD	0.039	0.032	0.026	0.021	0.013	0.024	0.014	0.011	0.011	0.008
	% RSD	2.89	4.87	7.44	11.08	10.44	3.43	4.21	5.26	7.90	7.750

After observing the results from the experiments, the thicknesses of the membrane material (cut from the same sheet of membrane as that used for this study) were measured using an optical microscope. Overall, the thickness was found to deviate by as much as ± 75% from the manufacturer's specification (75 μm) at different locations on a one square foot sheet of the membrane. When measured at different locations of a specific 1 square inch piece of the membrane, the thicknesses were within 100 ± 20 μm. The pieces of membranes required for the samplers were cut from a small area which would have avoided large variations in the thickness. The results of this experiment indicated the importance of proper control of the membrane thickness. It was not practically possible to determine the variations in the thickness within the small area of 21.4 mm^2 used for each and every passive sampler. To avoid any problems due to such variations, the membranes cut with the cutting tool were weighed, and the weights were used as a control for the membrane thickness used for the exposure experiments for all subsequent exposure studies.

As discussed in Chapter 3, there was a good correlation of ln(*k*) plot against LTPRI when the *k* was measured with the 75 μm thick membranes. The same correlation was then tested for *k* determined with different thicknesses of the membrane. The plots for the n-alkanes are shown in Figure 5-1 for the three membrane thicknesses. A slight deviation from a straight line correlation was observed for all three membrane thicknesses with the curvature being more pronounced for the 25 μm thick membranes (correlation coefficient of 0.9552). This can be attributed to the starvation effect, which affects the net uptake rates of the various analytes differently depending on the permeability of PDMS towards these analytes. The ln (k) vs LTPRI correlations with 75 μm and 150 μm membranes were generally good, suggesting that they were equally good choices for vial-based passive samplers. It should however be possible to use the 25 μm membrane when the air flow velocity around the sampler is expected to be high (to reduce the starvation effect), in which case lower quantification limits and lower residence times (as discussed in Chapter 2, Section 2.1.2) could be obtained. Further, shorter deployment time would be required when compared to 75 or 150 μm thick membranes to obtain the same quantification limits.

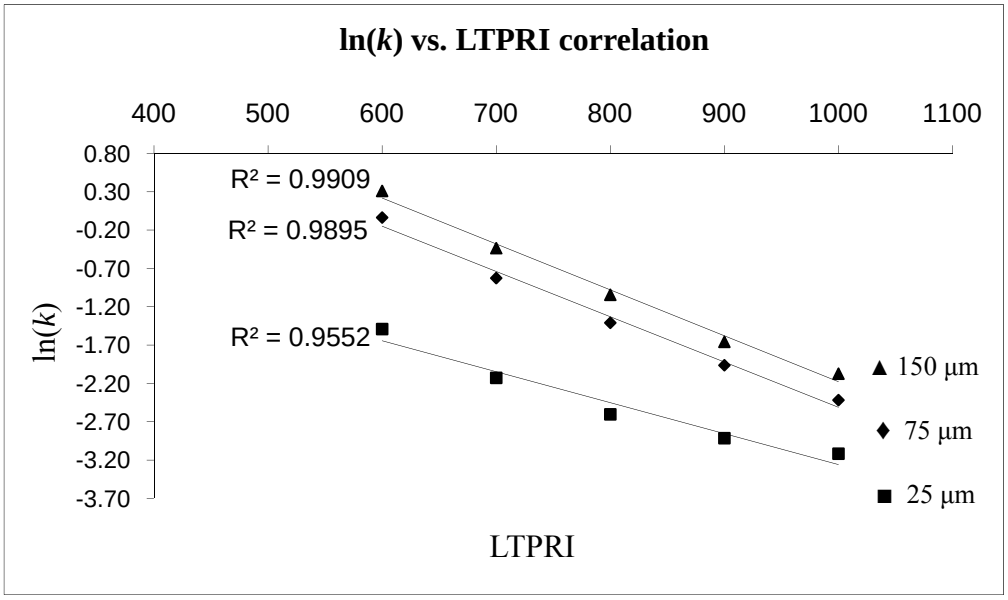

Figure 5-1: ln(*k*) vs. LTPRI correlations for n-alkanes and for various membrane thicknesses

Similarly to the observation for the n-alkanes, a larger deviation from straight line correlation was observed for aromatic compounds with the 25 µm thickness membrane when compared to 75 and 150 µm thick membranes (Figure 5-2). This reiterated the significance of the starvation effect observed for the 25 µm thick membranes.

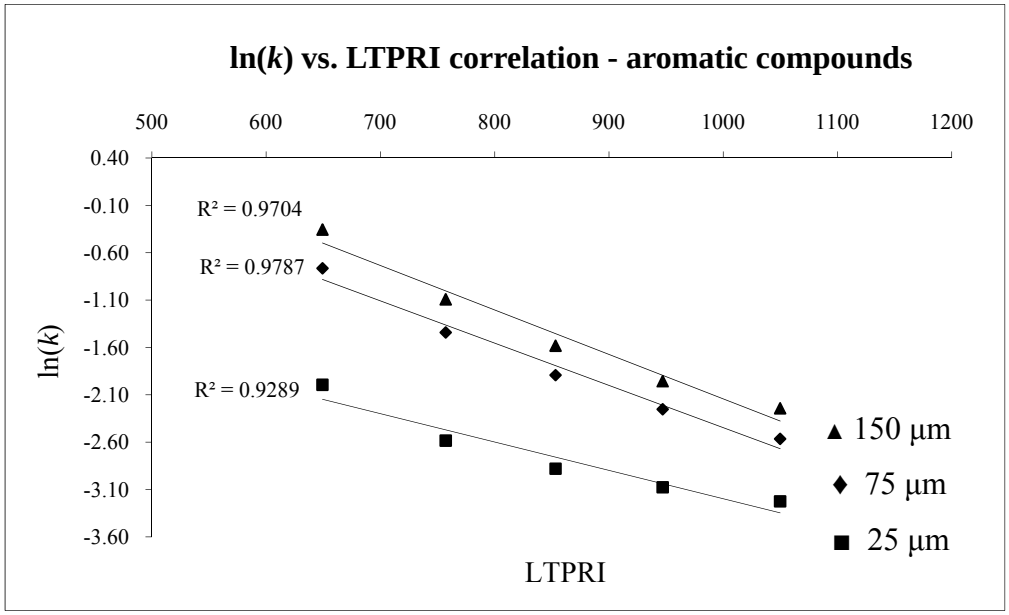

Figure 5-2: ln(*k*) vs. LTPRI correlations for aromatic compounds and for various membrane thicknesses

5.2.2 Effect of membrane area

The calculated area of the membrane exposed to air for the 1.8 mL vial was 21.4 mm^2, and that for the 0.8 mL vial was 11.5 mm^2. Accordingly, the calibration constants for any analyte determined using the 0.8 mL vial should be higher by ~1.9 times than those determined using the 1.8 mL vial. The calibration constants determined using the two types of vials and their ratios for each analyte are provided in Table 5-2. The ratios of the calibration constants ranged from 3.05 for n-hexane to 2.20 for butyl benzene, and there was a clear decreasing trend with an increase in LTPRI.

The observed results could be attributed to several factors. The most important factor is that the opening in the aluminum cap, which should define the area of exposure for the sampler, is slightly smaller than the inner diameter of the glass vial (Figure 3-5, Chapter 3). Consequently, there is a possibility for the air to penetrate between the membrane and the aluminum cap. Analyte transport into these tiny crevices will occur by molecular diffusion and hence the effect will be less pronounced for compounds with lower diffusion coefficients.

Table 5-2: Calibration constants and their reproducibilities for n-alkanes and aromatic hydrocarbons determined with 1.8 mL and 0.8 mL vials.

	k	n-hexane	Benzene	n-heptane	Toluene	n-octane	Ethyl benzene	n-nonane	o-xylene	Propyl benzene	n-decane	Butyl benzene
1.8 mL vials	Average (n=3)	0.671	0.384	0.337	0.189	0.170	0.117	0.102	0.100	0.082	0.074	0.063
	STDev	0.115	0.053	0.050	0.026	0.019	0.014	0.009	0.010	0.007	0.006	0.005
	%RSD	17.058	13.904	14.852	13.701	11.062	11.829	8.905	10.248	8.660	8.345	8.633
0.8 mL vials.	Average (n=4)	2.048	1.055	0.916	0.498	0.431	0.292	0.242	0.245	0.191	0.167	0.138
	STDev	0.102	0.073	0.082	0.046	0.045	0.030	0.027	0.026	0.020	0.019	0.016
	%RSD	4.960	6.878	8.932	9.200	10.322	10.163	11.153	10.776	10.225	11.519	11.490
Ratio of average $k_{0.8}/k_{1.8}$		3.05	2.75	2.72	2.64	2.53	2.49	2.37	2.45	2.32	2.24	2.20

Another factor which could result in disproportionate changes in the uptake rates is perhaps due to analyte transfer mechanism from the inner surface of the membrane to the sorbent. The concentration "on" the membrane surface, on the sorbent side, is required to be zero for the sampler to work properly. However, this might not necessarily be the case. The diameter of the membrane area exposed to the sample for the 0.8 mL vial was 3.8 mm. The packing of the sorbent within this area was visually examined and it was found that the first layer of the sorbent particles did not cover the entire area of the membrane uniformly, as illustrated in Figure 5-3. This uneven packing could be attributed to the adhesive nature of the membrane and could affect the uptake rate ratios disproportionately for different analytes. This is due to the different diffusion coefficient of the analytes within the interstitial space between the membrane and the first layer of sorbent particles.

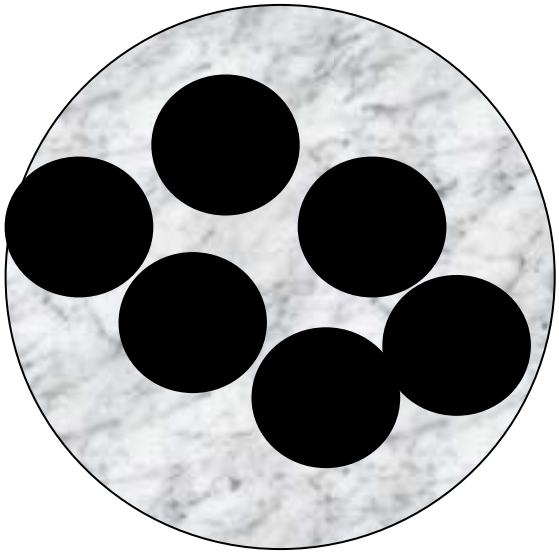

Figure 5-3: The monolayer of sorbent particles in contact with the PDMS membrane of the sampler.

A plot of ln(k) vs. LTPRI however showed similar correlation as observed before, as illustrated in Figure 5-4. This indicates that the correlations are still valid when the vial size is 0.8 mL as opposed to the 1.8 mL vial used in this project.

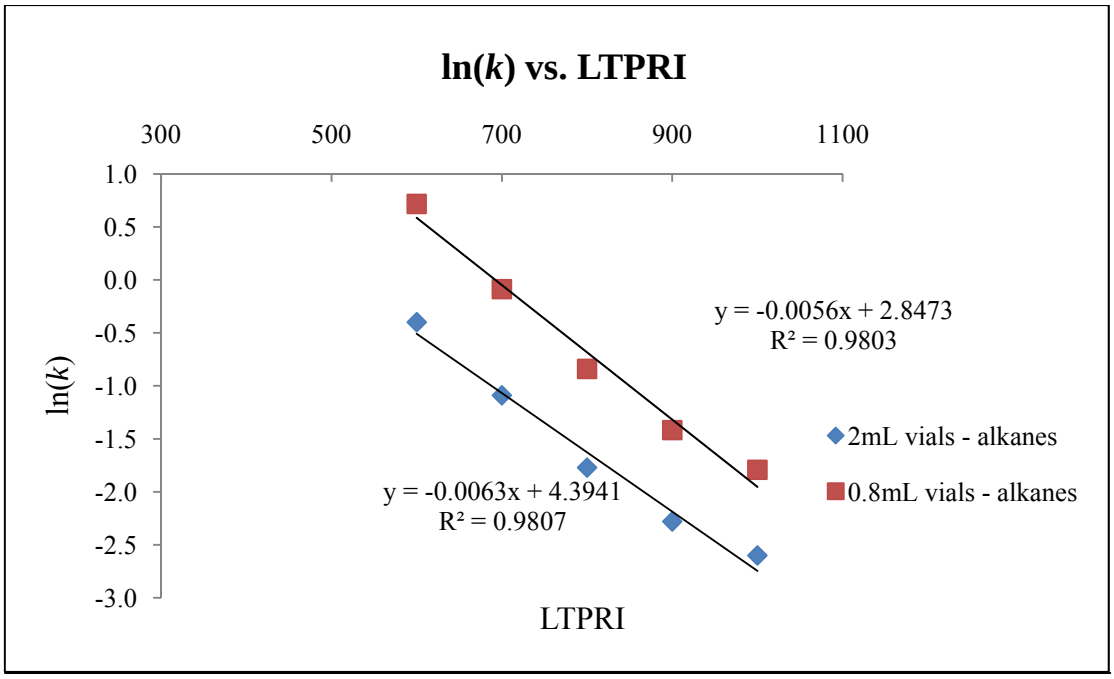

Figure 5-4: ln(*k*) vs. LTPRI correlation determined for n-alkanes with 1.8 mL and 0.8 mL vials.

5.2.3 Effect of exposure duration

The calibration constants of n-hexane determined by exposing the TWA-PDMS samplers for durations ranging from 1 to 9 days are shown in Table 5-3. The calibration constant could not be determined for exposures shorter than 24 hours because the amount of the analyte collected by the sampler was too small at the concentration selected for quantification. Data presented in Table 5-3 are remarkably consistent, proving that exposure duration did not have a significant effect on the uptake rates up to 9 days. This observation is critical for TWA concentration determination as it allows for the sampler to be deployed for long time periods without compromising the quality of the data. Consequently, the limits of detection and quantification for the analytes can be reduced.

Table 5-3: Calibration constants of n-hexane for different exposure durations.

Concentration ($\mu g/m^3$)	Exposure duration (days)	Average calibration constant (min/mL)	STD (n=6)	%RSD
806.3	1	0.850	0.072	8.5
759.2	3	0.835	0.018	2.2
923	5	0.862	0.052	6.0
605.2	7	0.842	0.019	2.3
700.2	9	0.860	0.082	9.5

5.3 Conclusions

In principle, the geometry of the membrane used in the fabrication of the TWA-PDMS sampler should define the calibration constant based on Fick's laws of diffusion. However, the ratios of the calibration constants for different analytes were different when the thickness or the area of the membrane exposed to the sample was changed. This can be explained based on the starvation effect, difference in the size of the opening of the aluminum cap and glass vial, as well as the non-ideal surface coverage of the PDMS membrane by the sorbent particles inside the sampler. These three factors affect the calibration constants of the sampler towards various analytes to a different extent, depending on their permeability through the PDMS membrane.

There were no observable effects of deployment period up to 9 days on the calibration constants of the samplers towards n-hexane. The validity of the conclusions from these studies should come from additional laboratory experiments in future which will be conducted as part of program funded by Environmental Security Technology Certification Program (ESTCP) (a US Department of Defence program) titled "Development of more cost-effective methods for long-term monitoring of soil vapor intrusion to indoor air using quantitative passive diffusive-adsorptive sampling techniques".

CHAPTER 6

Indoor and outdoor air sampling at various field locations

Indoor and outdoor air sampling was performed at several locations in North America, Europe and Asia using both the TWA-PDMS samplers and conventional methods. A representative selection of the methods and analytical results will be provided in this Chapter. All field sampling described in this Chapter was performed by Geosyntec Consultants, Inc., of Guelph, Ontario. All samplers were fabricated and analyzed at the University of Waterloo. The comparison between the TWA-PDMS samplers and conventional methods was a "blind" comparison, because no prior information on the background of the field site and/or analyte concentrations was available to the University of Waterloo due to client confidentiality agreements between Geosyntec Consultants and the site owners, and no information from the conventional samples was available to the University of Waterloo until all the results from the TWA-PDMS samplers were generated.

The objective of this chapter is to provide a comparison of the results obtained from TWA-PDMS passive samplers with commercially available samplers. The sampling projects that will be presented in this chapter are as follows:

- Indoor air sampling with SUMMA™ canisters and TWA-PDMS samplers,
- Indoor and outdoor air sampling with 3M™ OVM 3500 sampler and TWA-PDMS sampler,
- Sampling from vent pipes and high purge volume (HPV) flow cells using TWA-PDMS and SUMMA™ canisters and
- Indoor air sampling with TWA-PDMS sampler and SUMMA™ canisters or TAGA unit.

6.1 Field sampling and analysis methods

Passive sampler calibration, fabrication and analysis were performed at the University of Waterloo. The method described in Chapter 3 was used for the fabrication of the sampler. Each sampler was transferred to a separate 20 mL scintillation vial and sealed with a

threaded, plastic, foil-lined cap and PTFE tape. The scintillation vial was then placed inside a self-sealing polyethylene bag, as shown in Figure 6-1, followed by shipping the sampler to the specified location. The samplers were removed from the scintillation vials and installed in the field either by hanging them from a flexible thread attached to the PTFE loop, or by fixing a rigid stainless steel wire attached to the mouth of the sampler as shown in Figure 6-2. A laboratory blank was retained in the laboratory, and one or more trip blanks were included with each shipment to test for any positive biases in the analytical results. After sampling, the samplers were repacked in the same scintillation vials, sealed again with the caps and PTFE tape and shipped back to the University of Waterloo for analysis.

Figure 6-1: Photograph of a TWA-PDMS sampler packed and shipped to the field.

Figure 6-2: Photograph showing supports for sampler installation.

The analytes were different for each of the projects discussed in this Chapter and are listed in the respective sections. The calibration constants used in the calculation of the concentrations of the analytes are listed in Table 3-12. The calibration constant of PCE (0.187 min/mL) was estimated using the ln(k/MW) vs. LTPRI correlation because the experimentally determined value was not available.

6.1.1 Indoor air sampling with SUMMA™ canisters and TWA-PDMS samplers

Sampling with SUMMA™ canisters followed by analysis using US-EPA method TO-15 is one of the most common methods for VOC sampling and analysis in air, therefore it was chosen as a benchmark for comparison purposes. An example of a SUMMA™ canister is shown in Figure 6-3,[224] and a photograph of the SUMMA™ Canister and TWA-PDMS samplers deployed concurrently in the field is shown in Figure 6-4.

TWA-PDMS samplers were deployed in a crawl space inside a dwelling to monitor selected chlorinated organic compounds (1,1,1-TCA, chloroform, cis-DCE, PCE, trans-DCE and TCE). Seven passive samplers were deployed for approximately one week (exact exposure periods are shown in Table 6-1) at four different locations in the crawl space. Analyte concentrations were monitored concurrently by SUMMA™ canister method over the same exposure period as that for TWA-PDMS samplers at each of the four locations. The time-weighted average concentration obtained using the SUMMA™ canisters over a period of 7 days was then used for comparison with the concentration determined using the TWA-PDMS samplers. All the analyses of SUMMA™ canisters were performed by a commercial laboratory, while all the TWA-PDMS samplers were analyzed at the University of Waterloo.

The TWA-PDMS samplers were analyzed as described in Chapter 3 except that chromatographic separation and quantification were performed using the method detailed in Table 6-2.

Table 6-1: Deployment duration of TWA-PDMS samplers and the IDs of SUMMA™ canisters deployed concurrently.

Location	Geosyntec SUMMA™ Canister ID	TWA-PDMS sampler code	Deployment Date/Time	Retrieval Date/Time	Total time (mins)
A	SUMMA 1	GS-009	6/1/07 10:56 AM	6/8/07 9:22 AM	9986
B	SUMMA 2	GS-005	6/1/07 10:56 AM	6/8/07 9:22 AM	9986
		GS-007	6/1/07 10:56 AM	6/8/07 9:22 AM	9986
C	SUMMA 3	GS-004	6/1/07 10:40 AM	6/8/07 9:53 AM	10033
		GS-006	6/1/07 10:40 AM	6/8/07 9:53 AM	10033
D	SUMMA 4	GS-008	6/1/07 9:20 AM	6/8/07 8:56 AM	10056
		GS-010	6/1/07 9:20 AM	6/8/07 8:56 AM	10056

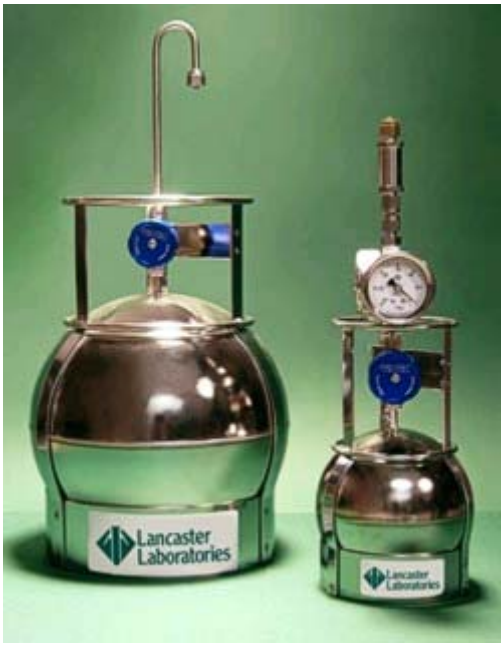

Figure 6-3: SUMMA™ canisters with flow controllers.[224]

Figure 6-4: SUMMA™ canister and TWA-PDMS samplers deployed for comparison purpose.

Table 6-2: Gas chromatographic method used for the separation and quantification of chlorinated compounds.

Gas chromatograph	Agilent Technologies, 6890 GC
Detector	Electron Capture Detector at 350˚C
Injection mode	Split, 275˚C
Split ratio	1:10
Injection volume	1 μL
Carrier gas	Helium at 1.2 mL/min
Oven temperature program	35˚C, 7˚C/min to 220˚C, held for 2 min
Data acquisition and processing	Chemstation software
Capillary column	RTX-5 (95% methyl and 5% phenyl), 30 m x 0.25 mm, 0.25 μm film thickness
Calibration method	External standard multipoint calibration

6.1.2 Indoor and outdoor air sampling with 3M™ OVM 3500 samplers and TWA-PDMS samplers

TWA-PDMS samplers were deployed in a building to test for the presence of chlorinated VOCs (same set as listed in Section 6.1.1). Commercially available diffusive-type passive samplers, 3M™ OVM 3500, were also deployed concurrently to compare the results obtained from the two samplers. The design of the 3M™ OVM 3500 sampler is described in detail in Section 1.5.2. One week prior to the concurrent deployment of both types of samplers, several 3M™ OVM 3500 samplers were deployed for 24 hours. The results of this measurement will be used in this thesis to show the temporal variability of the concentrations in the field. All analyses of the 3M™ OVM 3500 samplers were performed by a commercial laboratory, while the TWA-PDMS samplers were analyzed at the University of Waterloo. The sampling locations of the TWA-PDMS samplers are listed in Table 6-3. Quantification

of the analytes in the samplers was performed using the GC-MS method detailed in Table 6-4.

Table 6-3: TWA-PDMS sampler codes and the locations at which they were deployed.

Sampler code	Location
PS-652	2nd floor of office, inside building
PS-653	1st floor or office, lobby area, inside building
PS-654	1st floor of office, training room, inside building
PS-655	1st floor of office, shop area, inside building
PS-656	Behind office building, outside building
PS-657	main door of office, outside building

Table 6-4: GC-MS method used for the separation and quantification of chlorinated compounds.

Gas chromatograph-Mass spectrometer Instrument	Agilent Technologies, 6890 GC - 5973 MS
Injection mode	Split, 275˚C
Split ratio	1:10
Injection volume	1 μL
Carrier gas	Helium at 2.0 mL/min
Oven temperature program	35˚C for 5 mins, 5˚C/min to 120˚C (held for 0 mins), 30˚C/min to 350˚C (held for 3 minutes)
Data acquisition and processing	Chemstation software
Capillary column	Rxi-1 Ms (100% methylsiloxane), 60 m x 0.32 mm, 1.0 μm film thickness
Quantitation mode	Selected Ion Monitoring (three ions for each target analyte as listed in Table 7-3 in the next chapter)
Calibration method	External standard, multipoint calibration

6.1.3 Sampling from vent pipes and high purge volume (HPV) flow cells using TWA-PDMS samplers and SUMMA™ canisters

Vent pipes are used in many buildings to connect the sub-slab (below the floor) space to the atmosphere. Their main function is to minimize vapor intrusion into the building through the floor of the house, which is achieved by providing a path for the contaminated vapors to be released into the atmosphere. TWA-PDMS samplers and SUMMA™ canisters were used to monitor vapor concentrations inside such vent-pipes of a passive (wind-driven) sub-slab venting system in New Jersey. A photograph of one of the vent pipes is shown in Figure 6-5. In this project, the samples were collected by deploying the TWA PDMS samplers inside the vent pipe and just above ground level when there was upward air flow in the pipes. The flow in the vent pipe was expected to reduce any starvation effect. The TWA-PDMS samples and the SUMMA™ canisters samples were both taken over a period of 24 hours for TWA concentration determination.

Figure 6-5: Passive vent pipe

HPV testing, pioneered by Geosyntec Consultants, involves withdrawing sub-slab soil gas at a steady rate and monitoring the pollutant concentration in the vapor phase over a period of

time. In the HPV testing method, samplers are deployed or sampled from a flow-through cell in the effluent path. At a site in Mexico, the sub-slab soil gas sampling was performed using TWA-PDMS sampler and SUMMA™ canisters. TWA-PDMS samplers were deployed in the flow cell for half an hour to an hour, and SUMMA™ canister samples were collected over a period of 5 minutes during the period the TWA-PDMS sampler was deployed. Because of the substantial air flow through the flow cell, the starvation effect was expected to be minimal.

The TWA-PDMS samplers were analyzed using the GC-MS method listed in Table 6-4. The target analytes were c-DCE, TCE, and PCE for both of the above two sampling projects, and the TWA-PDMS samplers were analyzed using GC-MS method shown in Table-6-4.

6.1.4 Indoor air sampling with TWA-PDMS sampler and SUMMA™ canisters or TAGA unit

Indoor air sampling was performed at two buildings at a former military arsenal in New Jersey to quantify PCE concentrations. These buildings were decommissioned and redeveloped for commercial use prompting the requirement of pollution monitoring. A number of TWA-PDMS samplers were deployed for a 2-week period, and the analyte concentrations obtained from them were compared to those obtained a week earlier from US EPA TAGA mobile laboratory that makes real-time pollutant concentration measurements. The principle of operation of TAGA is briefly described in Section 1.1.1.

Figure 6-6: US EPA TAGA mobile laboratory

At another location in Massachusetts, indoor air samples were also collected with TWA-PDMS samplers and SUMMA™ canisters for the quantification of PCE. The TWA-PDMS sampling was performed over a period of 3 days and compared to samples collected over a period of 8 hours using SUMMA™ canisters (analyzed by EPA Method TO-15). The SUMMA™ canister samples were taken immediately after the TWA-PDMS samplers' deployment period. All the TWA-PDMS sampler analysis in the laboratory was performed using the GC-MS method listed in Table 6-4.

6.2 Results and discussion

The results obtained from the comparison of the TWA-PDMS samplers with commercially available active and passive sampling systems indicated the former's reliability in terms of cost effectiveness, sampler-sampler to sampler reproducibility, accuracy and over three orders of magnitude dynamic concentration range. These results are discussed in the sub-sections 6.2.1 through 6.2.4.

6.2.1 Indoor air sampling with SUMMA™ canisters and TWA-PDMS samplers

The concentrations of the target analytes determined by the two methods are provided in Table 6-5. 1,1 DCE, cis-DCE and trans-DCE were not quantified with either SUMMA™ canisters or by the TWA-PDMS samplers at any of the locations. Only chloroform was quantified at location D.

The comparison of the PCE concentrations obtained using the SUMMA™ canister and TWA-PDMS samplers at locations B and C shows not only good TWA-PDMS sampler-to-sampler reproducibility for PCE (< 2%), but also good correlation between the two different methods (< ~ 8%) in spite of the use of the estimated calibration constant for the quantification process. This provides strong evidence in support of the ln(*k/MW*) vs. LTPRI calibration constant estimation model. At location A, PCE concentration was quantified by TWA-PDMS samplers, but not by the SUMMA™ canister method owing to differences in the reporting limits for the two methods (0.25 $\mu g/m^3$ vs. 0.50 $\mu g/m^3$, respectively).

Results from duplicate TWA-PDMS samplers for all analytes except chloroform showed the consistency of the sampling device with respect to uptake rate, extraction efficiency and

chromatographic quantification methods. At location A, a concentration of 0.83 $\mu g/m^3$ of chloroform was quantified by the SUMMA™ canister method but not by the TWA-PDMS sampler (GS-009 in Table 6-5), even though the quantification limit was 0.21 $\mu g/m^3$. In contrast, at location B, a higher concentration was determined using TWA-PDMS sampler than that obtained with SUMMA™ canisters. This indicated possible short-term chloroform concentration variations during sampling with the SUMMA™ canisters. However that could not be confirmed as the sampler to sampler reproducibility for chloroform was good for one pair of duplicates (~11.5% difference between GS-005 and GS-007) and low for another (~76.7% difference between GS-004 and GS-006). At location D, the concentration of chloroform in one of the TWA-duplicates was 0.31 $\mu g/m^3$ and was < 0.21 $\mu g/m^3$ for the other. The reason for this discrepancy with chloroform could not be established.

Table 6-5: Comparison of the results from SUMMA™ canisters / TWA-PDMS sampler pairs and comparison of duplicate TWA-PDMS sampler results. Concentrations are reported in µg/m^3. The number followed by "U" indicates that the concentration was below the reporting limits, and the number itself represents the reporting limit for the specific analyte. Entries with N/A were not analyzed by the TWA-PDMS sampler.

Location	A		B			C			D		
	SUMMA™ canister	TWA-PDMS Sampler	SUMMA™ canister	TWA-PDMS Sampler Duplicates		SUMMA™ canister	TWA-PDMS Sampler Duplicates		SUMMA™ canister	TWA-PDMS Sampler Duplicates	
VOCs	SUMMA 1	(GS-009)	SUMMA 2	(GS-005)	(GS-007)	SUMMA 3	(GS-004)	(GS-006)	SUMMA 4	(GS-008)	(GS-010)
Sample Start Time:	6/1/07 10:56	6/1/07 10:56	6/1/07 10:56	6/1/07 10:56	6/1/07 10:56	6/1/07 10:40	6/1/07 10:40	6/1/07 10:40	6/1/07 9:20	6/1/07 9:20	6/1/07 9:20
Sample End Time:	6/8/07 9:22	6/8/07 9:22	6/8/07 9:22	6/8/07 9:22	6/8/07 9:22	6/8/07 8:56	6/8/07 8:56	6/8/07 9:53	6/8/07 8:56	6/8/07 8:56	6/8/07 8:56
1,1,1-Trichloroethane	**1.2**	**0.88**	**1.2**	**0.98**	**1.02**	**1.7**	**1.36**	**1.29**	0.5 U	0.32 U	0.32 U
1,1-Dichloroethene	0.48 U	2.5 U	0.48 U	2.5 U	2.5 U	0.48 U	2.5 U	2.5 U	0.48 U	2.5 U	2.5 U
Chloroform	**0.83**	0.21 U	**0.81**	**1.66**	**1.47**	**0.73**	**1.29**	**0.3**	0.49 U	0.21 U	**0.31**
cis-1,2-Dichloroethene	0.52 U	1.04 U	0.52 U	1.04 U	1.04 U	0.52 U	1.04 U	1.04 U	0.52 U	1.04 U	1.04 U
Tetrachloroethene	0.5 U	**0.46**	0.5 U	**0.52**	**0.52**	**0.54**	**0.58**	**0.57**	0.5 U	0.25 U	0.25 U
trans-1,2-Dichloroethene	0.52 U	N/A	0.52 U	N/A	N/A	0.52 U	N/A	N/A	0.52 U	N/A	N/A
Trichloroethene	**8.2**	**5.84**	**8.1**	**6.69**	**6.88**	**12**	**8.45**	**8.17**	0.5 U	0.12 U	0.12 U

6.2.2 Indoor and outdoor air sampling with 3M™ OVM 3500 samplers and TWA-PDMS samplers

The concentrations of all analytes obtained from 3M™ OVM 3500 samplers and TWA-PDMS samplers are shown in Tables 6-6 and 6-7. In each of the 6 locations shown in these tables, the first column shows the concentrations of the analytes determined using the 3M™ OVM 3500 samplers deployed at least 5 months before the rest of the sampling and analysis to give an indication of the temporal variability of the concentrations of different analytes.

Most of the analytes in the sample matrix which were not detected or quantified with the 3M™ OVM 3500 samplers were also not detected or quantified by the TWA-PDMS samplers. 1,1-DCA and 1,1-DCE were not detected using either of the two samplers. At one of the locations, trans-1,2-DCE was quantified by the TWA-PDMS samplers, but not by the 3M™ OVM 3500 sampler. In the absence of a reference method for comparison, this could be perceived as either a false positive result from TWA-PDMS sampler, or a false negative result from the 3M™ OVM 3500.

The results obtained from both TWA-PDMS and 3M™ OVM 3500 samplers indicated that the contaminants at the specific locations were mostly TCE and PCE, and little or no breakdown products (1,1-DCE, trans-1,2-DCE and cis-1,2-DCE) of these two compounds were present. The higher analyte uptake rates of the 3M™ OVM 3500 (and hence a lower reporting limit) samplers enabled TCE to be detected at all locations. When using the TWA-PDMS sampler, however, TCE was detected only at location 2. This should not be perceived as a disadvantage of the TWA-PDMS sampler, as the duration of the exposure can easily be increased to improve the quantification limits. Also, the quantification limits of the chromatographic method can be lowered by making large volume injections of the CS_2 extract, using thermal desorption instead of solvent extraction, or adjusting the ratio of solvent to adsorbent. The concentrations of PCE were high enough to be detected by the TWA-PDMS samplers at all locations. The concentrations of PCE determined by TWA-PDMS samplers were in all cases slightly lower than those obtained using 3M™ OVM samplers with the difference ranging from 9.5% to 41.2%. Again, in the absence of a reference method it is impossible to say whether either of the methods was biased.

Table 6-6: Comparison of results between 3M™ OVM 3500 sampler (abbreviated as 3M-OVM) and TWA-PDMS samplers. The concentrations are reported in µg/m^3. The number followed by "U" indicates that the concentration was below reporting limits and the number itself represents the reporting limit for the specific analyte.

Sample Type:	**Indoor Air**													
Sample Location:	Location 1			Location 2				Location 3			Location 4			
Sample I.D.:	PS-03	PDM-03	PS-653	PS-04	PS-04D	PDM-04	PS-654	PS-05	PDM-05	PS-655	PS-06	PDM-01	PDM-02	PS-652
Sampler Type	3M-OVM	3M-OVM	TWA-PDMS	3M-OVM	3M-OVM	3M-OVM	TWA-PDMS	3M-OVM	3M-OVM	TWA-PDMS	3M-OVM	3M-OVM	3M-OVM	TWA-PDMS
Sample Start Time:	9/21/08 15:23	2/27/09 17:13	2/27/09 17:16	9/21/08 15:28	9/21/08 15:29	2/27/09 17:23	2/27/09 17:25	9/21/08 15:30	2/27/09 17:33	2/27/09 17:35	9/21/08 15:40	2/27/09 16:55	2/27/09 17:03	2/27/09 17:00
Sample End Time:	9/22/08 15:25	3/6/09 11:25	3/6/09 11:23	9/22/08 15:28	9/22/08 15:30	3/6/09 11:53	3/6/09 11:57	9/22/08 15:33	3/6/09 11:36	3/6/09 11:39	9/22/08 15:41	3/6/09 11:09	3/6/09 11:14	3/6/09 11:17
1,1-Dichloroethane	0.2 U	0.1 U	2.0 U	0.2 U	0.2 U	0.1 U	2.0 U	0.2 U	0.1 U	2.0 U	0.2 U	0.1 U	0.1 U	2.0 U
1,1-Dichloroethene	0.2 U	0.1 U	2.6 U	0.2 U	0.2 U	0.1 U	2.6 U	0.2 U	0.1 U	2.6 U	0.2 U	0.1 U	0.1 U	2.6 U
1,2-Dichloroethene (cis)	0.2 U	**0.55**	1.2 U	0.2 U	0.2 U	**0.46**	1.2 U	0.2 U	**0.81**	1.2 U	0.2 U	**0.55**	**0.64**	1.2 U
1,2-Dichloroethene (trans)	0.2 U	0.1 U	1.6 U	0.2 U	0.2 U	0.1 U	**2.0**	0.2 U	0.1 U	1.6 U	0.2 U	0.1 U	0.1 U	1.6 U
1,1,1-Trichloroethane	0.2 U	0.1 U	1.5 U	0.2 U	0.2 U	**0.13**	1.5 U	0.2 U	**0.11**	1.5 U	0.2 U	**0.12**	**0.10**	1.5 U
Tetrachloroethene (PCE)	**1.68**	**3.27**	**2.3**	**1.70**	**1.60**	**3.98**	**3.6**	**1.76**	**1.23**	**0.9**	**1.62**	**2.91**	**3.05**	**1.9**
Trichloroethene (TCE)	**1.46**	**0.22**	0.6 U	**1.74**	**1.62**	**0.26**	**0.7**	**1.67**	**0.24**	0.6 U	**0.91**	**0.21**	**0.25**	0.6 U

Table 6-7: Comparison of results between 3M™ OVM 3500 sampler (abbreviated as 3M-OVM) and TWA-PDMS samplers. Concentrations are reported in μg/m^3. The number followed by "U" indicates that the concentration was below reporting limits and the number itself represents the reporting limit for the specific analyte.

Sample Type:	**Outdoor Air**					
Sample Location:	Location 5			Location 6		
Sample I.D.: Sampler Type	PS-01 3M-OVM	PDM-07 3M-OVM	PS-657 TWA-PDMS	PS-02 3M-OVM	PDM-06 3M-OVM	PS-656 TWA-PDMS
Sample Start Time:	9/21/08 15:15	2/27/09 17:50	2/27/09 17:51	9/21/08 15:18	2/27/09 17:41	2/27/09 17:43
Sample End Time:	9/22/08 15:15	3/6/09 11:28	3/6/09 11:31	9/22/08 15:19	3/6/09 11:46	3/6/09 11:49
1,1-Dichloroethane	0.2 U	0.1 U	2.0 U	0.2 U	0.1 U	2.0 U
1,1-Dichloroethene	0.2 U	0.1 U	2.6 U	0.2 U	0.1 U	2.6 U
1,2-Dichloroethene (cis)	0.2 U	**0.97**	1.2 U	0.2 U	**0.57**	1.2 U
1,2-Dichloroethene (trans)	0.2 U	0.1 U	1.6 U	0.2 U	0.1 U	**2.5**
1,1,1-Trichloroethane	0.2 U	**0.24**	1.5 U	0.2 U	**0.14**	1.5 U
Tetrachloroethene (PCE)	**0.41**	**1.87**	**1.1**	**0.42**	**0.98**	**0.8**
Trichloroethene (TCE)	**0.58**	**0.35**	0.6 U	**0.50**	**0.22**	0.6 U

6.2.3 Vent pipe and HPV test sampling with TWA-PDMS samplers and SUMMA™ canisters

Figure 6-7 shows the correlation plot of the concentrations of PCE determined using the TWA-PDMS samplers and by either the SUMMA™ canister or TAGA. The experiments indicated a very strong correlation between the two methods over two to three orders of magnitude for each analyte and an overall correlation over ~4 orders of magnitude for all the analytes put together. The correlation indicated two data points (marked as A in the chart) for which the deviations from the 1:1 correlation line was higher than that for the rest. However,

the TCE to PCE ratio in that sample was the same as that observed for other samples taken at the same location. The correlation also indicated no negative bias in the concentrations obtained from TWA-PDMS samplers which indicated that there was no starvation effect. These experiments suggested that TWA-PDMS passive samplers could be an economic alternative to expensive conventional methods of quantifying pollutant concentration in sub-slab soil gas.

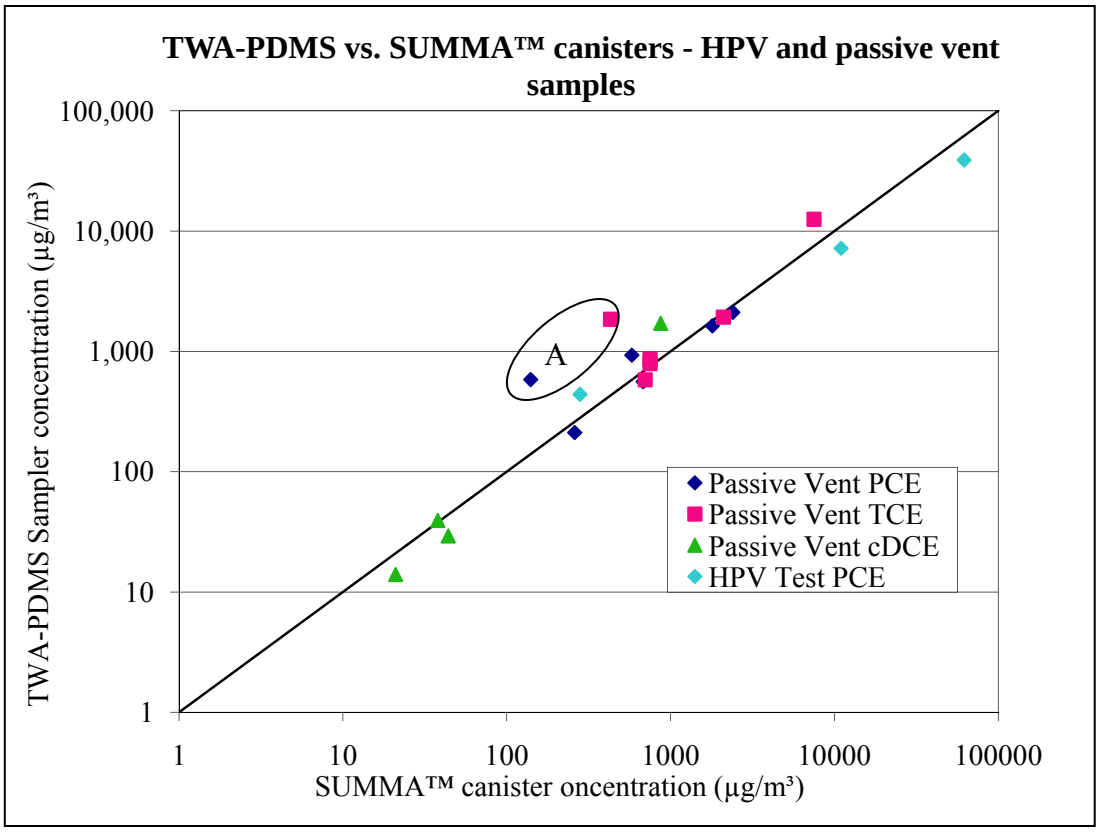

Figure 6-7: Correlation between the concentrations determined in HPV flow cell and passive vent-pipe using TWA-PDMS samplers and SUMMA™ canisters. "A" indicates two data points for which the deviations from the 1:1 correlation were higher than that for the rest.

6.2.4 Indoor air sampling with TWA-PDMS samplers and SUMMA™ canisters or TAGA unit

Correlation of PCE concentrations obtained from TWA-PDMS samplers, SUMMA™ canisters and TAGA unit are shown in Figure 6-8. Similar to the observation made in section

6.2.3, excellent correlation was observed between TWA-PDMS samplers and the other reference methods. The correlation further reiterated the wide dynamic range of the TWA-PDMS samplers (over 3 orders of magnitude). Considering that the samples from TWA-PDMS samplers were collected over 3 days, SUMMA™ canisters over 8 hours and TAGA measured the concentrations instantaneously, the correlation observed can be considered excellent.

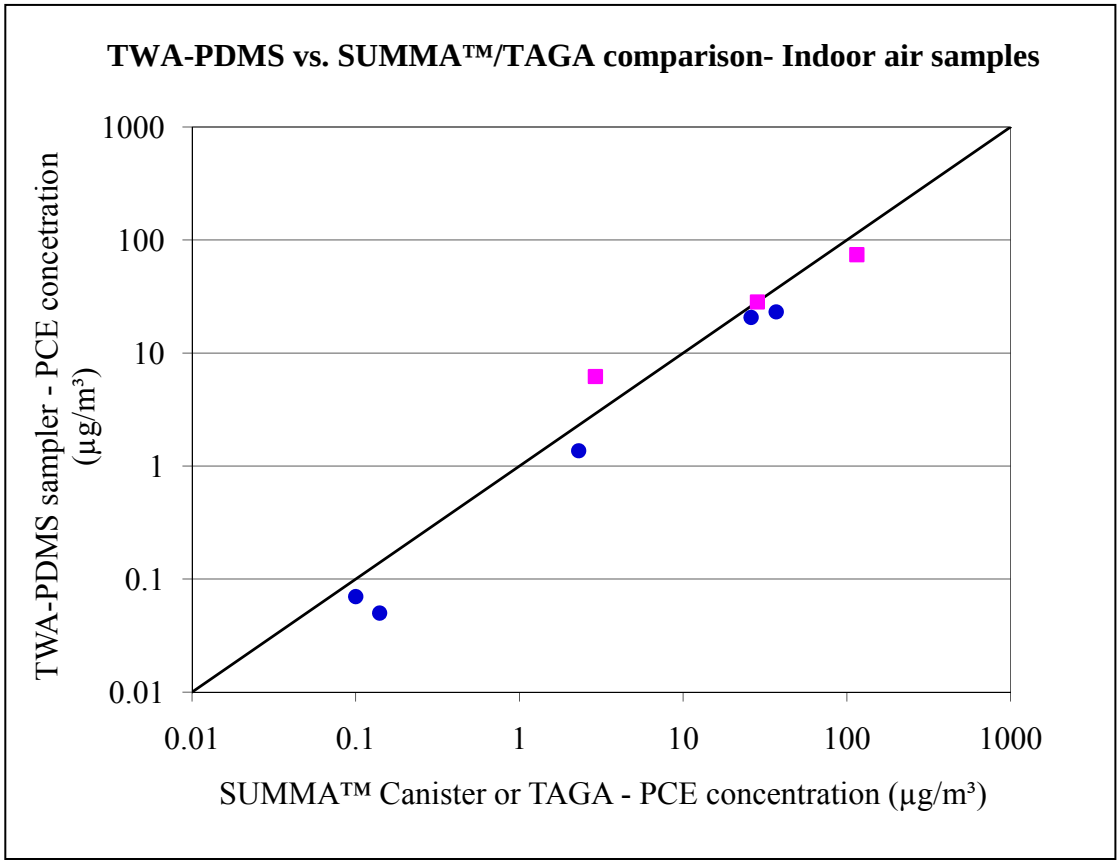

Figure 6-8: Comparison of PCE concentrations determined by TWA-PDMS samplers and either SUMMA™ canisters or TAGA.

6.3 Conclusions

The results of the analysis performed using TWA-PDMS samplers and commercially available sampling systems such as SUMMA™ canisters, 3M™ OVM 3500 sampler, and TAGA mobile laboratory were discussed in this chapter. SUMMA™ canisters are often considered "gold standards" for comparison with new sampling methods. In the indoor air

sampling experiments, excellent correlations were observed between the concentrations determined using SUMMA™ canisters and the TWA-PDMS samplers for all analytes but chloroform. Furthermore, comparison of the concentrations obtained from SUMMA™ canisters and TAGA with TWA-PDMS samplers indicated good correlation between the two methods and an overall linearity of 6 orders of magnitude for the TWA-PDMS samplers.

3M™ OVM 3500 sampler is a commercially available passive sampler for the analysis of volatile organic compounds in air. The results obtained from the two methods generally showed comparable concentrations. Analyte uptake rates for TWA-PDMS samplers were lower than those for the 3M™ OVM samplers, hence the latter could quantify TCE at lower concentration levels than the former.

The HPV testing method pioneered by Geosyntec Consultants in combination with the use of TWA-PDMS samplers proved to be a useful tool in monitoring temporal variability of analyte concentration without any bias related to starvation effects. TWA-PDMS sampling in wind driven passive vents using TWA-PDMS samplers also showed very good correlations with the results obtained with SUMMA™ canisters and indicated no starvation effect. The results obtained from TAGA compared well with those obtained from TWA-PDMS samplers.

In all the comparisons, PCE concentrations determined using TWA-PDMS samplers were estimated from the ln(k/MW) vs. LTPRI correlation rather than determined experimentally, yet they still showed good correlations with the values obtained using the reference methods, which is another indication that the calibration constant estimation model works well.

CHAPTER 7

Soil gas sampling and analysis

Soil gas surveys are important for determining the presence, composition, source and distribution of contaminants in soil. The application of TWA-PDMS samplers for such purposes was tested at several locations and a representative selection of the methods and analytical results will be presented in this thesis. All field sampling projects described in this chapter were performed either by Geosyntec Consultants, Inc. of Guelph, ON, or Tauw Scientific Inc., Belgium, for their clients at various locations in Europe and in North America. Soil gas sampling application described here included samples collected at various depths and distances from buildings under evaluation for potential vapor intrusion (exterior samples), as well as samples collected at shallow depths beneath floor slabs (interior samples). The consultants' goal was to characterize or monitor the nature and extent of subsurface VOC vapors. Our research goal at the University of Waterloo was to demonstrate the applicability and advantages of the TWA-PDMS sampling technology for such contaminant mapping purposes by comparing it with existing technologies whenever possible along with prior knowledge of the contaminant history at the selected locations.

Soil gas sampling is often challenging because of high soil moisture content, variable permeability, different drilling methods and inter-operator variability. With respect to soil gas sampling using TWA-PDMS samplers, the aspects discussed in section 4.5.5, related to the effect of the linear flow velocity of air on the sampling rate are critical to understand and properly interpret the soil gas concentrations determined. This will be dealt with under the discussion sections for each of the sampling programs described in this chapter.

7.1 Field sampling and analysis methods

Passive sampler calibration, fabrication and analysis were performed at the University of Waterloo. The method described in Chapter 3 was used for the fabrication of the sampler. The method described in Chapter 6 was used for the packing and shipping of the samplers to and from the laboratory. The holding time between sampling and analysis was generally less than 30 days, and the samples were refrigerated during storage.

In this section, sampling performed at three different locations will be described:

- Sub-slab vapor sampling using TWA-PDMS samplers and SUMMA™ canisters at Knoxville, TN,
- Soil gas sampling in Belgium using TWA-PDMS samplers and GORE™ modules, and
- Sub-slab vapor sampling at a location in Italy using TWA-PDMS samplers.

The first method involved comparison with standard methods, the second involved comparison with a commercially available diffusive-type sampler, and the third was an application in soil gas concentration mapping.

7.1.1 Sub-slab vapor sampling using TWA-PDMS samplers and SUMMA™ canisters

Sub-slab vapor samples were collected with TWA-PDMS samplers and SUMMA™ canisters at a location in Knoxville, TN. SUMMA™ canister samples were collected one week prior to the deployment of the TWA-PDMS samplers from 0.5 inch holes drilled into the floor. The vapour samples were collected for a period ranging between 5 and 10 minutes at 200 mL/min using the flow controller in the SUMMA™ canister. The TWA-PDMS samplers were introduced into holes of 0.75 inch diameter (of varying depths depending on the thickness of the concrete). The samplers were hung from a rigid metal wire in such a way as to be approximately an inch from the bottom of the hole, and the hole was sealed with a temporary seal made of rubber wrapped with aluminum foil sufficient to prevent air-flow into or out of the drilled hole. The major target analytes at the site were TCE and PCE. All sample processing was performed using GC-ECD as shown in Table 6-2 earlier.

7.1.2 Soil gas sampling in Belgium with TWA-PDMS samplers and GORE™ modules

In this study, soil gas sampling was performed at a contaminated site using 438 TWA-PDMS samplers deployed at a regular spacing of about 30 m throughout the site. The area of the test site was approximately 1000 m long and 600 m wide. The contaminants possibly present at the site included chlorinated ethanes, ethenes and benzenes, BTEX, PAHs and PCBs. The contaminants originated from different industries located in the area. Head-to-head comparison was made between the results obtained from TWA-PDMS samplers and the

commercially available GORE™ modules at 80 locations (see Chapter 1 for the description of the GORE™ module). The GORE™ modules were installed, retrieved and analyzed independently by their manufacturer.

The list of the target analytes, determined based on the history of the manufacturing facilities and their activities in the region, is shown in Table 7-1. The analytes marked with asterisks are those for which the calibration constants were estimated based on the correlation of the calibration constant with the linear temperature programmed retention index of the analytes. Table 7-1 also indicates the minimum concentration (reporting limits) that could be quantified using the TWA-PDMS samplers calculated based on the calibration constant, one week deployment period and quantification limits of the chromatographic methods. The low calibration constants (or high uptake rates) for PAHs indicate that very high linear flow velocity of air across the surface of the sampler is required for sampling without starvation effect.

Table 7-1: Target analytes, their calibration constants and reporting limits for a one week exposure of the TWA-PDMS sampler used for soil gas sampling in Belgium. "*" indicates analytes for which estimated calibration constants were used for quantitfication purposes.

Analyte	Calibration constant (min/mL)	Reporting limit for 1 week exposure period in $\mu g/m^3$
1,1-Dichloroethylene	1.223	2.48
t-Dichloroethylene	0.755	1.55
1,1-Dichloroethane	0.964	1.86
c-Dichlroethylene	0.524	1.12
Chloroform	0.514	1.08
1,2-Dichloroethane	0.388	0.80
1,1,1-Trichloroethane	0.787	1.54
Benzene	0.466	0.85
Carbontetrachloride	0.667	1.35
Trichloroethylene	0.305	0.56
1,1,2-Trichloroethane*	0.255	0.55
Toluene	0.236	0.48
Perchloroethylene*	0.187	0.43
Chlorobezenze*	0.276	0.69
1,1,1,2-Tetrachloroethane*	0.166	0.29
Ethylbenzene	0.151	0.29
p,m-Xylene	0.146	0.30
1,1,2,2-Tetrachloroethane*	0.112	0.26
o-Xylene	0.131	0.31
1,3-Dichlorobenzene*	0.134	0.38
1,4-Dichlorobenzene*	0.131	0.38
1,2-Dichlorobenzene*	0.118	0.38
Naphthalene*	0.039	0.039
Acenaphthylene*	0.009	0.009
Acenaphthene*	0.009	0.009
Fluorene*	0.008	0.008
Phenanthrene*	0.003	0.003
Anthracene*	0.002	0.002
Fluoranthene*	0.002	0.002
Pyrene*	0.0008	0.001

7.1.2.1 Sampler deployment methods

A 2 inch diameter borehole was drilled to a depth of 1.2 meters using a core barrel shown in Figure 7-1. The TWA-PDMS samplers were then suspended inside the borehole at a depth of 1 m from the ground surface. The water table depth in that area was around 4 m. Once the sampler was in place, the borehole was sealed with a simple technique illustrated in Figure 7-2. A rigid metal rod was first inserted into a black plastic bag and an aluminum foil was wrapped snugly enough to hold during insertion and removal, but loosely enough to expand out against the walls of the borehole after insertion (Figure 7-2 (A) and (B)). The assembly was then pushed into the borehole to a depth of approximately 0.7 m from the surface (Figure 7-2 (C) and (D)) which allowed vapor sampling for the TWA-PDMS samplers from a 0.5 m long segment of the borehole. The surface of the borehole was then sealed with a wooden tapered cork.

Figure 7-1: Field personnel coring a hole for the deployment of TWA-PDMS samplers and GORE™ Modules

Figure 7-2: Photographs of (A) – Aluminum foil being wrapped around the plastic cover, (B) – crunching the aluminum foil for snug fit, (C) – the assembly being inserted into the borehole and (D) – the completed borehole sealing process.

GORE™ modules were deployed into separate boreholes at a lateral distance of 0.3 m from the selected boreholes where the TWA-PDMS samplers were deployed. The GORE™

module (the white part in Figure 7-3) was inserted into the borehole and secured using a thread on the outside such that the module rested at approximately the same distance from the ground surface as that of the TWA-PDMS samplers in their respective boreholes. The boreholes were then sealed at the surface with wooden corks. The surface appearance of the ground after the boreholes were sealed is shown in Figure 7-4. It has to be noted that the effective vapor space in the borehole from where TWA-PDMS sampling was performed was 0.5 m of the borehole, while it was the entire 1.2 m for the GORE™ modules (proprietary specification). On the other hand, the sealing method used for the TWA-PDMS samplers was much more effective, and the risk of soil gas dilution with atmospheric air in the borehole was much smaller than with the GORE™ modules.

Figure 7-3: Deployment of the GORE™ module inside a borehole.

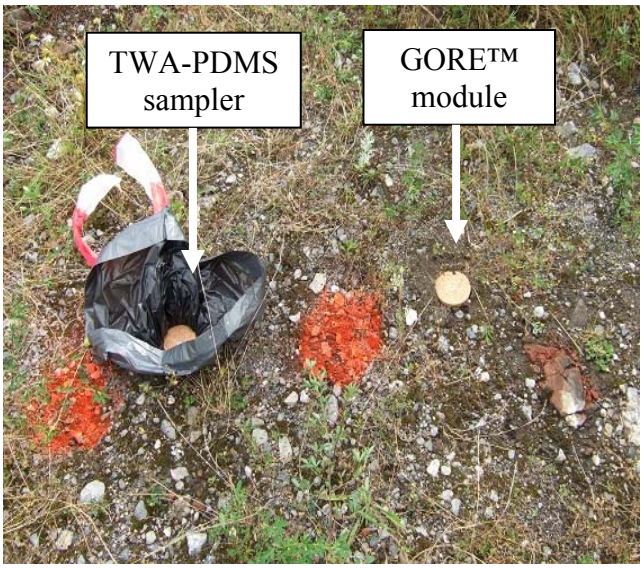

Figure 7-4: Ground surface appearance after the deployment of the TWA-PDMS samplers and the GORE™ modules.

Figure 7-5 shows locations of the 438 TWA-PDMS samplers. The lateral spacing between the samplers was different at different locations, but was generally kept at 30 m whenever possible. Figure 7-6 shows the locations of the 80 GORE™ modules installed for head-to-head comparison purposes.

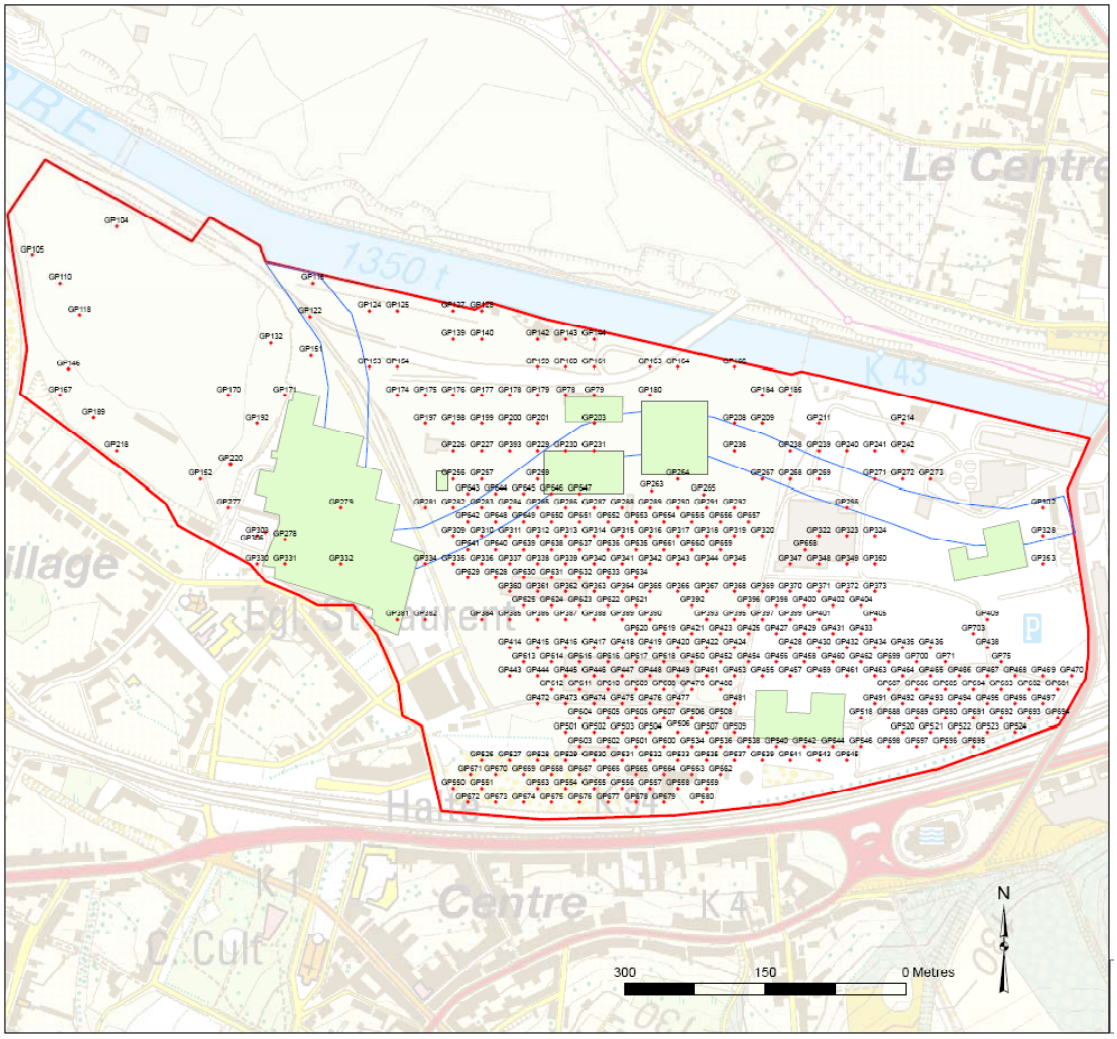

Figure 7-5: Borehole locations for the TWA-PDMS sampler's deployment

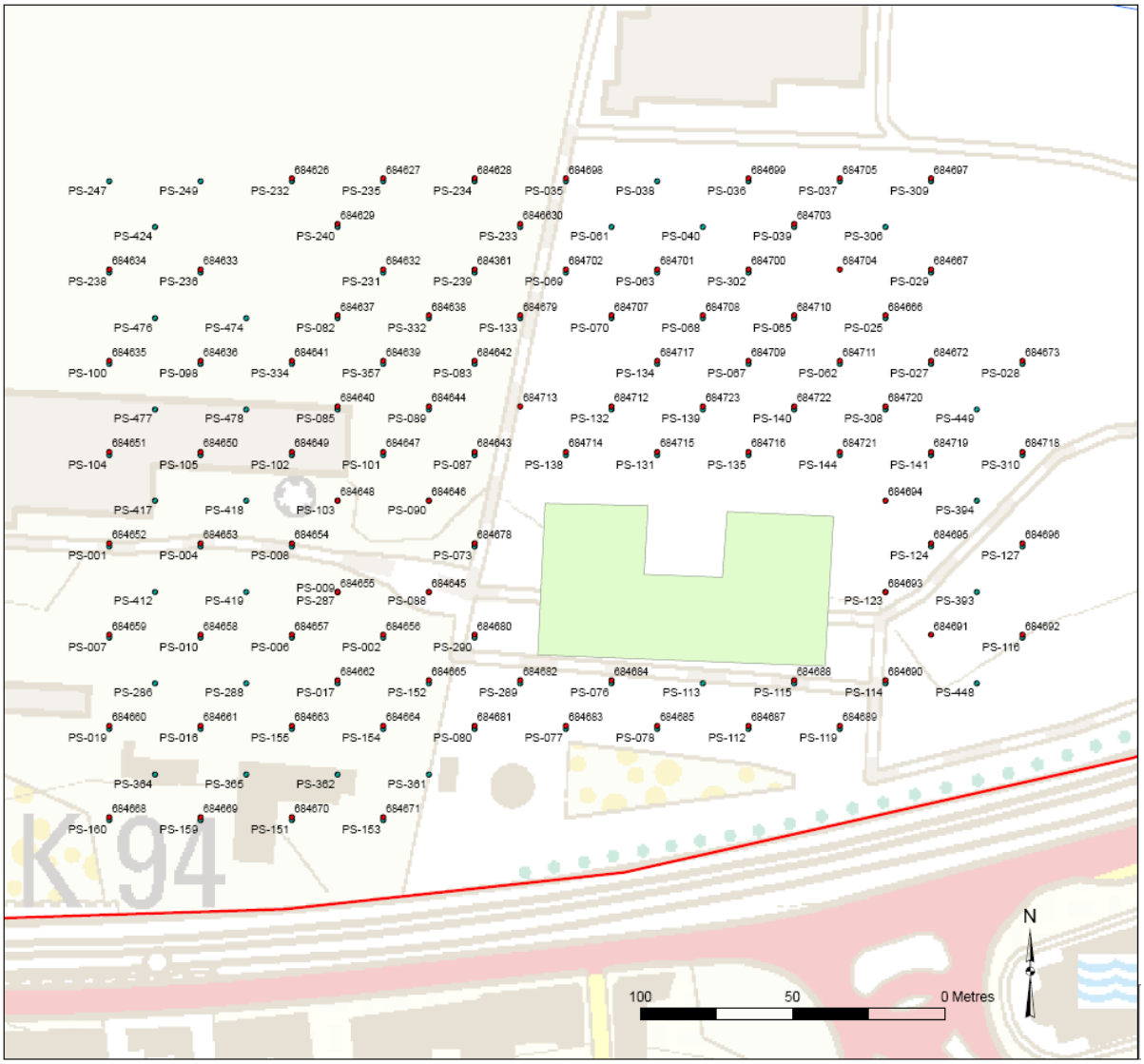

Figure 7-6: Borehole locations where the TWA-PDMS samplers and GORE™ modules were deployed within 30 cm of each other. Red spots indicate GORE™ modules, and green spots indicate TWA-PDMS samplers.

7.1.2.2 TWA-PDMS sampler solvent desorption and chromatographic methods

The extraction scheme shown in Figure 7-7 was used for the quantification of the target analytes trapped in the TWA-PDMS samplers. The target analytes included PAHs, which are extracted from Anasorb 747® with poor efficiency using CS_2. The extraction method was therefore modified by including a second extraction with

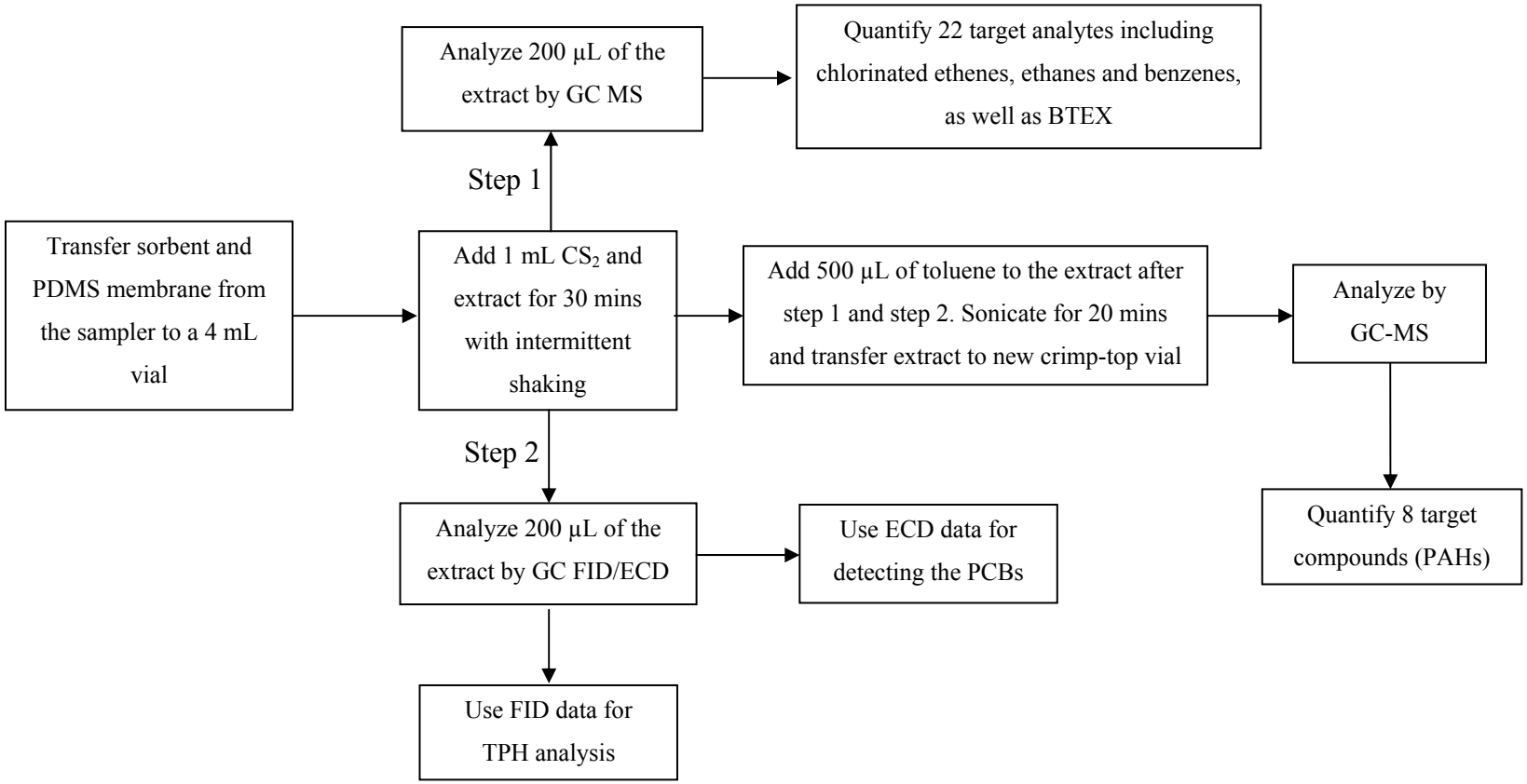

Figure 7-7: Schematic of the solvent desorption and subsequent chromatographic analysis peformed for the quantification of the various groups of target analytes.

toluene combined with sonication for the extraction and analysis of the PAHs. The respective recovery rates for the PAHs were determined based on this extraction method and applied while estimating the concentrations in the sample as described in more detail in the paragraphs below.

The sorbent in the sampler along with the PDMS membrane were transferred to 4 mL vials and extracted with 1 mL aliquots of freshly distilled CS_2 for 30 minutes with intermittent shaking. 0.4 mL of the extract was transferred to two GC crimp cap vials with 200 µL inserts in each of them, and then crimped to seal. The content of the first vial was analyzed by GC-MS for all analytes except the PAHs and PCBs using the method listed in Table 7-2. GC-MS was operated in the SIM mode and the ions used for the quantification of each analytes are listed in Table 7-3.

Table 7-2: GC-MS method used for the separation and quantification of BTEX and chlorinated compounds.

GC-MS Instrument	Agilent Technologies, 6890 GC - 5973 MS
Injection mode	Split, 275˚C
Split ratio	1:10
Injection volume	1 µL
Carrier gas	Helium at 2.0 mL/min
Oven temperature program	35˚C for 5 mins, 5˚C/min to 120˚C (held for 0 mins), 30˚C/min to 350˚C (held for 3 minutes)
Data acquisition and processing	Chemstation software
Capillary column	Rxi-1 MS (100% methylsiloxane), 60 m x 0.32 mm, 1.0 µm film thickness
Quantification mode	Selected Ion Monitoring (three ions for each analyte, except where noted, as in Table 7-3)
Calibration method	External standard, multipoint calibration

Table 7-3: Ions used for the quantification of the analytes in the GC-MS SIM mode.

Analyte	Ions used for the analytes in the SIM mode (m/z)
1,1-Dichloroethylene	61, 96, 98
t-Dichloroethylene	63, 65, 98
1,1-Dichloroethane	61, 96, 98
c-Dichlroethylene	61, 96, 98
Chloroform	83, 85, 47
1,2-Dichloroethane	62, 64, 49
1,1,1-Trichloroethane	97, 99, 61
Benzene	78, 77, 51
Carbontetrachloride	117, 119, 121
Trichloroethylene	95, 130, 132
1,1,2-Trichloroethane	97, 83, 61
Toluene	91, 92, 65
Perchloroethylene	166, 131, 164
Chlorobezenze	112, 77
1,1,1,2-Tetrachloroethane	131, 117
Ethyl benzene	91, 106, 65
p,m-Xylene	91, 106, 105
1,1,2,2-Tetrachloroethane	83, 85
o-Xylene	106, 91
1,3-Dichlorobenzene	146, 148, 111
1,4-Dichlorobenzene	146, 148, 111
1,2-Dichlorobenzene	146, 148, 111
Naphthalene	128, 102
Acenaphthylene	310, 353, 121
Acenaphthene	153, 154, 76
Fluorene	166, 165, 82
Phenanthrene	178, 176, 152
Anthracene	178, 176, 152
Fluoranthene	202, 200, 101
Pyrene	202, 200, 101

The second vial was used for the determination of the Total Petroleum Hydrocarbon (TPH) concentration and screening for PCBs in the sample. The determination of TPH requires a GC with an FID (sensitive to most organic compounds), while the detection of PCBs requires a GC with an ECD (sensitive to chlorinated compounds). To achieve this, the eluent from the GC capillary column was split into two using a Graphpack® "Y" splitter, and the eluent was analyzed by both FID and ECD. The GC method listed in Table 7-4 was used for this purpose. Total petroleum hydrocarbons were then estimated based on the procedure described in Chapter 3.

Table 7-4: GC method used for the separation and quantification of total petroleum hydrocarbons and for the detection of PCBs.

GC Instrument	Agilent Technologies, 6890 GC
Injection mode	Split, 275˚C
Split ratio	1:10
Injection volume	1 µL
Carrier gas	Helium at 1.20 mL/min
Oven temperature program	35˚C for 0 mins, 5˚C/min to 120˚C (held for 0 mins), 30˚C/min to 350˚C (held for 3 minutes)
Data acquisition and processing	Chemstation software
Capillary column	VF-1 Ms (100% methylsiloxane), 15 m x 0.25 mm, 0.5 µm film thickness
Detector / calibration method for TPH estimation	Flame Ionization detector / external standard, multipoint calibration with benzene
Detector / calibration method for the detection of PCB's	Electron Capture Detector / no calibration performed.

No theoretical and/or experimental work was performed to determine the uptake rates of the PCBs by the TWA-PDMS samplers, as quantitative analysis was not required by the customer. Consequently, only a visual comparison of the peak pattern in the chromatograms obtained using the ECD for the samples with a chromatogram obtained by injecting a 1 µL sample solution containing 1 µg/mL of Aroclor 1254 (a mixture of PCB congeners) was

carried out to screen for the presence or absence of PCBs. The extraction efficiency of the PCB congeners in Aroclor 1254 was examined by spiking 10 µL of a 100 µg/mL solution in a 4 mL vial containing 250 mg of Anasorb 747®, and following the same procedure of extraction and sample injection as described earlier for PCB analysis.

A 0.5 mL aliquot of toluene was then added to the same 4 mL vial (from which 400 µL aliquot of the CS_2 extract was already removed) described in the above paragraphs, and further extracted with sonication for 20 minutes at room temperature. The toluene-CS_2 extract was centrifuged, and the supernatant was transferred to another vial containing a 100 µL insert and analyzed by GC-MS for the semi-quantification of PAHs. The GC-MS method (operated in the SIM mode) used for the analysis is listed in Table 7-5.

Table 7-5: GC-MS method used for the separation and quantification of PAHs in the extracted solvent.

GC-MS Instrument	Agilent Technologies, 6890 GC – 5975B MS
Injection mode	Split, 275˚C
Split ratio	1:10
Injection volume	1 µL
Carrier gas	Helium at 1.20 mL/min
Oven temperature program	35˚C for 0 mins, 5˚C/min to 120˚C (held for 0 mins), 30˚C/min to 350˚C (held for 3 minutes)
Data acquisition and processing	Chemstation software
Capillary column	VF-5 MS (95% methylsiloxane , 5% Phenyl), 30 m x 0.25 mm, 1.0 µm film thickness
Quantification mode	Selected Ion Monitoring (three ions for each analyte, except where noted, as in Table 7-3)
Calibration method	External standard, multipoint calibration

Recovery rates for all target analytes were determined by spiking standard solutions of the analytes onto the Anasorb 747® and a cut PDMS membrane (same dimension as that used in the samplers) in a 4 mL vial. The vials were capped after spiking and were allowed to equilibrate for 2 days for one set of 6 vials and 2 weeks for a a second set of 6 vials at room temperature before extraction with CS_2 and chromatographic analysis. This was done to

investigate any difference in recovery rates due to holding time of the sampler between its retrieval in the field and extraction/analysis in the laboratory. The target analytes were divided into four groups, and the recovery rates were determined for these groups separately in the maner explained above. Recovery rates obtained from the two-week storage period were applied when calculating analyte concentrations in the soil gas so as to correct for the time required for sampler transportation from Belgium to Waterloo, ON.

7.1.3 Sub-slab soil gas sampling in Italy with TWA-PDMS samplers

Sub-slab soil gas sampling was performed to determine the concentrations of chlorinated ethanes and ethenes at various locations in a manufacturing facility with known history of using various chlorinated solvents. A total of 37 PDMS samplers were deployed for sub-slab vapor sampling. A total of 6 target VOCs were analyzed: PCE, TCE, cis-DCE, vinyl chloride, 1,1-DCE and chloroform. The calibration constants of all the target analytes except vinyl chloride are listed in Table 7-1. An estimated calibration constant of 2.08 min/mL (based on ln(k/MW) vs. LTPRI correlation as described in Chapter 3) was used for the latter.

An electric hammer drill was first used to drill a one inch diameter hole in the floor as shown in Figure 7-8. A one foot temporary steel casing was used as a guide to insert the sampler to the desired depth into the drilled hole. The casing was then removed and the top of the hole was sealed to prevent air exchange across the slab during the deployment period. After five days of sampler exposure, the samplers were retrieved and shipped to the University of Waterloo for sample analysis. Both the deployment and the retrieval of the 37 samplers took only several hours, thereby reducing the field cost drastically compared to conventional soil gas sampling using SUMMA™ canisters which would have taken two to three days for the same number of samples. The samples received at the University of Waterloo were analyzed using the GC-MS method parameters listed in Table 7-2. Analyte extraction was performed using the sample extraction scheme presented in Figure 3-16. All analyses were performed within one week from the time the samples were retrieved from the field.

Figure 7-8: Photographs of (A) – a hole being drilled into the floor and (B) – deployment of the TWA-PDMS sampler at a predetermined depth in the hole.

7.2 Results and discussion

The results from the projects described above provided extensive information regarding the advantages and performance of the TWA-PDMS sampler when used for soil gas sampling applications. They are presented in the following three sub-sections.

7.2.1 Sub-slab vapor sampling using TWA-PDMS samplers and SUMMA™ canisters

The concentrations obtained from the two sampling systems at different locations shown in Figure 7-9 indicated a negative bias in the concentrations of both TCE and PCE determined by the TWA-PDMS samplers compared to those obtained using the SUMMA™ canister method. This was a direct consequence of the starvation effect, which is unavoidable due to the stagnant air matrix around the sampler. This effect resulted in a negative bias of approximately one order of magnitude for most of the samplers, and was less than two orders of magnitude for all but one sampler. If the starvation effects were to be identical for all the samplers at all the locations, a nearly constant negative bias should have been observed

(assuming that there were no temporal variations during the time the concentrations were determined by the two methods). The variation in negative bias indicated that the starvation effect was different for different samplers, which could be explained based on the different depths of the core holes, as well as the differences in soil matrix permeability towards TCE and PCE. There was however a positive correlation between the two methods sufficient for routine use of the TWA-PDMS sampler for such application in determining the relative concentrations of various pollutants at different locations. It should also be noted that the starvation effect is unavoidable for not just the sampler discussed here, but for any other passive sampler in general.

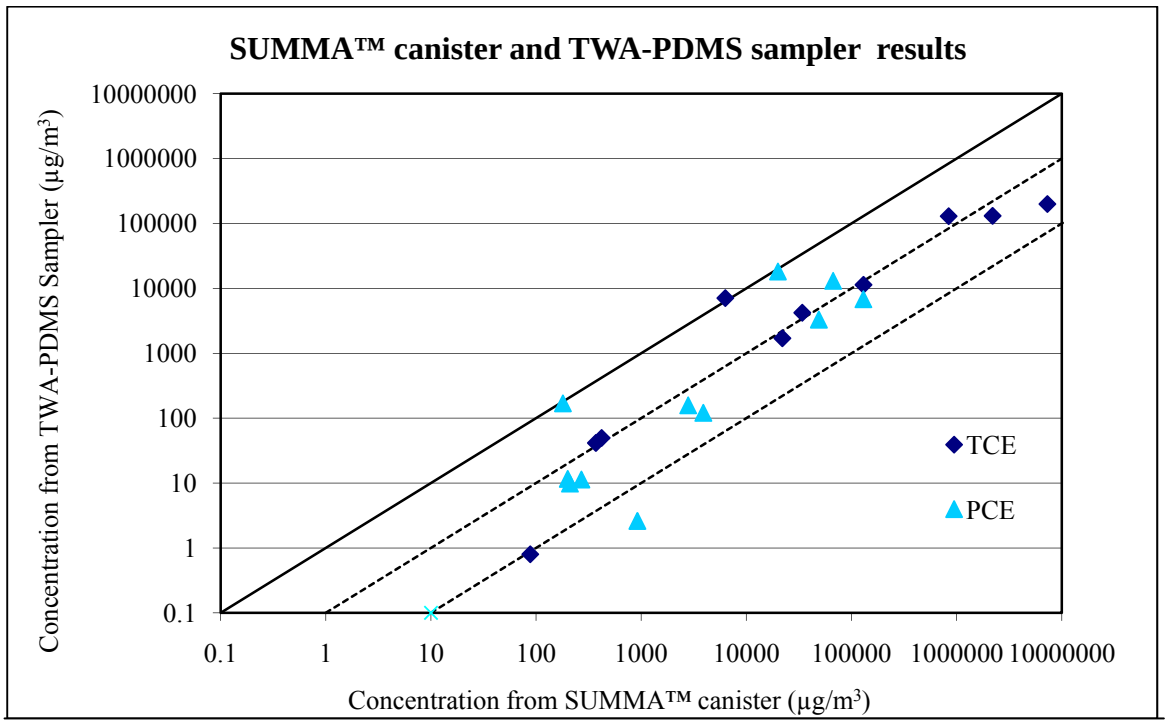

Figure 7-9: Comparison of PCE and TCE concentrations obtained from TWA-PDMS samplers and SUMMA™ canisters. The solid straight line represents a 1:1 correlation, and the dotted lines represent one and two orders of magnitude difference correlations.

The results of this project indicated the importance of the starvation effect as applied for soil gas sampling using the TWA-PDMS samplers. One potential method to reduce such starvation effect is to increase the depth and width of the core hole in which the sampler is

deployed. In that way, the inside surface area of the core hole can be increased, and consequently more analyte can diffuse into the core hole in unit time to compensate for its removal from the vapour phase due to uptake into the sampler. As a result, the core hole diameter was increased to 2 inches in the project which is discussed next.

7.2.2 Soil gas sampling in Belgium

Out of the 438 samplers deployed in the field, only 405 were retrieved and analyzed, as some of the samplers could not be retrieved due to the borehole collapsing onto them. A detailed analytical report on the concentrations of various target analytes at various locations is available in Excel spreadsheet format on the accompanying compact disc. The electronic version of the Excel sheet in pdf format is also available (Appendix A). The significant observations are discussed in this section.

Figure 7-10 shows a typical chromatogram of a standard solution of a mixture of chlorinated compounds and BTEX obtained using the GC-MS method outlined in Table 7-2. Chlorobenzene and 1,1,1,2-tetrachloroethane peaks co-eluted at 17.4 minutes, therefore their unique fragment ions, 112 and 131, respectively, were used for quantification. The same was true for 1,1,2,2-tetrachloroethane and o-xylene. In this case, the unique fragment ions m/z 83 and 91, respectively, were used for the quantification. Figure 7-11 shows a typical chromatogram of a sample solution obtained using the GC-MS method outlined in Table 7-2.

Figure 7-12 shows chromatograms obtained from the injection of the standard solution of 1 µg/mL of Aroclor 1254 in CS_2 and an equivalent concentration after extraction of the spiked Aroclor 1254 with 1 mL CS_2. These two chromatograms were used for comparison with the sample extracts to visually identify the presence/absence of PCBs in soil gas.

The extraction efficiencies of all the analytes (Table 7-6) except PAHs and dichlorobenzenes were greater than 84%, with relative standard deviations of less than 5.3% (n=6) for both 48 hours and 2 weeks holding period. The extraction efficiencies varied between 48% and 78% for the PAHs and dichlorobenzenes, with a relative standard deviations ranging between 3.2% and 12.3% (n=6). The low extraction efficiencies for PAHs and dichlorobenzenes were expected, as Anasorb 747® is known to be unsuitable for PAHs and SVOCs in general.

While a total of 405 TWA-PDMS samplers were analyzed, only 80 GORE™ modules were installed for comparison purposes. Accordingly, contaminant profiles determined on the basis of PDMS sampler results indicated more contaminated locations than the GORE™ modules. The major contaminants determined using both types of samplers were chlorinated compounds like TCE and PCE, as well as benzene and traces of naphthalene. No PCBs were detected using either of the two methods. This was consistent with the knowledge of the history of the location. Contamination profiles determined by TWA-PDMS samplers and GORE™ modules for these analytes were generally similar and indicated the same concentration hot spots.

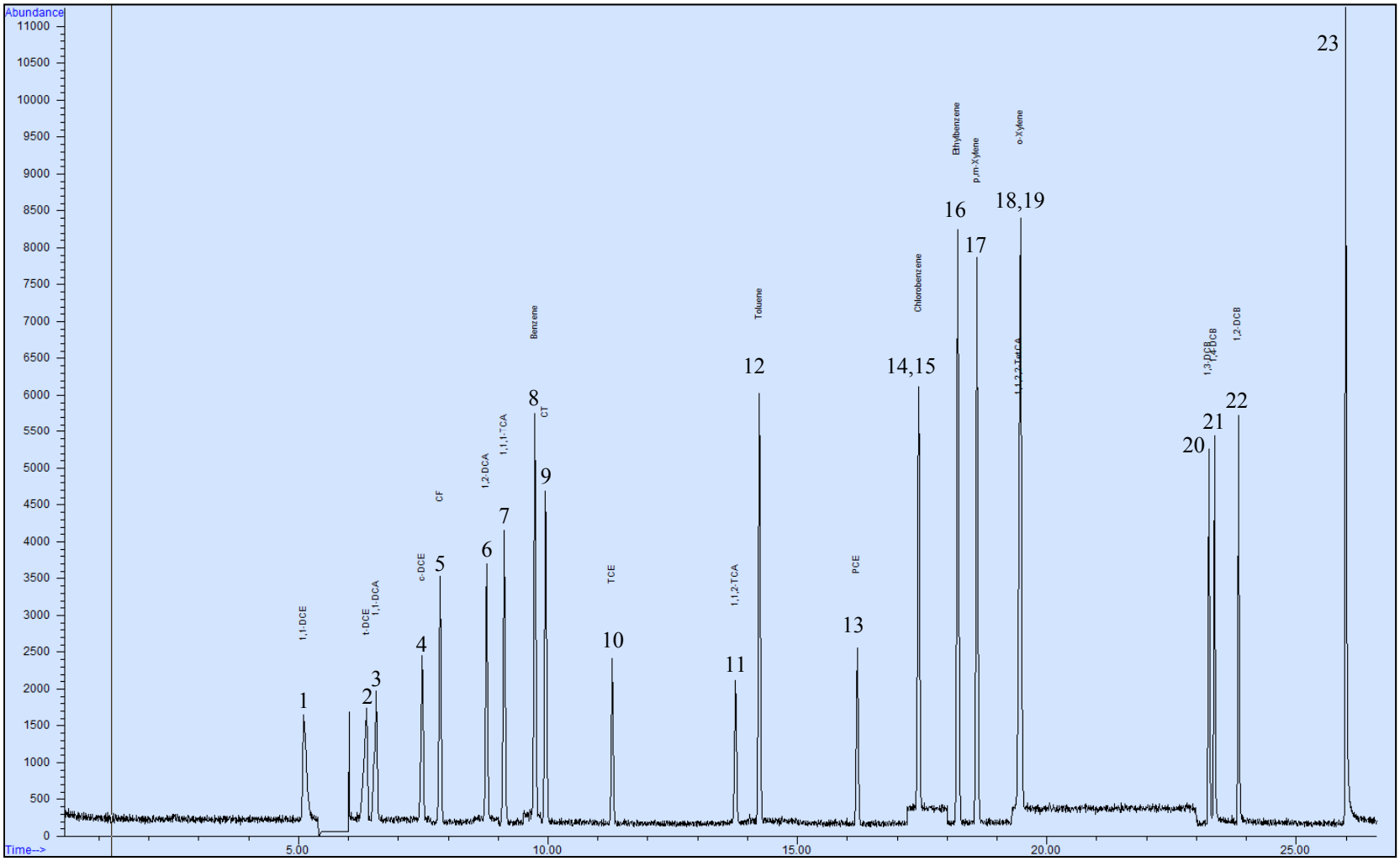

Figure 7-10: A typical chromatogram of a standard solution of chlorinated compounds and BTEX obtained using GC-MS method outlined in Table 7-2: (1) 1,1-DCE (2) t-DCE (3) 1,1-DCA (4) c-DCE (5) CF (6) 1,2-DCA (7) 1,1,1-TCA (8) benzene (9) CT (10) TCE (11) 1,1,2-TCA (12) toluene (13) PCE (14) chlorobenzene (15) 1,1,1,2-TetCA (16) ethyl benzene (17) p,m-Xylene (18) 1,1,2,2-TetCA (19) o-xylene (20) 1,3-DCB (21) 1,4-DCB (22) 1,2-DCB (23) naphthalene.

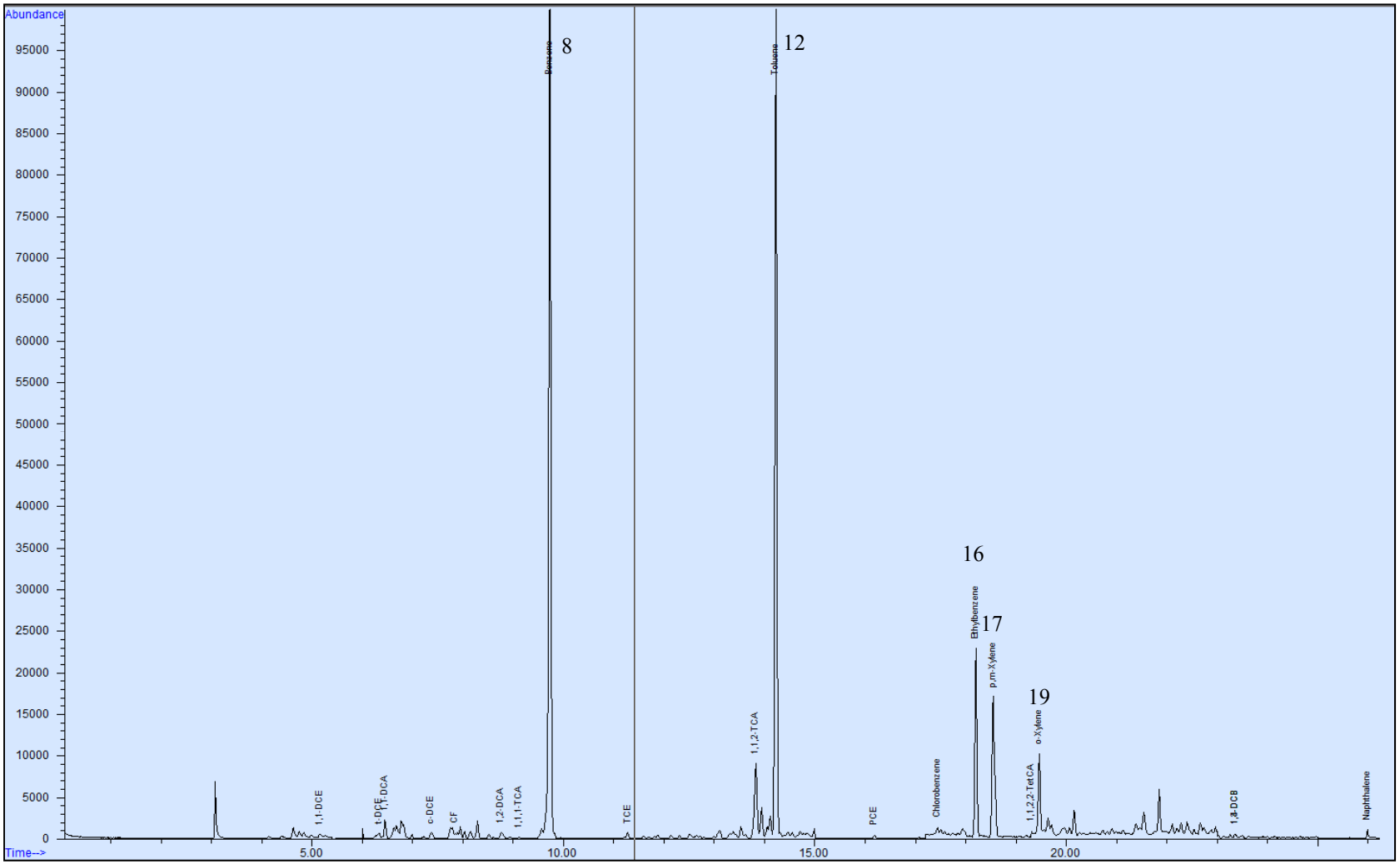

Figure 7-11: A typical chromatogram obtained from a sample solution using the GC-MS method outlined in Table 7-2: (8) benzene (12) toluene (16) ethyl benzene (17) p,m-xylene (19) o-xylene.

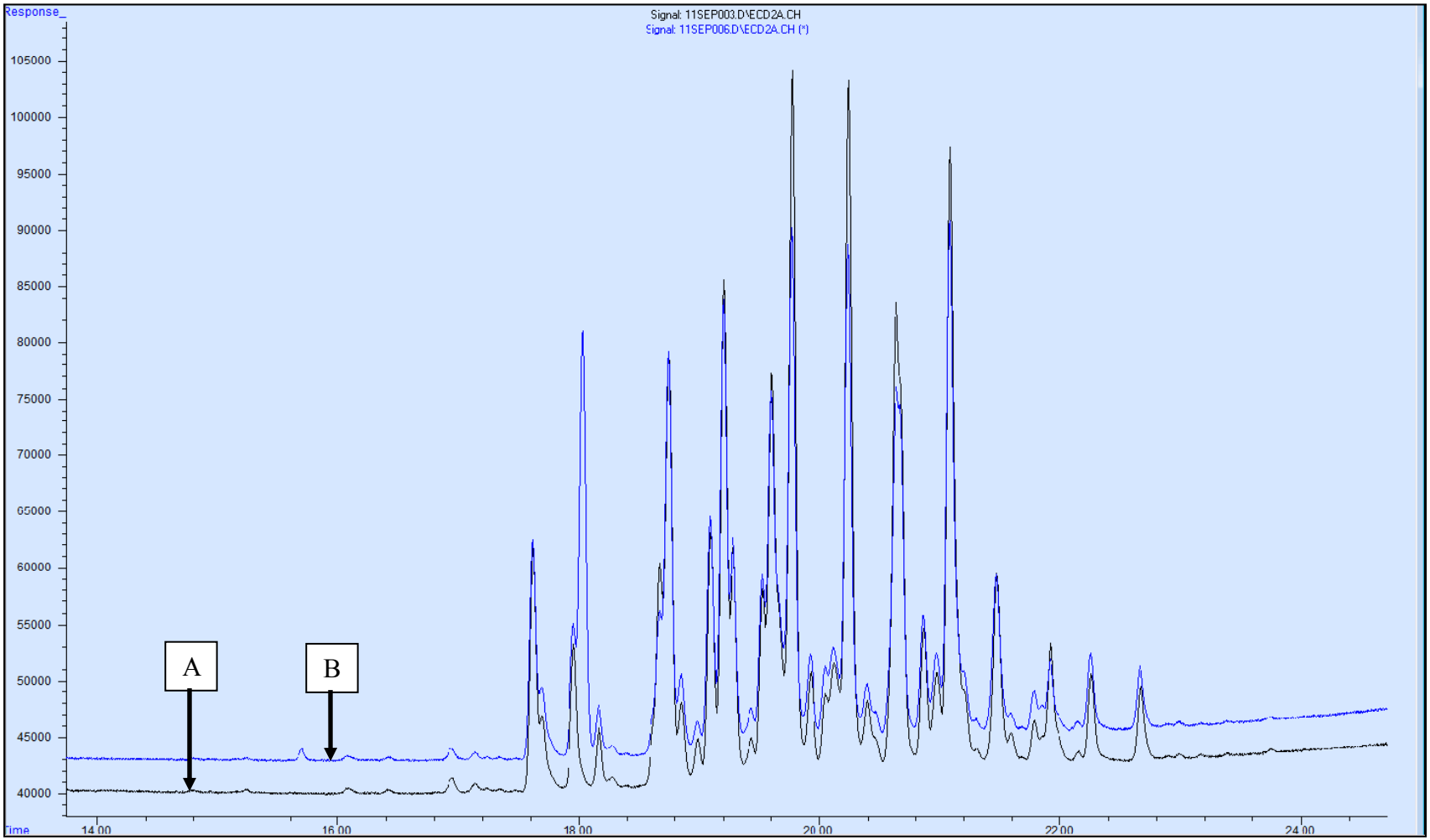

Figure 7-12: Chromatograms obtained by the injection of 1 µL of Aroclor 1254 in CS_2: (A) 1 µg/mL standard solution of Aroclor 1254 and (B) 1 µg Aroclor 1254 spiked onto to Anasorb 747® and PDMS membrane and extracted with 1 mL CS_2.

Table 7-6: Extraction efficiency of spiked target analytes determined for two different holding times. The superscripts next to the analytes indicate four groups into which the analytes were divided, a, b, c and d.: (A) Determined by solvent desorption and analysis after 14 days and (B) determined by solvent desorption and analysis after 48 hours.

Analyte	(A) Extraction after 2 weeks		(B) Extraction after 48 hours	
	Average percentage extraction efficiency (n=6)	% RSD	Average percentage extraction efficiency (n=6)	% RSD
1,1-Dichloroethylene[a]	97.7	4.8	96.9	5.1
t-Dichloroethylene[a]	96.7	3.2	97.2	3.7
1,1-Dichloroethane[a]	97.7	3.6	95.8	3.1
c-Dichlroethylene[a]	93.1	2.9	94.2	3.4
Chloroform[a]	94.8	4.1	96.1	2.8
1,2-Dichloroethane[a]	96.4	1.7	95.4	3.1
1,1,1-Trichloroethane[a]	101.2	2.6	100.1	3.2
Benzene[c]	97.5	2.2	97.3	1.7
Carbontetrachloride[a]	103.0	4.1	102.2	3.9
Trichloroethylene[a]	108.5	5.3	107.2	4.7
1,1,2-Trichloroethane[a]	92.4	4.7	93.1	6.1
Toluene[c]	97.7	3.1	95.6	2.9
Perchloroethylene[a]	94.2	3.5	95.4	3.5
Chlorobenzene[b]	87.6	3.4	86.3	3.9
1,1,1,2-Tetrachloroethane[b]	90.0	4.8	87.9	3.2
Ethylbenzene[c]	102.6	2.7	100.1	2.9
p,m-Xylene[c]	97.0	3.8	97.6	2.1
1,1,2,2-Tetrachloroethane[b]	84.5	3.9	84.5	4.9
o-Xylene[c]	84.5	5.2	85.3	4.8
1,3-Dichlorobenzene[b]	70.3	3.2	68.9	4.1
1,4-Dichlorobenzene[b]	67.7	5.8	65.3	4.9
1,2-Dichlorobenzene[b]	61.4	6.1	62.6	6.4
Naphthalene[d]	68.0	8.2	63.7	7.6
Acenaphthylene[d]	59.0	7.3	63.4	6.9
Acenaphthene[d]	78.5	9.5	65.0	10.1
Fluorene[d]	64.4	8.3	63.1	11.3
Phenanthrene[d]	51.5	9.6	42.5	9.1
Anthracene[d]	44.9	11.3	45.2	10.4
Fluoranthene[d]	57.3	12.3	62.9	9.9
Pyrene[d]	48.4	7.9	56.4	12.2

In the case of sampling and analysis with TWA-PDMS samplers, the soil gas sampling, analysis and calculations to convert the mass sorbed by the sampler into concentration in the gas phase were carried out in the same fashion as for air sampling discussed earlier. The calibration constants used in the calculations were determined (or estimated based on ln(k) vs. LTPRI correlation) under the conditions of optimum flow of air across the surface of the sampler. Since there was no air circulation in the sealed boreholes, the final concentration determined was most likely lower than the true concentration because of the starvation effect. Further, since the starvation effect increases with increasing uptake rates, the magnitude of the negative bias in principle should also be higher when moving down from 1,1-DCE to pyrene in Table 7-6. The magnitude of this starvation effect was discussed in Section 7.2.1. However, as the borehole dimensions and the depth at which the samplers were deployed were similar in all cases, the method still should have provided accurate relative concentrations provided that the permeability of the soil matrix at different locations was similar. In the case of GORE™ modules, a proprietary method for the calculation of the soil gas concentrations was used by the manufacturer.

The plot of benzene concentrations determined by the TWA-PDMS samplers vs. the corresponding concentrations determined by the GORE™ modules at different locations is shown in Figure 7-13. The plot revealed that the concentrations reported by the GORE™ modules were mostly lower than those determined using the TWA-PDMS samplers. None of the data points in the correlation plot approached the 1:1 line above 100 $\mu g/m^3$ as measured by the TWA-PDMS sampler, which indicated that GORE™ modules were not effectively estimating high benzene concentrations. This was in agreement with the findings of a project conducted by the US EPA Environmental Technology Certification Program on the use of GORE™ modules, which noted that pollutant concentrations were not effectively determined at high concentrations.[113]

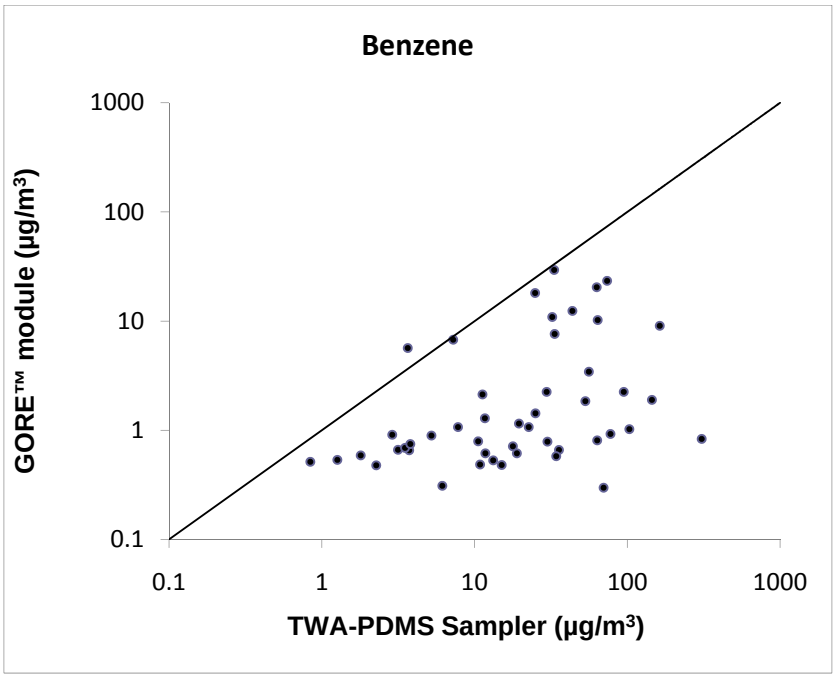

Figure 7-13: Correlation plot for benzene concentrations determined at different locations using the TWA-PDMS samplers and the GORE™ modules. The straight line represents a 1:1 correlation.

As noted in Section 1.7.1, the uptake rate of the GORE™ module is substantially higher because of its geometry, as well as the diffusive properties of the GoreTex® material used as the barrier. For example, the uptake rate of toluene is ~ 13 mL/min for the GORE™ modules as opposed to 4.2 mL/min for the TWA-PDMS samplers.[225] The GoreTex® material prevents liquid water from being transported across it. However, it still lets water vapor to pass through (with the sampler having a higher uptake rate for water vapor than for the rest of the target analytes), which could have very likely led to premature sorbent saturation in the GORE™ modules. The exposure to humid environment and to high analyte concentrations can easily saturate the sorbent resulting in the correlation plot similar to that observed for benzene. The PDMS membrane used as a barrier in the TWA-PDMS samplers on the other hand has low permeability towards water compared to other analytes (and hence lower uptake rate), which allows the sorbent and the sampler to function properly at higher concentrations and/or for longer deployment times. The potential bias of TWA-PDMS sampler results is mainly related to the starvation effect, whereas the results from the GORE™ modules might be biased due to the starvation effect, sorbent saturation and lack of

a proper theoretical model for converting the amounts found in the samplers into analyte concentrations in the soil gas. Consequently, it can be concluded that the results from the TWA-PDMS samplers should be closer to true values than those from the GORE™ modules.

Figures 7-14 and 7-15 show the concentration contour plots of benzene determined using the TWA-PDMS samplers and the GORE™ modules, respectively. Comparing the two figures, the concentration maps identify some of the same areas of elevated concentrations (it should however be pointed out that the color scales in two contour maps are different by more than an order of magnitude, reflecting the negative bias of the GORE™ modules as indicated in Figure 7-13). For example, it can be noticed that locations A and B in Figure 7-14 show concentration profiles similar to locations A1 and B1 in Figure 7-15. There were also locations where benzene was detected by the TWA-PDMS samplers, but not by the GORE™ modules. This was partly due to the fact that a larger number of TWA-PDMS samplers were used to generate the profiles compared to the number of GORE™ modules.

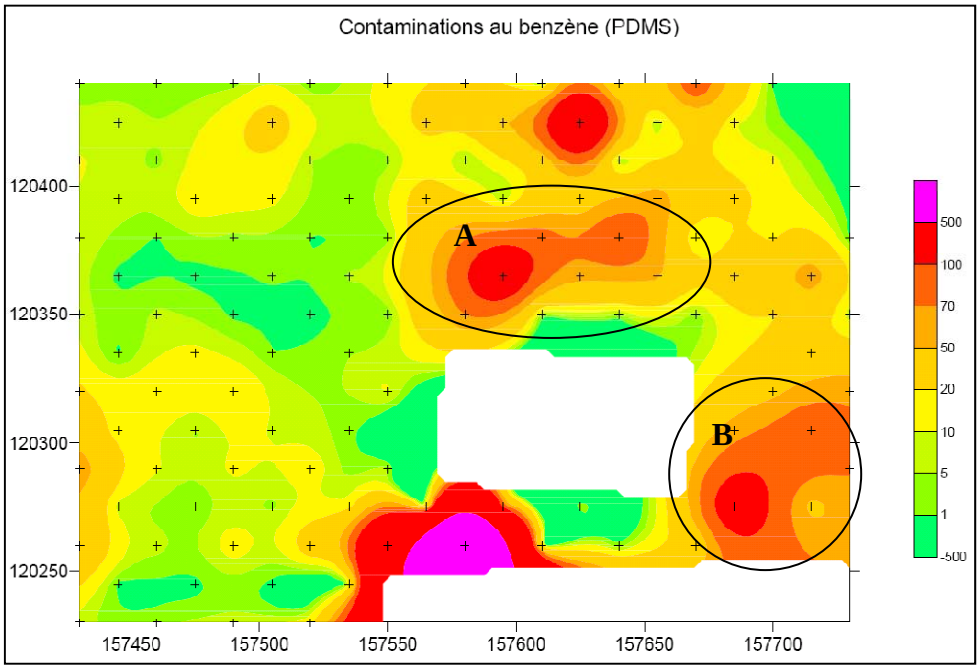

Figure 7-14: Benzene concentration profile determined using the TWA-PDMS samplers. A and B are locations in the field that can be compared with locations A1 and B1 in Figure 7-15.

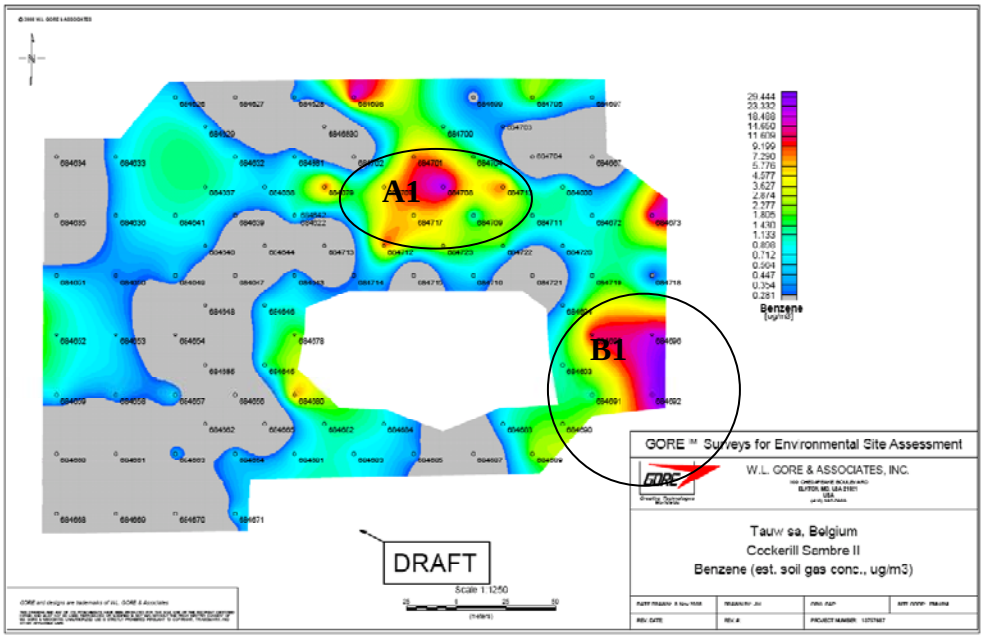

Figure 7-15: Benzene concentration profile determined using the GORE™ modules. A1 and B1 are locations in the field that can be compared with locations A and B in Figure 7-14.

The correlation plot of the corresponding BTEX concentrations obtained by the two types of samplers (shown in Figure 7-16) indicated again a trend similar to that seen for benzene. This was likely due to the fact that of all the BTEX, only benzene was found in considerable amounts at various locations by both samplers. Similar to the benzene correlation, none of the data points in the plot approached the 1:1 line above 100 µg/m^3 as determined by the TWA-PDMS samplers attributable to sorbent saturation and increased starvation effects for the GORE™ modules. The highest BTEX concentration determined by TWA-PDMS sampler was ~ 3100 µg/m^3, while that determined by GORE™ module was only ~ 69 µg/m^3. The concentration profiles of total BTEX determined by the two samplers are shown in Figures 7-18 and 7-19. Visually, the similarities in the concentration profiles were not entirely obvious because of the 1-2 order of magnitude difference in the color scale.

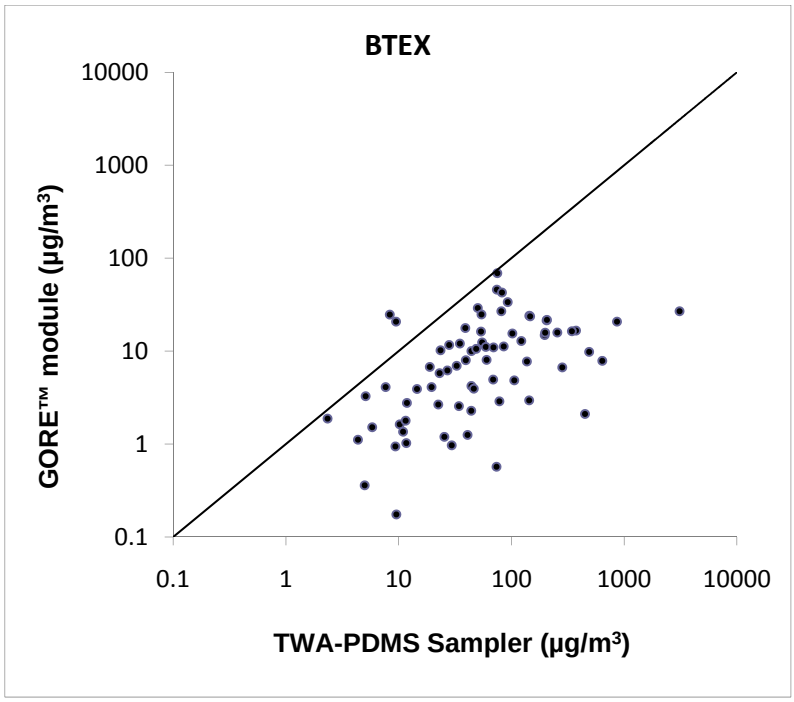

Figure 7-16: Correlation plot for BTEX concentrations determined at different locations using the TWA-PDMS samplers and the GORE™ modules. The straight line represents a 1:1 correlation.

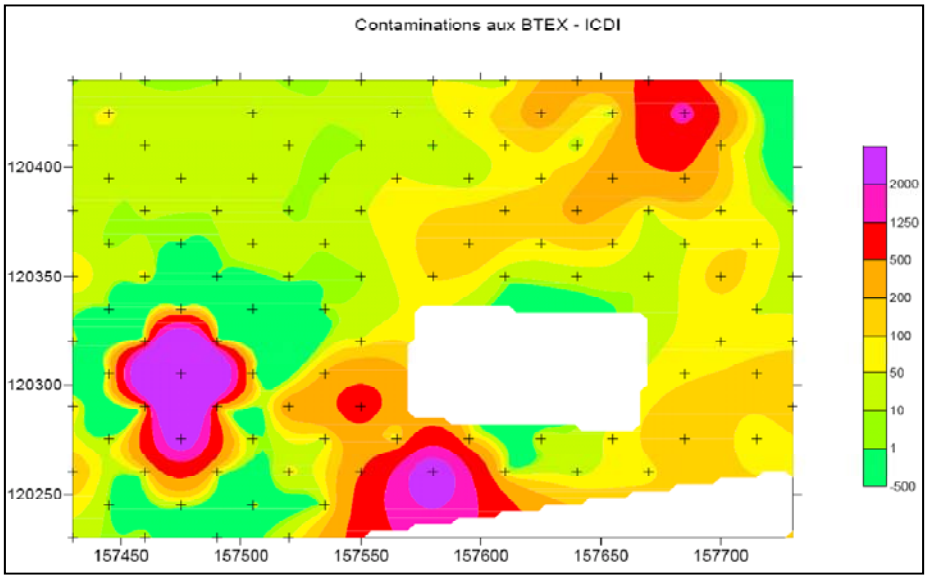

Figure 7-17: BTEX concentration profile determined using the TWA-PDMS samplers

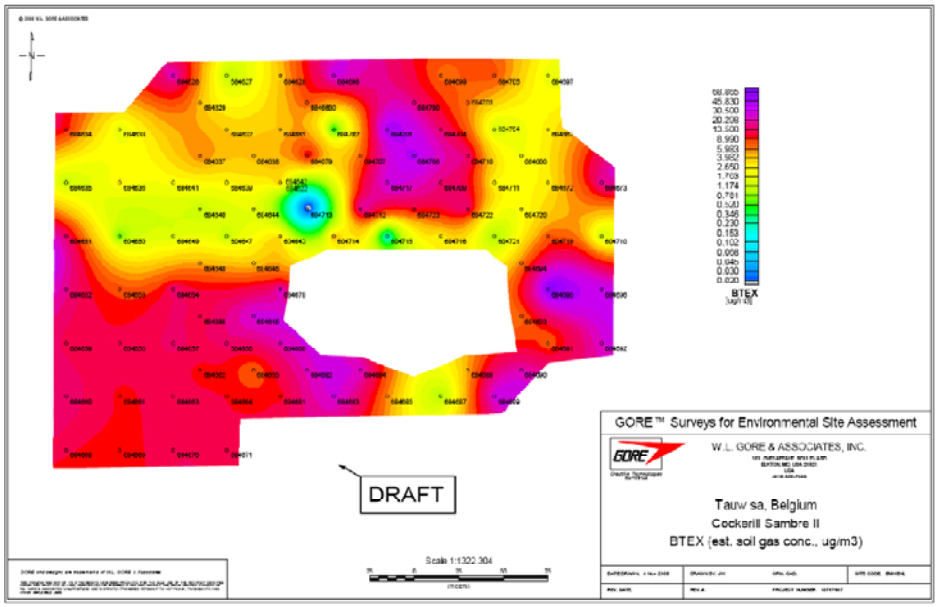

Figure 7-18: BTEX concentration profile determined using the GORE™ modules

Figure 7-19 shows that naphthalene concentrations reported by the GORE™ modules were generally 1-3 orders of magnitude higher than those reported using TWA-PDMS samplers, which is in contrast to the trend with benzene and BTEX concentrations (as well as TCE and PCE profiles which will be discussed later). A possible reason for this observation could be the increased starvation effect experienced by the TWA-PDMS samplers, which becomes worse with increasing air – PDMS partition coefficient. The estimated uptake rate of naphthalene is ~ 25.6 mL/min for TWA-PDMS samplers, which should be greater than that for the GORE™ modules (since uptake rate is ~ 13 mL/min for toluene by GORE™ modules as per ref. 2, it should be much lower than that for naphthalene owing to the lower diffusion coefficient of naphthalene in air). Further, the TWA-PDMS sampler has not been tested in the laboratory for its applicability to the determination of semi-volatile organic compounds. As the partition coefficient of the analyte increases to a level like that for naphthalene, a potential problem could be that PDMS itself becomes a good sink, hence the analyte might not be as efficiently transferred to the sorbent in the sampler as with smaller molecules. The concentration contour plots of naphthalene determined by the two samplers are shown in Figures 7-20 and 7-21. The elevated concentrations determined at locations C, D and E in

Figure 7-20 from TWA-PDMS samplers were similar to those at locations C1, D1 and E1 determined using GORE™ modules as shown in Figure 7-21.

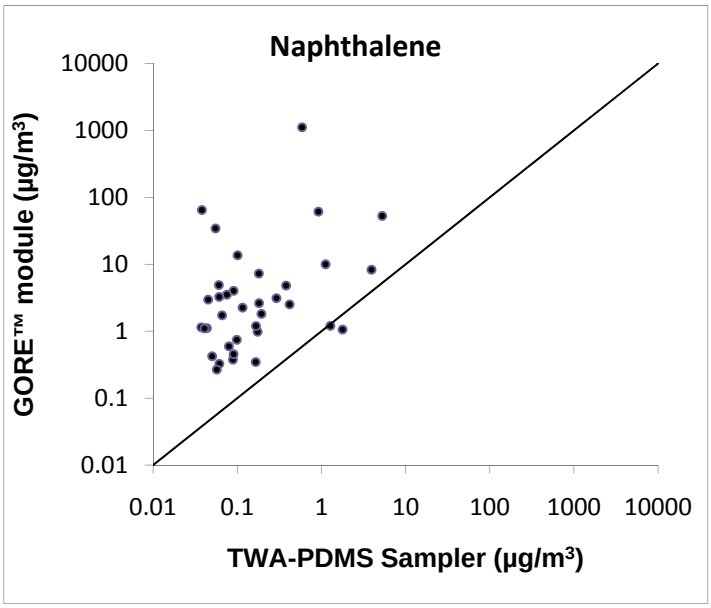

Figure 7-19: Correlation plot for naphthalene concentrations determined at different locations using the TWA-PDMS samplers and the GORE™ modules. The straight line represents a 1:1 correlation.

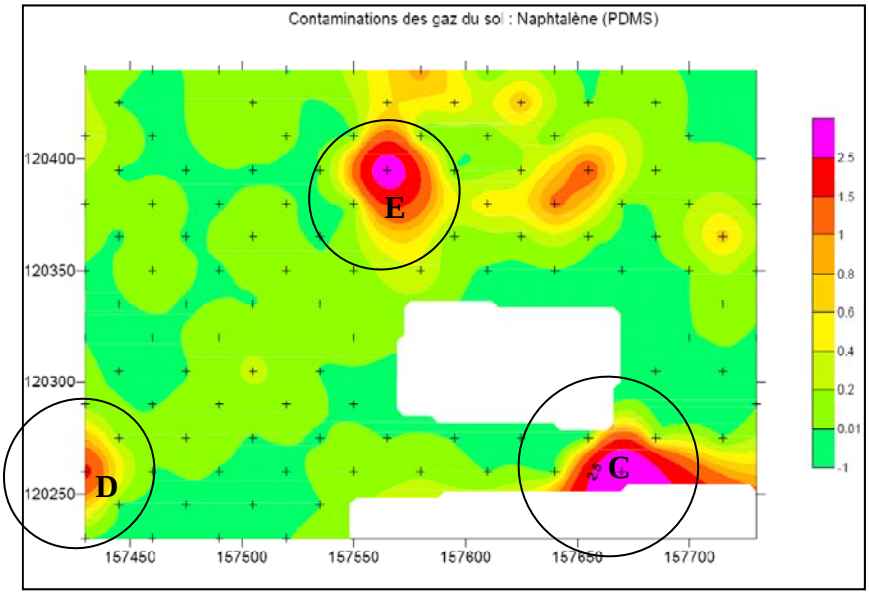

Figure 7-20: Naphthalene concentration profile determined using the TWA-PDMS samplers. C, D and E are the locations in the field which can be compared with C1, D1 and E1 in Figure 7-21.

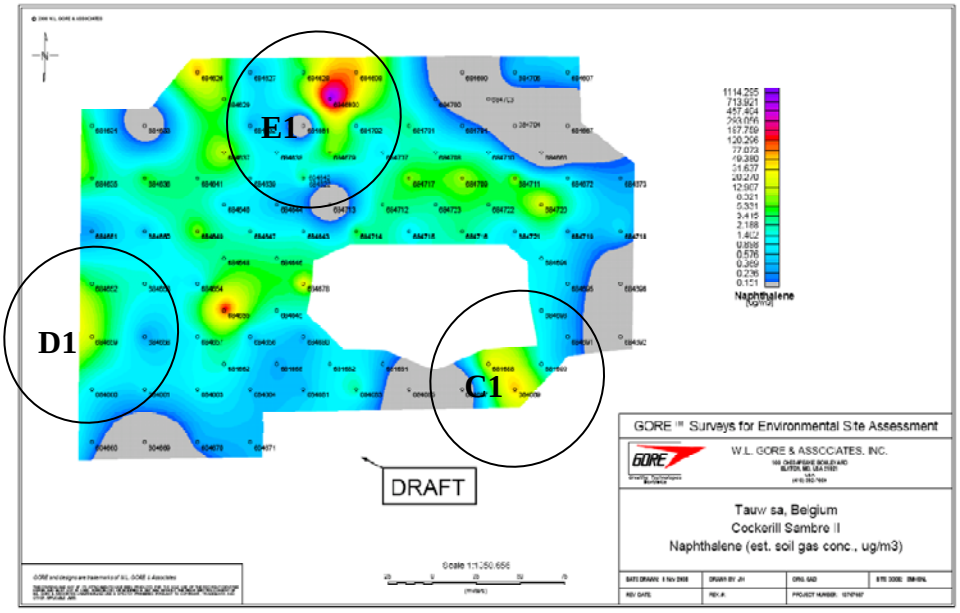

Figure 7-21: Naphthalene concentration profile determined using the GORE™ modules. C1, D1 and E1 are the locations that can be compared with locations C, D and E in Figure 7-20.

There was a relatively good correlation between the absolute concentrations obtained using the two samplers for PCE (shown in Figure 7-22) when compared to the other analytes discussed so far. The correlation plot indicated no saturation effect for PCE determined by the GORE™ module at concentrations up to ~ 120 µg/m^3. As a result of the good correlation, the concentration contour plots of PCE obtained by the two methods, shown in Figures 7-22 and 7-23, identified similar elevated concentrations levels (locations E and E1 in Figures 7-23 and 7-24).

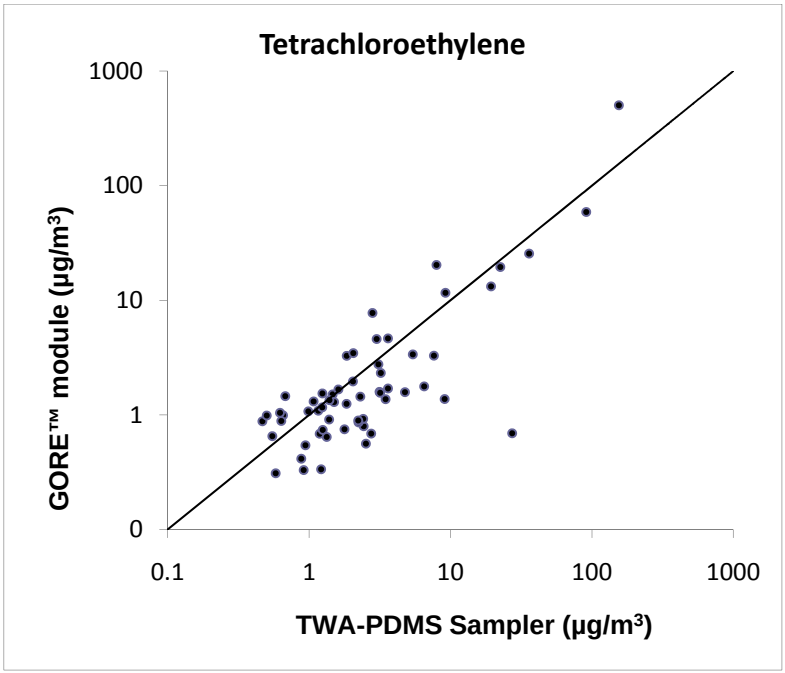

Figure 7-22: Correlation plot for PCE concentrations determined at different locations using the TWA-PDMS samplers and the GORE™ modules. The straight line represents a 1:1 correlation.

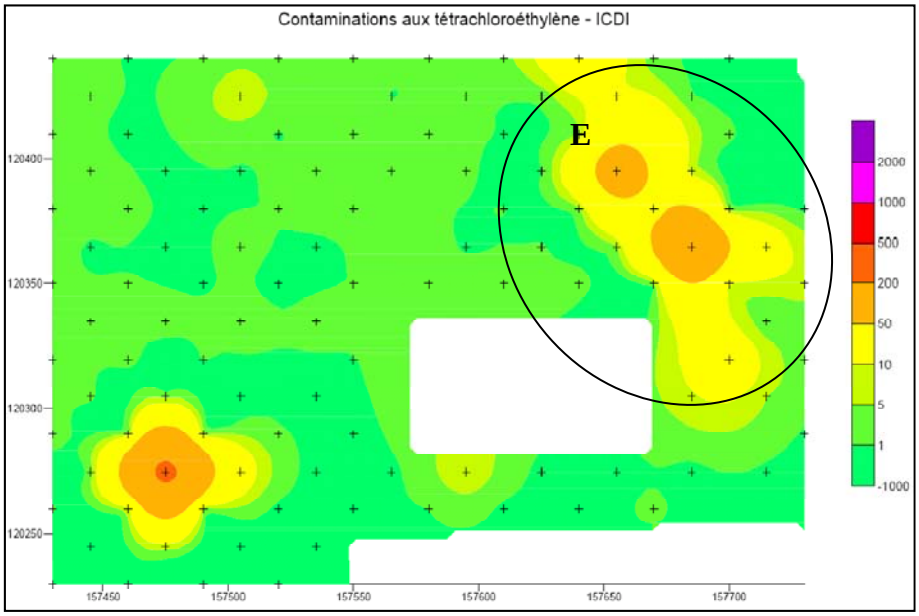

Figure 7-23: PCE concentration profile determined using the TWA-PDMS samplers. E is the location that can be compared with the location E1 in Figure 7-24.

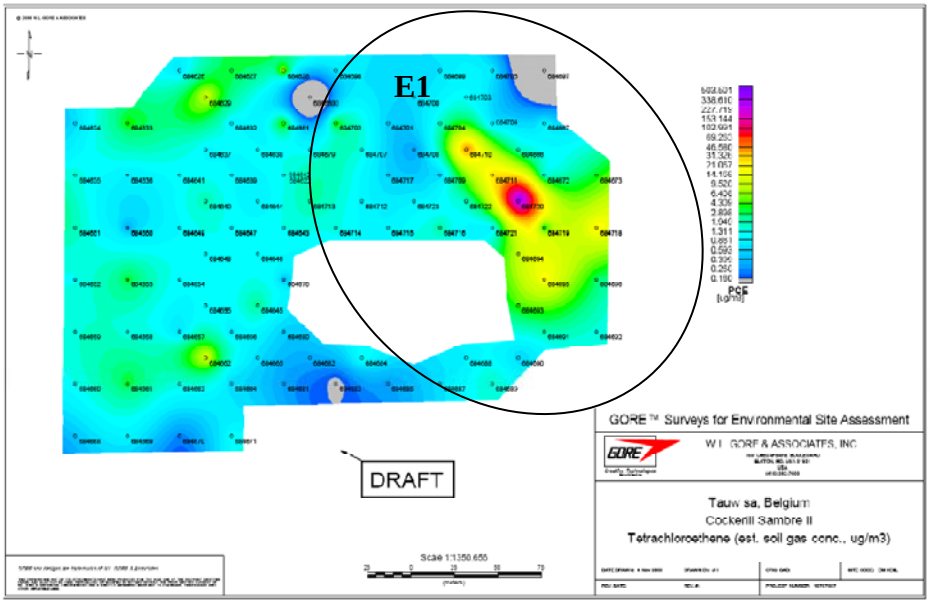

Figure 7-24: PCE concentration profile determined using the GORE™ modules. E1 is the location that can be compared with location E in Figure 7-23.

The comparison of absolute concentrations of TCE (Figure 7-25), indicated that the concentrations obtained from GORE™ modules were generally lower than those obtained using the TWA-PDMS samplers. This was similar to the trends observed with benzene and BTEX and can be attributed to starvation and saturation effect for the GORE™ modules. Furthermore, this is consistent with results presented at the Midwestern States Risk Assessment Symposium - Soil Gas Demonstration Program in 2006, where the GORE™ modules showed good correlation to active soil gas samples for PCE, but underestimated TCE concentrations by typically a factor of 7.[226] The difference in the concentrations measured at any location by the two methods was however within one order of magnitude at most of the locations and within 3 orders of magnitude at all the locations. Nevertheless, there was still a similarity in the concentration hot spot locations identified in the two contour plots. (Figures 7-27 and 7-28). Examples are regions F and G in Figure 7-26 corresponding to the regions F1 and G1 in Figure 7-27.

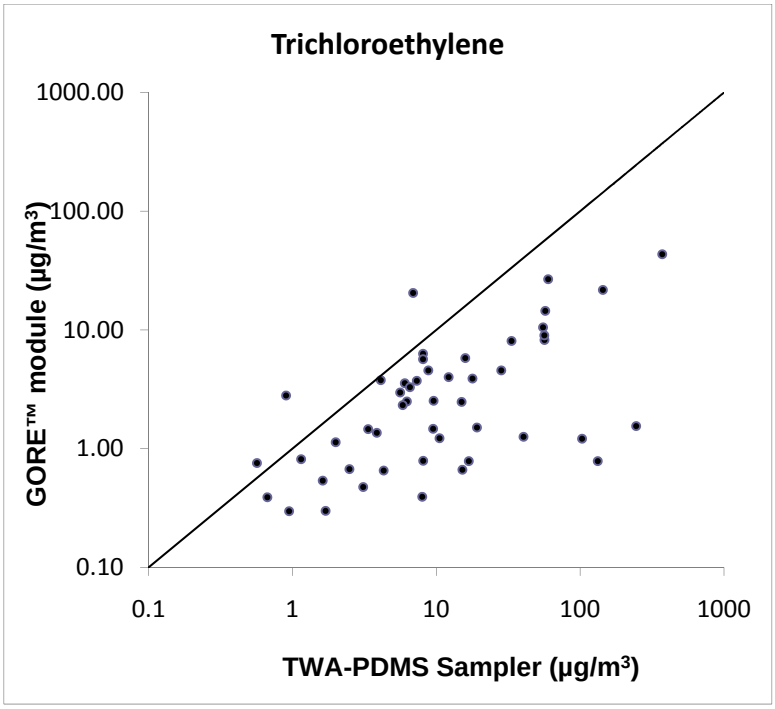

Figure 7-25: Correlation plot for trichloroethylene concentrations determined at different locations using the TWA-PDMS samplers and the GORE™ modules. The straight line represents a 1:1 correlation.

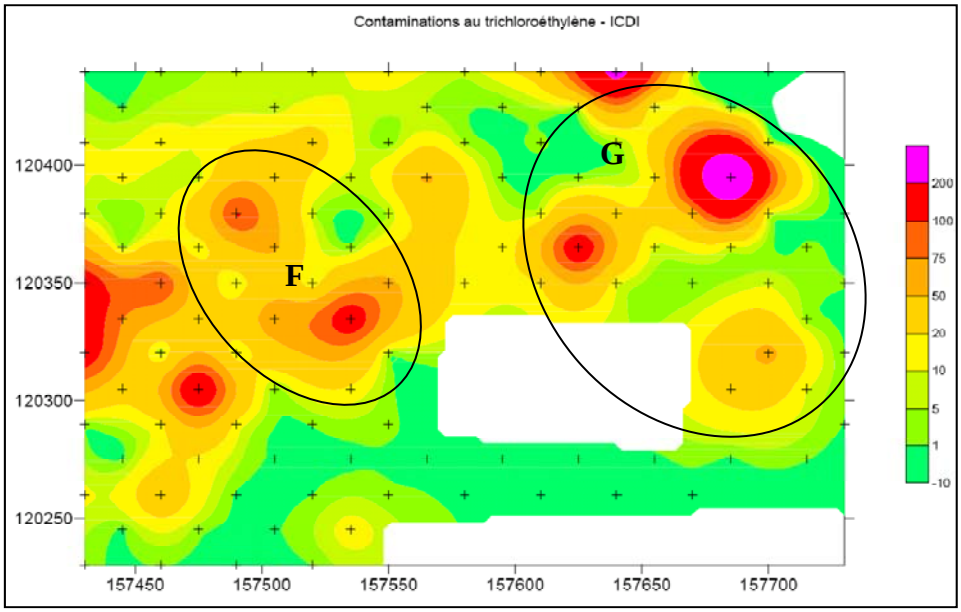

Figure 7-26: Trichloroethylene concentration profile determined using the TWA-PDMS samplers. F and G are locations that can be compared with location F1 and G1 in Figure 7-27.

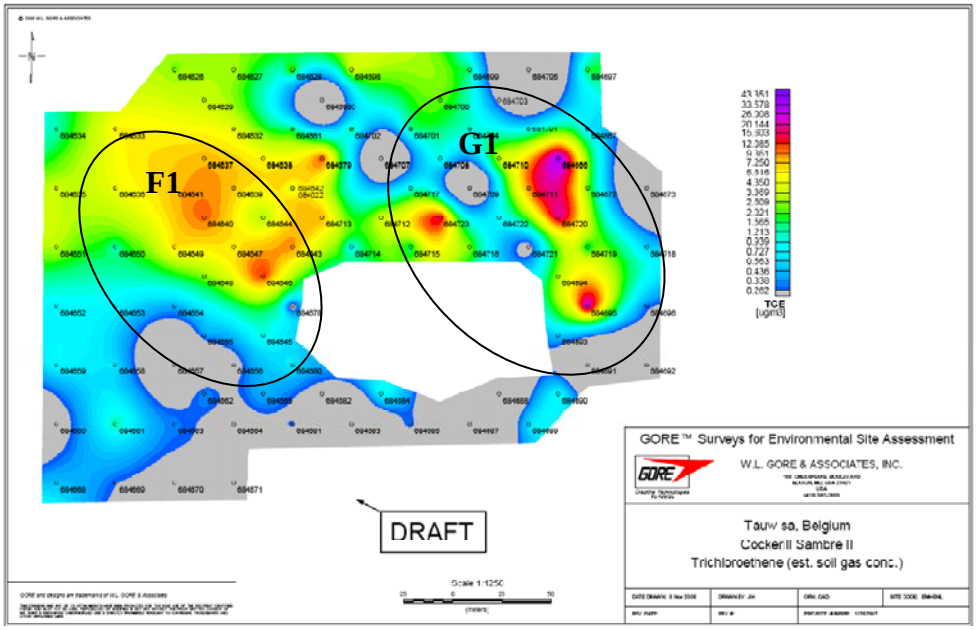

Figure 7-27: Trichloroethylene concentration profile determined using the GORE™ modules. F1 and G1 are locations that can be compared with locations F and G in Figure 7-26.

The correlation for TPH concentrations determined using the two samplers was poor, as shown in Figure 7-28. With two exceptions, all the data points indicated a negative bias in the concentrations reported by GORE™ modules. In the cases discussed above for benzene, BTEX, and TCE, the saturation effect for GORE™ module was noticeable above 100 µg/m^3 as determined by the TWA-PDMS samplers. The TPH correlation plot shown here is a further proof for such an effect. The TWA-PDMS samplers were found to have a much broader dynamic range of 6 orders of magnitude.

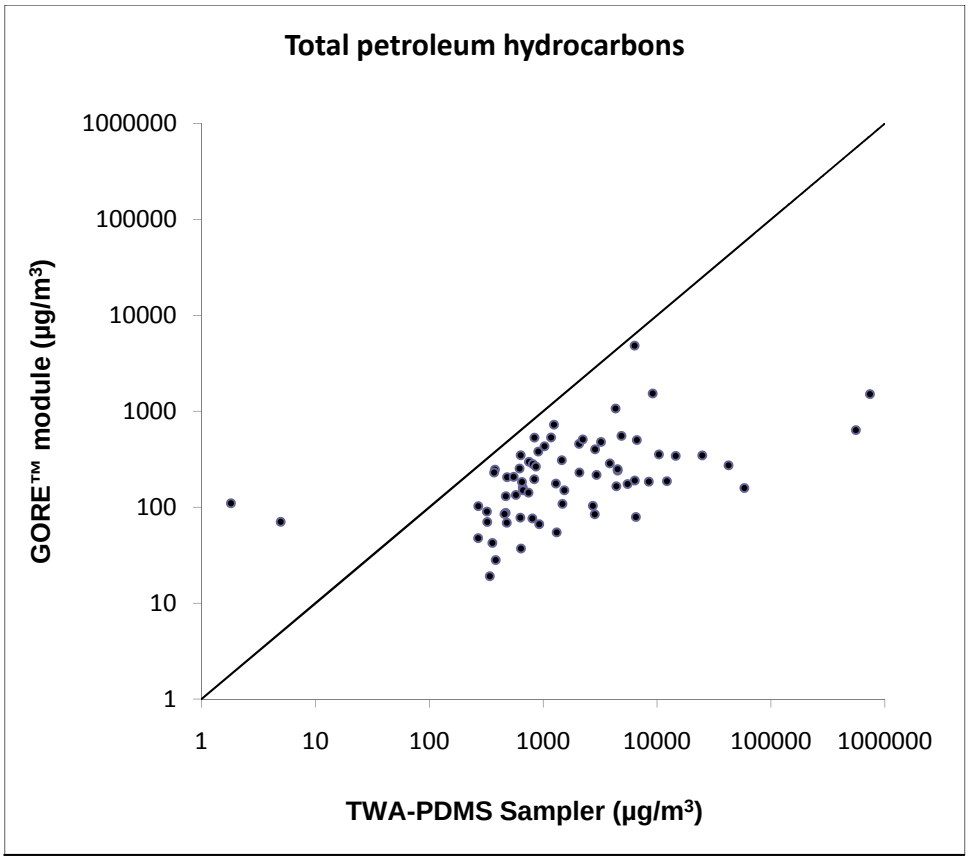

Figure 7-28: Correlation plot for total petroleum hydrocarbon concentrations determined at different locations using the TWA-PDMS samplers and the GORE™ modules. The straight line represents a 1:1 correlation.

Concentration contour plots of total petroleum hydrocarbons (TPH) determined by the two samplers are shown in Figures 7-29 and 7-30. It was difficult to compare the two profiles because of the large variation in the color scales for the two profiles due to the large negative bias in the results reported using the Gore modules. However, there were still concentration hot-spots which were identified using both samplers. The variation could also have arisen due to the different quantification methods used to arrive at the final TPH concentration. The GORE™ modules analysis method used GC-MS for quantification, while TPH quantification with the TWA-PDMS samplers was based on GC-FID analysis and estimated calibration constants. The GORE™ method is based on the assumption that all organic compounds have similar response factors when using a MS as a detector, which is not true. Furthermore, the uptake rates of most of the compounds detected by GC-MS were unknown. Consequently,

the estimate of the TPH concentrations obtained using the GORE™ method, based on a proprietary model, is subject to unknown errors. In the case of TWA-PDMS sampler, a GC-FID was used for the quantification of TPH. The method, as described in earlier chapters, is based on the uniform response of FID towards hydrocarbons. Furthermore, the uptake rate of each compound in the sample can be easily estimated based on the calibration constant vs. LTPRI correlation. The results from TWA-PDMS samplers can therefore be considered more accurate than those from the GORE™ modules.

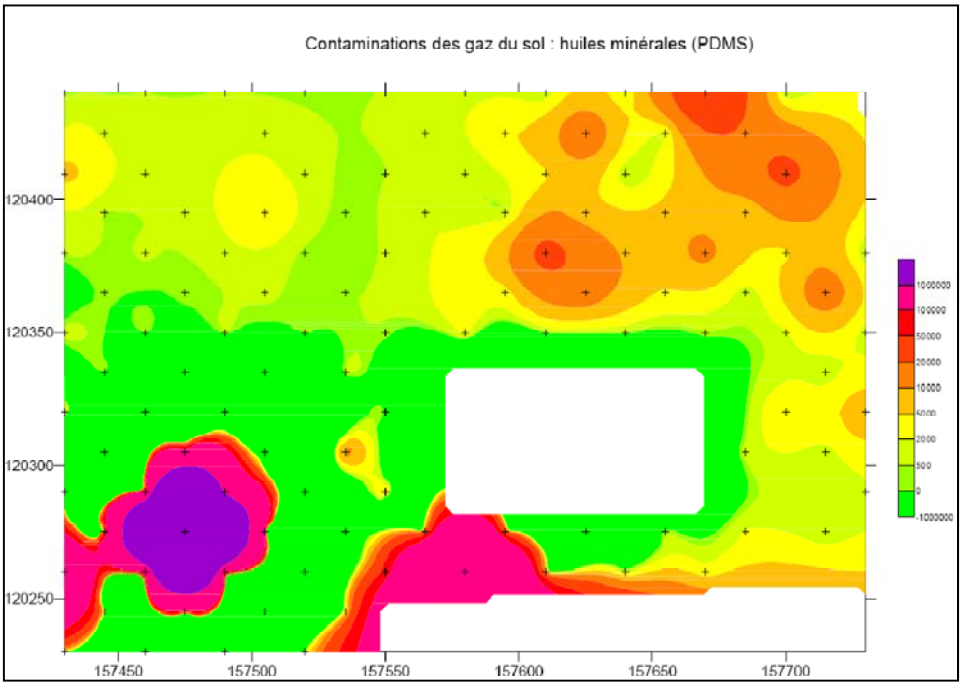

Figure 7-29: Total petroleum hydrocarbons concentration profile determined using the TWA-PDMS samplers.

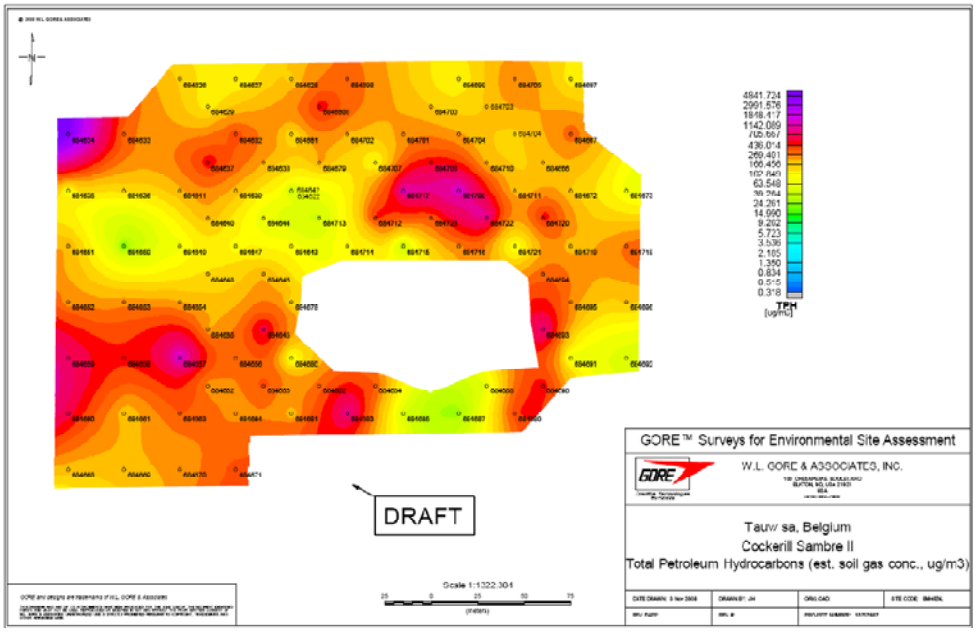

Figure 7-30: Total petroleum hydrocarbons concentration profile determined using the GORE™ modules.

In general, except for naphthalene, the majority of the concentrations reported using the GORE™ modules were lower than those found using the TWA-PDMS samplers. The interpretation of the variations cannot however be confirmed in the absence of the knowledge of the model used for calculating the concentrations of the target analytes from the mass trapped in the GORE™ module.

The cost of TWA-PDMS passive samplers is approximately 25% of that of GORE™ modules and the chromatographic analysis cost is approximately the same. Consequently, the TWA-PDMS samplers proved to be very economic and efficient in determining the concentration profiles in soil gas matrix for the majority of the target analytes considered in the project. The TWA-PDMS sampler was not originally designed for the sampling and analysis of PAHs (or SVOCs in general). Since the GORE™ modules also did not report any substantial amounts of PAHs in the location, it is not possible to explore the applicability of the TWA-PDMS samplers for PAHs. The same was true for PCBs, as they were not detected using either of the two methods.

7.2.3 Sub-slab soil gas sampling in Italy using TWA-PDMS samplers

Analysis of all samplers indicated that vinyl chloride (reporting limit 14.6 μg/m^3) and 1,1-DCE (reporting limit 16.0 μg/m^3) were not present in quantifiable amounts in any of the samples. The concentrations of c-DCE (reporting limit 8.6 μg/m^3), chloroform (reporting limit 1.5 μg/m^3), TCE (reporting limit 0.86 μg/m^3) and PCE (reporting limit 0.58 μg/m^3) are presented in Table 7-7. The results showed that PCE was the dominant VOC in the soil gas at the specific site, followed by TCE and traces of c-DCE and chloroform. The elevated concentrations depicted in Figure 7-31 seemed to be restricted to locations where it was known that PCE had been used. It was also noticed that the concentration of PCE generally decreased as the location was further away from the "hot spots" of relatively high concentrations.

On the basis of the soil gas survey performed during this project, eight locations with the highest concentrations were selected for drilling, and soil samples were collected for further analysis for regulatory purposes. The analysis of bulk soil samples had indicated the absence of any VOCs at the site. This demonstrates that the TWA-PDMS sampler provides sensitivity that can probe soil samples with much lower concentrations, which is very useful for assessing the potential health risks via subsurface vapor intrusion to indoor air.

Table 7-7: Concentrations of the target analytes determined using the TWA-PDMS samplers at Lomazzo, Italy.

Sampler code	c-DCE (µg/m^3)	$CHCl_3$ (µg/m^3)	TCE (µg/m^3)	PCE (µg/m^3)
Apr-03	59.1	2.82	51.7	8.98
Apr-04	11.5	1.62	20.3	12.7
Apr-05	U	1.44	31.1	7.85
Apr-06	9.84	1.85	5	12
Apr-07	21.5	1.97	5.43	12.2
Apr-08	U	1.65	1.53	10.4
Apr-09	U	1.85	2.92	7.07
Apr-10	U	1.62	1.5	25.7
Apr-11	106	2.1	187	6170
Apr-12	22.8	1.54	61.3	1460
Apr-13	8.94	1.75	16.7	536
Apr-14	U	1.49	19.2	450
Apr-15	13.4	1.93	140	10200
Apr-16	13.5	3.55	1610	1550
Apr-17	27.4	1.74	30.2	974
Apr-18	U	U	26.5	47
Apr-19	U	2.31	122	16100
Apr-20	U	2.93	133	11800
Apr-21	U	1.7	73.4	4090
Apr-22	U	1.9	62.8	128
Apr-23	U	1.67	8.11	3160
Apr-24	U	2.13	355	13300
Apr-25	116	72.3	4350	729000
Apr-26	U	1.54	26.7	313
Apr-27	U	1.58	1.21	44.8
Apr-28	U	U	1.27	1250
Apr-29	U	U	21.7	23.3
Apr-30	U	U	9.19	33.6
Apr-31	U	2.08	18.1	30.6
Apr-32	U	1.79	100.6	12.7
Apr-33	U	1.8	1.85	9.93
Apr-34	U	1.7	8.03	15.7
Apr-35	U	1.91	18.2	13.6
Apr-36	23.9	3.01	459	108000
Apr-37	23.3	8.55	857	45400
Apr-38	U	1.67	1.92	31.3
Apr-39	U	2.05	9.85	11.4
Apr-40	U	1.58	51.7	2.24

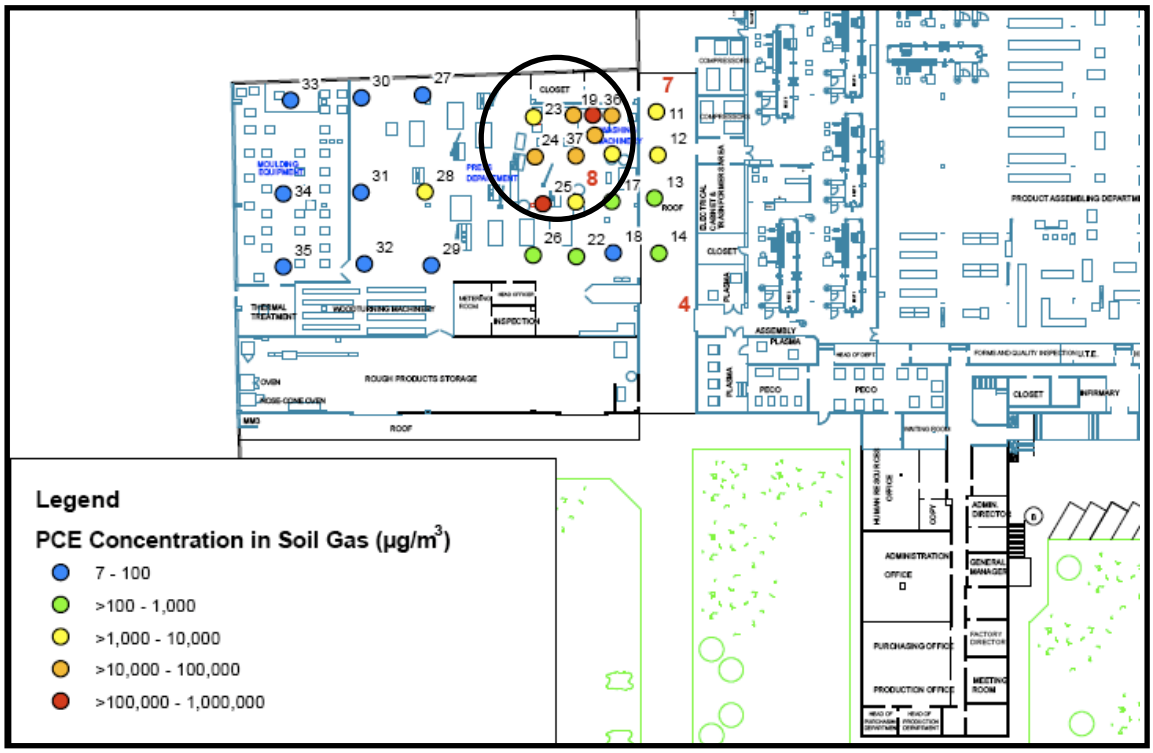

Figure 7-31: Concentrations of PCE at various locations determined using TWA-PDMS samplers. The circled region shows areas of maximum concentration of PCE.

7.3 Conclusions

Soil gas sampling at various indoor as well as outdoor locations was performed using TWA-PDMS samplers and compared with GORE™ modules and SUMMA™ canisters sampling. The project at Knoxville, TN, using both the TWA-PDMS samplers and SUMMA™ canisters, showed the importance of the starvation effects in the determination of analyte concentrations by the TWA-PDMS samplers. The concentrations determined by the TWA-PDMS samplers showed a general positive correlation, and were within two orders of magnitude of those determined using SUMMA™ canisters for all the samplers but one.

Soil gas sampling performed at an outdoor location in Belgium alongside commercially available GORE™ modules showed that concentration profiling can be done with TWA-PDMS sampler at least as well as with the GORE™ modules, and most likely more accurately because of the many advantages of the TWA-PDMS samplers in this particular application. Low permeability of PDMS towards water allowed TWA-PDMS samplers to

determine analyte concentrations over a large dynamic range. The major error(s) in determining the actual concentration from the TWA-PDMS samplers can be attributed only to the starvation effect, while for the GORE™ modules they can be attributed to the starvation effect (greater than that for TWA-PDMS samplers for most of the analytes), the use of a proprietary uptake rate model rather than experimentally determined values, and sorbent saturation due to high moisture uptake rate. The starvation and saturation effects together resulted in the GORE™ modules not being able to determine high concentrations accurately, as opposed to a wide dynamic concentration range for the TWA-PDMS samplers.

Deployment of the TWA-PDMS samplers can be done as easily as with the GORE™ modules at only a fraction of the cost of fabrication. The TWA-PDMS samplers were not intended for use in sampling of PAHs and need to be further developed in terms of the sorbent choice and extraction method if this direction is to be pursued further. The GORE™ module on the other hand has been widely used for PAH sampling and analysis.

Sub-slab soil gas sampling and analysis are critical in examining vapor intrusion pathways and subsequent remediation requirements. TWA-PDMS samplers were demonstrated to be useful for such an application at Lomazzo, Italy. The concentrations obtained by the TWA-PDMS samplers were not compared to any accepted method in this project for comparison, but the general concentration ranges corresponded well to the locations where there was prior knowledge of the contaminant use. Sub-slab soil gas sampling and analysis is an important tool to determine pollutant distribution, which is crucial in modeling vapor intrusion pathways.

CHAPTER 8

Summary and future work

8.1 Summary

Passive sampling technology is more advantageous compared to traditional active/grab sampling techniques due to its low cost, low maintenance requirements, unattended operation and independence from power sources. In the current project, a new passive sampler was designed to further improve the potential of the passive sampling technology for routine use in the field. The merits of the technology have resulted in upcoming commercialization of the sampler.

One of the fundamental ideas of the project was to design a sampler which would be inexpensive, allow easy automation of the analytical procedure and reduce the number of sample preparation steps. The design of the TWA-PDMS sampler developed proved to be highly economic, and the device can be easily fabricated using supplies available in a laboratory with little training. Solvent extraction can be carried out within the sampler itself, followed by introducing the sampler into the GC auto-sampler after changing the aluminum crimp cap. This method results in reduced potential for contamination, as well as makes the whole procedure easy for automation.

Calibration constants of 41 model compounds were determined, and a model was developed to estimate them based on the physicochemical properties of the analytes. The 41 model analytes included compounds from highly non-polar alkanes to highly polar alcohols. While it is possible to estimate the calibration constants of diffusive passive samplers by theoretical calculations using the diffusion coefficients of the analytes in air, it has not been the case thus far for permeation passive samplers, as the permeability coefficients of the analytes in the permeation membranes used in the samplers are not easily available. The model developed within this project based on LTPRI allows for the sampler to be deployed in the field without prior knowledge of specific analytes in the sample matrix. This is due to the fact that LTPRIs determined using columns with polydimethylsiloxane stationary phases depend on partitioning coefficients of the analyte molecules between the carrier gas and the

stationary phase, just as the calibration constants of the permeation passive samplers do. Such a concept of estimation of the calibration constants is very useful not only when the identity of the analyte is unknown at the time of sampling, but also when determining summary parameters like total petroleum hydrocarbons in the gas phase using a GC equipped with a flame ionization detector.

Determining the calibration constants of the 41 model compounds also allowed the determination of the permeability of polydimethylsiloxane towards various analytes. Determination of such fundamental properties is an important scientific information for similar analytical sample preparation/introduction techniques such as PDMS membrane extraction with a sorbent interface (MESI), PDMS thin film extraction and PDMS membrane inlet mass spectrometry (MIMS).

An important issue with the performance of passive samplers is the sampling rate variation when environmental conditions considerably deviate from the laboratory conditions under which it was determined. Owing to the hydrophobic properties of polydimethylsiloxane, it was shown that the calibration constants of the sampler towards various analytes are largely independent on the humidity in the sampling environment. Anasorb 747®, the sorbent used in the fabrication of the sampler, is characterized by good analyte recovery rates for VOCs during solvent desorption with carbon disulphide, which positively affects the performance of the TWA-PDMS sampler.

The calibration constant for a particular analyte is a function of the geometry of the sampler and the permeability of PDMS towards the analyte. Permeability on the other hand is the product of the diffusion coefficient of the analyte in PDMS and the partition coefficient of the analyte between air and the PDMS membrane. With varying temperature, the diffusion coefficient and the partition coefficient of an analyte vary in opposite directions, which leads to a partial trade-off in the net permeability. As a result, the dependence of the uptake rate on temperature is weak. The variations in the calibration constants with temperature were quantified for various groups of compounds. The variations were in general found to be slightly larger than those observed with diffusive-type passive samplers. However, with the knowledge of temperature variations in the field environment, appropriate corrections can

always be used based on the energy of activation of permeation values determined in this project. These values are not only important in understanding the function of the sampler designed in this project, but also to understand the fundamental transport properties of PDMS. Such fundamental transport properties in turn can be successfully used for other PDMS-based analytical techniques, including those mentioned above.

Field sampling and analysis are important parts of validation of any new sampler design. A number of field sampling events were therefore planned and performed in collaboration with Geosyntec Consultants and Tauw Scientific Inc. to study the performance of the samplers under actual field conditions. The analytical results obtained from the TWA-PDMS samplers were compared to several currently available passive samplers such as SUMMA canisters, 3M™ OVM 3500 samplers, GORE™ modules, and TAGA.

Sampling and analysis by SUMMA™ canisters/EPA method TO-15 are accepted as the "gold standard" for comparison purposes. Concentrations obtained using TWA-PDMS samplers indicated excellent correlation with SUMMA™ canister method over 4 orders of magnitude. Similar excellent results were observed when compared with TAGA mobile laboratory results also, which, together with the results from SUMMA™ canisters, indicated an overall dynamic concentration range of the TWA-PDMS samplers of 6 orders of magnitude. The results from the field sampling and analysis procedures showed that the TWA-PDMS samplers provided comparable and/or better results when compared to 3M™ OVM 3500 sampler and GORE™ modules. Considering that the cost of the TWA-PDMS samplers is significantly lower than that of the above mentioned sampling systems, the overall performance of the sampler can be considered to be very good. The TWA-PDMS samplers have been shown to work well in indoor air, outdoor air and soil gas matrices.

The project presented in the thesis included theoretical details, determination of the fundamental calibration data and the effect of geometric and environmental parameters on the calibration constants. The excellent performance of the sampler observed in the laboratory resulted in sampling and analysis being performed at more than 20 locations in North America, Europe, and Asian countries in the past three years alone. The sample matrices included indoor air, outdoor air, and soil gas. The results from the samplers were

used for vapor intrusion studies, soil gas remediation work and screening for pollutants in dwellings, offices and manufacturing areas. The TWA-PDMS samplers have been shown to work at least as good as commercially available samplers at a considerably reduced cost and increased ease of use. The potential for the sampler to be used routinely in the field is therefore considerable and warrants more detailed studies in many areas which have not been touched upon in the thesis due to the limited amount of time.

8.2 Future work

The good performance and advantages of the TWA-PDMS sampler resulted in it being included in a project entitled "Development of more cost-effective methods for long-term monitoring of soil vapor intrusion to indoor air using quantitative passive diffusive-adsorptive sampling techniques" and funded by Environmental Security Technology Certification Program (ESTCP), a US Department of Defence program. The project involves the comparison of four passive sampling techniques including TWA-PDMS, Radiello®, Automated Thermal Desorption (ATD®) tube, and SKC Ultra II® samplers. Various aspects of the different samplers will be considered in this project including a comparison with industry-accepted standards using statistically designed laboratory and field experiments. The matrices studied will include indoor air, outdoor air, sub-slab soil gas and soil gas.

The development of the model for the estimation of the calibration constants was based on the assumption that the diffusion coefficients of the analytes were practically constant, and that consequently the calibration constants were determined mainly by the partition coefficients of the analytes between air and the PDMS membrane. While the model worked well, there are opportunities to further correct for variations in the diffusion coefficients of the analytes in PDMS membranes. One such method would be to use the concept of inverse gas chromatographic (IGC) techniques to determine not only the partition coefficients, but also the diffusion coefficients of the analytes in the membrane. The method of determining the diffusion coefficients is based on the fact that the chromatographic retention time and the profile of the eluting peaks are functions of the partition coefficient of the analyte between the carrier gas and the stationary phase and the diffusion coefficients of the analytes in the stationary phases and the mobile phase among many other variables. Pawlisch and co-

workers determined the diffusion coefficients and solubility parameters for analytes such as benzene, toluene, and ethylbenzene in polystyrene as early as in 1987.[227] Jackson and Huglin measured diffusion coefficients of chlorobenzene in cross-linked amine-cured epoxy resin.[228] Cankurtaran and Yilmaz determined the enthalpy and entropy parameters of selected n-alkanes in PDMS, a method which could be useful when determining the variations of the calibration constants of the TWA-PDMS samplers with temperature.[229] Zhao and co-workers demonstrated the applicability of IGC for the determination of the diffusion coefficients of various n-alkanes in crosslinked PDMS.[230]

Since determining these parameters using GC can be quicker and easier when compared to experimentally determining the calibration constants of the analytes in the laboratory, this method can result in a better model for correlating the calibration constant with retention parameters in gas chromatography.

An added advantage of developing models based on retention parameters is that the PDMS membrane can be replaced by various other materials. Such materials can then be conveniently used as stationary phases in gas chromatographic columns for developing models for estimating the calibration constants with the changed membrane material. Alternatively, a custom membrane material can be proposed based on studies of the retention parameters in columns coated with this material.

The TWA-PDMS sampler developed during this project has been applied mainly for vapour phase volatile organic compounds sampling and analysis. However, since PDMS is highly hydrophobic, in principle the sampler should be applicable for sampling volatile organic compounds from water matrix as well. Demonstrating the applicability of the sampler in water (and pore water) matrices could in theory provide one sampler for all matrices.

Currently, the analytical extraction method involves solvent desorption with carbon disulphide. Typically, the carbon disulphide volume used for extraction is 1 mL, and only 1 μL of this extract is injected into the GC for quantifications. Consequently, the quantification limit for the extraction and analysis is considerably higher than it potentially could be. The quantification limit can be further reduced either by using large volume injection in GC (with injection volumes potentially as high as 100 μL), or by switching to a thermally desorbable

sorbent. The latter would allow solvent desorption to be replaced with thermal desorption, which makes it possible to transfer all the analytes collected by the sorbent into the GC column, thereby greatly reducing the quantification limit of the method. Alternatively, supercritical fluid extraction of the sorbent can be performed followed by transferring the analytes completely into the GC using a method similar to the extraction of toluene from Anasorb 747® demonstrated by Glaser and Shulman.[231]

The project detailed in this thesis has resulted in a new, highly cost effective permeation-type passive sampler and has been validated in the laboratory and under field conditions. Many potential improvements can be made to understand and further develop the technology. The author firmly believes that the sampler will be well accepted for widespread use in air and soil gas monitoring applications.

Appendix A

Soil gas sampling in Belgium: Analyte concentrations

This appendix is a pdf file containing analyte concentrations determined using TWA-PDMS samplers at a contaminated site in Belgium.

The file name of this pdf file is “Belgium Project Results – Thesis.pdf”

If you accessed this thesis from a source other than the University of Waterloo, you may not have access to this file. You may access it by searching for this thesis at http://uwspace.uwaterloo.ca

References

[1]S. Seethapathy, T. Górecki, X. Li, J. Chromatogr. A 1184 (2008) 234.

[2]T. Górecki, J. Namieśnik, Trends Anal. Chem. 21 (2002) 276.

[3]Directive 2004/42/EC of the European Parliament and of the Council on the Limitation of Emissions of Volatile Organic Compounds Due to the Use of Organic Solvents in Decorative Paints and Varnishes and Vehicle Refinishing Products and Amending Directive 1999/13/EC, Strasbourg, 2004.

[4]EPA Compendium Method TO-17, Determination of Volatile Organic Compounds in Ambient Air Using Active Sampling onto Sorbent tubes, United States Environmental Protection Agency, Cincinnati, OH, 1999.

[5]M. Harper, J. Chromatogr. A 885 (2000) 129.

[6]Hazardous Materials Training Institute, in Site Characterization, Wiley, NJ, 1997.

[7]K. Badjagbo, S. Sauve, Trends Anal. Chem. 26 (2007) 931.

[8]M. Liess, M. Leonhardt, Meas. Sci. Technol. 14 (2003) 427.

[9]Technical note TN-102, http://www.conceptcontrols.com/file/164, accessed on 30th Jul, 2009.

[10]B.G. Willoughby (Ed.) in Air Monitoring in the Rubber and Plastics Industries, Smithers Rapra Technology, Billingham, UK, 2003.

[11]E.D. Palmes, A.F. Gunnison, Am. Ind. Hyg. Assoc. J. 34 (1973) 78.

[12]P. Mayer, J. Tolls, J.L. M. Hermens, D. Mackay, Environ. Sci. Technol. 37 (2003) 185A.

[13]J. Pawliszyn, in D. Barceló (Ed.), Comprehensive Analytical Chemistry, Vol. 37, Elsevier, Amsterdam, 2002, p. 253.

[14]T.M. Madkour, S.K. Mohamed, A.K. Barakat, Mater. Sci. Technol. 18 (2002) 1235.

[15]J. Namieśnik, T. Górecki, E. Kozlowski, L. Torres, J. Matheieu, Sci. Total. Environ. 38 (1984) 225.

[16]J. Comyn (Ed.), Polymer Permeability, Elsevier, England, 1985.

[17]K.J. Saunders, Int. Environ. Safety, August (1981) 54.

[18]A. Berlin, R.H. Brown, K.J. Saunders (Eds.), Diffusive Sampling: An Alternative Approach to Workplace Air Monitoring, CEC Pub. No. 1055EN, Commission of European Communities, Brussels, 1987.

[19]B.A. Byrne, R.I. Aylott, Concentrator for Removing Organic Materials from Aqueous Systems, British Patent 1566253, London, UK, 1980.

[20]A. Södergren, Environ. Sci. Technol. 21 (1987) 855.

[21]R.H. Brown, M. Curtis, K.J. Saunders, S. Vandendriessche (Eds.), Clean Air at Work - New Trends in Assessment and Measurement for the 1990s (Proceedings of an International Symposium Held in Luxenbourg, 9-13 September 1990), Royal Society of Chemistry, London, 1991.

[22]J.N. Huckins, J.D. Petty, K. Booij (Eds.), Monitors of Organic Chemicals in the Environment: Semipermeable Membrane Devices, Springer, NY, 2006.

[23]R. Greenwood, G. Mills, B. Vrana (Eds.), Passive Sampling Techniques in Environmental Monitoring, Vol. 48, Elsevier, Amsterdam, 2007.

[24]W.K. Fowler, Am. Lab. 14 (1982) 80.

[25]V.E. Rose, J.L. Perkins, Am. Ind. Hyg. Assoc. J. 43 (1982) 605.

[26]M. Harper, C.J. Purnell, Am. Ind. Hyg. Assoc. J. 48 (1987) 214.

[27]R.H. Brown, Pure Appl. Chem. 65 (1993) 1859.

[28]O.J. Levin, R. Lindahl, Analyst 119 (1994) 79.

[29]B. Kozdron-Zabiegała, J. Namieśnik, A. Przyjazny, Indoor Environ. 4 (1995) 189.

[30]R.H. Brown, J. Environ. Monit. 2 (2000) 1.

[31]A. Kot, B. Zabiegała, J. Namieśnik, Trends Anal. Chem. 19 (2000) 446.

[32]Y. Lu, Z. Wang, J. Huckins, Aquat. Toxicol. 60 (2002) 139.

[33]R.M. Cox, Environ. Pollut. 126 (2003) 301.

[34]F. Stuer-Lauridsen, Environ. Pollut. 136 (2005) 503.

[35]J. Namieśnik, B. Zabiegała, A. Kot-Wasik, M. Partyka, A. Wasik, Anal. Bioanal. Chem. 381 (2005) 279.

[36]Technology Overview of Passive Sampler Technologies, DSP-4, Interstate Technology and Regulatory Council (ITRC), Washington, DC, 2006.

[37]B. Vrana, I.J. Allan, R. Greenwood, G.A. Mills, E. Dominiak, K. Svensson, J. Knutsson, G. Morrison, Trends Anal. Chem. 24 (2005) 845.

[38]M. Partyka, B. Zabiegała, J. Namieśnik, A. Przyjazny, Crit. Rev. Anal. Chem. 37 (2007) 51.

[39]G.A. Mills, B. Vrana, I. Allan, D.A. Alvarez, J.N. Huckins, R. Greenwood, Anal. Bioanal. Chem. 387 (2007) 1153.

[40]EPA Compendium Method TO-14A, Determination of Volatile Organic Compounds (VOCs) in Ambient Air Using Specially Prepared Canisters with Subsequent Analysis by Gas Chromatography, United States Environmental Protection Agency, Cincinnati, OH, 1999.

[41]EPA Compendium Method TO-15, Determination of Volatile Organic Compounds in Air Collected in Specially-Prepared Canisters and Analyzed by Gas Chromatography/Mass Spectrometry, United States Environmental Protection Agency, Cincinnati, OH, 1999.

[42]www.lancasterlabs.com/environmental/analytical/9050_02.doc, accessed on 31st Jul, 2009.

[43]A. Rossner, J.P. Farant, J. Occup. Environ. Hyg. 1 (2004) 69.

[44]S. Heekmann, Non-enantioselective and Enantioselective Determination of Microbial Volatile Organic Compounds as Tracer for Human Exposure to Mould Growth in Buildings, Ph.D thesis, University of Basel, Switzerland, 2006.

[45]N. Yomamoto, T. Matsubasa, S. Mori, K. Suzuki, Anal. Chem. 74 (2002) 484.

[46]http://products.aerotechpk.com/ProductList.aspx?cid=92912dc1-cdc8-4390-8b8e-5973583cdd1b&sid=237bcf6a-48e1-448d-8a02-c3b7bbffe1f2, accessed on 23rd Jun, 2009.

[47]S.A.S. Wercinski and J. Pawliszyn (Eds.), Solid-phase Microextraction - A Practical Guide, Mercel Dekker, NY, 2009.

[48]Y. Chen, J. Pawliszyn, Anal. Chem. 75 (2003) 2004.

[49]M. Vogel, Anal. Bioanal. Chem. 381 (2005) 84.

[50]M. Shoeib, T. Harner, Environ. Sci. Technol. 36 (2002) 4142.

[51]T. Harner, K. Pozo, T. Gouin, A. Macdonald, H. Hung, J. Cainey, A. Peters, Environ. Pollut. 144 (2006) 445.

[52]T. Harner, M. Shoeib, M. Diamond, G. Stern, B. Rosenberg, Environ. Sci. Technol. 38 (2004) 4474.

[53]B.H. Wilford, T. Harner, J. Zhu, M. Shoeib, K.C. Jones, Environ. Sci. Technol. 38 (2004) 5312.

[54]F.M. Jaward, N.J. Farrar, T. Harner, A.J. Sweetman, K.C. Jones, Environ. Sci. Technol. 38 (2004) 34.

[55]J.R. Kucklick, P.A. Helm, Anal. Bioanal. Chem. 386 (2006) 819.

[56]S. Harrad, S. Hunter, Organohalogen Compd. 66 (2004) 3786.

[57]http://www.pops.int/documents/meetings/effeval/gmp_guidance/Annex_5/Annex%205%20SOPs_GAPS_PUF-DiskSampler_Dec11_06.pdf, accessed on 8th Aug, 2009.

[58]J.F. Muller, D.W. Hawker, D.W. Connell, P. Komp, M.S. McLachlan, Atmos. Environ. 34 (2000) 3525.

[59]N.J. Farrar, K. Prevedouros, T. Harner, A.J. Sweetman, K.C. Jones, Environ. Pollut. 144 (2006) 423.

[60]N.J. Farrar, T.J. Harner, A.J. Sweetman, K.C. Jones, Environ. Sci. Technol. 39 (2005) 261.

[61]T. Harner, N.J. Farrar, M. Shoeib, K.C. Jones, A.P.C. Gobas Frank, Environ. Sci. Technol. 37 (2003) 2486.

[62]M.E. Bartkow, D.W. Hawker, K.E. Kennedy, J.F. Mueller, Environ. Sci. Technol. 38 (2004) 2701.

[63]F. Wania, L. Shen, Y.D. Lei, C. Teixeira, D.C.G. Muir, Environ. Sci. Technol. 37 (2003) 1352.

[64]H. Plaisance, Atmos. Environ. 38 (2004) 6115.

[65]D.L. McDermott, K.D. Reiszner, P.W. West, Environ. Sci. Technol. 13 (1979) 1087.

[66]K.D. Reiszner, P.W. West, Environ. Sci. Technol. 7 (1973) 526.

[67]P.W. West, K.D. Reiszner, Am. Ind. Hyg. Assoc. J. 39 (1978) 645.

[68]D.R. Bell, K.D. Reiszner, P.W. West, Anal. Chim. Acta 77 (1975) 245.

[69]A. Hagenbjork-Gustafsson, R. Lindahl, J. Levin, D. Karlsson, Analyst 127 (2002) 163.

[70]Y.S. Tang, J.N. Cape, M.A. Sutton, The Scientific World 1 (2001) 513.

[71]Yanagisawa, H. Nishimura, Environ. Int. 8 (1982) 235.

[72]J. Begerow, E. Jermann, T. Keles, L. Dunemann, Fresenius J. Anal. Chem. 363 (1999) 399.

[73]Y.Z. Tang, P. Fellin, R. Otson, in E.D. Winegar, L.H. Keith (Eds.), Lewis Publishers, FL, 1993.

[74]M. De Bortoli, L. Moelhave, D. Ullrich, in A. Berlin, R.H. Brown, K.J. Saunders (Eds.), Diffusive Sampling; An Alternate Approach to Workplace Air Monitoring; Proceedings of an International Symposium Held in Luxembourg, Royal Society of Chemistry, London, 1987, p. 238.

[75]T.L. Hafkenscheid, J. Mowrer, Analyst 121 (1996) 1249.

[76]A. Sunesson, I. Liljelind, M. Sundgren, A. Pettersson-Stromback, J. Levin, J. Environ. Monit. 4 (2002) 706.

[77]E. Yamada, M. Kimura, K. Tomozawa, Y. Fuse, Environ. Sci. Technol. 33 (1999) 4141.

[78]R. Liard, M. Zureik, Y. Le Moullec, D. Soussan, M. Glorian, A. Grimfeld, F. Neukirch, Environ. Res. 81 (1999) 339.

[79]M.J. Roadman, J.R. Scudlark, J.J. Meisinger, W.J. Ullman, Atmos. Environ. 37 (2003) 2317.

[80]H. Hori, I. Tanaka, Ann. Occup. Hyg. 40 (1996) 467.

[81]M. Ferm, P. Svanberg, Atmos. Environ. 32 (1998) 1377.

[82]M. Ferm, H. Rodhe, J. Atmos. Chem. 27 (1997) 17.

[83]M. Ferm, Atmos. Environ. 13 (1979) 1385.

[84]TOPAS/TDS – Badge-Type Thermodesorption Passive Sampler Based on TENAX for Air Sampling - Development Study, http://www.gerstel.com/an-2001-06.pdf, Berlin, accessed on 10th May, 2007.

[85]W.J. May, Ann. Occup. Hyg. 33 (1989) 69.

[86]K.H. Pannwitz, Draeger Review 52 (1984) 1.

[87]K.H. Pannwitz, Draeger Review 48 (1981) 8.

[88]U. Giese, H. Stenner, E. Ludwig, A. Kettrup, Fresenius J. Anal. Chem. 338 (1990) 610.

[89]W.J. Lautenberger, E.V. Kring, J.A. Morello, Am. Ind. Hyg. Assoc. J. 41 (1980) 737.

[90]G. Bertoni, A. Cecinato, R. Mabilia, R. Tappa, Chromatographia 56 (2002) 361.

[91]B. Oury, F. Lhuillier, J. Protois, Y. Morele, J. Occup. Environ. Hyg. 3 (2006) 547.

[92]M. Carrieri, E. Bonfiglio, M.L. Scapellato, I. Macca, G. Tranfo, P. Faranda, E. Paci, G.B. Bartolucci, Toxicol. Lett. 162 (2006) 146.

[93]J. Delcourt, J.P. Sandino, Int. Arch. Occup. Environ. Health. 74 (2001) 49.

[94]SKC 575 Series Passive Samplers for Organic Vapors, SKC Publication 40087, http://www.skcinc.com/instructions/40087.pdf, PA, accessed on 10th May, 2007.

[95]K.A. Charron, M.A. Puskar, S.P. Levine, Am. Ind. Hyg. Assoc. J. 59 (1998) 353.

[96]M. Harper, L.V. Guild, Am. Ind. Hyg. Assoc. J. 57 (1996) 1115.

[97]W. Hendricks, The Marines Project: A laboratory Study of Diffusive Sampling/Thermal Desorption/Mass Spectrometry Techniques for Monitoring Personal Exposure to Toxic Industrial Chemicals, Industrial Hygiene Division, OSHA, Salt Lake Technical Center, Salt Lake City, UT, April 2002.

[98]E. Yamada, Y. Hosokawa, Y. Furuya, K. Matsushita, Y. Fuse, Anal. Sci. 20 (2004) 107.

[99]B. Zabiegała, M. Partyka, T. Górecki, J. Namieśnik, J. Chromatogr. A. 1117 (2006) 19.

[100]B. Zabiegała, T. Górecki, J. Namieśnik, Anal. Chem. 75 (2003) 3182.

[101]N. Shinohara, K. Kumagai, N. Yamamoto, Y. Yanagisawa, M. Fujii, A. Yamasaki, J. Air Waste Manag. Assoc. 54 (2004) 419.

[102]SKC Publication 1636 Rev 0702, http://www.skcinc.com/instructions/1636.pdf, PA, accessed on 10 May, 2007.

[103]R. Lindahl, J. Levin, K. Andersson, J. Chromatogr. 643 (1993) 35.

[104]S. Seethapathy, T. Górecki, B. Zabiegała, J. Namieśnik, presented at the Pittsburg Conference on Analytical Chemistry and Applied Spectroscopy (PITTCON), abstract no. 1680-3, Chicago, IL, February 2007.

[105]M. Shoeib, T. Harner, B. Wilford, K. Jones, J. Zhu, Organohalogen Compd. 66 (2004) 3999.

[106]M. Bartkow, K. Jones, K. Kennedy, N. Holling, D. Hawker, J. Muller, Organohalogen Compd. 66 (2004) 138.

[107]K. Pozo, T. Harner, M. Shoeib, R. Urrutia, R. Barra, O. Parra, S. Focardi, Environ. Sci. Technol. 38 (2004) 6529.

[108]R. D. Morrison, in Environmental Forensics: Principles and Applications, CRC Press, FL,1999.

[109]San Diego County, Site Assessment and Mitigation Manual, CA, 2004.

[110]D.A. Vroblesky, J.F. Robertson, M. Fernandez, C.M. Aelion, in Proceedings of the Sixth National Outdoor Action Conference, National Water Well Association, Las Vegas, NV, 1992, p. 3.

[111]J. Wilson, J.E. Whetzel, W.W. Wells, Combining Passive Soil Gas Sampling, GC-MS Analysis, and Non-Conventional Interpretation to Identify Fuel Sources, Presented at the

Annual International Conference on Soils, Sediments, Water and Energy, Oct 18 – 20, Amherst, MA, 2004.

[112]http://www.lascaux.ch/english/restauro/pdf/58322_02.pdf, accessed on 8th Aug, 2009.

[113]Environmental Technology Verification Report: Soil Gas Sampling Technology, W.L. Gore & Associates Inc., GORE-SORBER® Screening Survey, USEPA 600/R-98/095, 1998.

[114]K. Monks, M. Godwin, Proceedings of the 2001 International Containment & Remediation Technology Conference and Exhibition, Florida State University, FL, 2001.

[115]M. Anderson, G. Church, J. Environ. Eng. 124 (1998) 555.

[116]R. Sadler, D. Connell, Analytical Methods for the Determination of Total Petroleum Hydrocarbons in Soil, proceeding of the Fifth National Workshop on the Assessment of Site Contamination, Adelaide, Australia, 2002.

[117]D.C. Gomes, M. Alarsa, M.C. Salvador, C. Kupferschmid, Water Sci. Technol. 29 (1994) 161.

[118]J.N. Huckins, M.W. Tubergen, G.K. Manuweera, Chemosphere 20 (1990) 533.

[119]T.D. Hayes, B.K. Soni, Soil Sed. Contam. 15 (2006) 511.

[120]J. Cáslavský, P. Kotlaríková, in E. Lichtfouse, J. Schwarzbauer, D. Robert (Eds.) Environmental Chemistry, Springer, NY, 2005.

[121]R.P. Lanno, J. Wells, K. Duncan, M. Carey, P. Rider, A. Stepp, B. Miller, Estimating the Bioavailability of Hydrocarbons in Soils Using Passive Sampling Devices, proceedings of the 7th International Petroleum Environmental Conference, Albuquerque, NM, 2000.

[122]http://www.est-lab.com/spmd.php, accessed on 8th Aug, 2009.

[123]G. Ouyang, J. Pawliszyn, Anal. Bioanal. Chem. 386 (2006) 1059.

[124]W.J. Havenga, E.R. Rohwer, J. Chromatogr. A 848 (1999) 279.

[125]Z. Zhang, J. Pawliszyn, Anal. Chem. 65 (1993) 1843.

[126]Technology Overview of Passive Sampler Technologies, DSP-4, Interstate Technoloy and Regulatory Council (ITRC), Washington, DC, 2006.

[127]T. Dragoo, J. Hicks, D. Vroblesky, R. Vazquez, in E.J. Calabrese, P.T. Kostecki, J. Dragun (Eds.), Contaminated Soils, Sediments and Water: Science in the Real World, Springer, NY, 2005, p. 537.

[128]US EPA Environmental Technology Verification Report: Soil Sampler, SimulProbe Technologies, Inc., Quadrel Services, Inc. (Quadrel), EMFLUX, EPA/600/R-98/096, Washington DC, August 1998.

[129]M.D. McVey, T.J. Goering, J.L. Peace in Passive and Active Soil Gas Sampling at the Mixed Waste Landfill, Technical Area Ill, Sandia National Laboratories/New Mexico, Sandia National Laboroatories, February 1996.

[130]http://www.atsdr.cdc.gov/HAC/PHA/memphisschools/mcs_p1.html#disca, accessed on 2nd Sep, 2009.

[131]http://www.eswp.com/brownfields/Frishkorn%20Andrew.pdf, accessed on 2nd sep, 2009.

[132]S. Tumbiolo, L. Vincent, J. Gal, P. Maria, Analyst 130 (2005) 1369.

[133]B. Flaconneche, J. Martin, M.H. Klopffer, Oil Gas. Sci. Technol. 56 (2001) 261.

[134]K. Booij, R. Van Bommel, H.M. Van Aken, H. Van Haren, G. Brummer, H. Ridderinkhof, Passive Samplers on Semi-Permanent Moorings at Three Deep-ocean Sites, presented at the 7th Passive Sampling Workshop and Symposium, abstract no. 24, Reston, VA, April 2007.

[135]E.R. Alley (Ed.), Water Quality Control Handbook, II Ed, McGraw Hill, Berkshire, UK, 2006.

[136]J. Ballach, B. Greuter, E. Schultz, W. Jaeschke, Sci. Total Environ. 243/244 (1999) 203.

[137]M. Bates, N. Gonzalez-Flesca, V. Cocheoc, R. Sokhi, Analyst 122 (1997) 1481.

[138]P.P. Ballesta, E.G. Ferradas, A.M. Aznar, Am. Ind. Hyg. Assoc. J. 56 (1995) 171.

[139]R.G. Lewis, J.D. Mulik, R.W. Coutant, G.W. Wooten, C.R. McMillin, Anal. Chem. 57 (1985) 214.

[140]K. Booij, R. Van Bommel, A. Mets, R. Dekker, Chemosphere 65 (2006) 2485.

[141]G.S. Ellis, J.N. Huckins, C.E. Rostad, C.J. Schmitt, J.D. Petty, P. MacCarthy, Environ. Toxicol. Chem. 14 (2005) 1875.

[142]D.R. Luellen, D. Shea, Environ. Sci. Technol. 36 (2002) 1791.

[143]J. Thomas, T.M. Holsen, S. Dhaniyala, Environ. Pollut. 144 (2006) 384.

[144]J.N. Huckins, J.C. Meadows, G.K. Manuweera, J.A. Lebo, presented at the 12th Annual Meeting of the Society of Environmental Toxicology and Chemistry, 3-7 November, Seattle, WA, 1991.

[145]J.N. Huckins, G.K. Manuweera, J.D. Petty, D. Mackay, J.A. Lebo, Environ. Sci. Technol. 27 (1993) 2489.

[146]K. Booij, H.M. Sleiderink, F. Smedes, Environ. Toxicol. Chem. 17 (1998) 1236.

[147]W.A. Ockenden, B.P. Corrigan, M. Howsam, K.C. Jones, Environ. Sci. Technol. 35 (2001) 4536.

[148]K. Booij, H.E. Hofmans, C.V. Fischer, E.M. Van Weerlee, Environ. Sci. Technol. 37 (2003) 361.

[149]B. Vrana, G. Schueuermann, Environ. Sci. Technol. 36 (2002) 290.

[150]J.N. Huckins, J.D. Petty, J.A. Lebo, F.V. Almeida, K. Booij, D.A. Alvarez, W.L. Cranor, R.C. Clark, B.B. Mogensen, Environ. Sci. Technol. 36 (2002) 85.

[151]H.S. Söderström, P. Bergqvist, Environ. Sci. Technol. 38 (2004) 4828.

[152]D. Alvarez, POCIS - Current Applications, On-going Research and Future Needs, presented at the 7th Passive Sampling Workshop and Symposium, abstract no. 1, Reston, VA, April 2007.

[153]N. Mazzella, T. Debenest, F. Delmas, Dissipation of Polar Xenobiotics From Pharmaceutical POCIS and Suggestion of a Performance Reference Compound, presented at the 7th Passive Sampling Workshop and Symposium, abstract no. 3, Reston, VA, April 2007.

[154]Y. Chen, J. O'Reilly, Y. Wang, J. Pawliszyn, Analyst 129 (2004) 702.

[155]M.E. Bartkow, K.C. Jones, K.E. Kennedy, N. Holling, D.W. Hawker, J.F. Mueller, Environ. Pollut. 144 (2006) 365.

[156]L. Tuduri, T. Harner, H. Hung, Environ. Pollut. 144 (2006) 377.

[157]T. Harner, M. Shoeib, T. Gouin, P. Blanchard, Environ. Sci. Technol. 40 (2006) 5333.

[158]Methods for the determination of Hazardous Substances: Protocol for Assessing the Performance of a Diffusive Sampler, MDHS 27, Health and Safety Executive (HSE), London, 1983.

[159]J.G. Firth, in A. Berlin, R.H. Brown, K.J. Saunders (Eds.), Diffusive sampling; An Alternate Approach to Workplace Air monitoring; Proceedings of an International Symposium held in Luxembourg, Royal Society of Chemistry, London, 1987, p. 177.

[160]R.H. Brown, R.P. Harvey, C.J. Purnell, K.J. Saunders, Am. Ind. Hyg. Assoc. J. 45 (1984) 67.

[161]R.H. Brown, in A. Berlin, R.H. Brown, K.J. Saunders (Eds.), Diffusive sampling; An Alternate Approach to Workplace Air Monitoring; Proceedings of an International Symposium Held in Luxembourg, Royal Society of Chemistry, London, 1987, p. 185.

[162]M.E. Cassinelli, R.D. Hull, J.V. Crable, A.W. Teass, in A. Berlin, R.H. Brown, K.J. Saunders (Eds.), Diffusive Sampling; An Alternate Approach to Workplace Air Monitoring; Proceedings of an International Symposium Held in Luxembourg, Royal Society of Chemistry, London, 1987, p. 190.

[163]The NIOSH Manual of Analytical Methods, Third Edition, 1984.

[164]Methods for the Determination of Hazardous Substances: Protocol for Assessing the Performance of a Diffusive Sampler, MDHS 27, Health and Safety Executive (HSE), London, 1994.

[165]Methods For the Determination of Hazardous Substances: Volatile Organic Compounds in Air - Laboratory Method Using Diffusive Solid Sorbent Tubes, Thermal Desorption and Gas Chromatography, MDHS 80, Health and Safety Executive (HSE), London, 1995.

[166]Methods for the Determination of Hazardous Substances: Volatile Organic Compounds - Laboratory Method Using Diffusive Samplers, Solvent Desorption and Gas Chromatography, MDHS 88, Health and Safety Executive (HSE), London, 1997.

[167]Workplace Air Quality - Sampling and Analysis of Volatile Organic Compounds by Solvent Desorption/Capillary Gas Chromatography - Part 2: Diffusive Sampling Method, ISO 16200-2, International Organization for Standardization (ISO), Geneva, 2000.

[168]Workplace Air Quality - Sampling and Analysis of Volatile Organic Compounds in Ambient Air, Indoor Air and Workplace Air by Sorbent Tube/Thermal Desorption/Capillary Gas Chromatography - Part 2: Diffusive Sampling, ISO 16017-2, International Organization for Standardization (ISO), Geneva, 2000.

[169]ASTM Method D 6246-02, Annual Book of ASTM Standards, American Society for Testing and Materials, Philadelphia, PA, 2005.

[170]ASTM Method D 4597 – 03, Annual Book of ASTM Standards, American Society for Testing and Materials, Philadelphia, PA, 2005.

[171]ASTM Method 4598, Annual Book of ASTM Standards, American Society for Testing and Materials, Philadelphia, PA, 1995.

[172]ASTM Method D 4599 - 03, Annual Book of ASTM Standards, American Society for Testing and Materials, Philadelphia, PA, 2005.

[173]ASTM Method D 6306 - 098, Annual Book of ASTM Standards, American Society for Testing and Materials, Philadelphia, PA, 2005.

[174]CEN EN 482:1994, Workplace Atmospheres - General Requirements for the Performance of Procedures for the Measurement of Chemical Agents, European Committee for Standardization, Brussels, 1994.

[175]CEN EN 838, Workplace Atmospheres - Requirements and Test Methods for Diffusive Samplers for the Determination of Gases and Vapours, European Committee for Standardization, Brussels, 1995.

[176]CEN EN 13528-1, Ambient Air Quality - Diffusive Samplers for the Determination of Concentrations of Gases and Vapours – Requirements and Test Methods, Part 1: General Requirements. Brussels, Belgium: European Committee for Standardization, Brussels, 2002.

[177]CEN EN 13528-2, Ambient Air Quality - Diffusive Samplers for the Determination of Concentrations of Gases and Vapours - Requirements and Test Methods, Part 2: Specific Requirements and Test Methods, European Committee for Standardization, Brussels, 2002.

[178]CEN EN 13528-3, Ambient Air Quality - Diffusive Samplers for the Determination of Concentrations of Gases and Vapours - Requirements and Test Methods, Guide to Selection, Use and Maintenance, European Committee for Standardization, Brussels, 2003.

[179]Technical and Regulatory Guidelines for Using Polyethylene Diffusion Bag Samplers to Monitor Volatile Organic Compounds in Groundwater, DSP-3, Interstate Technology and Regulatory Council (ITRC), Washington, DC, 2004.

[180]Protocol for Use of Five Passive Samplers to Sample for a Variety of Contaminants in Groundwater, DSP-5, Interstate Technology and Regulatory Council (ITRC), Washington, DC, 2004.

[181]E.C. da Rocha, F. Augusto, A.L.P. Valente, J. Michrocolumn Sep. 11 (1999) 29.

[182]R.A. Ketola, M. Ojala, H. Sorsa, T. Kotiaho, R.K. Kostianen, Anal. Chim. Acta. 349 (1997) 359.

[183]J. Pawliszyn, in D. Barceló (Ed.), Comprehensive Analytical Chemistry, Vol. 37, Elsevier, Amsterdam, 2002, p. 253.

[184]F.C. Tompkins, R.L. Goldsmith, Am. Ind. Hyg. Assoc. J. 38 (1977) 8.

[185]M.E. Bartkow, K. Booij, K.E. Kennedy, J.F. Muller, D.W. Hawker, Chemosphere 60 (2005) 170.

[186]D.L. Bartley, L.J. Doemeny, D.G. Taylor. Am. Ind. Hyg. Assoc. J. 44 (1983) 24.

[187]E. Langlois, Am. Occup. Hyg. 52 (2008) 239.

[188]E. Boscaini, M.L. Alexander, P. Prazeller, T.D. Maerk, Int. J. Mass. Spectrom. 239 (2004) 179.

[189]R.H. Brown, J. Environ. Monit., 2 (2000) 1.

[190]S. Seethapathy, Calibration of Permeation Passive Samplers Based on Physicochemical Properties of the Analytes, M.Sc. thesis, University of Waterloo, ON, 2005.

[191]J.G. Wijmans, J. Membr. Sci. 237 (2004) 39.

[192]T.C. Merkel, V.I. Bondar, K. Nagai, B.D. Freeman, I. Pinnau, J. Polym. Sci. Part B. 38 (2000) 415.

[193]S.V. Dixon-Garret, K. Nagai, B.D. Freeman, J. Polym. Phys. 38 (2000) 1461.

[194]J.M. Kong, S.J. Hawkes, J. Chromatogr. Sci. 14 (1976) 279.

[195]http://www.wacker.com/, accessed on 12th Aug, 2009.

[196]J.M. Watson, P.A. Payne, J. Membr. Sci. 49 (1990) 171.

[197]D.A. Skoog, F.J. Howler, T.A. Nieman, (Eds.), Principles of Instrumental Analysis, Fifth edition, Brooks Cole, CA, 1998, p 679.

[198]H.V. Dool, P.D. Kratz, J. Chromatogr. 11 (1963) 463.

[199]F.R. Gonzalez, A.M. Nardillo, J. Chromatogr. A, 842 (1999) 29.

[200]A. Kłoskowski, W. Chrzanowski, M. Pilarczyk, J. Namieśnik, J. Chem. Therm. 37 (2005) 21.

[201]P.A. Martos, A. Saraullo, J. Pawliszyn, Anal. Chem. 69 (1997) 402.

[202]C.A. Cramers, C.E. van Tilburg, C.P.M. Schutjes, J.A.Rijks, G.A. Rutten, R. de Jijs, J. Chromatogr. A. 279 (1983) 3.

[203]http://www.sspinc.com/prodspecs/ssp-m100.cfm, accessed on 15th July 2009.

[204]Personal communication, J. Namieśnik, Technical University of Gdańsk, Poland.

[205]D. Monca, L. Feron, J. Weber, Clin. Chem. 35/4 (1989) 601.

[206]http://massfinder.com/wiki/Retention_index_guide, accessed on 29th August 2009.

[207]M. Gjølstad, K. Bergemalm-Rynell, G. Ljungkvist, S. Thorud, P. Molander, J. Sep. Sci. 27 (2004) 1531.

[208]M. Harper, Analyst 119 (1994) 65.

[209]http://www.weber.hu/PDFs/SKC/ShelfLife_SKCmedia.pdf, accessed on 15th July, 2009.

[210]C.J. Guo, D. Dee Kee, Chem. Eng. Sci. 46 (1991) 2133.

[211]E. Favre, P. Schaetzel, Q.T. Nguygen, R. Clement, J. Neel, J. Membr. Sci. 92 (1994) 169.

[212]I. Blume, P.J.F. Schwering, M.H.V. Mulder, C.A. Smolders, J. Memb. Sci. 61 (1991) 85.

[213]C. Dotremont, B. Brabants, K. Geeroms, J. Mewis, C. Vandecasteele, J. Mem. Sci. 104 (1995) 109.

[214]D.A. Skoog, D.M. West, F.J. Holler, S.R. Crouch in Fundamentals of Analytical Chemistry (8th Ed.), Brooks/Cole, Florence, KY, 2003.

[215]L.M. Costello, W.J. Koros, Ind. Eng. Chem. Res. 31 (1992) 2708.

[216]M.A. LaPack, J.C. Tau, and C.G. Enke, Anal. Chem. 62 (1990) 1265.

[217]M.W. Denny (Ed.), Air and Water, the Biology and Physics of Life's Media, Princeton University Press, NJ, 1995, p. 89.

[218]D.W. Underhhill, C.E. Feigley, Anal. Chem. 63 (1991) 1011.

[219]R.H. Brown, J. Environ. monit. 2 (2002) 1.

[220]A. Pennequin-Cardinal, H. Plaisance, N. Locoge, O. Ramalho, S. Kircher, J.C. Galloo, Atmos. Environ. 39 (2005) 2535.

[221]A. Piechocki-Minguy, H. Plaisance, S. Garcia-Fouque, J.C. Galoo, R. Guillermo, Environ. Technol. 24 (2003) 1527.

[222]A.L. Sunesson, C.A. Nilsson, B. Andersson, J. Chromatogr. A 699 (1995) 203.

[223]I. Cinnau, A. Chiriac, A. Caprita, J. Chromatogr. A 964 (2002) 1.

[224]http://www.lancasterlabs.com/, accessed on 11th Aug, 2009.

[225]http://iavi.rti.org/attachments/Resources/Hodny_Passive_Sampling.pdf, accessed on 15th Aug, 2009.

[226]R. Truesdale, D. Grosse, T. McAlary, Field Demonstration of Soil Gas Sampling and Analytical Methods, presented at the Midwestern States Risk Assessment Symposium - Soil Gas Demonstration Program, Indianapolis, IN, 21-24 Aug, 2006.

[227]C.A. Pawlisch, A. Marcris, R.L. Laurence, Macromolecules 20 (1987) 1564.

[228]P.L. Jackson, M.B. Huglin, Eur. Polym. J. 31 (1995) 63.

[229]O. Cankurtaran, F. Yilmaz, Polym. Int. 41 (1996) 307.

[230]C. Zhao, J. Li, Z. Jing, C. Chen, Eur. Polym. J. 42 (2006) 615.

[231]R.A. Glaser, S.A. Shulman, Chromatographia 42 (1996) 665.F